MICROCOPY RESOLUTION TEST CHART
NATIONAL BUREAU OF STANDARDS - 1963 - A

AFWAL-TR-82-3040
Part II
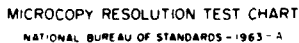
AD A131402

DEVELOPMENT AND FLIGHT TEST OF AN ACTIVE FLUTTER
SUPPRESSION SYSTEM FOR THE F-4F WITH STORES

PART II.   GROUND TESTS AND SUBCRITICAL
FLIGHT TESTS

H. Hönlinger
D. Mussman
R. Manser
Messerschmitt-Bölkow-Blohm GmbH
Ottobrunn, Federal Republic of Germany

and

C. J. Huttsell
Air Force Wright Aeronautical Laboratories
Wright-Patterson Air Force Base, Ohio 45433

April 1982

Final Report for Period March 1978 - March 1980

DTIC FILE COPY

LAWRENCE J. HUTTSELL
Aerospace Engineer
Aeroelastic Group

FREDERICK A. PICCHIONI, LT COL, USAF
Chief, Analysis & Optimization Branch
Structures & Dynamics Division

FOR THE COMMANDER

RALPH L. KUSTER, JR., Colonel, USAF
Chief, Structures & Dynamics Division

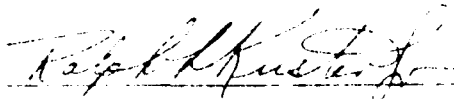| REPORT DOCUMENTATION PAGE		READ INSTRUCTIONS BEFORE COMPLETING FORM
1. REPORT NUMBER AFWAL-TR-82-3040, Part II	2. GOVT ACCESSION NO. AD A131 452	3. RECIPIENT'S CATALOG NUMBER
4. TITLE (and Subtitle) DEVELOPMENT AND FLIGHT TEST OF AN ACTIVE FLUTTER SUPPRESSION SYSTEM FOR THE F-4F WITH STORES, PART II. GROUND TESTS AND SUBCRITICAL FLIGHT TESTS		5. TYPE OF REPORT & PERIOD COVERED Final Report March 1978 - March 1980
		6. PERFORMING ORG. REPORT NUMBER
7. AUTHOR(s) H. Hönlinger, D. Mussman, R. Manser, and L. Huttsell		8. CONTRACT OR GRANT NUMBER(s) Memorandum of Understanding
9. PERFORMING ORGANIZATION NAME AND ADDRESS Messerschmitt-Bolkow-Blohm GmbH. (MBB) Ottobrunn, Federal Republic of Germany		10. PROGRAM ELEMENT, PROJECT, TASK AREA & WORK UNIT NUMBERS PE 62201F 2401/02/23
11. CONTROLLING OFFICE NAME AND ADDRESS Flight Dynamics Laboratory (AFWAL/FIBR) Air Force Wright Aeronautical Laboratories, AFSC Wright-Patterson Air Force Base, Ohio 45433		12. REPORT DATE April 1983
		13. NUMBER OF PAGES 156
14. MONITORING AGENCY NAME & ADDRESS(if different from Controlling Office)		15. SECURITY CLASS. (of this report) Unclassified
		15a. DECLASSIFICATION DOWNGRADING SCHEDULE

16. DISTRIBUTION STATEMENT (of this Report)

Approved for public release; distribution unlimited.

17. DISTRIBUTION STATEMENT (of the abstract entered in Block 20, if different from Report)

18. SUPPLEMENTARY NOTES

19. KEY WORDS (Continue on reverse side if necessary and identify by block number)

Active Controls
Aeroservoelasticity
Flutter
Flutter Suppression
Wing/Store Flutter

20. ABSTRACT (Continue on reverse side if necessary and identify by block number)

Extensive research programs have been conducted at MBB and at AFWAL to investigate the application of active controls for the suppression of wing/store flutter. A flutter suppression system was developed and flight tested on an F-4F aircraft. The control law was designed by MBB using optimal control theory to minimize the control surface motion and to provide the required stability margins. During the test it was found that the dynamic behavior of the wing-pylon-store changed considerably with excitation amplitude due to free

DD $_{1 JAN 73}^{FORM}$ 1473   EDITION OF 1 NOV 65 IS OBSOLETE

play and preload. The active flutter suppression system worked well and provided an increase in flutter speed.

FOREWORD

The research described in this report was conducted by Messerschmitt-Bolkow-Blohm GmbH. (MBB) under a joint U.S. Air Force/German Ministry of Defense Memorandum of Understanding. The Air Force Project Engineers for this effort (work unit 24010223) were Thomas E. Noll and Lawrence J. Huttsell of the Structures and Dynamics Division, Flight Dynamics Laboratory, Air Force Wright Aeronautical Laboratories. The MBB Project Engineer Was H. Hönlinger.

The authors wish to acknowledge the cooperation and support of the OTC E-61 of the Federal Armed Forces in Manching and DFVLR, Institute for Aeroelastics, in Gottingen.

This report (Part II) documents the ground vibration tests, the ground tests on the flutter suppression system, and the initial sub-critical flight tests. Part I documents the design of the active flutter suppression system and Part III documents the flight test demonstration.

This report covers work conducted from March 1978 to March 1980.

TABLE OF CONTENTS

LIST OF ILLUSTRATIONS

LIST OF ILLUSTRATIONS (Cont'd)

LIST OF ILLUSTRATIONS (Cont'd)

LIST OF ILLUSTRATIONS (Cont'd)

LIST OF ILLUSTRATIONS (Cont'd)

LIST OF ILLUSTRATIONS (Concluded)

LIST OF TABLES

SECTION I

INTRODUCTION

During the last several years, considerable interest has emerged in the U.S. and European community for the application of active control technology to suppress flutter. Both the U.S. Air Force and MBB have performed extensive research programs accompanied by wind tunnel tests in the field of active flutter and elastic mode suppression.

In 1975, MBB conducted a successful wind tunnel test which also led to a flight demonstration. This research demonstrated suppression of wing store flutter with store mounted vanes (Reference 1). On another program, flutter speed was increased on a fin-tailplane-aft fuselage with a hydraulically driven rudder (References 2, 3). Miniature model actuators and new wind tunnel test techniques were developed to investigate Flutter Suppression Systems (FSS) with flutter models. Special computer programs - utilizing optimal control theory - were adapted to find suitable control laws for flutter suppression (Reference 4). A very successful application of these programs is described in Reference 5. Analytical development of systems to reduce buffet induced pilot vibrations was presented in Reference 6. A system to improve ride comfort of a low wing loaded fighter was laid out recently (Reference 7).

Two full scale airplanes were equipped and flight tested to prove the feasibility of active flutter suppression. The first flight test was performed with a Fiat G 91/T3 which used additional control surfaces (vanes) to produce aerodynamic forces which counteract the store motion (Reference 8). In 1977, a much more challenging flight test program was launched in cooperation with the Bundesamt fur Wehrtechnik and Beschaffung (BWB) and the U.S. Air Force Flight Dynamics Laboratory (FDL). The objective of this program was to design and flight test a system for flutter suppression on an F-4F aircraft with stores. As flying test bed for this program, an F-4F aircraft of the German Air Force test center at Manching (Erprobungsstelle 61 der Bundeswehr) was chosen. This airplane was already equipped to perform flight flutter tests with stores. To generate the necessary unsteady aerodynamic control forces, existing control surfaces (ailerons) were used. Accelerometers located on the

wing provided the signals which were fed back through the existing
stability augmentation system of the airplane.

This report (Part II) documents the ground vibration tests, the
ground tests on the flutter suppression system, and the initial sub-
critical flight tests. Part I documents the analysis and design of the
active flutter suppression system for the F-4F aircraft with stores
(Reference 9). Part III documents the flight test demonstration of the
active flutter suppression system.

SECTION II

GROUND TEST RESULTS

1. GROUND VIBRATION TEST AND COMPARISON WITH ANALYSES

A ground vibration test was conducted with the LBFK external stores on the F-4F before flight test with an active flutter suppression system. The purpose of the test was to check the mathematical structural model of the F-4F wing with the critical external stores, as indicated by the aircraft manufacturer (References 10, 11). Special emphasis was placed on the measurement of the vibration modes critical for flutter and to study nonlinearities of the wing-pylon external store combination (Reference 12).

a. Description of the Ground Vibration Test

The ground vibration test was performed with the aircraft on the landing gear. To simulate free-free conditions, the tires were deflated to 50% of the required pressure. The excitation of the modes was performed by electrodynamic shakers with harmonic force input. The exciter locations and the applied force amplitudes are noted on the graphic representations of the measured mode shapes (Figure 8). For the measurement of the mode shapes a sufficient number of accelerometers were fixed on the surfaces, stores, and fuselage as shown on Figure 8.

Since practically all actual reasonant frequencies of elastic structures depend more or less on the vibration amplitude and thus on the exciter forces, so-called linearity checks were recorded together with each measured mode, i.e. the frequency and the amplitudes at some chosen measurement points versus exciter force.

3

Additionally a dimensionless nonlinearity number (NN) was defined and plotted to have a quick look at the degree of nonlinearity for each resonant vibration mode. NN is defined by:

$$NN = \frac{\Delta f}{\Delta a} \cdot \frac{a}{f} \qquad \text{where } f = \text{frequency (Hz)}$$

$$a = \text{an amplitude of the vibration mode.}$$

$$\frac{\Delta f}{\Delta a} = \text{frequency increase divided by the corresponding increase of amplitude}$$

For linear vibration NN = 0 and for nonlinear vibration NN $\gtrless$ 0. The magnitude of /NN/ is a measure for the degree of nonlinearity.

Two methods have been applied for evaluation of the damping values g (%): First decay curves were recorded and used for the evaluation of the logarithmic decrement D. Where $D = \frac{1}{m} \ln \frac{a_1}{a_{m+1}}$ and where $a_1, a_2, \ldots, a_m$ are consecutive amplitudes. The damping value g is approximately $= \frac{D}{\pi}$, if the damping is small. In the second method a "complex power" method was applied yielding the damping value g as well as the generalized masses, which were transformed (normalized) to the vibration amplitude of 1 m at a chosen reference point.

b. Comparison of Calculated and Measured Results

The first four calculated vibration modes were compared with those measured on the aircraft in order to check the mathematical structural model. The mass data of the external store configurations used for comparison of vibration modes are compiled in Table 1. Figures 1 through 8 present the first four measured modes and Figures 9 through 15 present the first four calculated modes for both the flutter critical and the safe store configuration. The vibration modes for wing bending, store yaw, and store roll are presented in Figures 9, 10, 12, 13, and 14. The external store pitching mode calculated as critical for flutter, however, demonstrates deviations from the experiment both in mode shape and in frequency. The nodal line of the measured mode (Figure 3) curves to the front (in the direction of flight). This shift of the nodal line in the pitching mode would indicate that a higher flutter speed may be

expected than was calculated. The nodal line of the vibration mode for the flutter stopper with the weights in the "safe" position (Figure 7), however, turns to the rear, indicating a lower flutter speed than calculated. This test result is opposite to the calculations with the mathematical model given by MDC (Figures 11 and 15).

Before it was possible to begin flight tests, this serious difference between calculation and experiment had to be explained and the mathematical model modified in such a manner that it correctly reflected the behavior of the real aircraft. Section III will discuss these modifications to the analysis.

2. COMPONENT TEST RESULTS

a. Impedance Test of the Aileron Actuator

The stiffness of the hydraulic actuator must be known in order to estimate the effect of aileron stiffness on flutter speed. Hydraulic actuators have a stiffness dependence on frequency (impedance), which cannot yet be satisfactorily determined by analysis. The DFVLR in Gottingen has developed an experimental analytical procedure to determine the actuator impedance. The DFVLR Gottingen, Institute for Aeroelastics, therefore carried out the impedance test with the Weston Power aileron actuator. The experimental results are compiled in a separate report (Reference 13). The resulting impedance of the aileron actuator did not lead to any great changes in the flutter speed calculated with real actuator stiffness.

b. Measurement of the Transfer Function of the Aileron

In Reference 14, the transfer function of the modified National Waterlift aileron actuator employed in flight tests was compared with that of the standard and the modified Weston Power actuator. The calculations of the control law for the flutter suppression system are based partially on these results. Since the flight tests were performed with the modified National Waterlift actuator for reasons of durability, it was necessary to measure the transfer function of the aileron control system with the National Waterlift actuator again for both wings, and to compare this with the calculated results. Figure 16 shows a block diagram

for the measurement of the aileron actuator transfer function. Figures 17 and 18 show the transfer functions of the left and right aileron control system for different electrical input signals.

The nonlinear behavior is clearly noticeable from the deviating amplitude and phase paths for various input signals. It was assumed for the interpretation of the control law that the actuator becomes even more nonlinear under the effect of the air load. Therefore the effect of the air load on the transfer function of the actuator was estimated in calculating the control law.

c. Modification and Testing of the Flutter Stopper

Because of the major differences between the calculated and measured vibration results, the flutter stopper had to be modified. The radius of gyration of the external store had to be increased to obtain a low flutter point on the basis of the measured vibration data. The mechanism to shift the mass in the flutter stopper had to be changed by 130° in order to increase flutter speed, as can be seen in Figure 19. The diagram of the altered flutter stopper is presented in Figure 20.

The necessary radius of gyration ($\cdot$ ~ 1.40 m) could be achieved without major changes in construction by increasing the total weight. Additional weights were installed for this purpose in the front and rear section of the external store, as can be seen in Figure 20. Figures 21 and 22 show the construction in detail.

Changing the shift mechanism for the trimming weights was also possible without large structural changes, because only individual components were shifted internally. Figure 23 shows the altered mounts of the guide rods for the trimming weights and the new position of the buffers for the trimming weights. The new location of holding mechanisms for the trimming weights and the installation of the solenoid switch can be seen in Figures 21 and 22.

The flutter stopper was equipped with accelerometers and terminal switches for controlling the position of the trimming weights as shown in Figure 20. The connection to the aircraft was established via a magnetic plug in the rear third of the external store. The cabling plan

for the external store can be seen in Figure 24 with details of the electrical equipment.

After completing the modification of the external stores with the built-in flutter stopper, the operation of the shift mechanism for the trimming weights was then checked in the laboratory. The springs employed shift both trimming weights of 150 kg each within 0.5 sec from the position critical for flutter to the safe position. The switching forces of the solenoid switch first proved to be insufficient and an additional spring had to be installed, as can be seen in Figures 21 and 22. With this modification, the flutter stopper functioned faultlessly. The inertial radius of gyration of the flutter stopper with the weights in "safe" and "critical" position were determined for the pitch axis with the standard pendulum test. This mass data are shown on Figure 25.

3. FUNCTIONAL TESTS ON THE FLUTTER SUPPRESSION SYSTEM

The detailed design of the flutter suppression system and the associated test equipment is given in Reference 9. Only the circuit diagram for the electronic control system is given in this report (Figure 26). The entire circuit for an aircraft wing with aileron was accommodated on one circuit board. The electronic control box together with the MBB limit value switch-off was mounted on an instrument carrier (Figure 27). The instrument carrier was constructed especially for accommodating the two instruments and achieving the installation weight prescribed by the aircraft manufacturer. A simple redundant switching logic was developed for the combination of the limit value cut-off and the emergency switch-off, installed in control panel 2 in the rear of the cockpit (Figure 28).

The following functional tests were performed, after the installation of the flutter suppression system, the switch-off devices, and the flutter stopper in the aircraft:

- checking the individual test programs which are possible with the electronic control and setting the aileron bias.

- checking the switch-off devices and adjusting the limit value cut-off.
- checking the operation of the flutter stopper.

During the function tests the test pilots also became acquainted with the flutter suppression system.

4. STRUCTURAL COUPLING TESTS

In contrast to the pure functional tests as described in previous paragraphs, the structural coupling test has special significance. The purpose of this test is to prove that the active suppression system is stable on the ground. Only after successful completion of this test was the control circuit of the active flutter suppression system closed.

For these tests, the air pressure in the tires was reduced to half the pressure in order to simulate the free-free aircraft not subject to the air forces. Two configurations were examined:

- Configuration 1 with critical external store.
- Configuration 2 with safe external store (flutter stopper released, trim weights in safe position).

The structure coupling test had to be conducted twice; once for the Weston Power actuator, with which the flight tests were begun and the second time after reequipping with the National Waterlift actuators. In order to gain information on the nonlinearities in the flutter suppression system, the tests were conducted with three different electrical input quantities, corresponding to three different amplitudes.

The structure coupling test was conducted in a frequency range of 2-25 Hz. At frequencies above 25 Hz, the actuator is too weak to excite the aircraft above the inertial force of the aileron. As a test signal, a sine wave was fed into the control electronics as an open loop circuit, as shown in the block diagram of Figure 16. The returning signal was set up as a ratio to the input signal and plotted for all frequencies as a Nyquist diagram. Figures 29 through 36 show the measured Nyquist diagrams for the critical external store configuration in each case for the three different input parameters Xi. Figures 37 through 40 show the

Nyquist diagrams for the safe external store configurations. The
critical point is situated at -1 for all Nyquist diagrams. Since none
of the curves passes to the left of the critical point with increasing
frequency, the system is stable on the ground both for the "critical"
and for the "safe" external store configuration. In the frequency range
under study, the amplitude boundary amounts to at least 6 dB. It was
only possible to attain these values, however, after the transfer function
of the control electronics was modified by an additional filter (Figure
41). This is presented in the Nichols diagrams (Figure 42) for the
cases with and without filters. The Nichols diagram for the wing
bending mode is shown on Figure 43. The ratio of output to input versus
the input signal for the flutter frequency was plotted in Figure 44 to
demonstrate the nonlinear behavior of the flutter suppression system.
At the same time, the corresponding phases for the generator signal are
given. This diagram (Figure 44) shows that in the area of very small
amplitudes a strongly nonlinear behavior may be expected, while the
nonlinear behavior is acceptable at normal amplitudes.

SECTION III

THEORETICAL RESULTS BASED ON TEST DATA

1. MODIFICATION OF THE ANALYTICAL PYLON PITCH STIFFNESS

The calculations for the wing alone (without external stores) with
MDC stiffness data (Reference 15) demonstrate good agreement with the
vibration test (References 12, 15). The main differences must therefore
stem from the pylon being incorrectly included in the calculations, the
weapon lock, or the nonlinearities in the pylon-external store com-
bination. The pylon bending stiffness in the pylon stiffness matrix
provided by MDC was varied to make the frequency and vibration mode of
the first four modes agree with the experimental results. The different
variations carried out for bending stiffness are compiled in Table 2.
The effect of this change in stiffness on the nodal position in the
external store pitching mode is shown in Figure 45. The best correlation
with the vibration tests was attained with an increase in bending
stiffness by a factor of 1.8. New vibration calculations were conducted
for the "safe" and "critical" external store configuration with the
mathematical model modified in this manner (Figures 46-54). The external
store pitching modes (Figures 48, 52) then agreed relatively well with
the modes measured in the experiment (Figures 3, 7).

2. FLUTTER TRENDS FOR DETERMINING FLUTTER CRITICAL CONFIGURATION

With the adjusted pylon bending stiffness, the calculated flutter
speed with LBFK external stores increased to more than 650 kts. Since
the demonstration of flutter suppression can only be carried out at flight
speeds of less than or equal 0.98 Mach because of flight limitations at
the flight test center in Manching, an attempt had to be made to find a
low flutter speed by changing the mass data of the LBFK external stores
to flutter at the desired speed of about 450-500 kts. Vibration
calculations with the LBFK external store configuration 1 M (1500 kg
mass and 1.45 radius of gyration) finally demonstrated a favorable nodal
position for the external store pitching mode (Figure 56), permitting
expectation of a low flutter speed. The yawing mode (Figure 54) thus
had a lower frequency than the wing bending (Figure 55), while there was

no great change for the external store roll mode (Figure 57). The
results of the trend study are compiled in Figures 19, 58, and 59. All
three diagrams explain the connection between flutter speed, mass of the
external store, and radius of gyration in different ways. All diagrams
show that a low flutter speed can only be achieved by increasing mass
and radius of gyration of the external store. Furthermore, the diagrams
show that the flutter speed can be increased significantly with constant
external store mass by reducing the radius of gyration from the
range ρ_y = 1.42 m.

In the original concept of the flutter stopper, it was assumed that
the flutter speed could be increased by expanding the radius of gyration.
It became necessary to restructure the flutter stopper on the basis of
these facts as presented in Section II.

Several other pertinent flutter calculations are provided in Figures
60 through 64, demonstrating that these are all "mild" cases of flutter
and are suitable for demonstrating a flutter suppression system. All
flutter calculations were made without structural damping.

3.   EFFECT OF CENTER OF GRAVITY ON FLUTTER SPEED

In addition to the variation in mass and radius of gyration of the
LBFK external store, the effect of the center of gravity of the external
store on flutter was also examined. Flutter calculations were conducted
for this purpose with a shift in center of gravity by ± 38 cm. In both
cases the shift in center of gravity resulted in higher flutter speed
(Figures 65, 66). The lowest flutter speeds were attained when the center
of gravity was situated between the suspension hooks, as in the study in
the previous paragraphs. These results are opposite to those values
provided by MDC in Reference 10.

4.   INFLUENCE OF STORE AERODYNAMICS AND MACH NUMBER ON FLUTTER

The unsteady air forces were calculated at Ma = 0.9 with both wing
theory and doublet lattice procedures (Reference 16). Both procedures
predicted approximately the same flutter speed. Unsteady aerodynamics
were calculated for external stores using slender body theory and were

included in the flutter calculations. As expected, this led to a negligible change in the flutter speed (Figure 67).

Flutter calculations were performed to study the effect of Mach number (Figure 68). A comparison of Figure 60 with Figure 68 shows a slight reduction in flutter speed at Ma = 0.95 compared to Ma = 0.9.

5.   CALCULATION OF THE FLUTTER SUPPRESSION CONTROL LAW
      BASED ON TEST DATA

The control law for active flutter suppression was altered based on the updated mathematical structural model. Figures 69 and 70 contain calculated Nyquist diagrams for the updated control law to be tested in the flight trials. In the desired speed range, a calculated increase in flutter speed of about 100 kts was achieved (Figure 71). Another optimization of the control law was carried out (Control Law 1112) after the completion of the initial flight tests. In this calculation, the transfer function of the actuators under air loads and the optimal sensor locations ascertained in the experiment were taken into consideration.

Figure 72 shows the flutter calcuation and Figures 73 and 74 show the Nyquist diagrams with this control law. As can be seen from the flutter calculation, Control Law 1112 is even more effective than that studied in the flight trials. It was possible to increase the calculated flutter speed by another 40 kts.

SECTION IV

INITIAL FLIGHT TESTS

1. FLIGHT TEST PROGRAM

The flight program for testing the active flutter suppression system involved a three step approach:

- Flight tests to determine the flutter point of the "critical" and "safe" external store configuration

- Open loop measurements for checking the phase positions of the suppression system and for optimizing the location of the sensors

- Flight tests with closed loop control in the subcritical and supercritical flight range

In the course of the flight tests, however, the program had to be expanded to study the effects of nonlinearities in the wing-pylon-external store combination on the flutter speed. This nonlinear problem will be examined more closely in Subsection 3.

Another important point for conducting the flight tests was the definition of the test area and the flight course. Since the expected flutter speeds were accompanied by relatively high dynamic pressures, the flights had to be conducted at low altitudes. In addition, a fault-less telemetry reception had to be ensured. The flights had to be con-ducted over the least populated area possible. The test area and flight course drawn in Figure 75 was chosen for the flight tests in cooperation with the telemetry experts at the test center.

It was difficult to obtain a flight permit for the F-4F with active flutter suppression system and the safety equipment, since no comparable active systems had been permitted in West Germany. Even the MIL specifications normally employed for flight permits of military aircraft

had no provisions for qualifications of active flutter suppression systems. Three steps were undertaken to obtain the flight permit:

- The control electronics and switching logic for the switch-off devices were subjected to the following qualification tests:
  - vibration
  - temperature
  - electromagnetic compatibility
  - high voltage spikes

  It had to be proven that the flutter stopper and the switch-off devices of the suppression system function faultlessly both in ground tests and in flight tests.

- The permit for the entire system was granted on the basis of the safety concept developed by MBB in agreement with the other partners of the program and on the basis of the qualifcation of the indivdual components of the active flutter suppression system.

Twenty test flights were conducted with the F-4F, W. No. 1126, from March 21 to August 14, 1979 within the framework of the joint F-4F flutter suppression program. The flight tests were conducted by E-61 Flight Test Center in Manching.

The flight tests were conducted with the modified LBFK dummies. The mass data, especially the radius of gyration, were increased in order to obtain the lowest possible flutter speed. It was possible to alter the radius of gyration during the flight by shifting the trim weights in the flutter stopper (Section II). The external stores were suspended on the outer pylon station (13.250) with the load lock MAU-12 C/A. The mass data for the configuration critical to flutter and the safe configuration can be seen in Figure 25. Since the wing-pylon-external store combination is a very nonlinear system, the tightening torque of the mounting elements from the pylon to the wing and pylon to external store must be known precisely as reference quantities. The individual tightening torques during the flight tests are compiled on Figure 76.

The first through the sixth flights were conducted with Weston Power High Gain aileron actuators. From the seventh flight on, the aircraft

was equipped with National Waterlift High Gain aileron actuators. Table 3 presents a list of the flight and configuration data.

An extensive measurement program was carried out in 18 flights with external stores. One-hundred-forty test points were included in the flights with the eight test programs built into the suppression system (Table 4). The following specific studies were conducted:

- Determination of damping and frequency as a function of speed for the critical external store configuration.

- Determination of the damping and frequency as a function of speed with disengaged flutter stopper.

- Study of the effect of nonlinearities of the wing-pylon-external store combination on the flutter speed.

- Flights with high dynamic pressures for more precise determination of the flutter point.

- Determination of optimal sensor combinations for the suppression system.

- Measurements with open loop and closed loop control circuits during the flights.

- Tests for finding the optimal phase positions for the suppression systems.

- Tests with an unstable damping system for automatic generation of vibration modes.

- Tests for determining the effectiveness of the suppression system in the subcritical velocity range.

It was not possible to demonstrate the effectiveness of the suppression system in the supercritical range because of flight speed limitations at the flight test center in Manching.

2. FLIGHT TEST RESULTS

Stability as a function of flight speed was determined for both external store configurations with the standard methods of flight testing. A frequency sweep (frequency range of 4-16 Hz, rise time of 30 sec/octave) was employed for exciting the individual vibration modes via the aileron. Stability was determined by means of filter correlation methods with an HP 5451 B Fourier analyzer. Figure 77 shows the damping trend and Figure 78 shows the frequency versus airspeed for the critical external store configuration. It can be seen from both diagrams that stability is zero at 600 KIAS; i.e., the flutter point is reached. However, flutter begins at higher speeds than expected on the basis of the nonlinearities in the wing-pylon-external store combination. This problem is examined more closely in the next paragraph. Figures 79 and 80 show damping and frequency trends for the flutter stopper. A comparison of Figure 79 with 77 shows that the flutter stopper is very effective. When the damping is extrapolated in Figure 79, the flutter point is around 750 KIAS for the flutter stopper (compare also Figure 58). There is good agreement with the calculations.

a. Effect of Nonlinearities in the Wing-Pylon-Store Combination on Flutter Speed

In the evaluation of frequency variation of the external store roll mode, a jump in frequency was discovered, as can be seen in Figure 81, leading to the conclusion of reduced roll stiffness of the external store or the pylon. A computation with reduced roll stiffness showed that this effect drastically increases flutter speed, so that it is above the flight range. In order to reduce these effects of nonlinearity, the tightening torque on the swaybrace, the adjustment screw, and the attachment bolt (Figure 76, Configuration A) was first increased to Configuration B. After a flight with the torques given in Configuration B for the swaybrace, it was discovered that the load lock was displaced. For this reason, all further flight tests were conducted with the torques of Configuration C. Increasing the torque of the adjustment screw, however, was not sufficient for the heavier external stores to avoid the

frequency jump in the external store mode at the high excitation levels. Therefore, either the tightening torque had to be further increased or the excitation forces (amplitude) had to be reduced. Since an increase in tightening torque was not permissible for structural reasons, the excitation forces were reduced to 25% or 17% of the maximum level. As can be seen in Figure 82, the frequency for the external store roll mode remains constant for all measured speeds with the reduced excitation forces. The effects of nonlinearity on the external store pitch mode and the wing bending mode were also examined. As can be seen from the compilation in Figure 83, the effect remains within the framework of measuring accuracy with the low excitation force. The elastic system may therefore be considered linear for small excitation forces or amplitudes. This also confirms the damping trend (Figure 84) of the critical external store configuration found with small excitation forces at high dynamic pressures, compared to small excitation calculated results.

b. Optimizing Sensor Locations

Figure 85 shows the location of the sensors and pick-ups for this program. In order to achieve a more precise experimental determination of the flutter point (shifted to higher speeds by the nonlinearities), two flights at less than Mach 1 but with high dynamic pressures were carried out at V_{max} = 610 KIAS. The time response record in Figures 86 through 90 show that the external stores vibrate harmonically at V = 600 KIAS (Figure 87). At V = 580 KIAS (Figure 86), however, the external store vibration is not yet harmonic. Especially when Figure 86 is compared With Figure 90, it can be seen that the amplitude of the harmonic vibration becomes larger with increasing speed.

The control law optimized for the flutter suppression system refers to the generalized coordinates as state variables (Reference 9). In order to employ the control law in the suppression system, the coefficients of the control law must therefore be converted with a transformation matrix to the individual sensor combinations, measuring the quantities corresponding to the generalized coordinates. The coefficients converted for three different sensor combinations I - III are compiled

17

in Table 5. Figures 91 through 93 show the geometrical position of the
sensor combinations in the wing and the control law. In order to
evaluate the individual sensor combinations, all representing the same
control law, the Nyquist diagrams at V = 520 or V = 500 KIAS of the sup-
pression system were compared with the three different sensor combinations
in Figure 94 (critical point in the Nyquist diagram is -1). It must
also be noted on the Nyquist diagram with the sensor combination III,
that the entire phase was rotated by 80° (counter clockwise).

The comparison shows that the sensor combination III is the
most favorable, since it essentially accommodates only the external store
modes and suppresses the outer wing mode at about 11 Hz. The sensor
location, FBL(R)4, had to be subsequently altered because of disturbing
aerodynamic effects, as can be seen in Figure 93.

c. Open Loop Tests

Very extensive open loop measurements were made in flight and
the results were plotted as Nyquist diagrams (critical point -1) with
the aim of checking the calculations (stability and phase position) and
for correcting the phase experimentally. This procedure is necessary,
since phase shifts occurring because of Mach number effects and non-
linearities in the actuator which were not accounted for in the analysis.

A review of the results, (Figures 95 through 98) indicates that:

- It was possible to identify the flutter modes clearly with
  the chosen sensor combinations. (Amplification of the
  external store pitch mode at high speeds, Figure 96).

- The entire phase position was not yet optimal for all three
  sensor combinations. A rotation of the entire phase of about
  90° counter clockwise was still required, because the control
  law was calculated using an actuator transfer function
  exhibiting a lag of about 80° instead of the 140° measured.

- The entire amplification was in the correct range, but it
  also had be optimized.

- The symmetry was good between the left and right wings, as
can be seen in the Figures 96, 97, and 98.

d. Tests with Unstable System for Automatic Excitation

One point of the flight test program was to test the procedure
developed by MBB for automatic mode excitation which can be used to
introduce an artificial flutter. This provides a determination of the
suppression capability in the flight vibration experiments with an
unstable system exciting one wing while the other wing is suppressing
this flutter. The calculations in Figures 99 through 102 show that an
automatic generation of the external store pitching mode should be pos-
sible with the unstable suppression system. At one point in the flight
test, the outer wing mode was excited at 11 Hz and at another point the
wing bending mode was excited at 5.2 Hz (Figure 103). It was not pos-
sible, however, to generate the external store pitching mode. The cause
can be easily seen in comparisons of the Nyquist diagrams in Figure 94.
The 11 Hz mode was generated when the suppression mode was tested with
sensor combination I. The 5.2 Hz mode was generated with sensor com-
bination III. In both cases the phase position was unfavorable for
generating the external store pitch mode (5.7 Hz). The experiments showed
that automatic generation of an unstable mode is possible with correct
phase position.

e. Effectiveness of the Flutter Suppression System in the
Subcritical Flight Range

In order to estimate the effectiveness of the suppression system
in the subcritical flight range, flight tests were carried out by means
of test programs 2 and 3 of Table 4. One system functioned as a sup-
pressor in these programs, while the other was generating a frequency
sweep via the aileron. This is presented in detail in the time responses
(Figures 104 through 109). Since it was not possible to conduct a flight
test with one-sided aileron excitation to which a reduction in amplitude
could be precisely related, it was assumed that at least 60% of the
generator energy reached the aircraft side on which the aileron functions
as a suppressor (estimations are based on structure coupling tests).
With this assumption, a reduction of the vibration amplitudes at the

external store tips (ZAL/ZAR) of 6dB and 8dB is achieved. The most
effective reduction is in the area of wing bending on the basis of the
not yet optimal phase position; however, the external store pitching
mode is also suppressed.

SECTION VI

CONCLUSIONS

A flutter suppression system was designed for the F-4F aircraft with external stores (Reference 9). The existing control surfaces (ailerons) were used as the active control surfaces. Accelerometers located on the wing provided signals which were compensated and fed back through the existing stability augmentation system.

During the ground vibration test, it was found that the dynamic behavior of the wing-pylon-store was different than that predicted. The analytical pylon pitch stiffness was modified to improve the agreement between analysis and test and the theoretical results were recomputed.

The flight test program was divided into three major sections: 1) classical flight flutter tests to find the passive flutter speed for both the critical and safe configurations, 2) open loop tests for substantiation and optimization of the analytically defined control law, and 3) closed loop tests to demonstrate flutter and mode suppression. The classical flight flutter tests indicated a limited amplitude flutter at 600 knots. Part III of this report documents the final flight test demonstration of the active flutter suppression system at supercritical speeds (i.e. above the passive flutter speed).

REFERENCES

1. G. Haidl, A. Lotze, O. Sensburg, "Active Flutter Suppression on Wings with External Stores," AGARDograph No. 175, July 1975.

2. O. Sensburg, H. Hönlinger, M. Kuhn, "Active Control of Empennage Flutter," AGARD-SMP Brussels, 13-18 April 1975.

3. H. Hönlinger, O.Sensburg, "Dynamic Simulation in Wind Tunnels," AGARD Conference Proceedings, No. 187.

4. G. Oesterheld, W. Kubbat, "Entwurf von Regelungssystemen mit Hilfe von Computer Aided Design and ihre Anwedung," MBB-Report GD 8-74.

5. H. Hönlinger, O. Sensburg, M. Kuhn, "Definition of the German Flutter Suppression Control Law for the YF-17 International Wind Tunnel Program," Paper presented at the 51st SMP of AGARD, Athens 13-18 April 1980.

6. O. Sensburg, J. Becker, H. Hönlinger, "Active Control of Flutter and Vibration of an Aircraft," IUTAM Symposium, Waterloo/Canada June 4-7, 1979, MBB-Report No. S/PUB/8.

7. J. Becker, W. Schmidts, "TKF-Boenbelastung," International MBB-Report TKF.

8. H. Hönlinger and A. Lotze, "Active Flutter Suppression of Aircraft Flutter," 11th ICAS-Congress, Lisbon/Portugal, 10-16 Sept. 1978.

9. H. Hönlinger, D. Mussman, R. Manser, and L. Huttsell, "Development and Flight Test of an Active Flutter Suppression System for the F-4F with Stores, Part I, Design of the Active Flutter Suppression System", AFWAL-TR-82-3040, Part I, September 1982.

10. H.R. Gongloff and J.W. Walker, "Model F-4E (Slat) Aircraft Wing Flutter Analysis with External Stores", MDC Report A 2560, November 30, 1973.

11. J.W. Walker and C.J. Moore, "Model F-4E (Slat) Thick Wing Flutter Analysis With and Without External Stores", MDC Report A 2770, June 15, 1974.

12. W. Gatter, "F-4F Flatterdämpfungsprogramm - Standschwingungsversuch am Flugzeug F-4F mit Flatter LBFK", MBB-Bericht UF1472, 1977.

13. R. Freymann and H. Giese, "Experimentell-rechnerische Ermittlung der dynamischen Obertragungsfunktionen des in einer F-4F Phantom zur Flatterunterdrucküng eigesetzten Querruderaktuators", DFVLR-interner Bericht Nr. IB 253-78 J 05, 1978.

REFERENCES (Concluded)

14. H. Hönlinger, "Versuche zur Flatterunterdruckung and Schwingungsdampfung mittels Querrunder an einer F-4F mit Außenlasten", MBB-Bericht UF1391, 1977.

15. G. Schneider, "Flatteruntersuchungen am Flugel der MDC-F-4F mit LBFK-Tragflugkorpern am außeren Flugelpylon", MBB-Bericht Nr. UFE 1280, Sept 1976.

16. H. Hönlinger, "F-4F Flutter Suppression Program - Flutter Analysis of F-4F with LBFK Stores Using an Adjusted Structural Model (Derived from Ground Resonance Tests)", MBB-Bericht UF 1473, 1978.

TABLE 1

MASS DATA FOR THE STORE CONFIGURATIONS

LBFK STORE CONFIGURATION	CALCULATION		GROUND VIBRATION TEST	
	MASS [kg]	RADIUS OF GYRATION ρ_y [m]	MASS [kg]	RADIUS OF GYRATION ρ_y [m]
1 CRITICAL	1500	1.28	1525	1.29
2 SAFE	1500	1.34	1525	1.36
MODIFIED STORE MASS DATA				
1M CRITICAL	1500	1.45		
2M SAFE	1500	1.39		

TABLE 2

VARIATIONS OF THE STORE PITCH STIFFNESS TO MATCH THE MATHEMATICAL MODEL

LBFK 15 CRITICAL	TEST	VARIATIONS OF THE PYLON PITCH STIFFNESS TO MATCH THE MATHEMATICAL MODEL				
MODE	FREQ. (HZ)	MDC DATA x 1.0	PYLON PITCH x 1.4	PYLON PITCH RIGID	x 1.4 FL x1.1	PYLON PITCH x 1.8
WING BENDING	5.63	5.33	5.43	5.52	5.43	5.46
STORE YAW	5.93	5.70	5.70	5.70	5.70	5.70
STORE PITCH	6.67	5.97	6.29	7.28	6.29	6.52
STORE ROLL	8.54	8.31	8.40	9.44	8.40	8.48
LBFK 1M (SAFE CONFIGURATION)						
WING BENDING	5.54	5.22				5.41
STORE YAW	5.62	5.46				5.47
STORE PITCH	6.48	5.97				6.36
STORE ROLL	8.53	8.30				8.45

TABLE 3
MEASURED TEST POINTS

| FLIGHT | FLIGHT DATA | | | CONFIGURATION | | | | FLIGHT TESTS | |
	ALT.[ft]	SPEED [KIAS]	Ma-NO.	STORE	ACTUAT.	SENSOR COMP.	PYLON T.MOM.	TEST PROGR.	REMARKS
175/1	6,000 - 10,000	300-500		clear	W.P. W.G.	I	A	1(50)	Freq. sweep 2.8-11.2 [Hz]
175/2	-"-	-"-		-"-	-"-	-"-	-"-	1(50)	
177/3	15,000	300	0.59	critical	-"-	-"-	-"-	1(100)	
-"-	-"-	350	0.69	-"-	-"-	-"-	-"-	-"-	
-"-	-"-	375	0.73	-"-	-"-	-"-	-"-	-"-	
-"-	-"-	400	0.78	-"-	-"-	-"-	-"-	-"-	
178/4	8,000	380	0.66	-"-	-"-	-"-	-"-	-"-	
-"-	-"-	400	0.69	-"-	-"-	-"-	-"-	-"-	
-"-	-"-	425	0.73	-"-	-"-	-"-	-"-	-"-	
-"-	-"-	450	0.78	-"-	-"-	-"-	-"-	-"-	
-"-	-"-	475	0.82	-"-	-"-	-"-	-"-	-"-	
-"-	-"-	500	0.86	-"-	-"-	-"-	-"-	-"-	
179/5	11,000	450	0.85	-"-	-"-	-"-	-"-	-"-	
-"-	-"-	475	0.90	-"-	-"-	-"-	-"-	-"-	
-"-	6,000	475	0.79	-"-	-"-	-"-	-"-	-"-	
-"-	-"-	500	0.83	-"-	-"-	-"-	-"-	-"-	
-"-	-"-	510	0.85	-"-	-"-	-"-	-"-	-"-	
-"-	-"-	300	0.51	safe	-"-	-"-	-"-	-"-	
-"-	-"-	350	0.58	-"-	-"-	-"-	-"-	-"-	
-"-	-"-	400	0.67	-"-	-"-	-"-	-"-	-"-	

TABLE 3 (Cont'd)

FLIGHT	FLIGHT DATA			CONFIGURATION				FLIGHT TESTS	
	ALT.[ft]	SPEED [KIAS]	Ma-No.	STORE	ACTUAT.	SENSOR COMB.	PYLON T.MGM.	TEST PROGR.	REMARKS
179/5	6,000	425	0.71	safe	W.P.HG.	i	A	1(100)	Freq. Sweep 2.2-11.2[Hz]
-"-	-"-	450	0.75	-"-	-"-	-"-	-"-	-"-	
-"-	-"-	475	0.79	-"-	-"-	-"-	-"-	-"-	
-"-	-"-	500	0.83	-"-	-"-	-"-	-"-	-"-	
181/7	7,000	400	0.69	critical	N.W.H.G.	-"-	-"-	-"-	Freq. Sweep 4-11.2[Hz]
-"-	-"-	450	0.76	-"-	-"-	-"-	-"-	-"-	
-"-	-"-	500	0.85	-"-	-"-	-"-	-"-	-"-	
-"-	-"-	400	0.68	safe	-"-	-"-	-"-	-"-	
-"-	-"-	450	0.76	-"-	-"-	-"-	-"-	-"-	
-"-	-"-	500	0.85	-"-	-"-	-"-	-"-	-"-	
-"-	-"-	520	0.88	-"-	-"-	-"-	-"-	-"-	
-"-	-"-	540	0.91	-"-	-"-	-"-	-"-	-"-	
182/8	7,000	500	0.85	critical	-"-	-"-	-"-	1(70%)	
-"-	-"-	500	0.85	-"-	-"-	-"-	-"-	1(100%)	
-"-	-"-	520	0.88	-"-	-"-	-"-	-"-	1(100)	
-"-	-"-	540	0.91	safe	-"-	-"-	-"-	1(100)	
-"-	-"-	550	0.92	-"-	-"-	-"-	-"-	1(100)	
-"-	-"-	560	0.93	-"-	-"-	-"-	-"-	1(100%)	
183/9	7,000	520	0.87	critical	-"-	-"-	-"-	1(70%)	
-"-	-"-	520	0.87	-"-	-"-	-"-	-"-	1(100%)	

TABLE 3 (Cont'd)

	FLIGHT DATA				CONFIGURATION				FLIGHT TESTS	
FLIGHT	ALT.[ft]	SPEED [KIAS]	Ma-NO.	STORE	ACTUAT.	SENSOR COMB.	PYLON T.MOM.	TEST PROGR.	REMARKS	
1.30	7,000	540	0.91	critical	N.W.F.G.	I	A	1(100)	Freq. Sweep 4-11.2[Hz]	
-"-	-"-	550	0.9	-"-	-"-	-"-	-"-	1(100)		
-"-	-"-	550	0.92	-"-	-"-	-"-	-"-	1(70)		
-"-	-"-	560	0.94	-"-	-"-	-"-	-"-	1(70)		
-"-	-"-	560	0.94	-"-	-"-	-"-	-"-	1(100)		
-"-	-"-	400	0.69	-"-	-"-	-"-	-"-	1(100)	Slats extended	
-"-	-"-	450	0.76	-"-	-"-	-"-	-"-	1(100)	-"-	
-"-	-"-	500	0.85	-"-	-"-	-"-	-"-	1(100)	-"-	
-"-	-"-	530	0.90	-"-	-"-	-"-	-"-	1(100)	-"-	
1.31/10	3,000	400	0.69	-"-	-"-	-"-	-"-	1(25)		
-"-	-"-	400	0.69	-"-	-"-	-"-	-"-	1(50)		
-"-	-"-	400	0.69	-"-	-"-	-"-	-"-	4		
-"-	-"-	450	0.77	-"-	-"-	-"-	-"-	1(25)	Freq. Sweep 4-11.2[Hz]	
-"-	-"-	450	0.77	-"-	-"-	-"-	-"-	1(50)	-"-	
-"-	-"-	450	0.77	-"-	-"-	-"-	-"-	4		
-"-	-"-	500	0.86	-"-	-"-	-"-	-"-	1(25)	Freq. Sweep 4-11.2[Hz]	
-"-	-"-	500	0.86	-"-	-"-	-"-	-"-	1(50)	-"-	
-"-	-"-	500	0.86	-"-	-"-	-"-	-"-	3	-"-	
-"-	-"-	500	0.86	-"-	-"-	-"-	-"-	4	-"-	
-"-	-"-	500	0.86	-"-	-"-	-"-	-"-	2	Freq. Sweep 4-11.2[Hz]	

TABLE 3 (Cont'd)

	FLIGHT DATA			CONFIGURATION				FLIGHT TESTS	
FLIGHT	ALT.[ft]	SPEED [KIAS]	Ma-NC.	STORE	ACTUAT.	SENSOR COMB.	PYLON T.MOM.	TEST PROGR.	REMARKS
184/10	8,000	500	0.86	critical	N.W.H.G.	I	A	3	Freq. Sweep 4-11.2[Hz]
-"-	-"-	520	0.89	-"-	-"-	-"-	-"-	1(25")	-"-
-"-	-"-	500	0.86	-"-	-"-	-"-	-"-	4	
-"-	-"-	510	0.87	-"-	-"-	-"-	-"-	4	
-"-	-"-	540	0.93	-"-	-"-	-"-	-"-	4	
185/11	10,000	450	0.84	-"-	-"-	-"-	B	1(25")	Freq. Sweep 4-16[Hz]
-"-	-"-	450	0.84	-"-	-"-	-"-	-"-	1(12")	
-"-	-"-	500	0.90	-"-	-"-	-"-	-"-	1(25")	
-"-	10,500	500	0.90	-"-	-"-	-"-	-"-	1(17)	
-"-	10,300	520	0.92	-"-	-"-	-"-	-"-	1(17")	
-"-	-"-	520	0.92	-"-	-"-	-"-	-"-	1(25")	
-"-	10,700	520	0.92	-"-	-"-	-"-	-"-	1(12")	
-"-	9,300	550	0.96	-"-	-"-	-"-	-"-	1(12")	
-"-	-"-	550	0.96	-"-	-"-	-"-	-"-	1(17")	
-"-	9,500	450	0.85	-"-	-"-	-"-	-"-	1(17")	Slats extended
187/13	5,900	450	0.75	-"-	-"-	II	-"-	1(17")	
-"-	-"-	450	0.75	-"-	-"-	-"-	-"-	1(25")	
-"-	-"-	450	0.75	-"-	-"-	-"-	-"-	1(50")	
-"-	-"-	500	0.83	-"-	-"-	-"-	-"-	1(17")	
-"-	-"-	500	0.83	-"-	-"-	-"-	-"-	1(25")	

TABLE 3 (Cont'd)

FLIGHT	FLIGHT DATA			CONFIGURATION				FLIGHT TESTS	
FLT.No.	ALT.[ft]	SPEED [KIAS]	Ma-No.	STORE	ACTUAT.	SENSOR COMB.	PYLON T.MOM.	TEST PROGR.	REMARKS
	5,900	500	0.??	mit Ball	-"-	II	B	1/?9	Freq. Sweep 4-16[Hz]
-"-	-"-	520	0.86	-"-	-"-	-"-	-"-	1/17	
-"-	-"-	520	0.?	-"-	-"-	-"-	-"-	1/2?	
-"-	-"-	520	0.8?	-"-	-"-	-"-	-"-	1/??	
-"-	-"-	450	0.??	-"-	-"-	-"-	-"-	1/??	
-"-	-"-	450	0.74	-"-	-"-	-"-	-"-	1/17	
-"-	-"-	520	0.??	-"-	-"-	-"-	-"-	1/17	
-"-	-"-	5?0	0.9?	-"-	-"-	-"-	-"-	1/25	
-"-	-"-	540	0.9?	-"-	-"-	-"-	-"-	1/17	
	12,000	450	0.86	-"-	-"-	-"-	C	1/17	
-"-	-"-	500	0.94	-"-	-"-	-"-	-"-	1/17	
-"-	12,000	520	0.94	-"-	-"-	-"-	-"-	1/17	
-"-	12,10?	520	0.94	-"-	-"-	-"-	-"-	1/25	
-"-	12,400	450	0.??	-"-	-"-	-"-	-"-	1/17	
-"-	12,000	500	0.90	-"-	-"-	-"-	-"-	1/17	Slats extended
-"-	12,500	520	0.95	-"-	-"-	-"-	-"-	1/17	-"-
-"-	13,000	520	0.97	-"-	-"-	-"-	-"-	1/25	-"-
189/15	8,650	500	0.87	-"-	-"-	-"-	-"-	1/17	-"-
-"-	8,220	520	0.90	-"-	-"-	-"-	-"-	1/17	
-"-	7,800	540	0.92	-"-	-"-	-"-	-"-	1/12	

TABLE 3 (Cont'd)

	FLIGHT DATA			CONFIGURATION				FLIGHT TESTS	
FLIGHT	ALT.[ft]	SPEED [KIAS]	Ma-NO.	STORE	ACTUAT.	SENSOR COMB.	PYLON T.MOM.	TEST PROGR.	REMARKS
189/15	7,650	540	0.92	critical	H.W.H.G.	II	C	1(25)	Freq. Sweep 4-16[Hz]
-"-	7,400	540	0.92	-"-	-"-	-"-	-"-	1(17)	-"-
-"-	3,550	540	0.92	safe	-"-	-"-	-"-	-	without system
-"-	-"-	560	0.94	-"-	-"-	-"-	-"-	-	-"-
-"-	-"-	450	0.78	-"-	-"-	-"-	-"-	-	-"-
-"-	3,200	540	0.92	-"-	-"-	-"-	-"-	-	-"-
190/16	5,900	540	0.99	critical	-"-	-"-	-"-	1(12)	Freq. Sweep 4-16[Hz]
-"-	-"-	560	0.91	-"-	-"-	-"-	-"-	1(12)	
-"-	-"-	560	0.91	-"-	-"-	-"-	-"-	1(17)	
-"-	-"-	540	0.89	safe	-"-	-"-	-"-	1(17)	
-"-	5,400	560	0.91	-"-	-"-	-"-	-"-	1(17)	
-"-	5,300	580	0.94	-"-	-"-	-"-	-"-	1(17)	
-"-	4,100	600	0.96	-"-	-"-	-"-	-"-	1(17)	
-"-	5,400	580	0.94	-"-	-"-	-"-	-"-	1(25)	
191/17	5,300	540	0.88	critical	-"-	-"-	-"-	1(17)	
-"-	4,800	580	0.94	-"-	-"-	-"-	-"-	1(12)	
-"-	-"-	580	0.94	-"-	-"-	-"-	-"-	1(17)	
-"-	3,800	600	0.94	-"-	-"-	-"-	-"-	1(12)	
-"-	-"-	600	0.95	-"-	-"-	-"-	-"-	1(17)	
-"-	3,500	610	0.98	-"-	-"-	-"-	-"-	1(17)	

TABLE 3 (Cont'd)

FLIGHT	FLIGHT DATA			CONFIGURATION					FLIGHT TESTS		
FLIGHT	ALT.[ft]	SPEED [KIAS]	Ma-No.	St. I	A-Drag	SENSOR COMB.	PYLON T.MOM.		TEST PROGR.	REMARKS	
193/1	1,000	530	0.78			II				side slipping	
- " -	- " -	600	0.8			- " -	- " -		-	- " -	
- " -	3,000	610	0.9			- " -	- " -		-	- " -	
- " -	2,200	610	0.9			- " -	- " -			- " -	
193/10	5,000	650	0.83			III	- " -			seen 4-16[Hz], phase changed	
- " -	5,400	650	0.85			- " -	- " -				
- " -	5,600	600	0.8			- " -	- " -				
- " -	6,250	460	0.7			- " -	- " -				
- " -	5,700	630	0.8			- " -	- " -				
- " -	5,900	580	0.78			- " -	- " -		1 ( )	Fr.Sw. 4-16[Hz], 57.60 changed	
- " -	5,900	450	0.75			- " -	- " -				
- " -	5,250	450	0.75			- " -	- " -		2(50)	Fr.Sw. 4-16[Hz] phase changed	
- " -	5,250	450	0.75			- " -	- " -		3(100)		
- " -	5,700	450	0.75			- " -	- " -		2(100)		
193/20	6,750	450	0.7			- " -	- " -		1(17)		
- " -	- " -	450	0.7			- " -	- " -		-	Pitch/Roll	
- " -	7,000	500	0.83			- " -	- " -		1(17)	Fr.Sw. 4-16[Hz] phase changed	
- " -	- " -	500	0.8			- " -	- " -		4	Pitch/Roll	
- " -	- " -	550	0.91			- " -	- " -		4	- " -	
- " -	- " -	550	0.91			- " -	- " -		1(17)	Fr.Sw. 4-16[Hz] phase changed	

31

TABLE 3 (Cont'd)

	FLIGHT DATA			CONFIGURATION				FLIGHT TESTS	
FLIGHT	ALT.[ft]	SPEED [KIAS]	Ma-No.	STORE	ACTUAT.	SENSOR COMB.	PYLON T.MOM.	TEST PROGR.	REMARKS
194/20	6,600	550	0.91	critical	W.W.H.G.	III	C	1(50)	Fr.Sw. 4-16[Hz], phase changed
-"-	-"-	550	0.91	-"-	-"-	-"-	-"-	8	
-"-	-"-	550	0.91	-"-	-"-	-"-	-"-	8	Roll
-"-	5,950	550	0.91	-"-	-"-	-"-	-"-	7(50%)	Freq. Sw. 4-16[Hz], phase changed
-"-	-"-	550	0.91	-"-	-"-	-"-	-"-	7(50)	
-"-	-"-	450	0.75	-"-	-"-	-"-	-"-	2(50)	

TABLE 1

TEST PROGRAMS OF THE FLUTTER SUPPRESSION SYSTEM

TEST PROGRAMM/TEST PROGRAM		AKTION/FUNCTION	
	BO.X GROUND VIBR.		BO. FLIGHT/ALTIT. WING
	GESCHL. KREIS M. GLEIT... OPEN LOOP W. FREQ...		GESCHL. KREIS M. GLEIT... OPEN LOOP W. FREQ...
	DÄMPFUNG/DAMPING		DÄMPFUNG/DAMPING
	GLEITFREQU./FREQUENCY SWEEP		GLEITFREQU./FREQUENCY SWEEP
	AUTOMATISCHE ERREGUNG AUTOMATIC EXCITATION		AUTOMATISCHE ERREGUNG AUTOMATIC EXCITATION
	DÄMPFUNG/DAMPING		AUTOMATISCHE ERREGUNG AUTOMATIC EXCITATION
	AUTOMATISCHE ERREGUNG AUTOMATIC EXCITATION		DÄMPFUNG/DAMPING
	GESCHL. KREIS M. GLEITFREQUENZ CLOSED LOOP W. FREQU. SWEEP		GESCHL. KREIS M. GLEITFREQUENZ CLOSED LOOP W. FREQU. SWEEP
	DÄMPFUNG/DAMPING		DÄMPFUNG/DAMPING

TABLE 5

COEFFICIENTS OF THE CONTROL LAW FOR VARIOUS SENSOR COMBINATIONS

SENSOR COMBINATION			CONTROL LAW			
			$K\varphi$	$K\gamma$	$K\dot{\varphi}$	$K\dot{\theta}$
$\varphi \cdot \dfrac{②-③}{L_1}$ $\dfrac{③-④}{L_2}$	I II		0.41571	0.44105	-0.3195×10^{-1}	-0.4637×10^{-1}
$\varphi \dfrac{③+④}{L_2}$ $\dfrac{③-④}{L_2}$	III		0.1484	0.2148	-0.11403×10^{-1}	-0.2898×10^{-1}
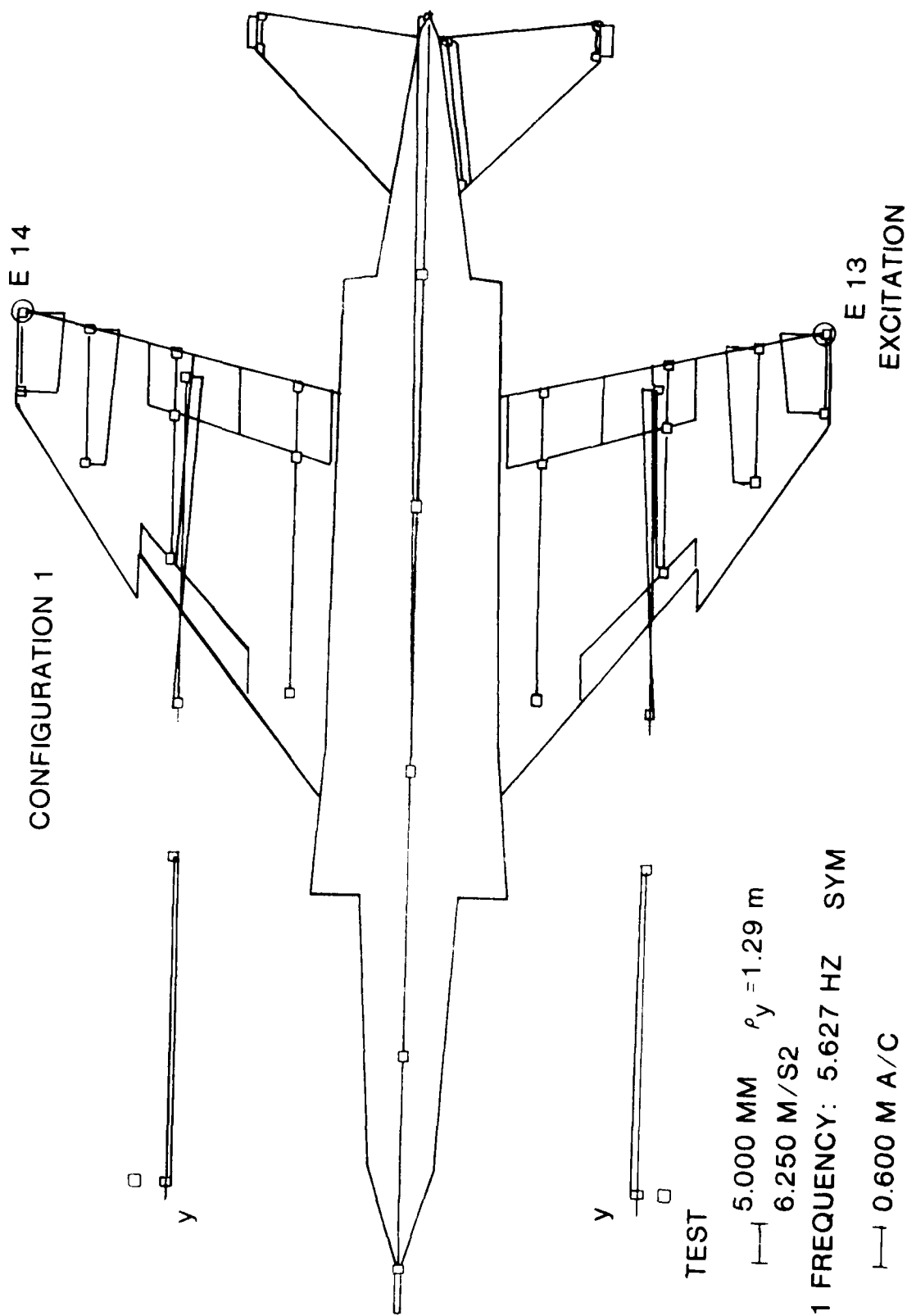
Figure 1. GVT, 1st Wing Bending, Configuration 1

CONFIGURATION 1

E8   94 N

y

E9   67 N

y
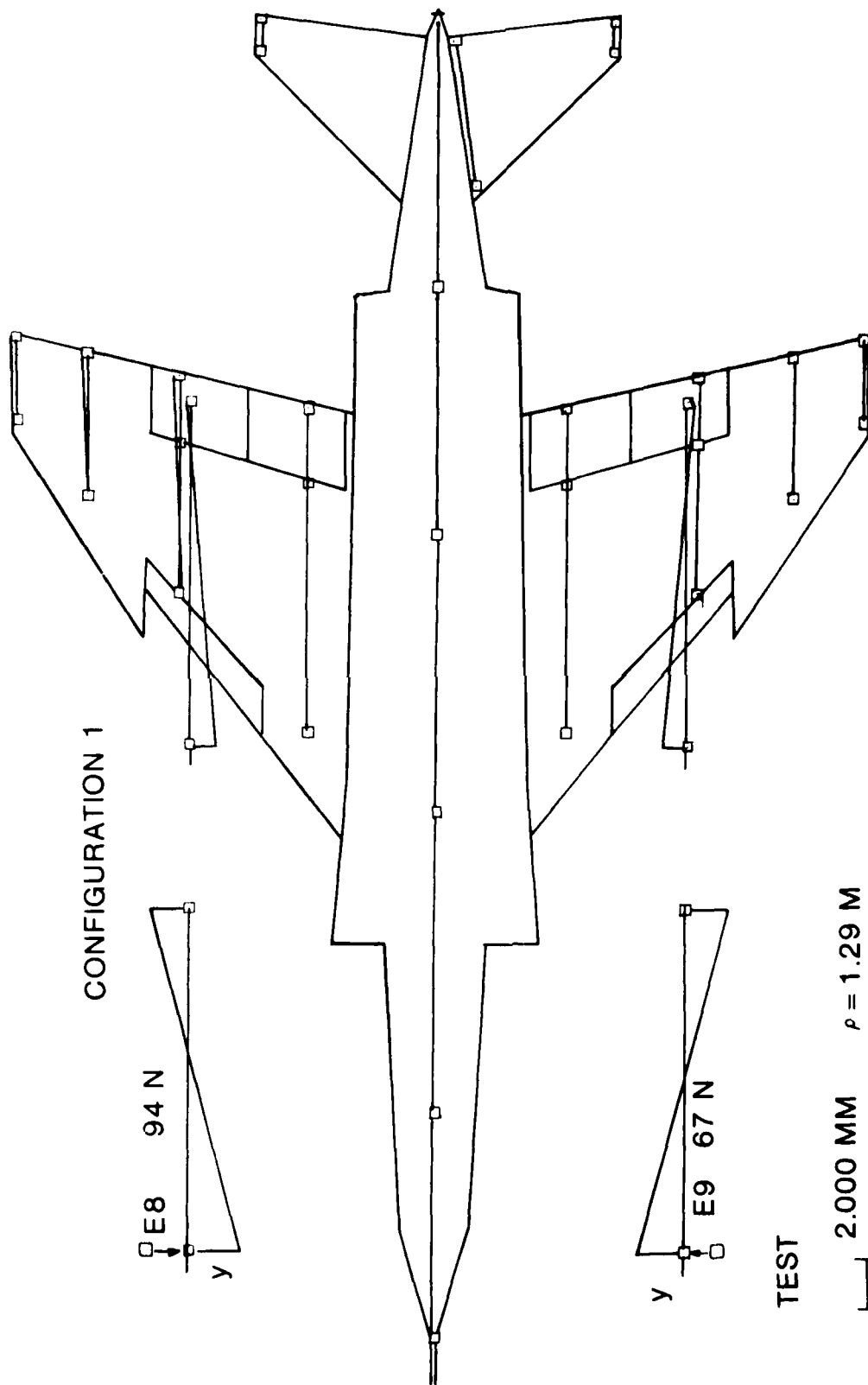
TEST

2.000 MM $\rho = 1.29$ M
2.748 M/S2

2 FREQUENCY: 5.899 HZ sym
0.600 M A/C

Figure 2. GVT, Store Yaw Mode, Configuration 1

CONFIGURATION 1

E8 229 N

E9 229 N

y

y

□
TEST
—┤— 2.000 MM ρ=1.29 M
—┤— 3.506 M/S2
3 FREQUENCY: 6.664 HZ SYM
—┌— 0.600 M A/C
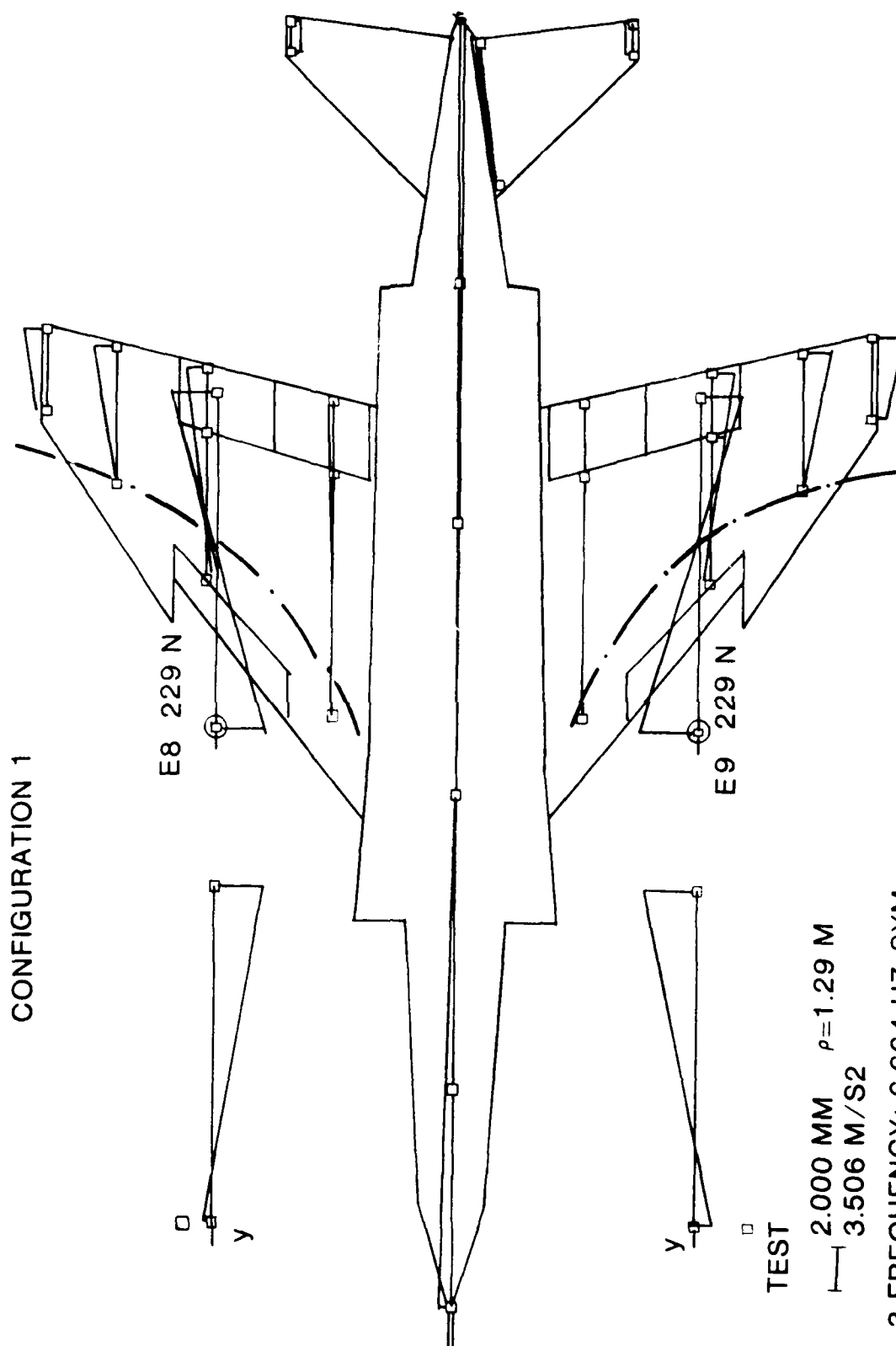
Figure 3.   GVT, Store Pitch Mode, Configuration 1

CONFIGURATION 1

94 N ☐ E10

94 N E11

-210 N
E8

-219 N
E9

TEST
━┤ 2.000 MM
5.753 M/S2   ρ=1.29 M

4 FREQUENCY: 8.536 HZ SYM
━┤ 0.600 M A/C
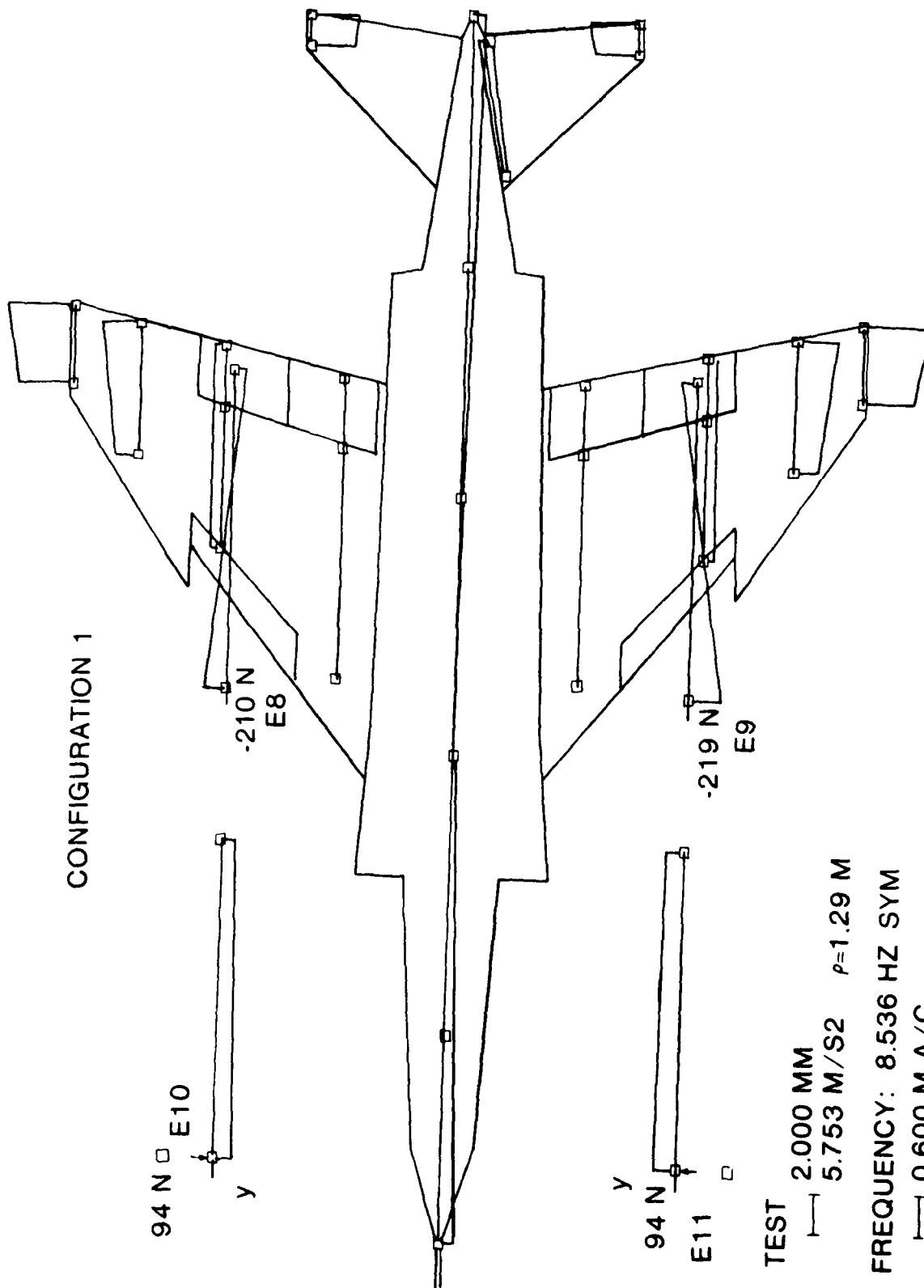
Figure 4. GVT, Store Roll Mode, Configuration 1

CONFIGURATION 2

E14   36N

E13

35 N

TEST 5.000 MM

6.067 M/S2 ρ = 1.36 M

1 FREQUENCY: 5.544 HZ SYM
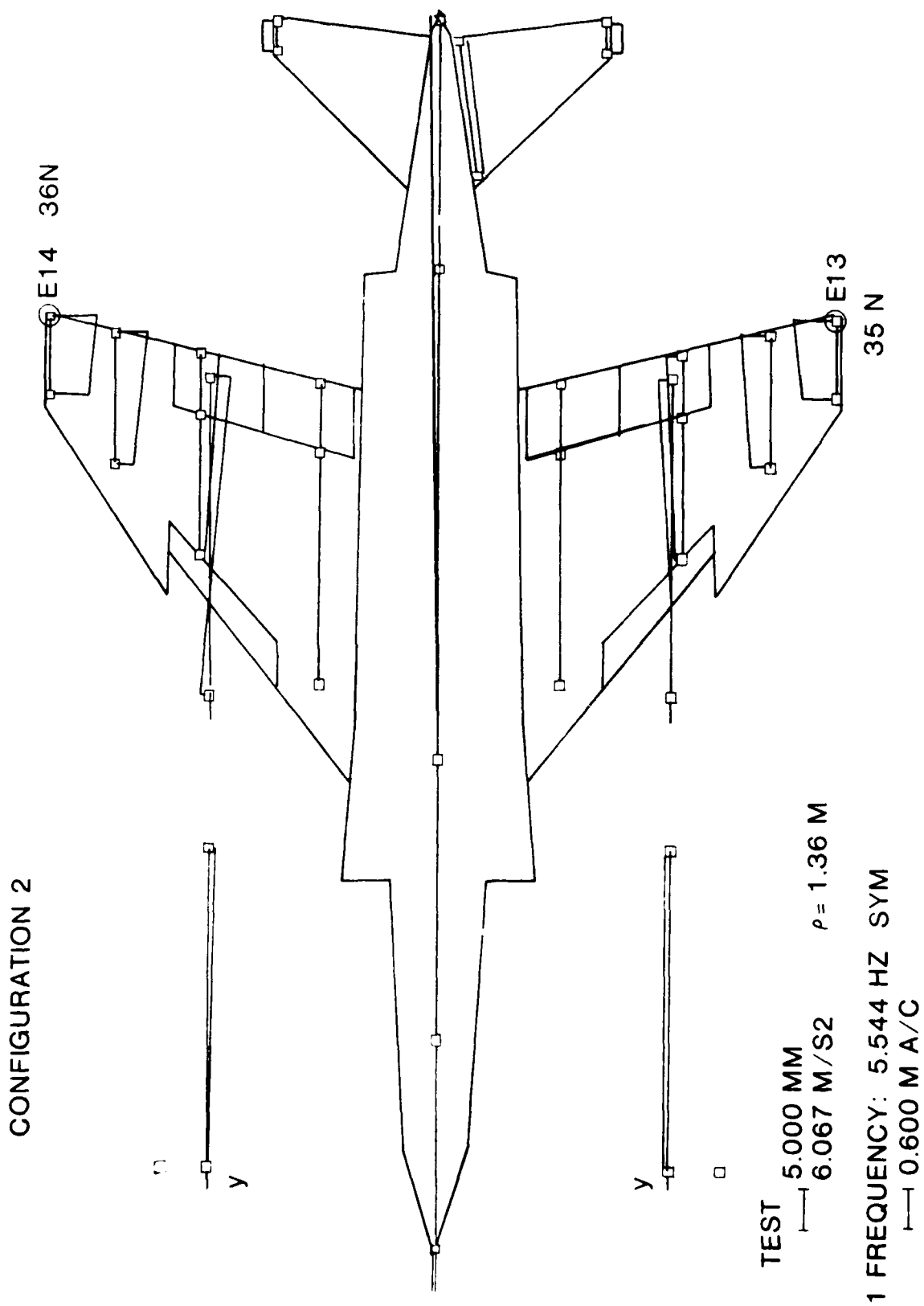
0.600 M A/C

Figure 5. GVT, 1st Wing Bending, Configuration 2

CONFIGURATION 2

124 N

107 N

TEST
2.000 MM $\rho = 1.36$ M
2.493 M/S2

2 FREQUENCY: 5.619 HZ SYM
0.600 M A/C
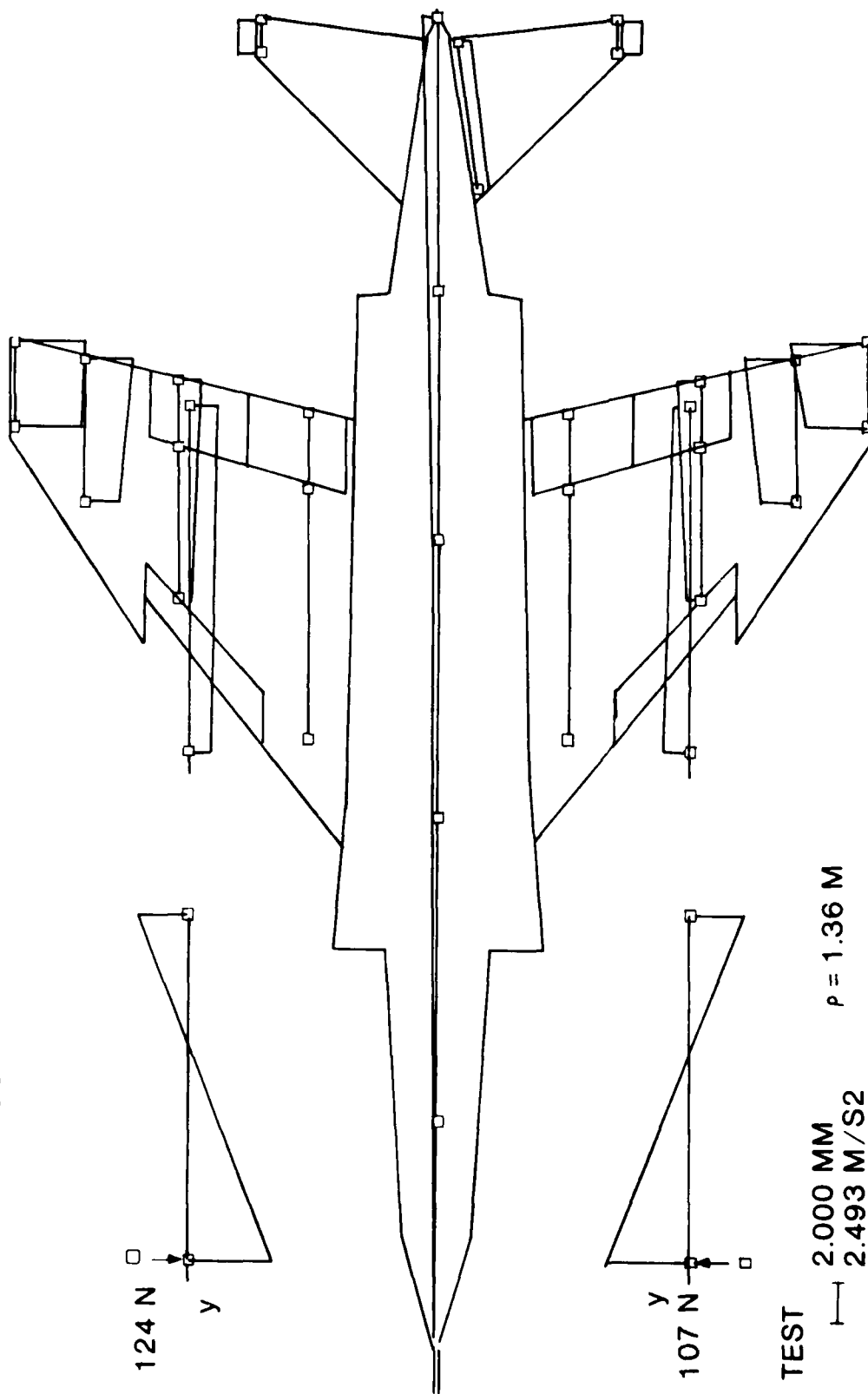
Figure 6. GVT, Store Yaw Mode, Configuration 2

CONFIGURATION 2

E8 229 N

E9 229 N
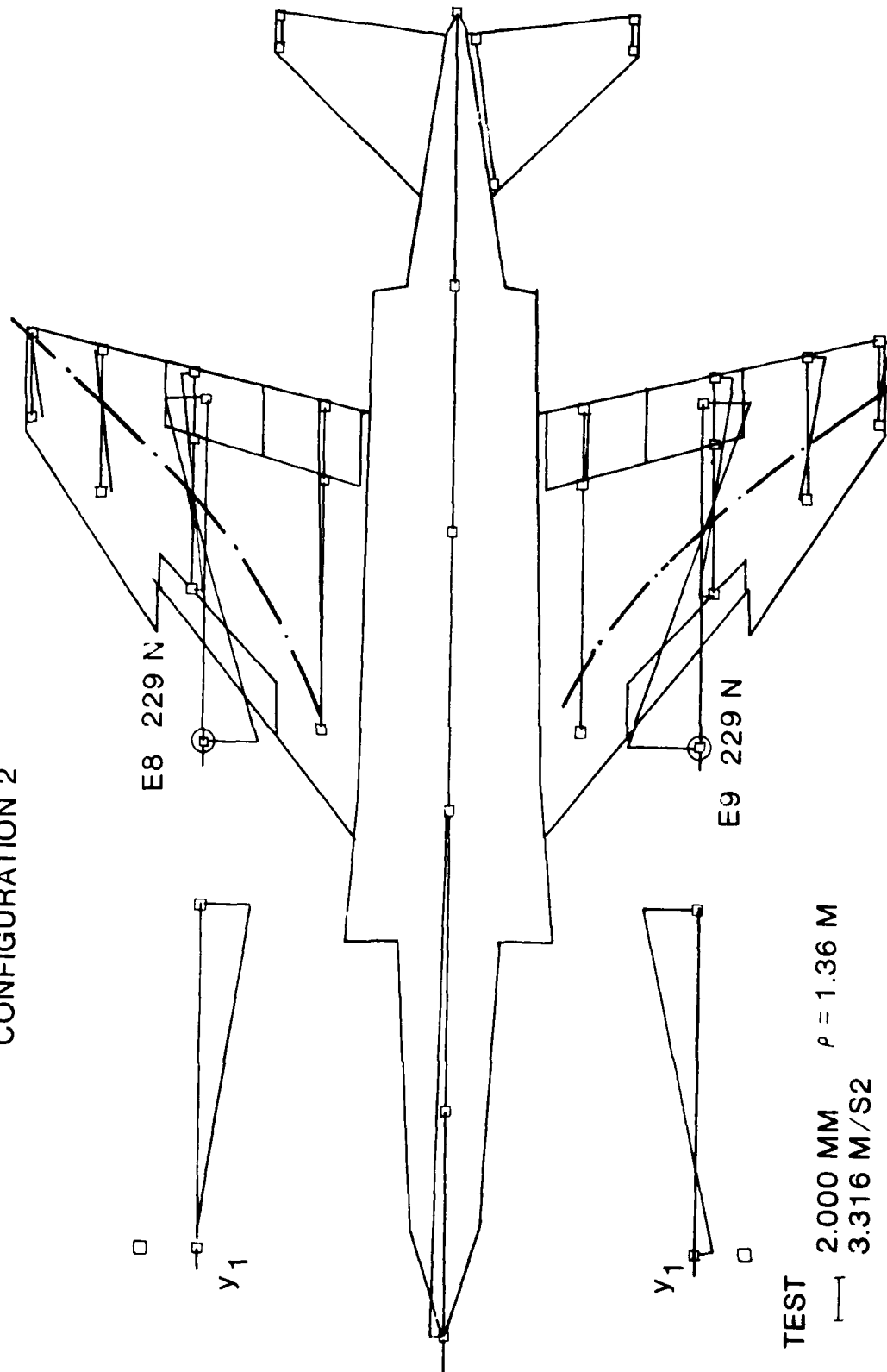
TEST
2.000 MM $\rho = 1.36$ M
3.316 M/S2
3 FREQUENCY: 6.481 HZ SYM
0.600 M A/C

Figure 7. GVT, Store Pitch Mode, Configuration 2

41

CONFIGURATION 2

-215 N
E8

-210 N
E9

90 N — E2
y

92 N — E1

2.000 MM
5.746 M/S2 $\rho = 1.36$

4 FREQUENCY: 8.531 HZ SYM
0.600 M A/C
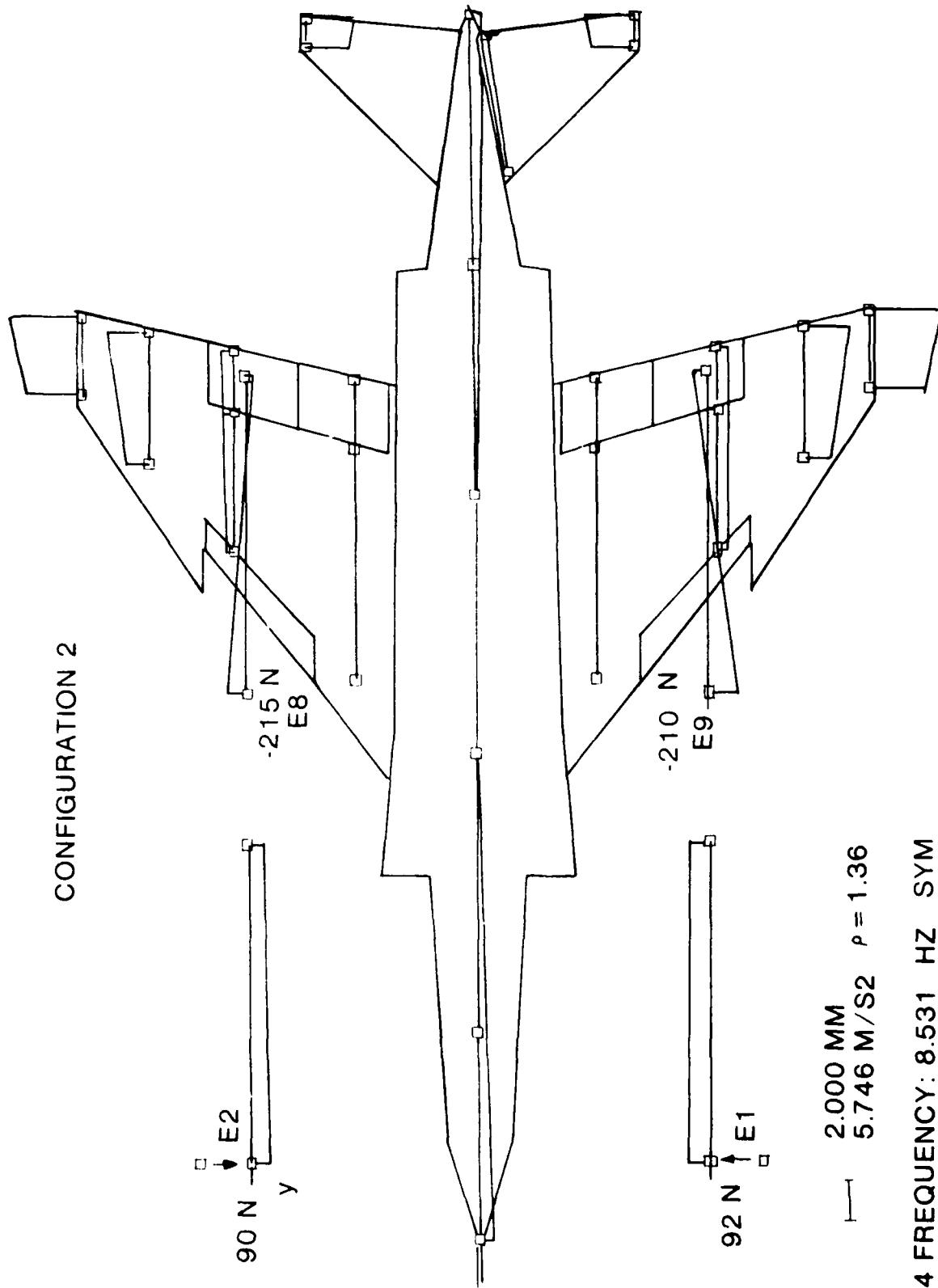
Figure 8. GVT, Store Roll Mode, Configuration 2

CONFIGURATION 1

y
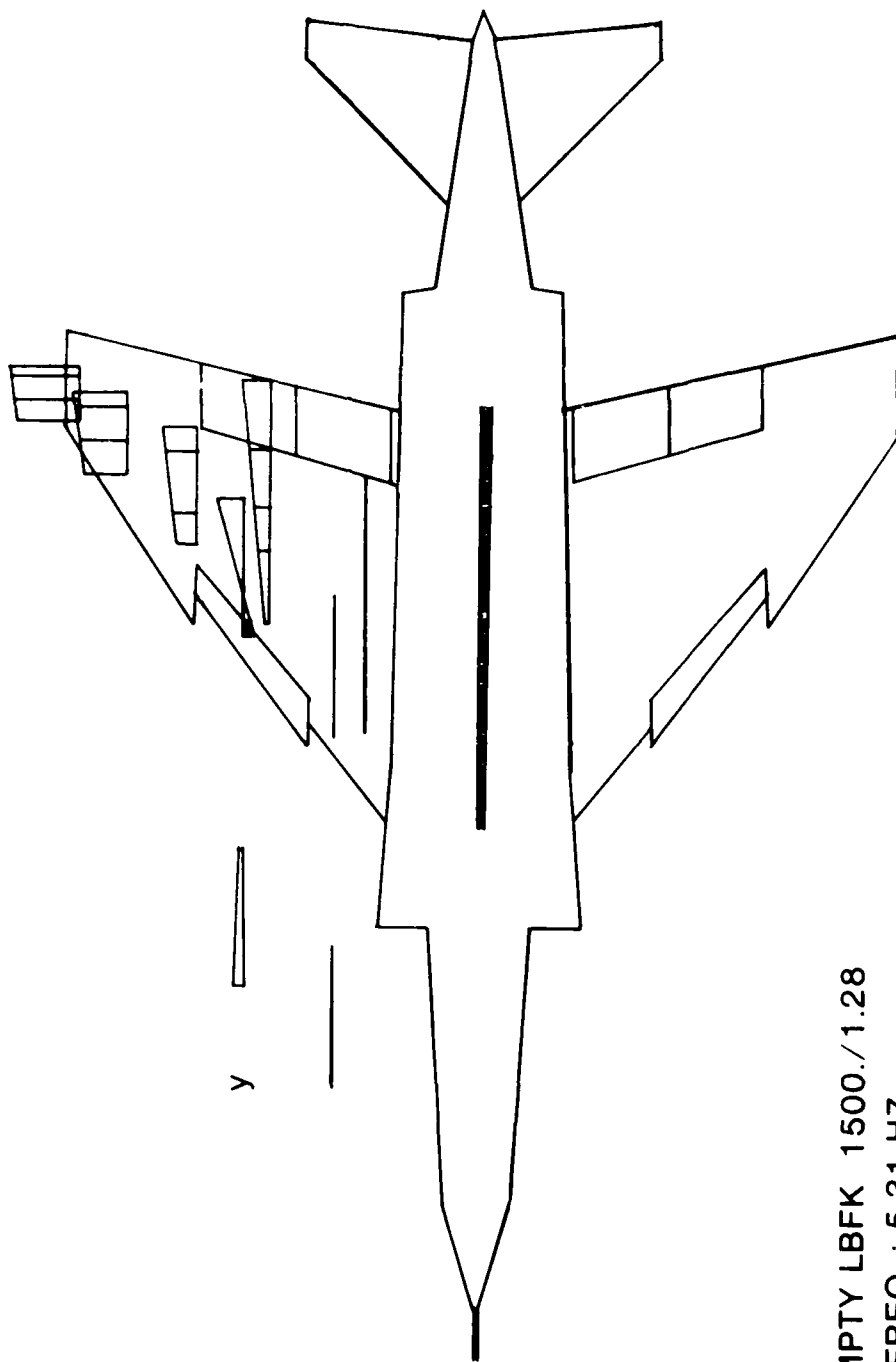
F-4 F EMPTY LBFK 1500./1.28
1.SYM FREQ.: 5.31 HZ

Figure 9. Calculated 1st Wing Bending, Configuration 1

CONFIGURATION 1

y
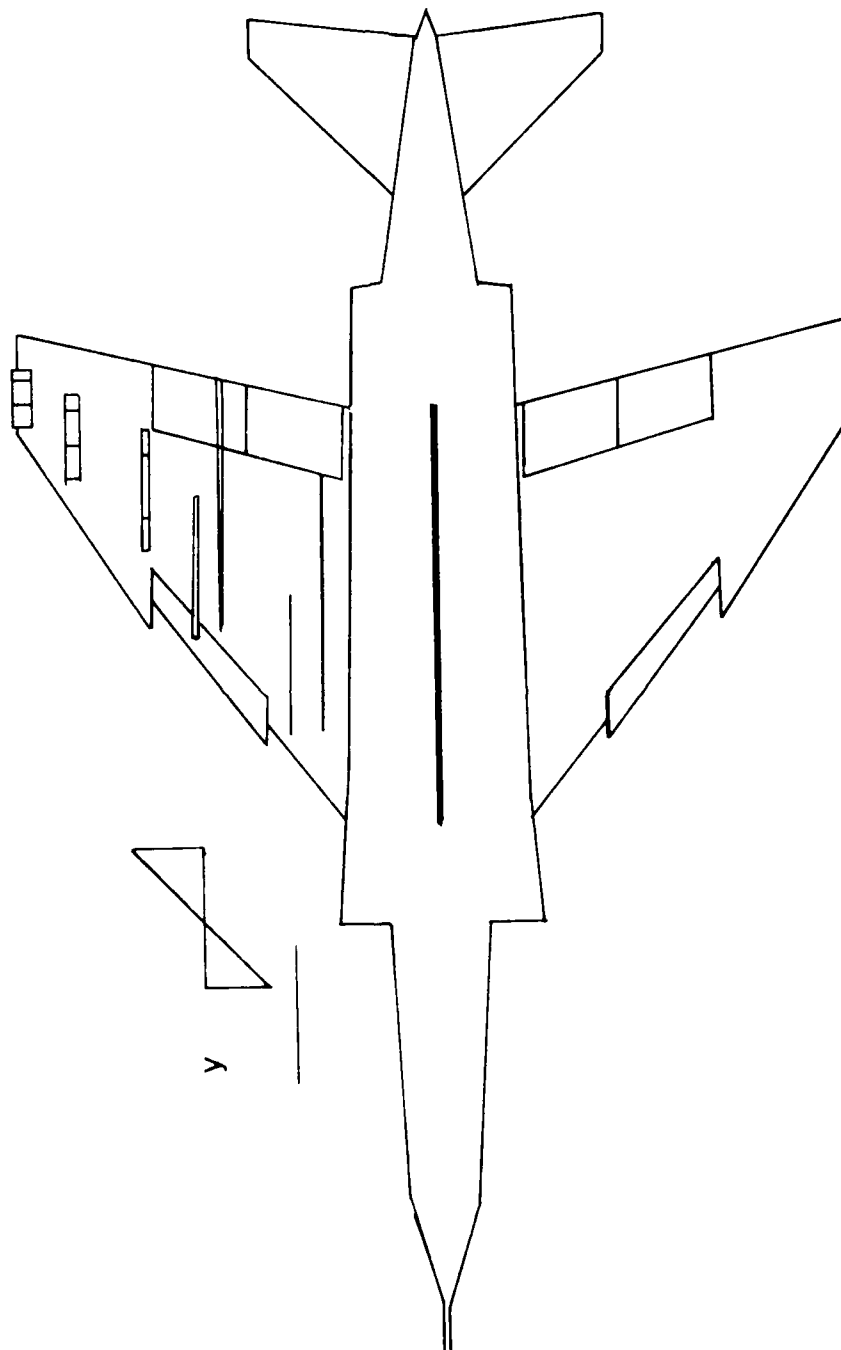
F-4 EMPTY LBFK 1500./1.28

2. SYM FREQ.: 5.70 HZ

Figure 10.   Calculated Store Yaw Mode, Configuration 1

CONFIGURATION 1

y

F-4 EMPTY LBFK 1500./1.28

3.SYM FREQ.: 5.97 HZ
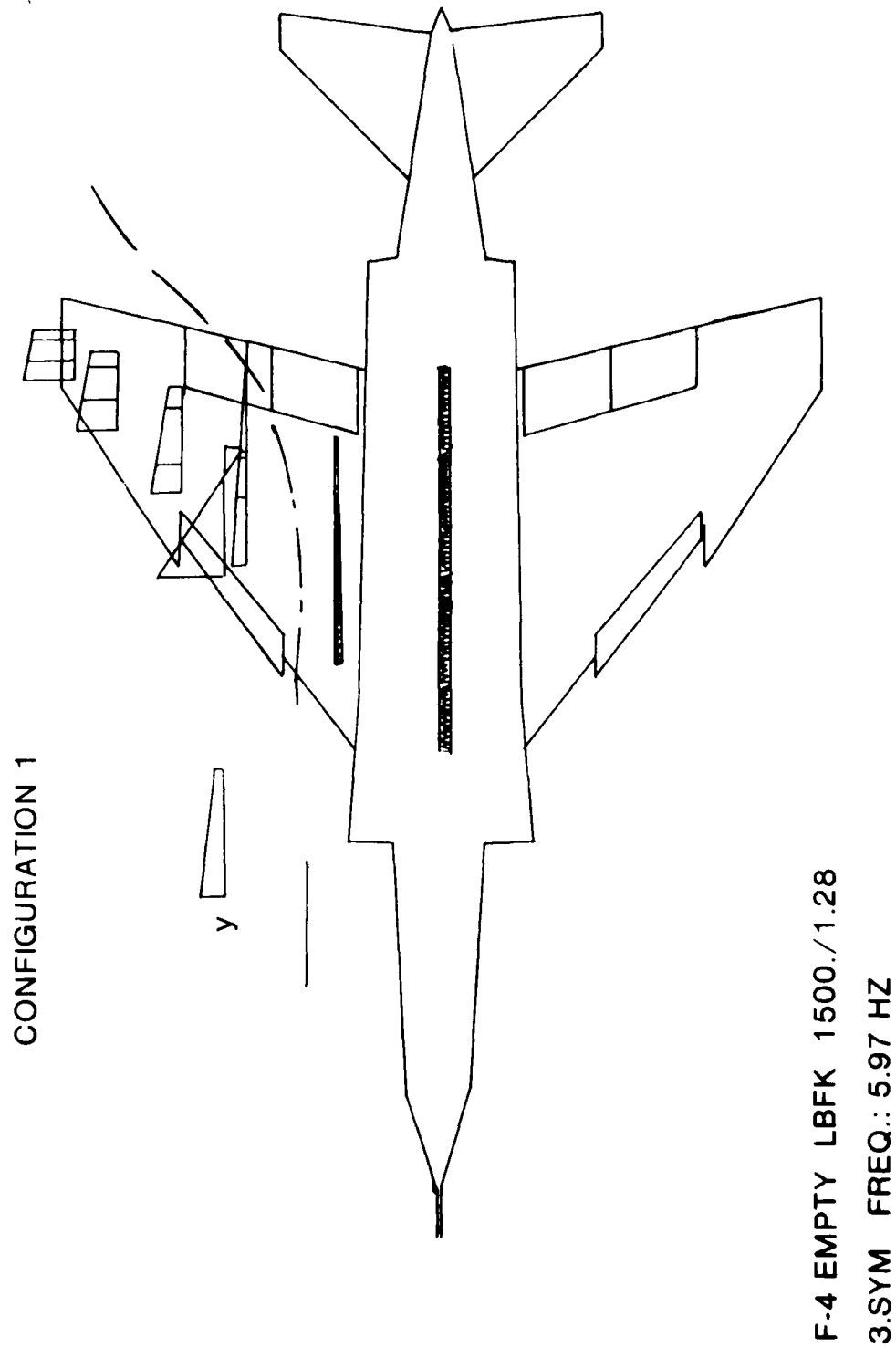
Figure 11. Calculated Store Pitch Mode, Configuration 1

CONFIGURATION 1

y

F-4 F EMPTY LBFK 1500./1.28
4.SYM FREQ.: 8.28 HZ
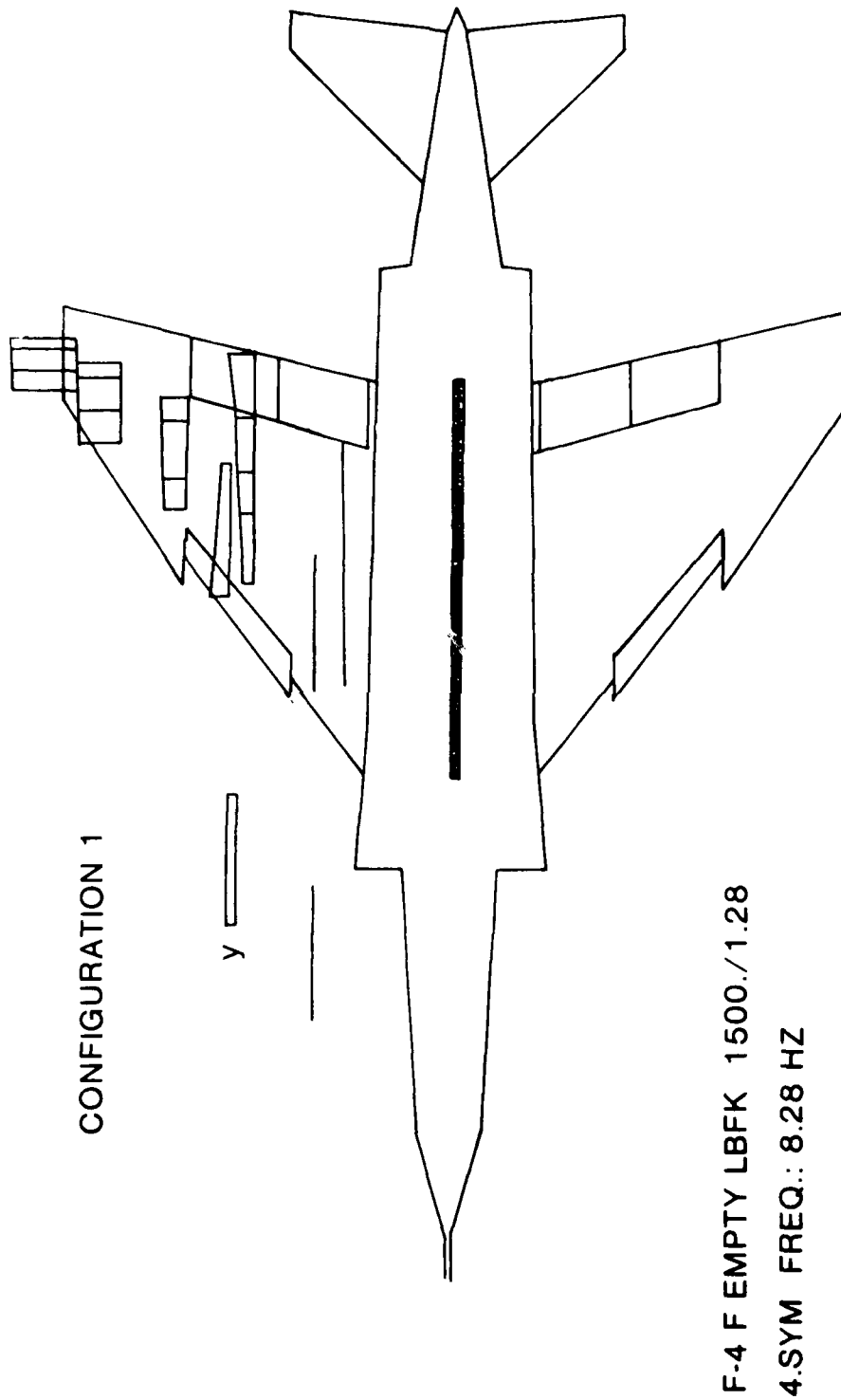
Figure 12. Calculated Store Roll Mode, Configuration 1

CONFIGURATION 2

F-4 EMPTY LBFK 1500./1.34
1.SYM   FREQ.: 5.22 HZ
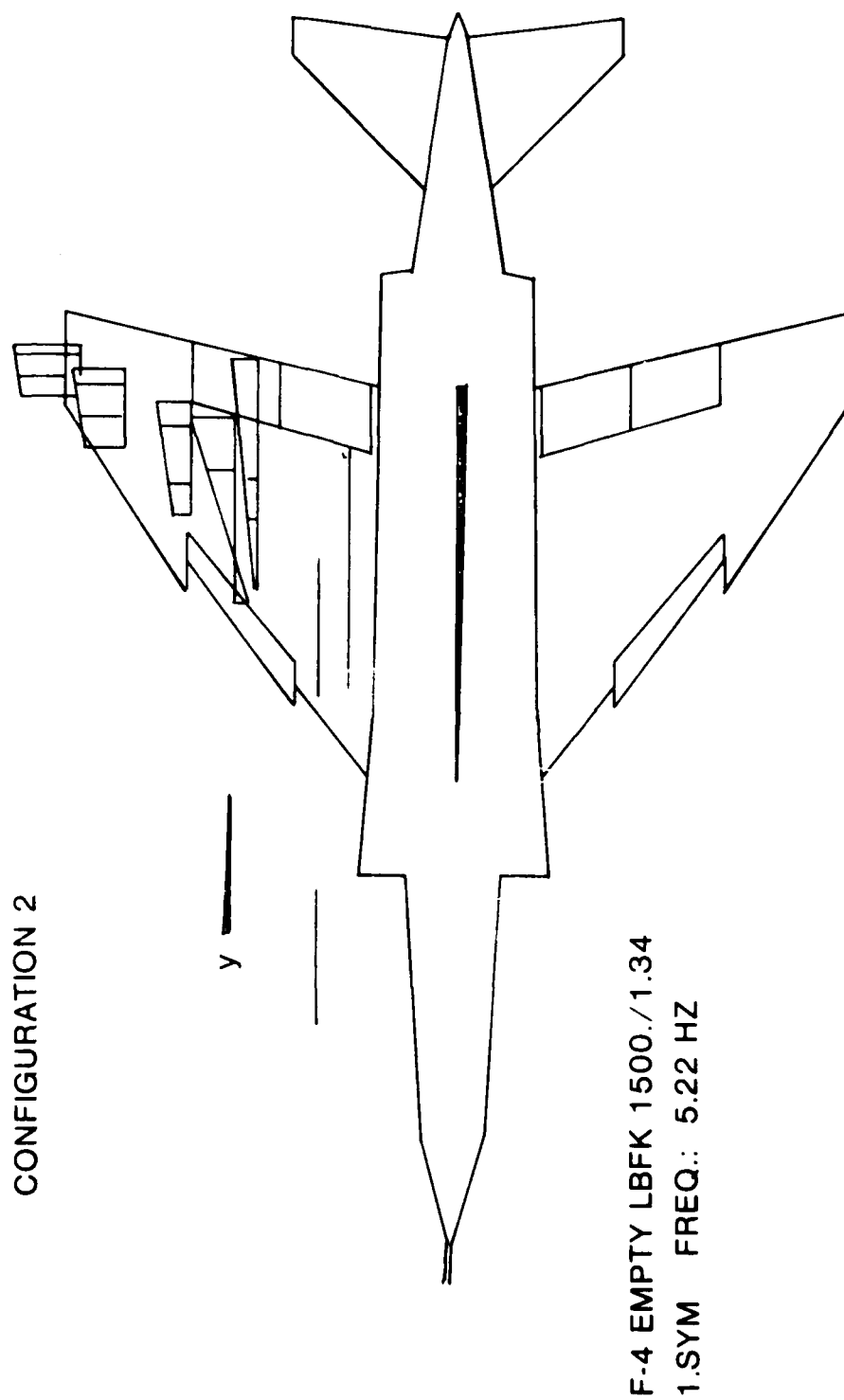
Figure 13.   Calculated 1st Wing Bending, Configuration 2
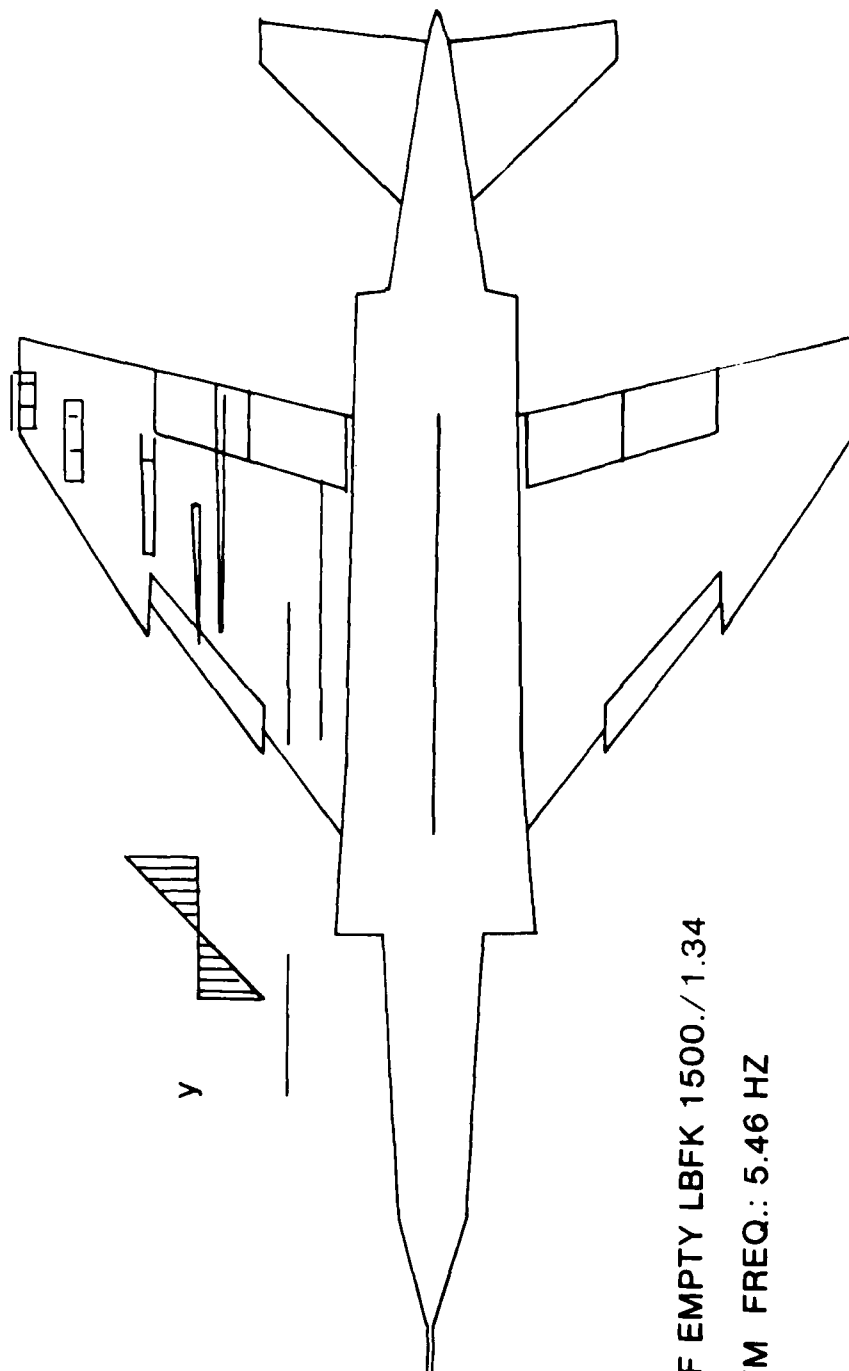
CONFIGURATION 2

F-4 F EMPTY LBFK 1500./1.34
2.SYM FREQ.: 5.46 HZ

Figure 14. Calculated Store Yaw Mode, Configuration 2

CONFIGURATION 2

y

F-4 EMPTY LBFK 1500./1.34

3.SYM FREQ. : 5.87 HZ
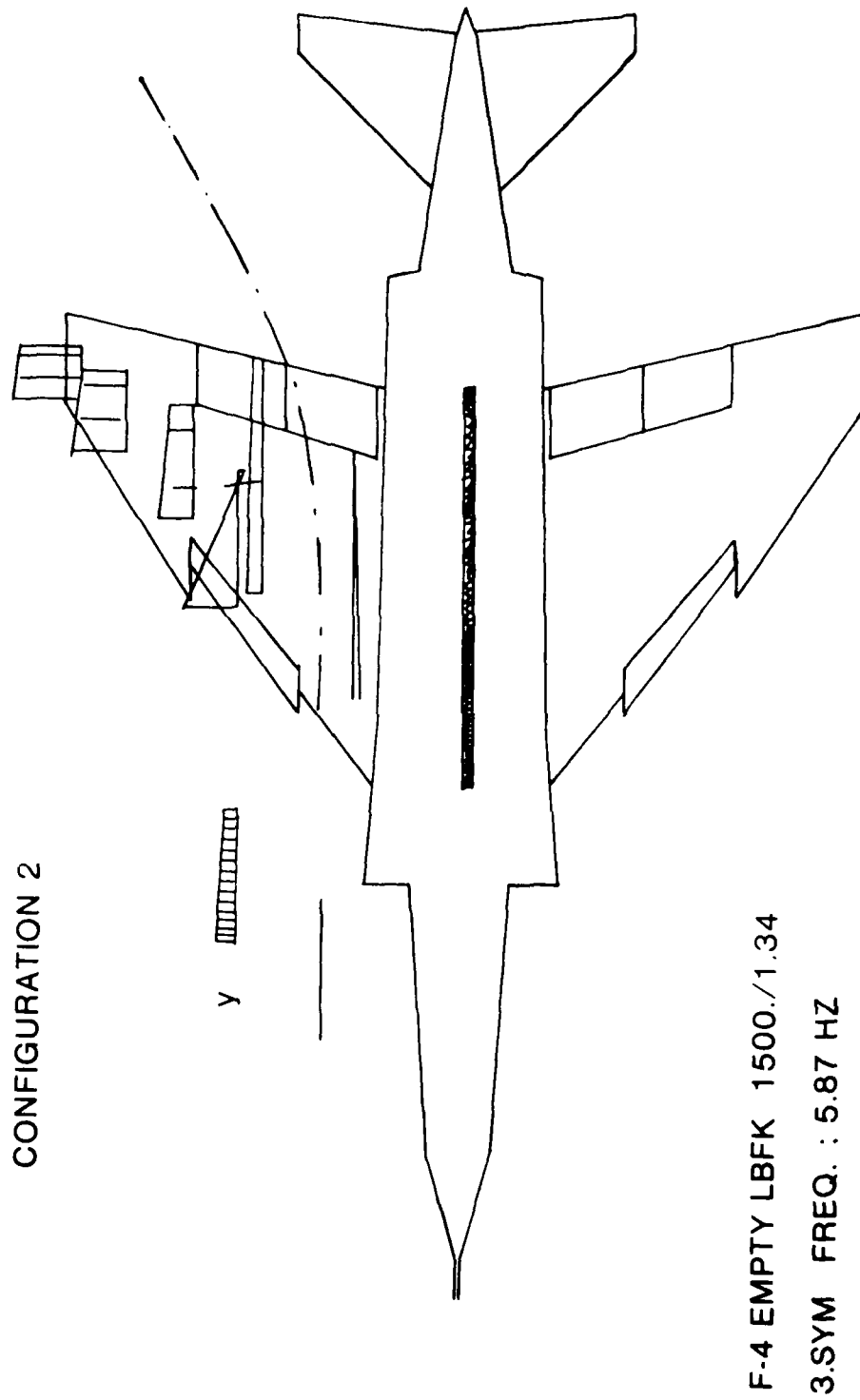
Figure 15.   Calculated Store Pitch Mode, Configuration 2

49
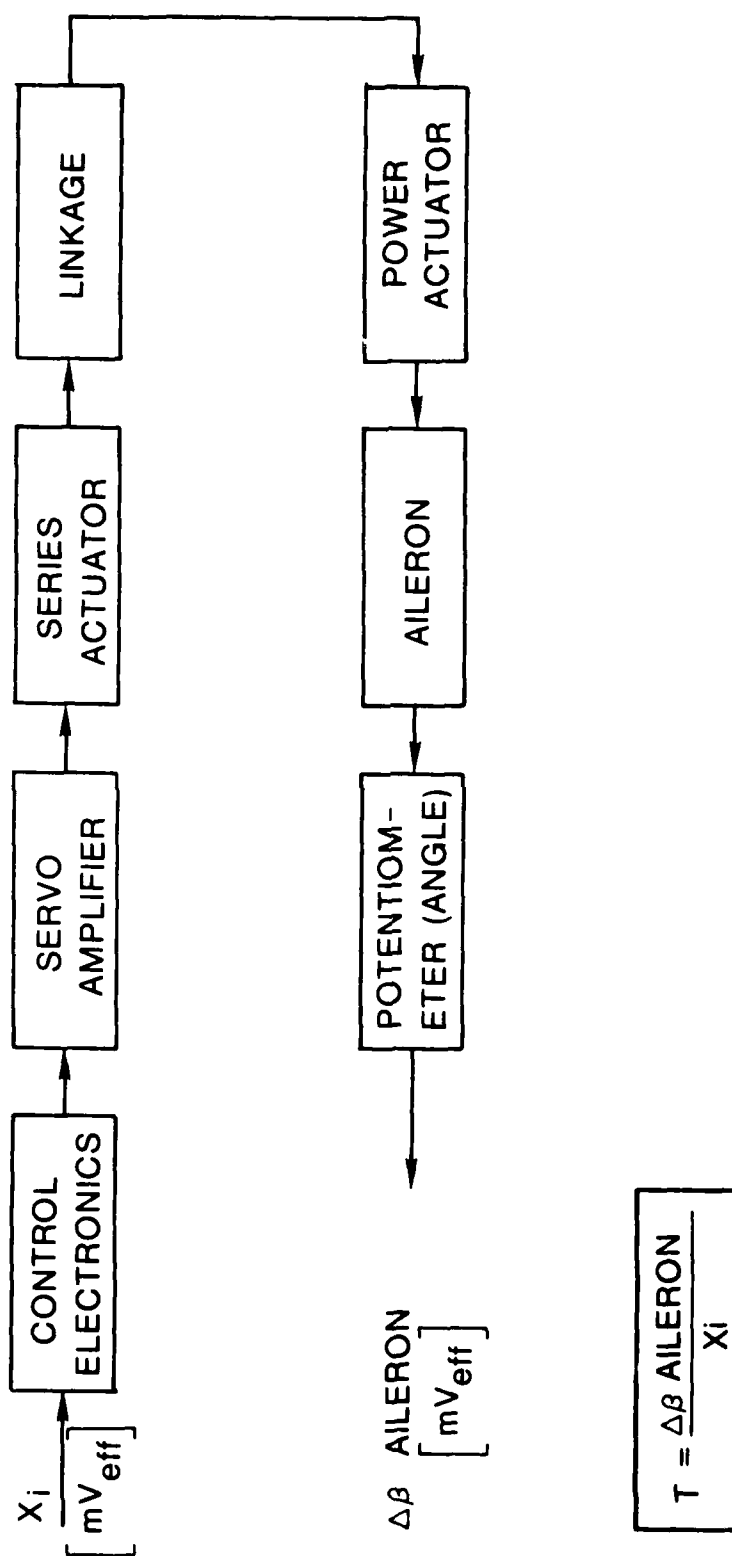
Figure 16.   Block Diagram for Measurement of Aileron Actuator Transfer
Function
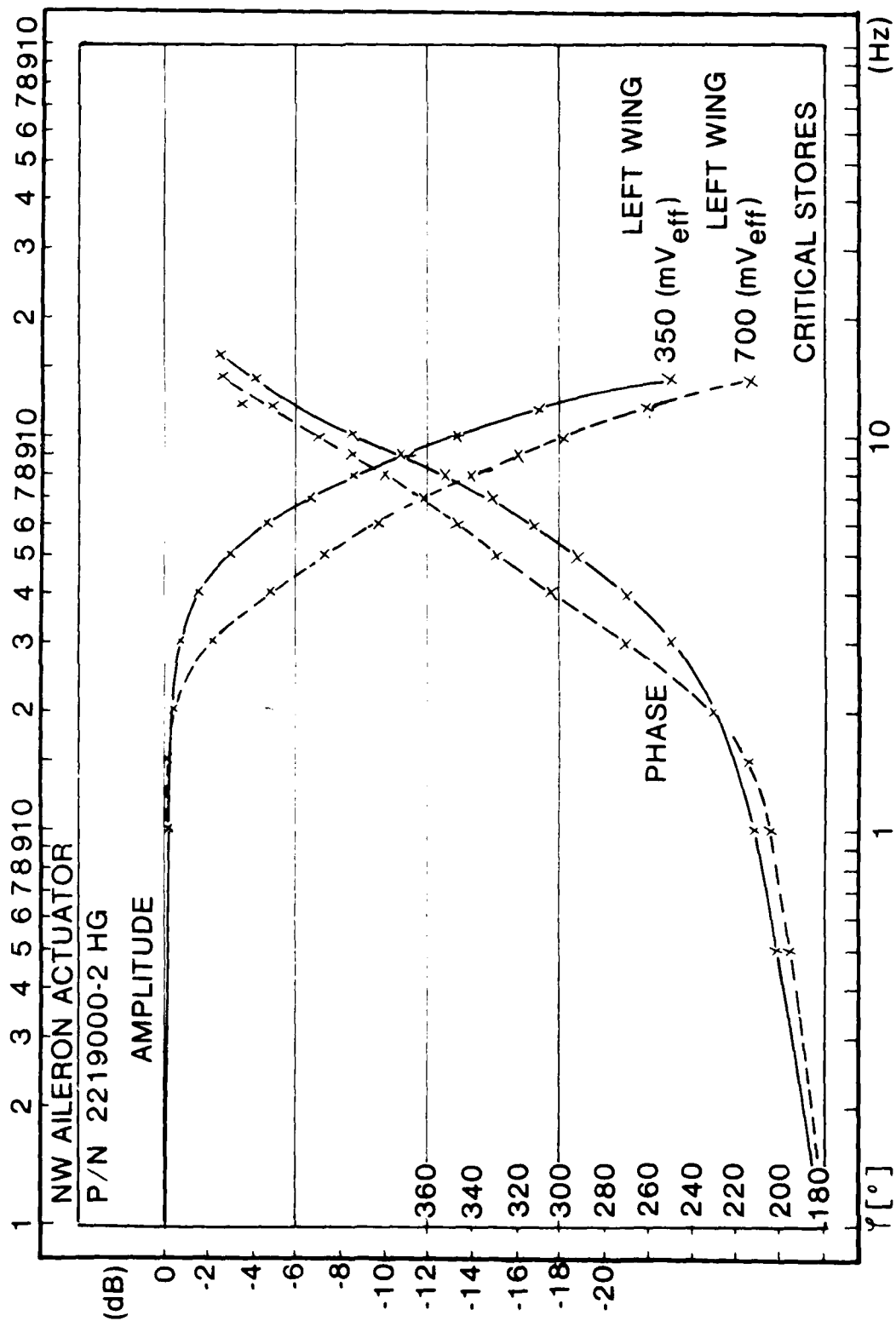
Figure 17. Measured Transfer Function of the Left Aileron
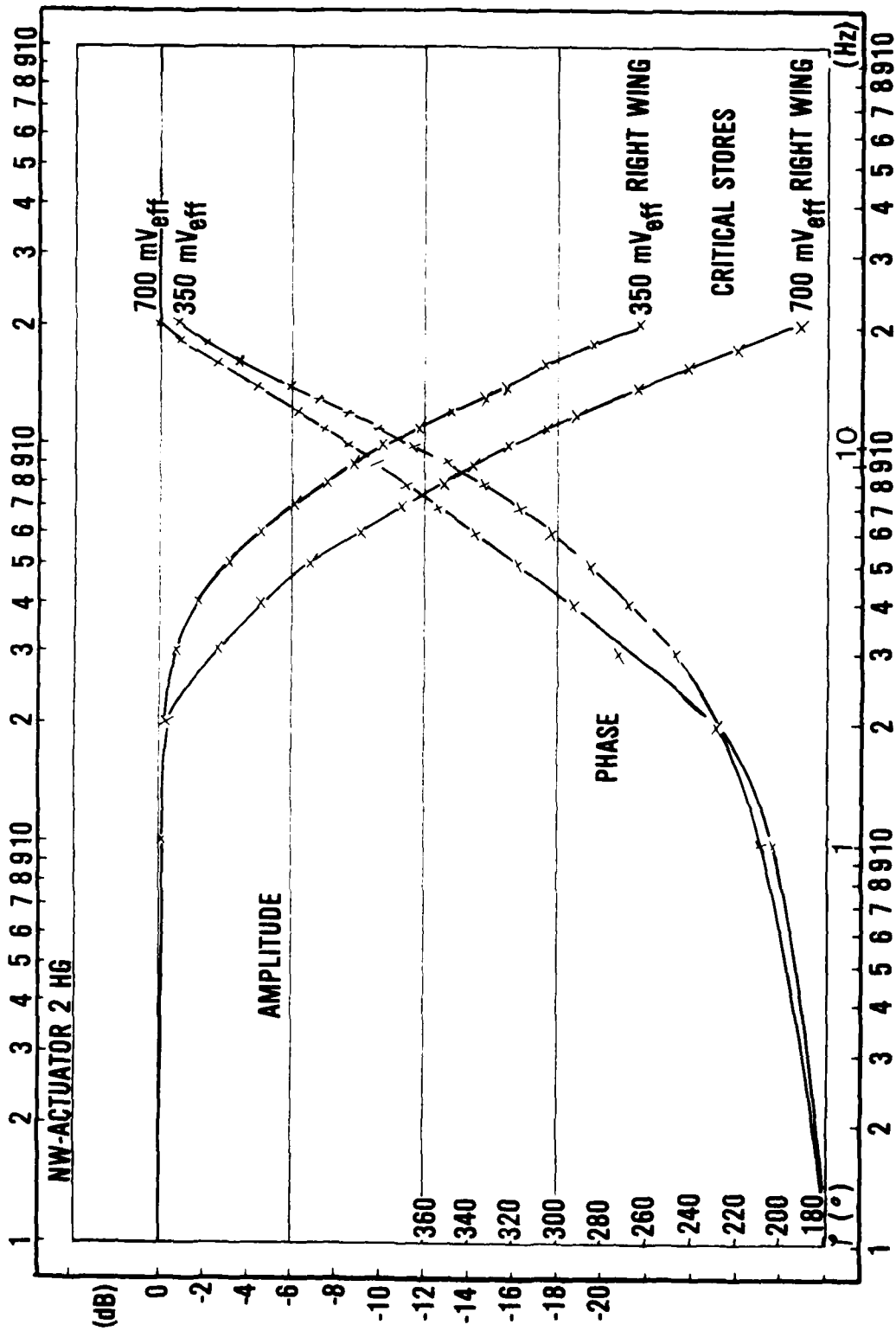
Figure 18. Measured Transfer Function of the Right Aileron
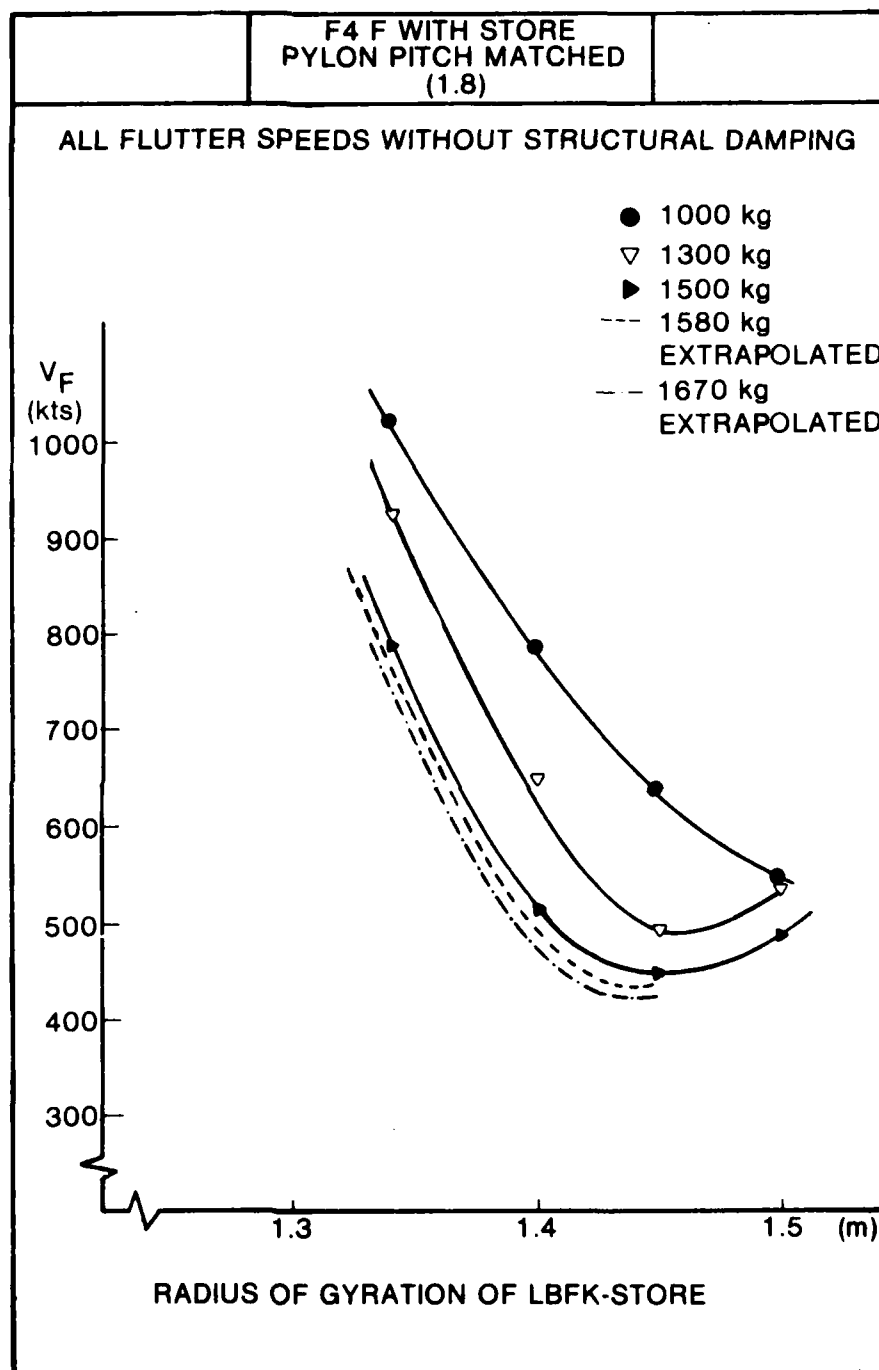
Figure 19. Flutter Speed vs Radius of Gyration of the LBFK-Store

● ACCELEROMETER

▲ SOLENOID-SWITCH

▲ SWITCH
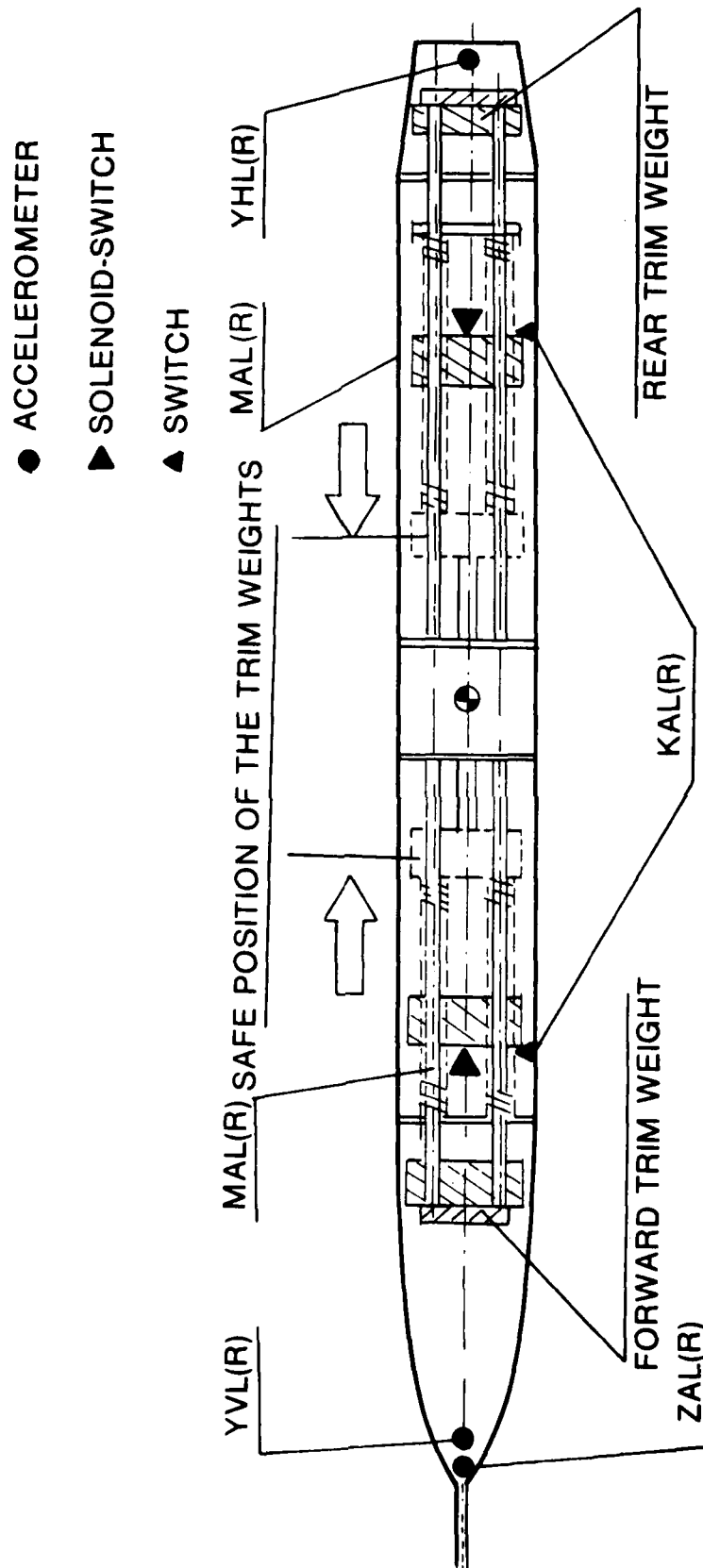
Figure 20.   Scheme for the Modified Flutter Stopper

FIXATION AND RELEASE UNIT

MOVABLE
TRIM
WEIGHT

MECHANIC BLOCKAGE

FORWARD TRIM WEIGHT

SPRING

MOVABLE
TRIM
WEIGHT
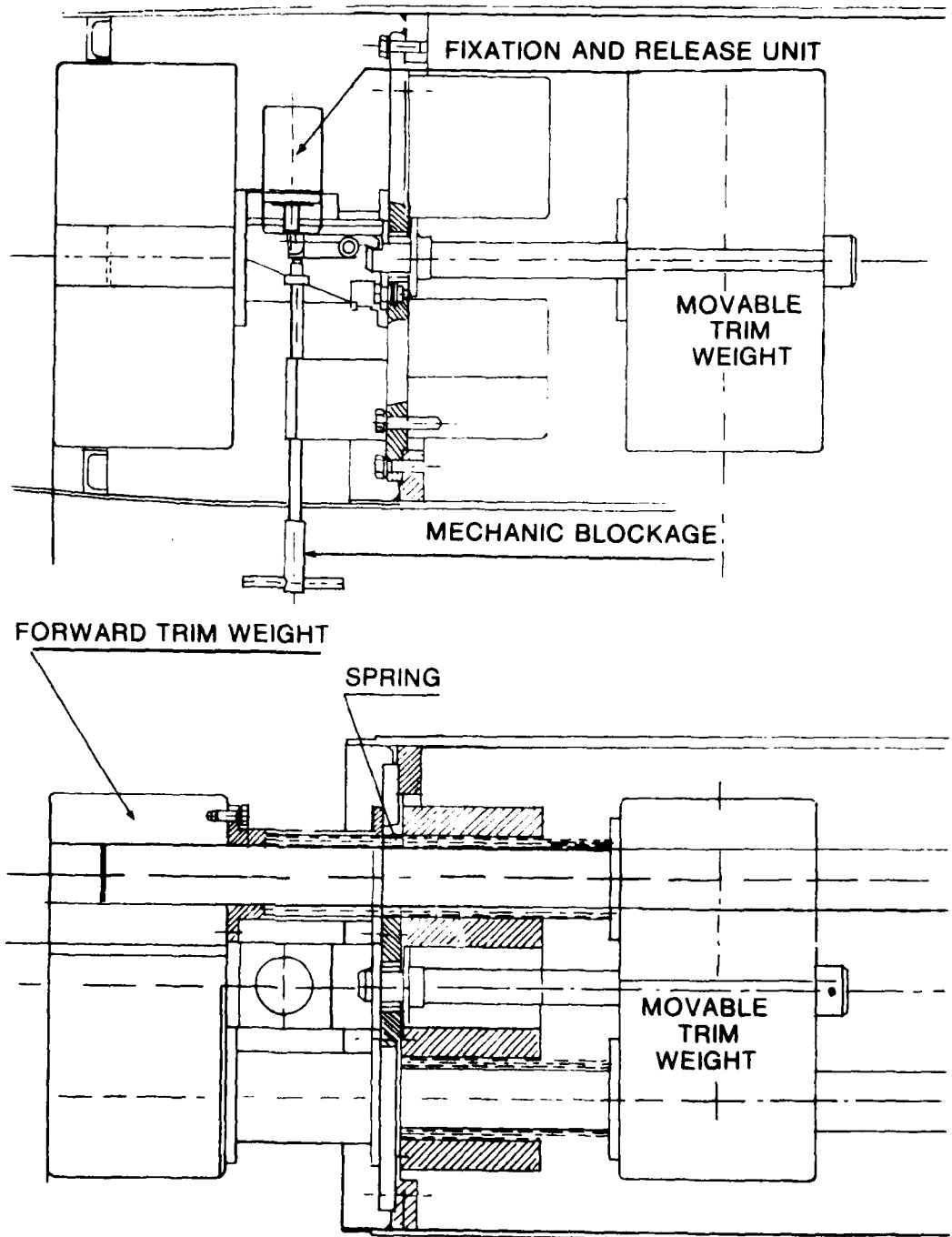
Figure 21.   Forward Part of the Flutter Stopper

FIXATION AND RELEASE UNIT
FOR THE REAR TRIM WEIGHT

REAR
TRIM WEIGHT

MECHANIC
BLOCKAGE

PRELOADED SPRING

ROD I

ROD II
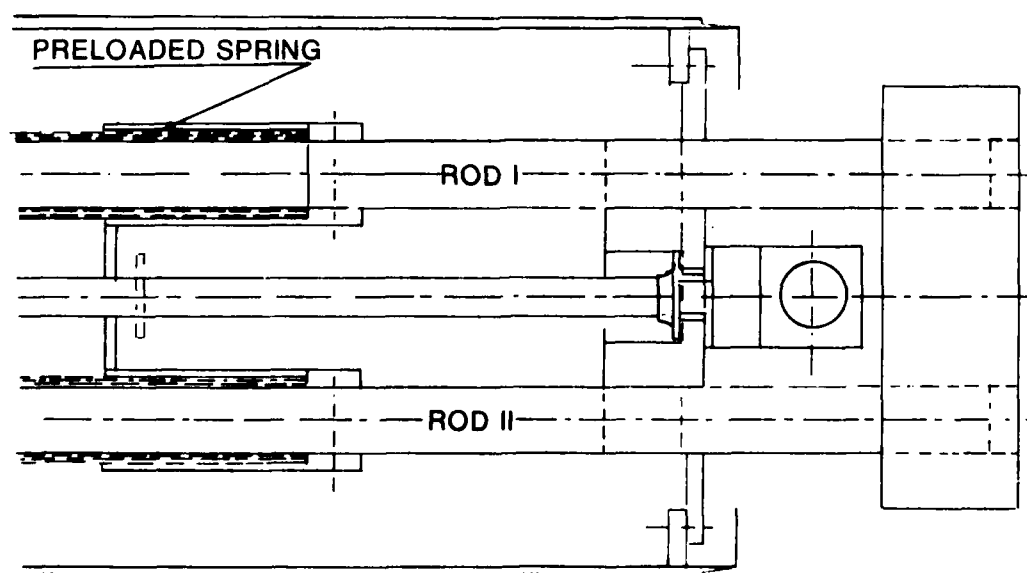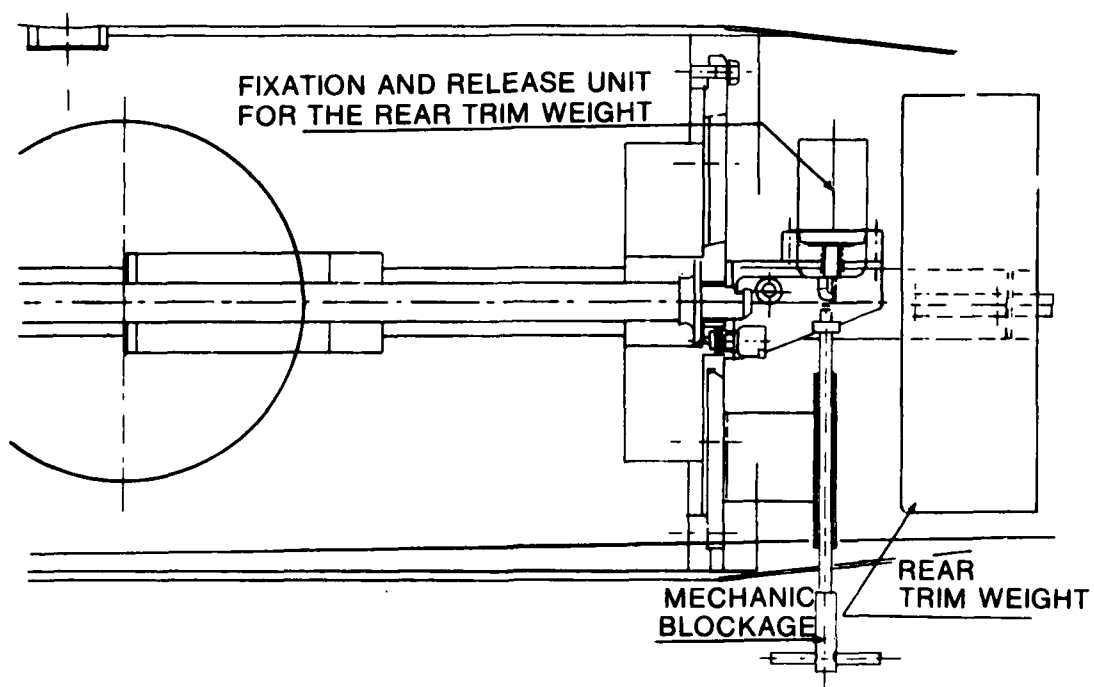
Figure 22.   Rear Part of the Flutter Stopper
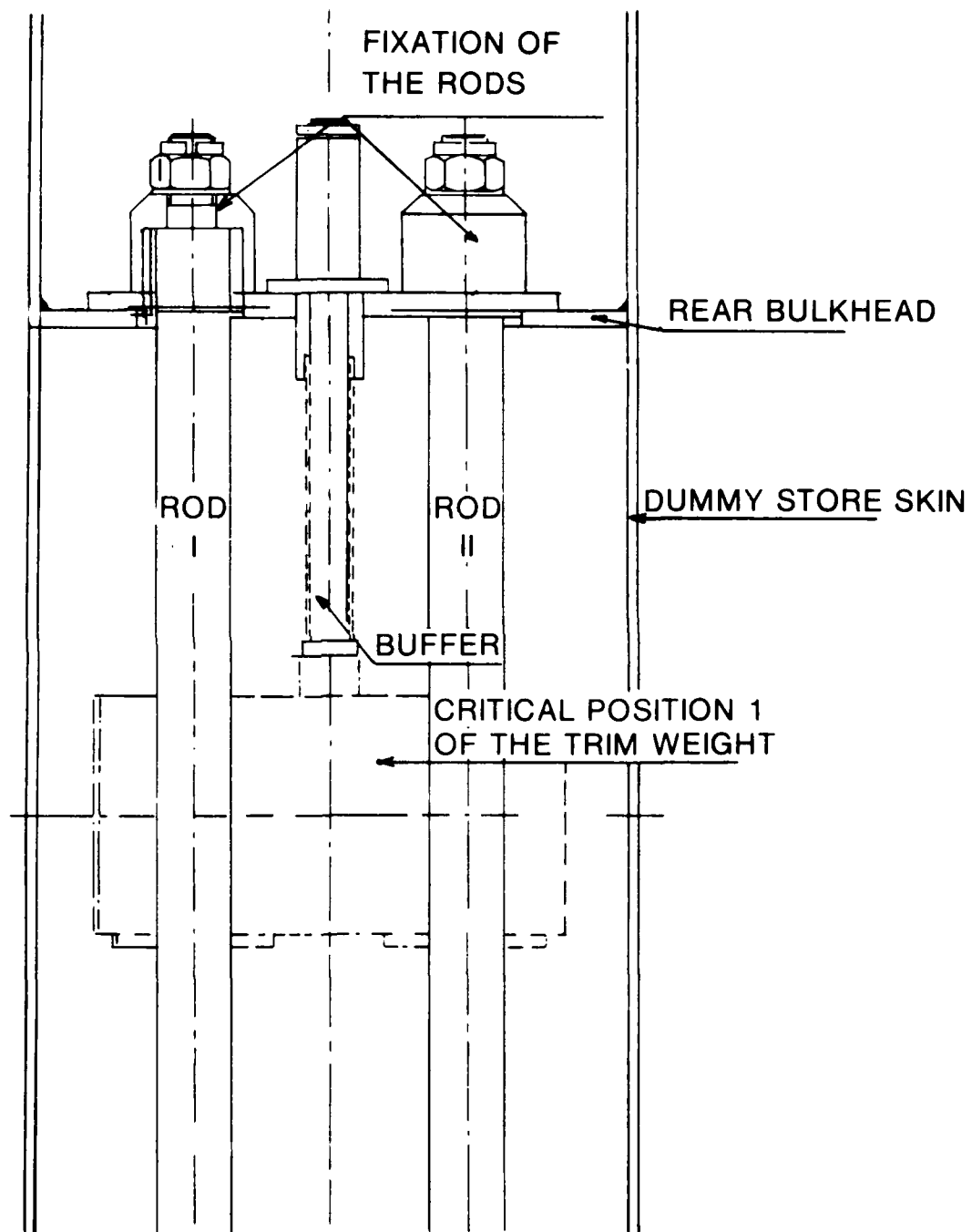
Figure 23. Fixation of the Rods in the LBFK Dummy Store
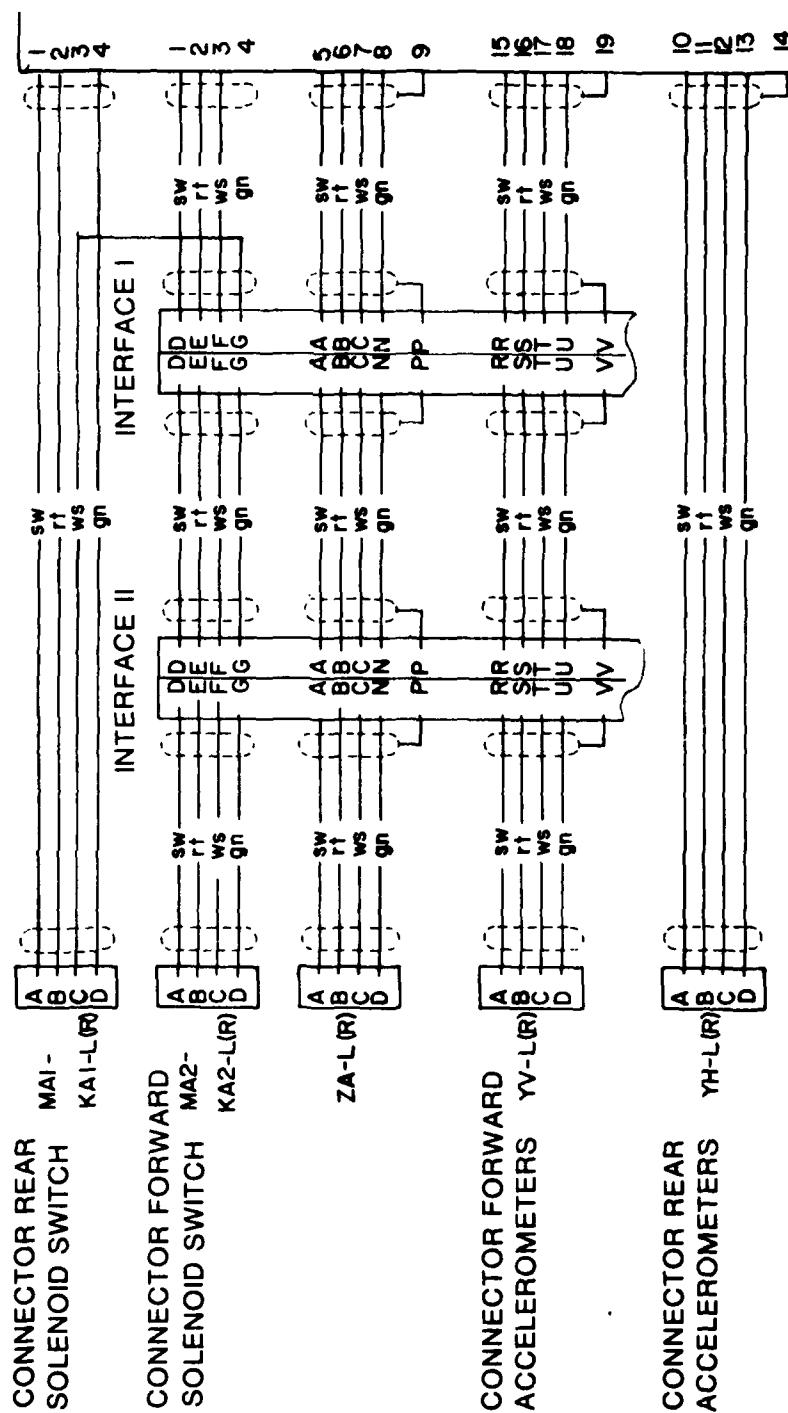
Figure 24. Wiring Plan for the Flutter Stopper

F-4F DUMMY STORE (LBFK)

5150

4675

(mm)

φ 500

762

381

c.g.

2750

1250
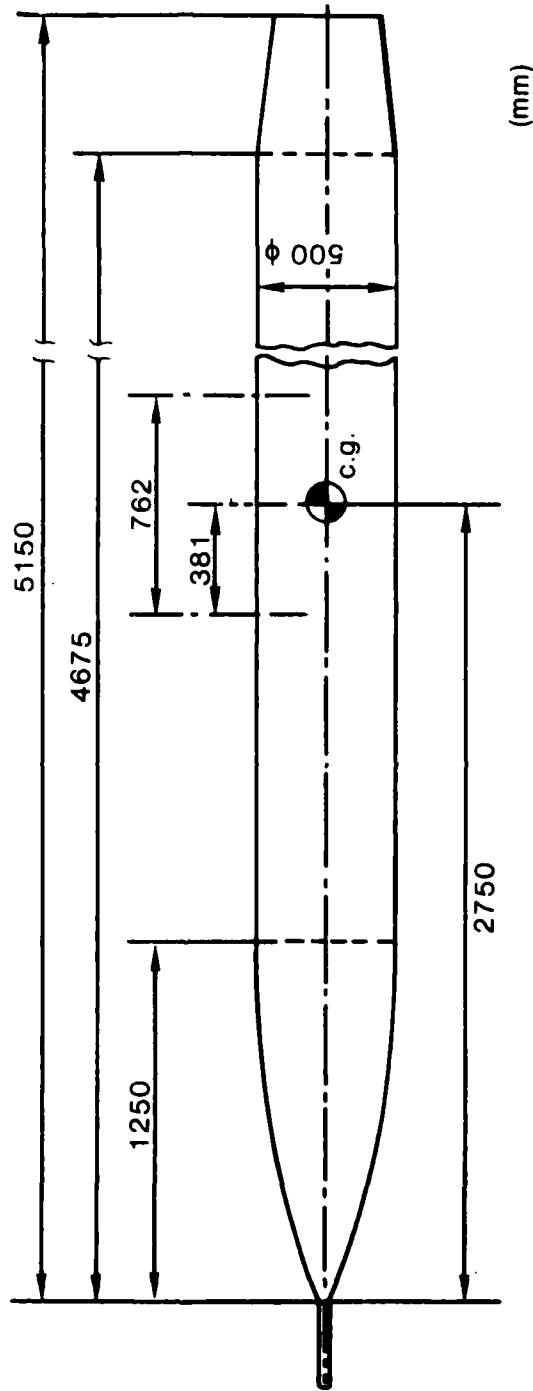
DUMMY D1 (LEFT WING)

W=1576 (kg)

ρ_y=1.341 (m) SAFE CONFIG.

ρ_y=1.409 1.341 (m) CRITICAL CONFIG

DUMMY D3: (RIGHT WING)

W=1583 (kg)

ρ_y=1.347 (m) SAFE CONFIG.

ρ_y=1.416 (m) CRITICAL CONFIG.

Figure 25. Geometry and Mass Data of the Modified Store

INPUT TO A/C SYSTEM

SENSOR INPUT

SENSOR INPUT
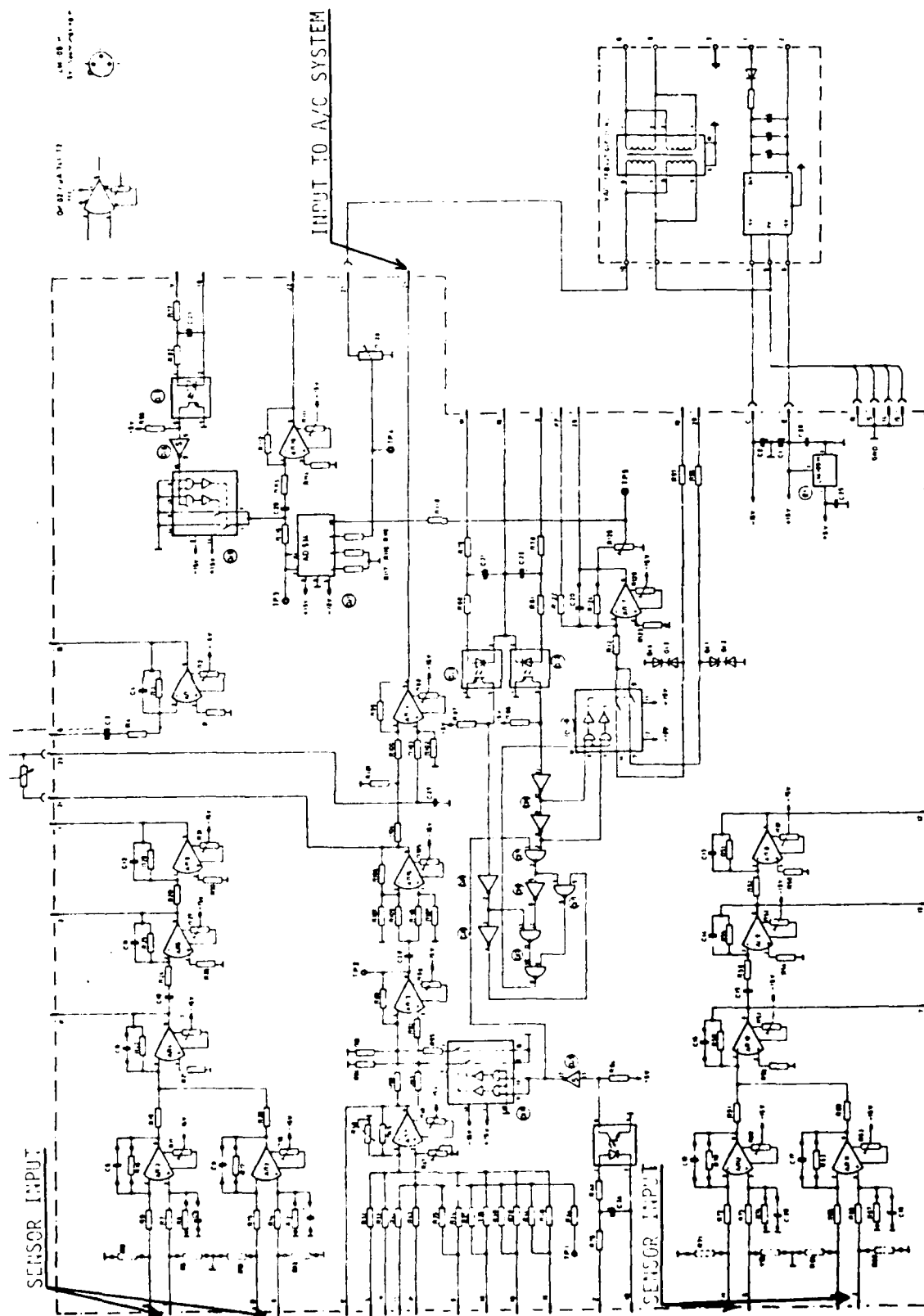
Figure 26. Design of the Control Electronics

60
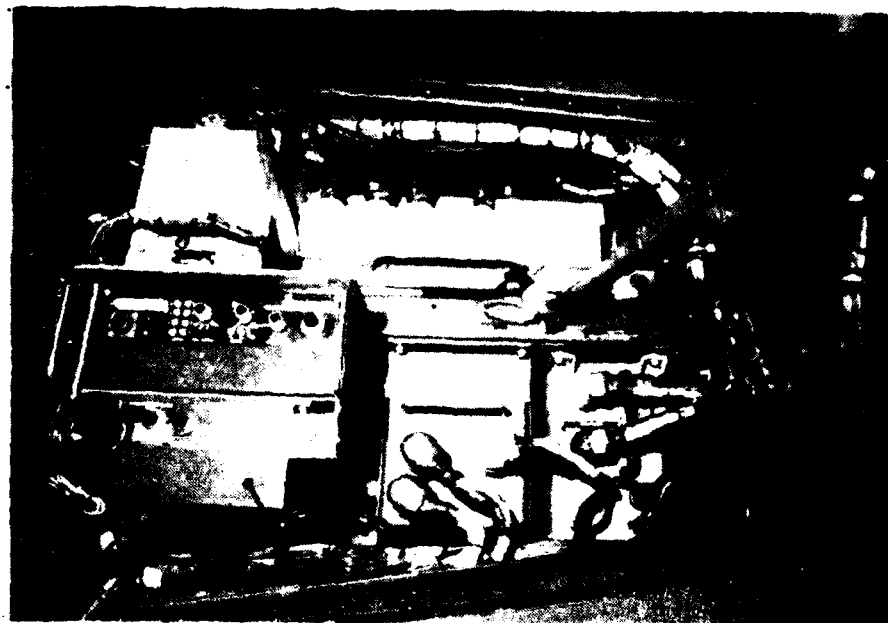
Figure 27. Installation of Control Electronics and Automatic Cut-Off System in the Aircraft
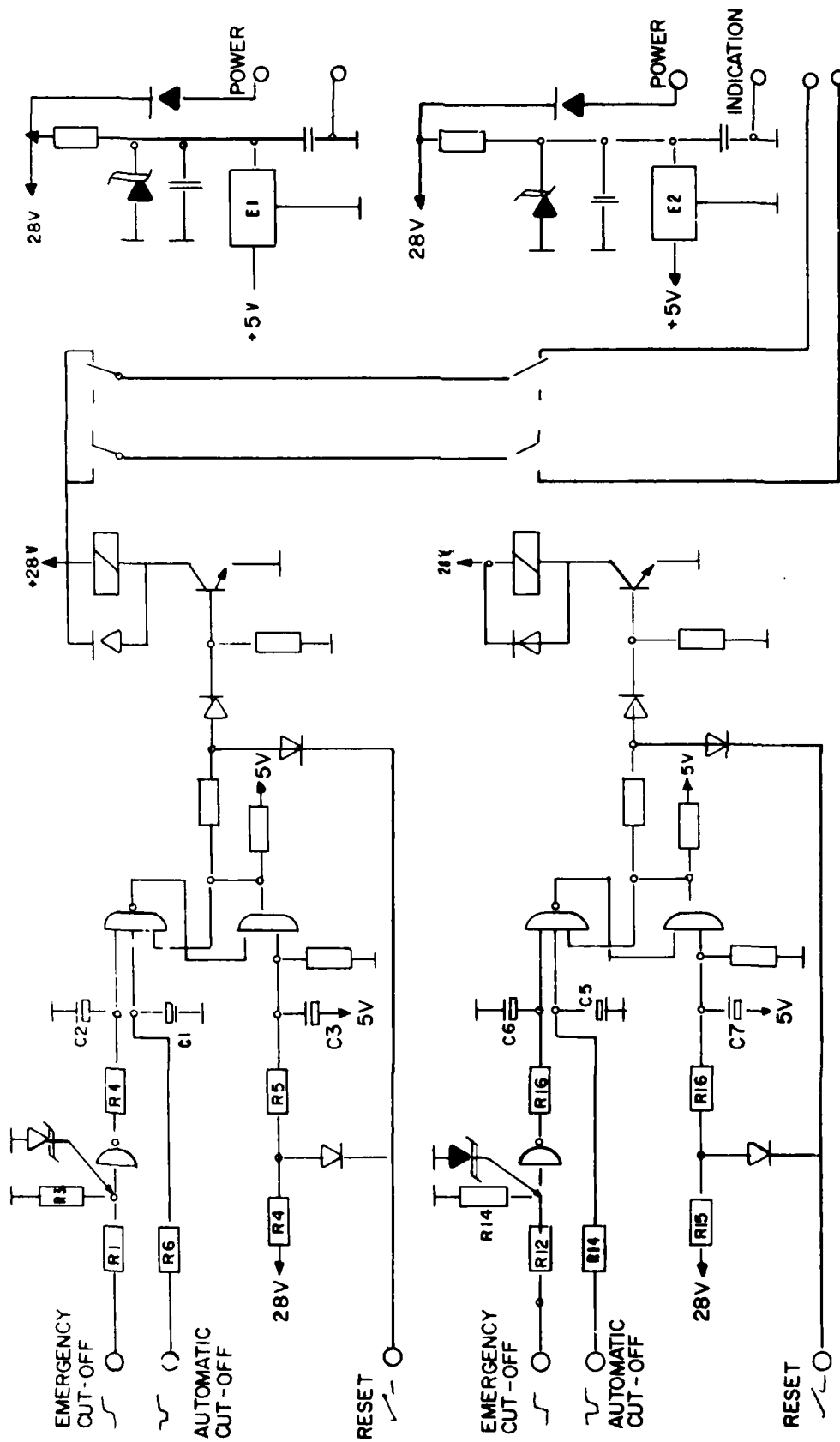
Figure 28. Design of the Cut-Off Logic

Test Nr $\frac{1}{S.1}$

1st WING BENDING

5.4 Hz 5.5 5.6

5.7

5.3

5.2

5.8Hz

180

5.1 4.9 5.9 360

(-) 0.1 4.5 6.8 6.0 (+) 0

6.6 6.4 Hz 6.2

270

90

LEFT / RIGHT WING

OPEN / CLOSED LOOP

INPUT 350 (mV_eff)

SAFE / CRITICAL
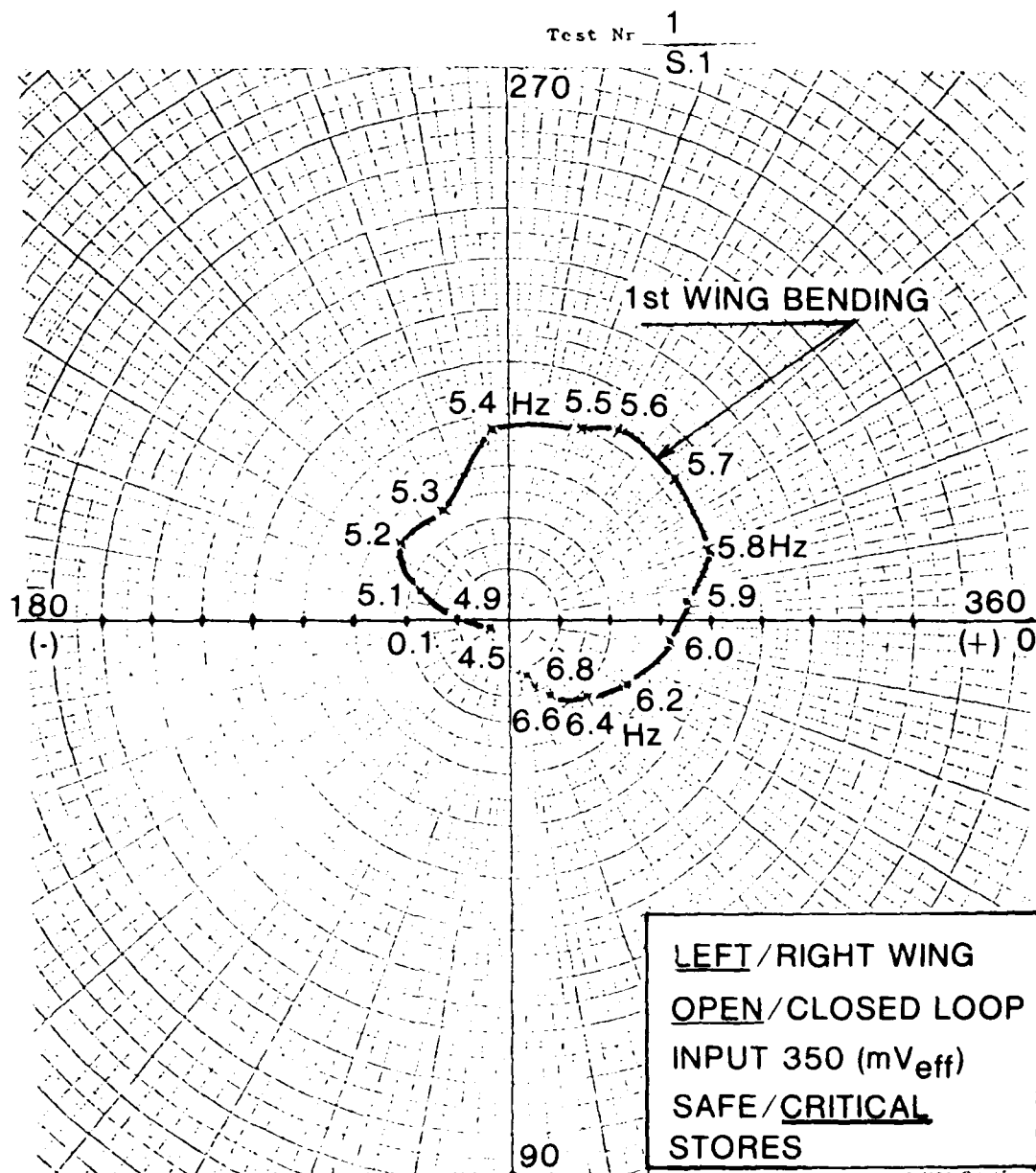
STORES

Figure 29.   Nyquist Diagram, Structural Mode Coupling Test, Left
Wing Bending
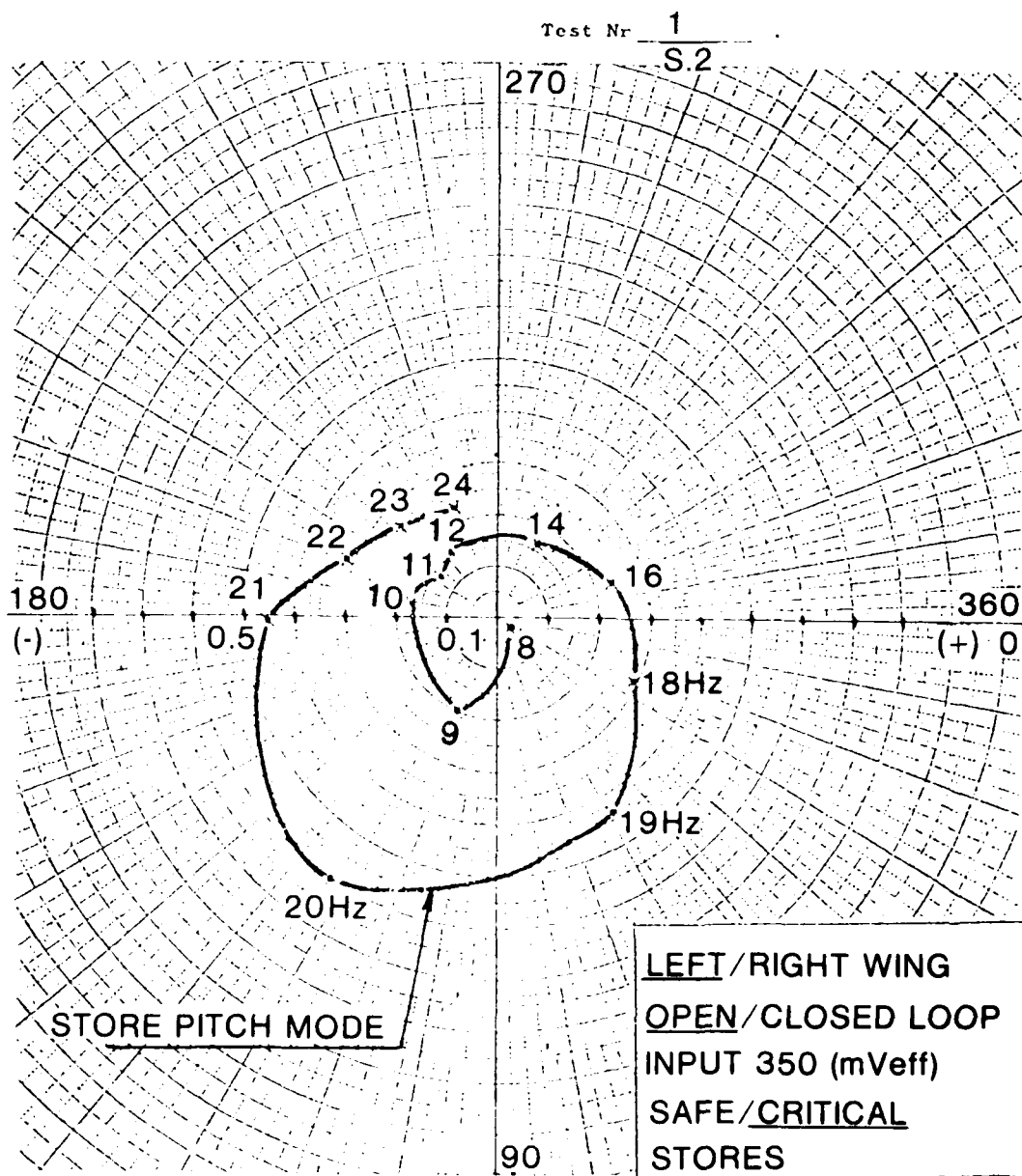
Figure 30. Nyquist Diagram, Structural Mode Coupling Test, Left
Wing Store Pitch
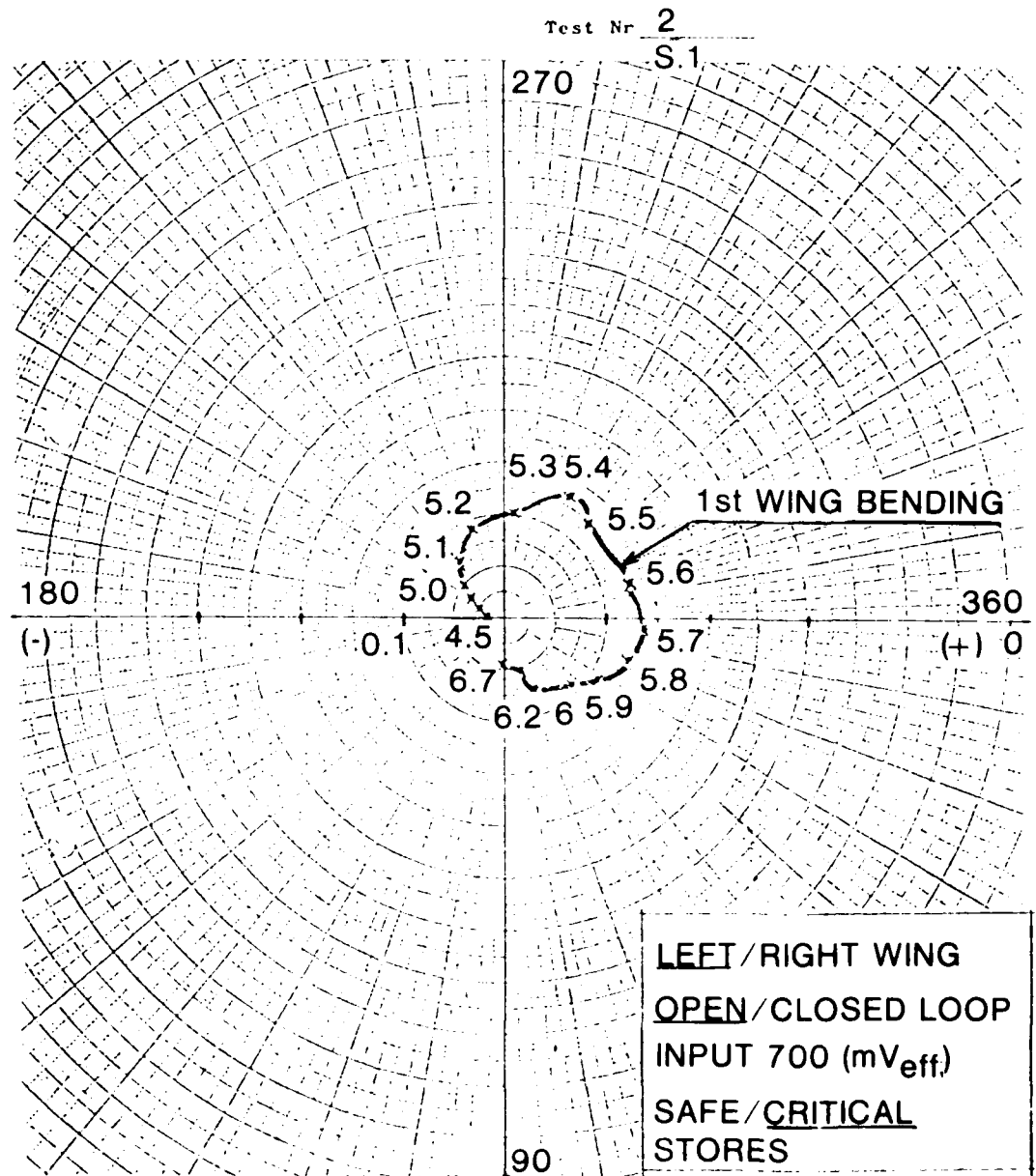
Figure 31. Nyquist Diagram, Structural Mode Coupling Test, Left Wing Bending

Test Nr $\dfrac{2}{S.2}$
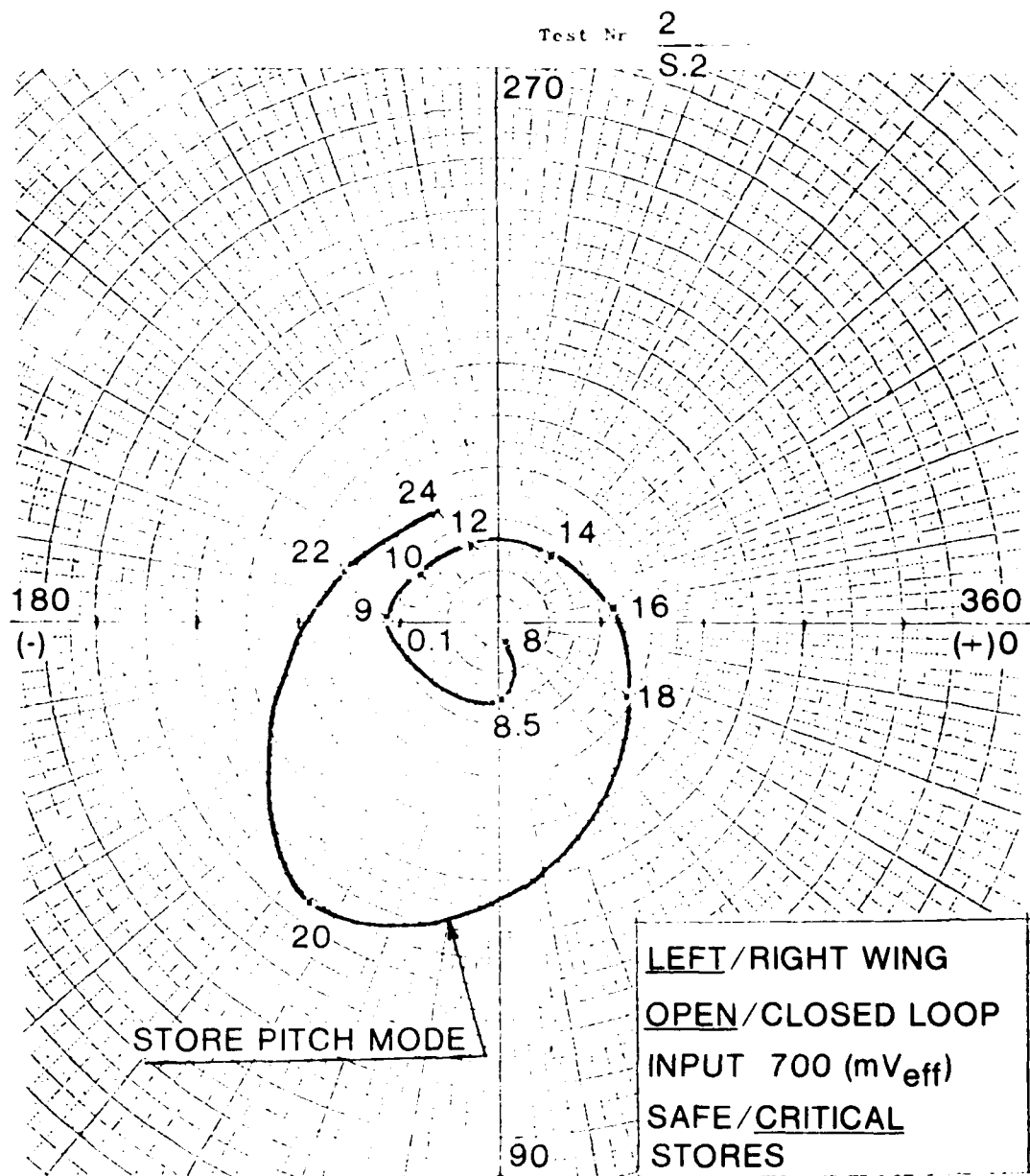
Figure 32. Nyquist Diagram, Structural Mode Coupling Test, Left
Wing Store Pitch
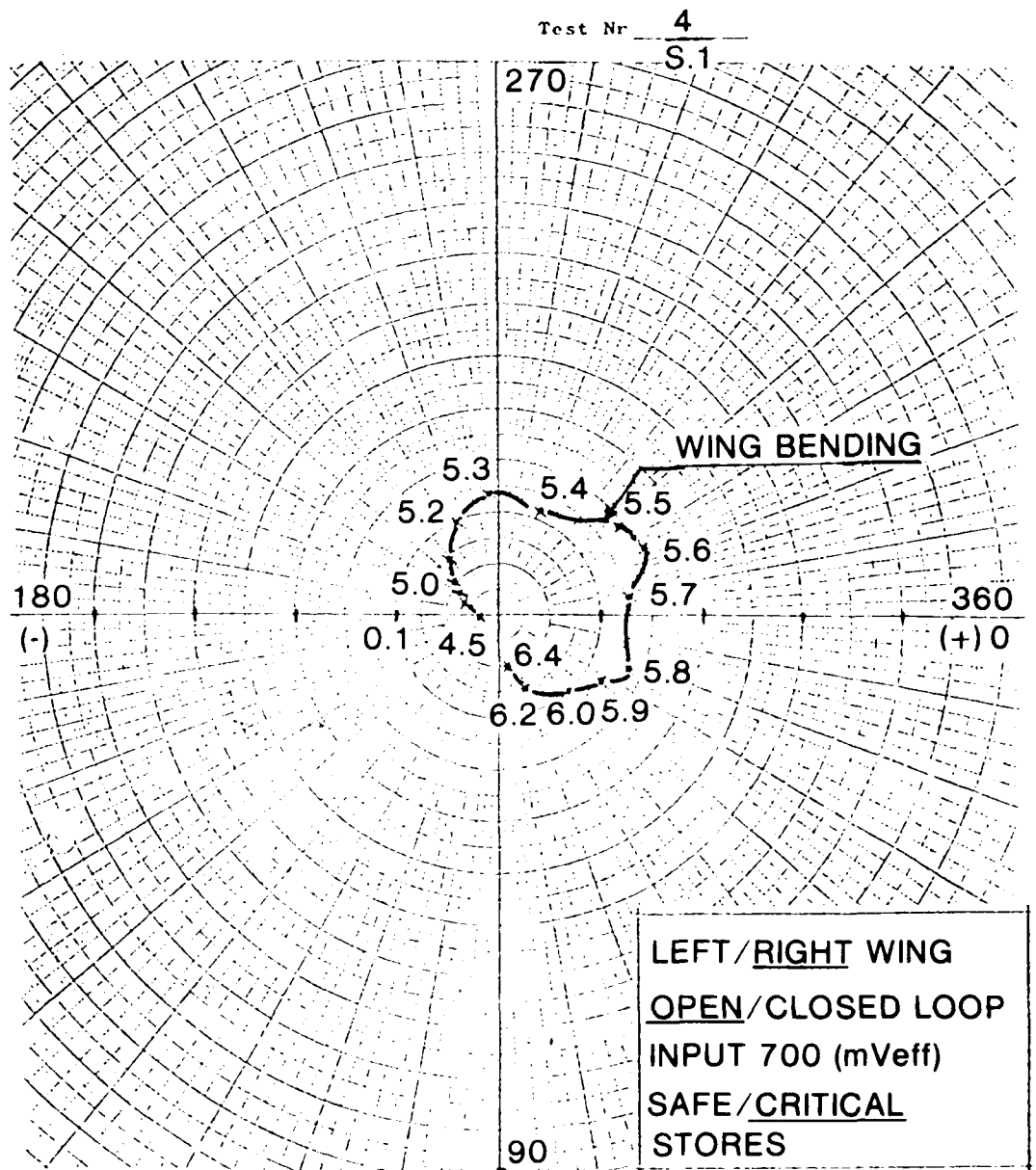
Figure 33.   Nyquist Diagram, Structural Mode Coupling Test, Right Wing Bending

Test Nr **4**
S.2
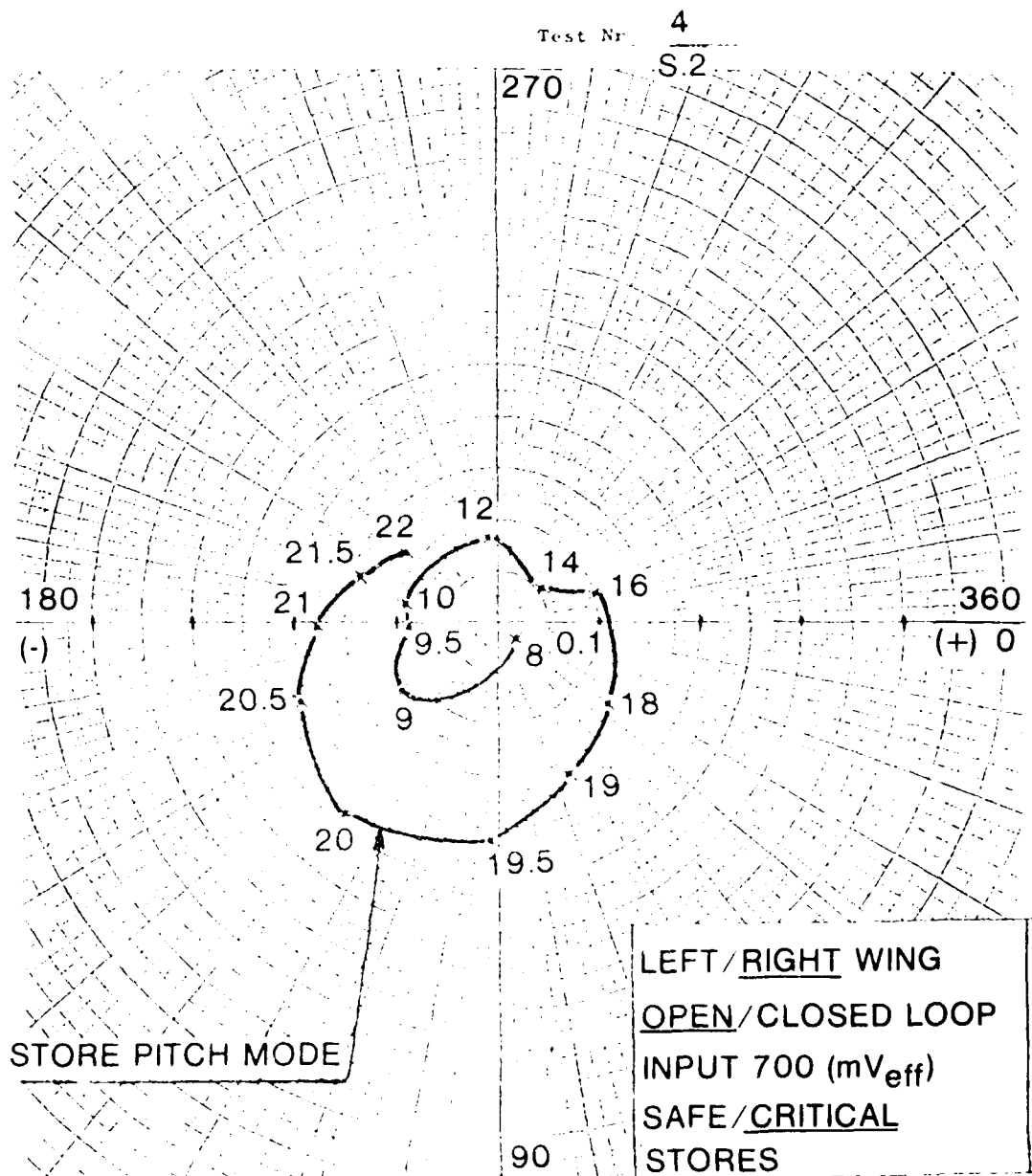
Figure 34. Nyquist Diagram, Structural Mode Coupling Test, Right
Wing Store Pitch

Test Nr __3__
                                                    __S.1__

270

WING BENDING

5.2
      5.4
5.0
180   360
(-)   0.1 4.5   5.6   (+) 0
                      6.2 6 5.7
                              5.8
                              90

LEFT/RIGHT WING
OPEN/CLOSED LOOP
INPUT 1050 (mV$_{eff}$)
SAFE/CRITICAL
STORES
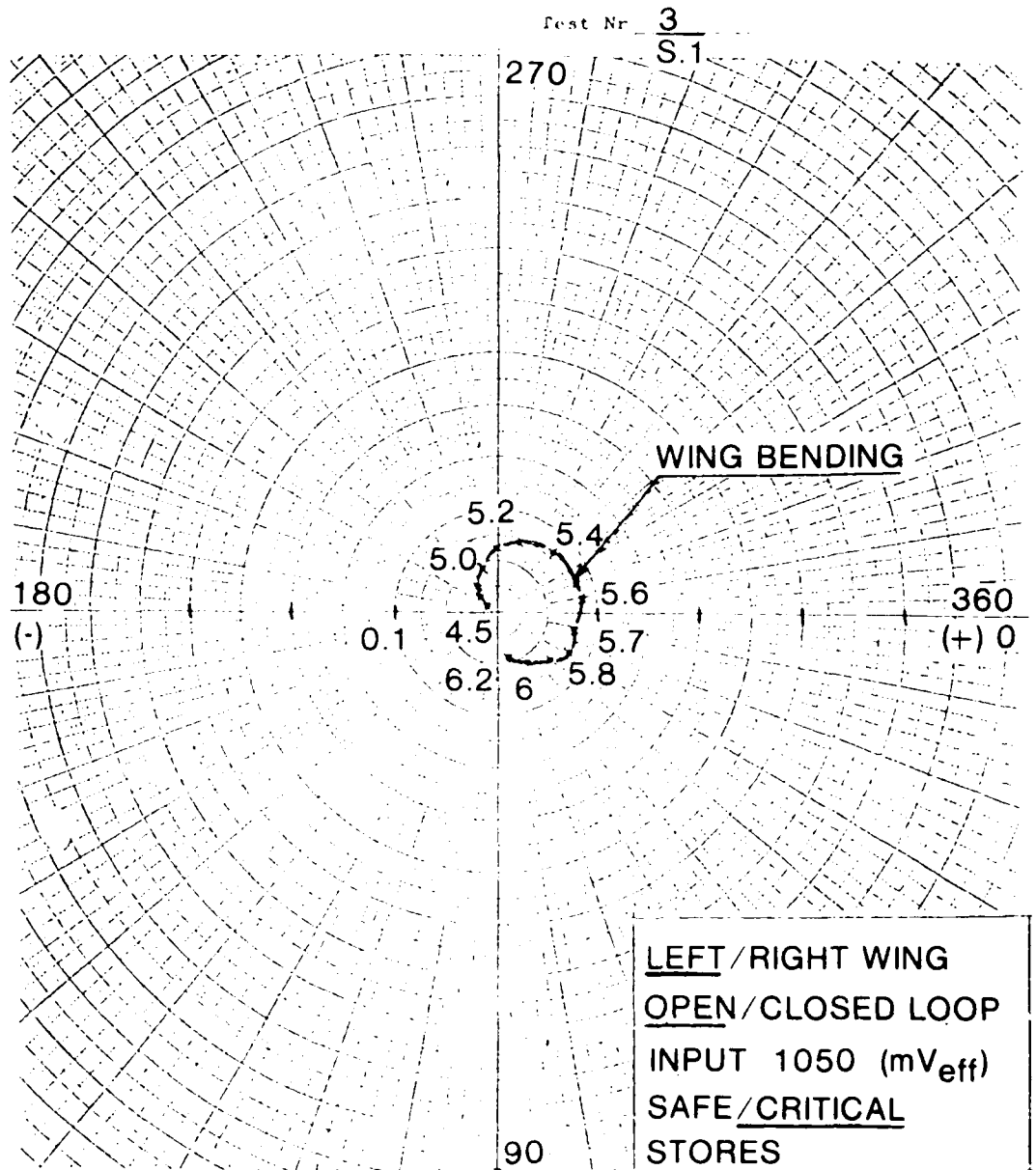
Figure 35.   Nyquist Diagram, Structural Mode Coupling Test, Left
             Wing Bending
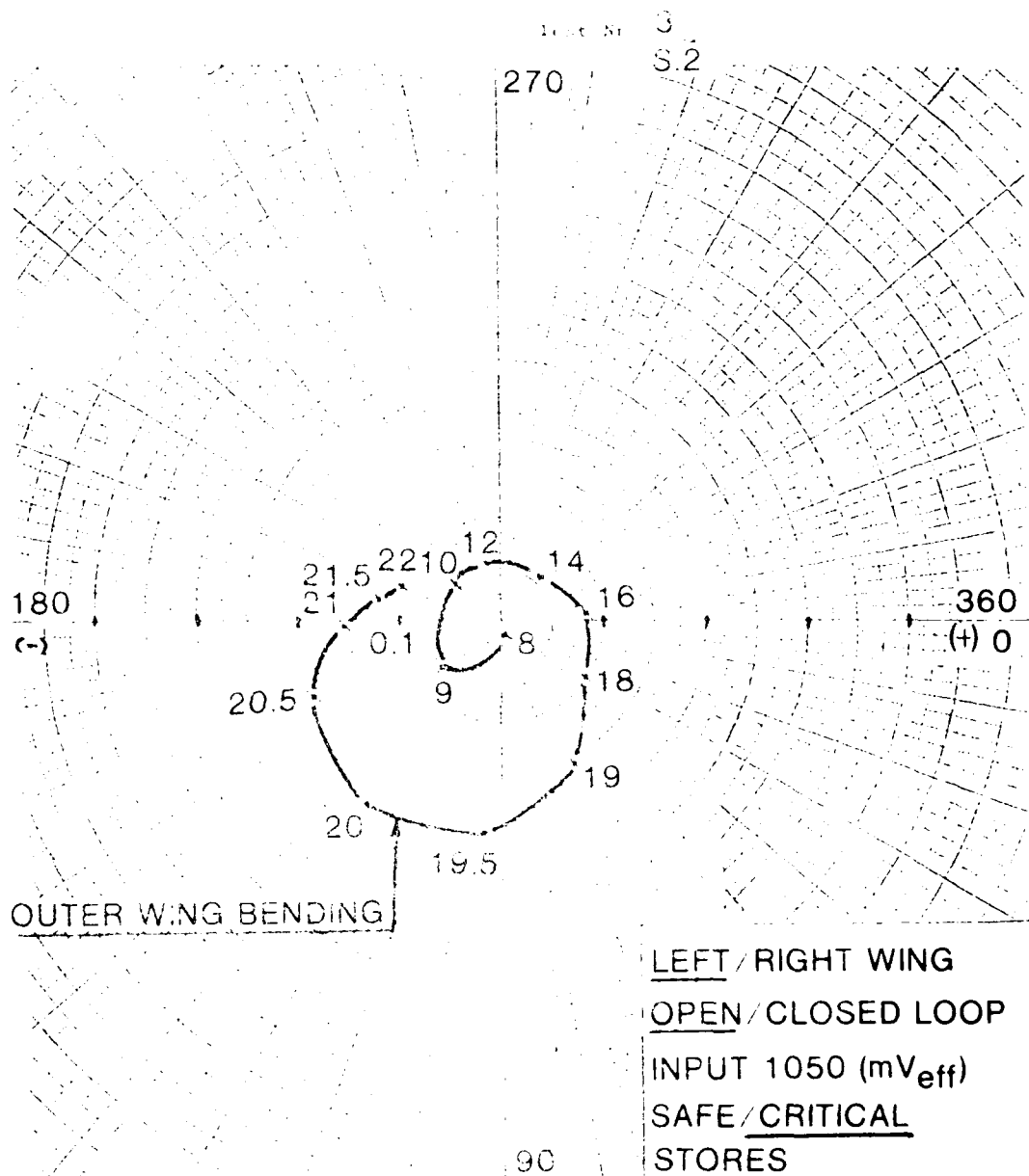
Figure ... Typical ... Structural Mode Coupling Test, Outer Wing Bending (Left)
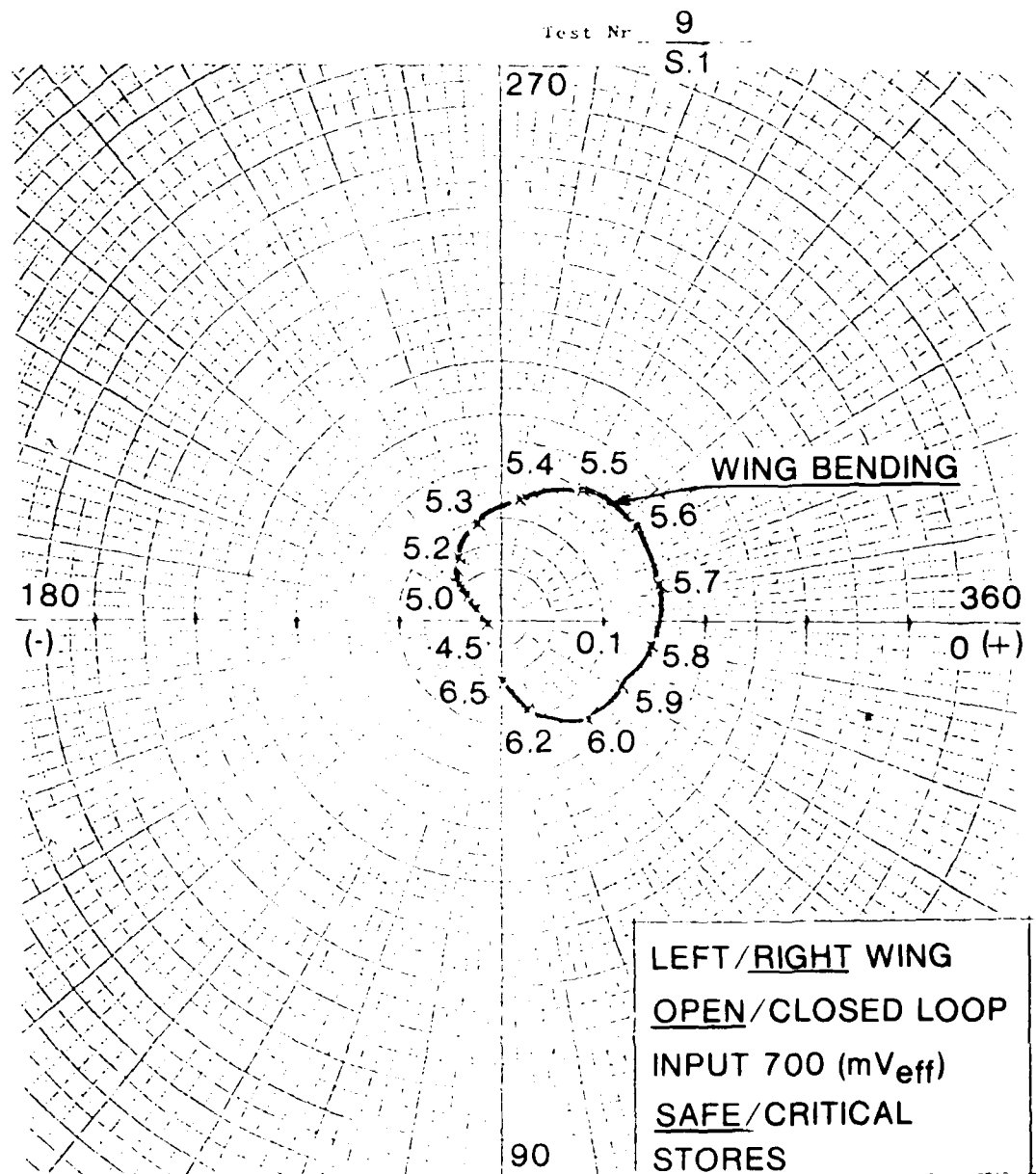
Figure 37. Nyquist Diagram, Structural Mode Coupling Test, Right
Wing Bending

Test Nr 9
S.2

LEFT/RIGHT WING

OPEN/CLOSED LOOP

INPUT 700 (mV$_{eff}$)

SAFE/CRITICAL
STORES
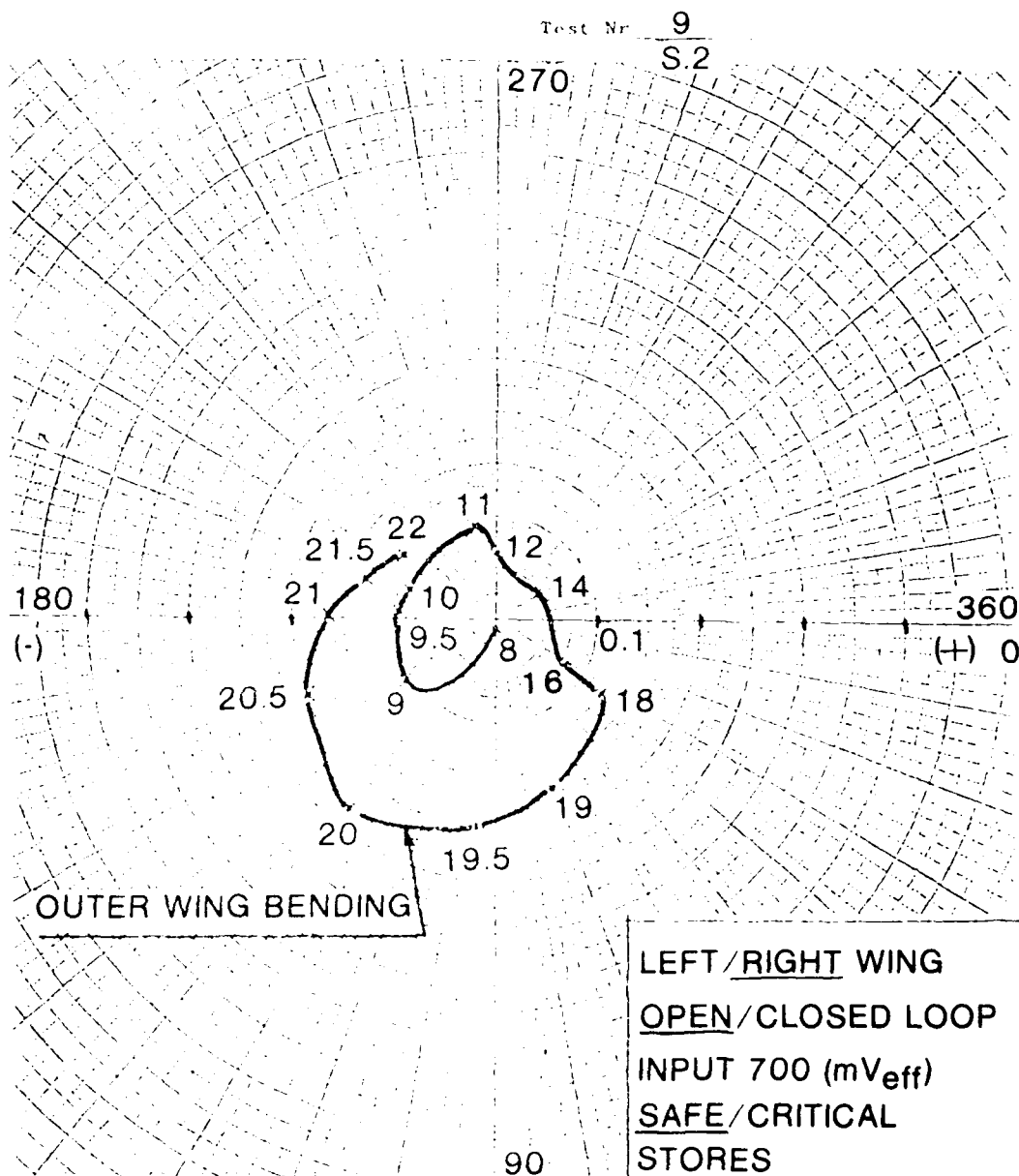
Figure 38. Nyquist Diagram, Structural Mode Coupling Test, Outer
Wing Bending (Right)

Test Nr. 10
S.1

WING BENDING

LEFT/RIGHT WING
OPEN/CLOSED LOOP
INPUT 700 (mV_eff)
SAFE/CRITICAL
STORES
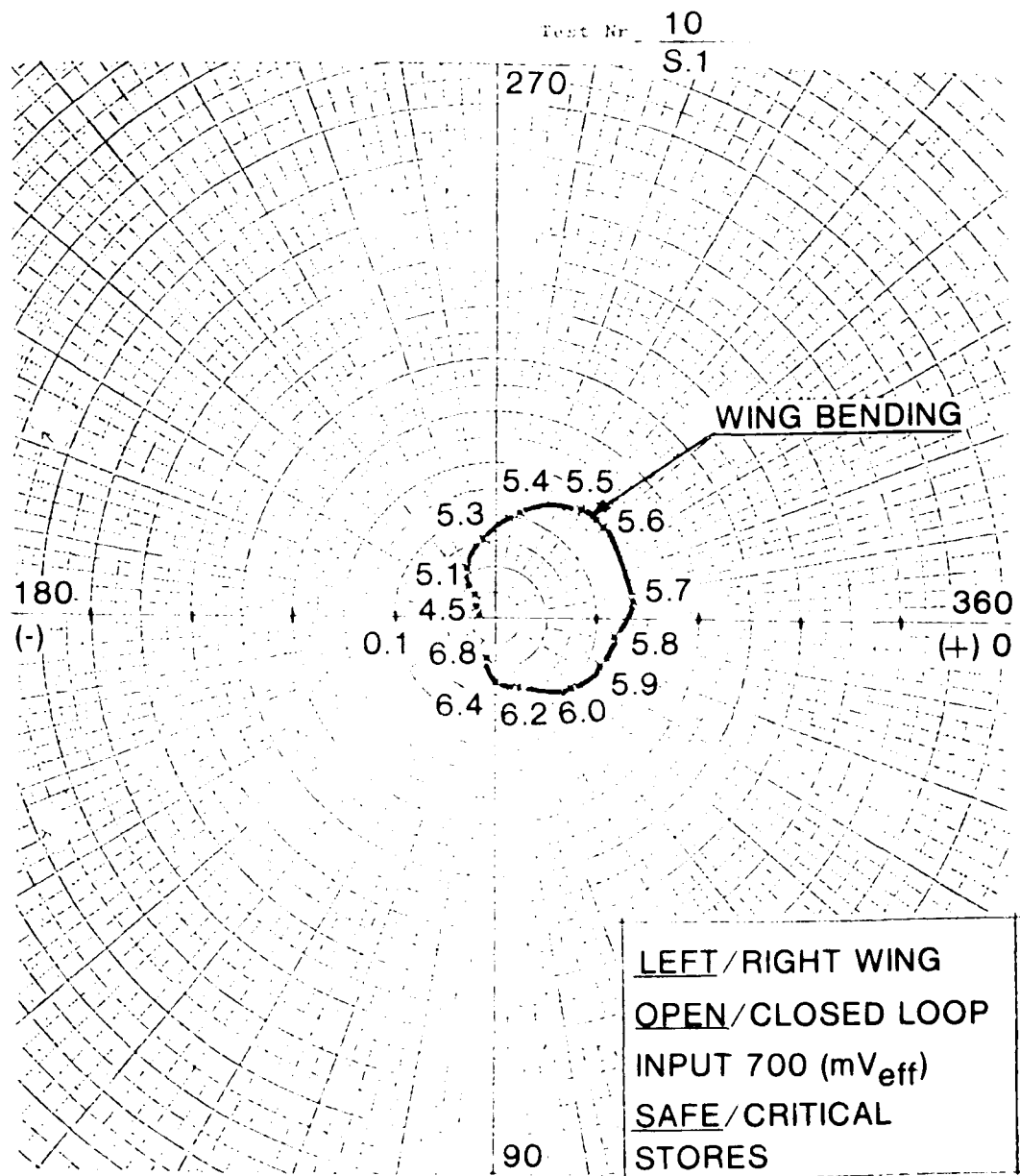
Figure 39.   Nyquist Diagram, Structural Mode Coupling Test, Left
            Wing Bending

73

270

25

22   10 12   14

21.5   16

180   21   9.5   0.1   360

(-)   8   0 (+)

9

18

18.5

20.5

19

20

19.5

OUTER WING BENDING

LEFT/RIGHT WING

OPEN/CLOSED LOOP

INPUT 700 (mV$_{eff}$)

SAFE/CRITICAL

90   STORES
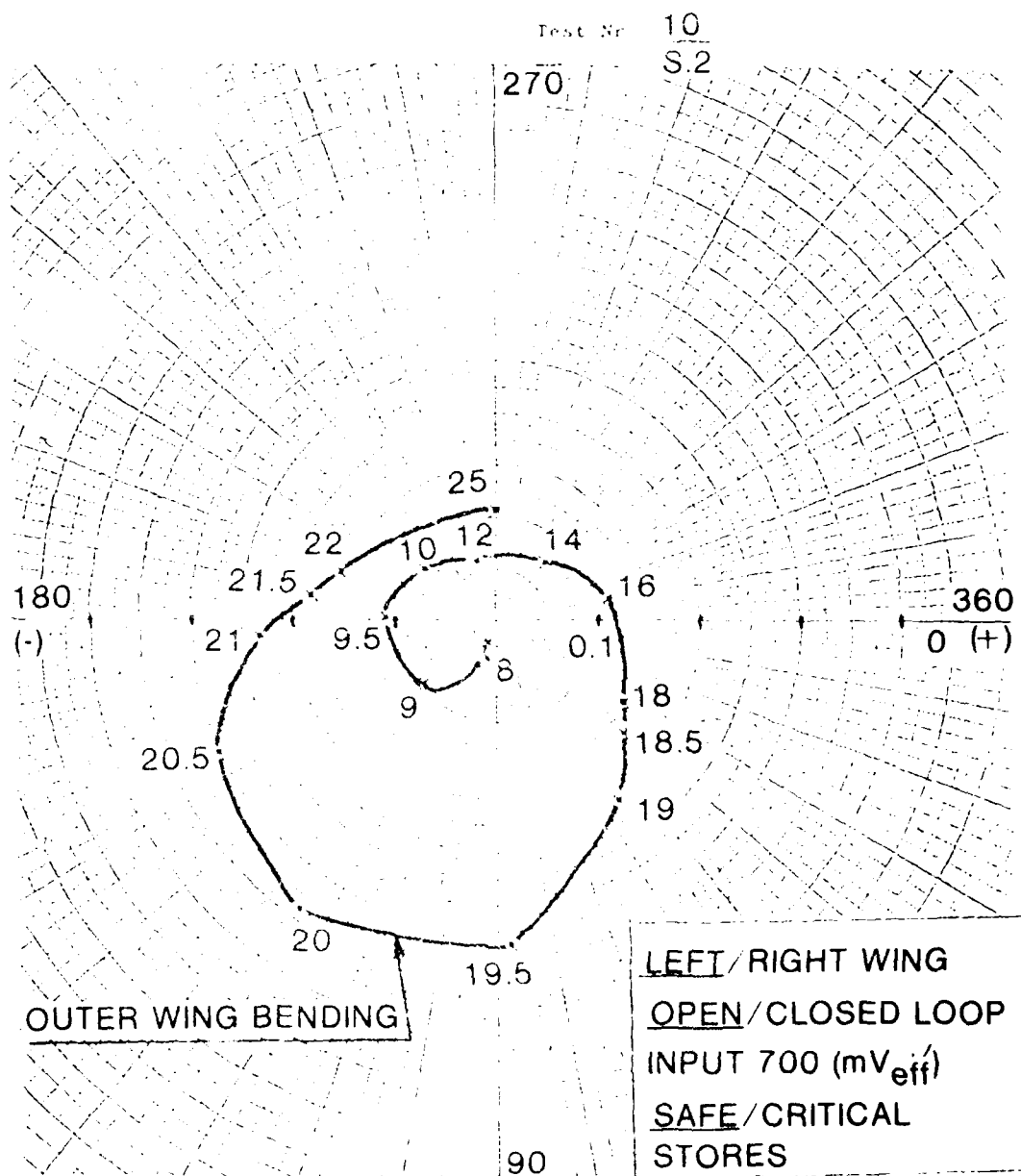
Figure 40.   Nyquist Diagram, Structural Mode Coupling Test, Outer
             Wing Bending (Left)
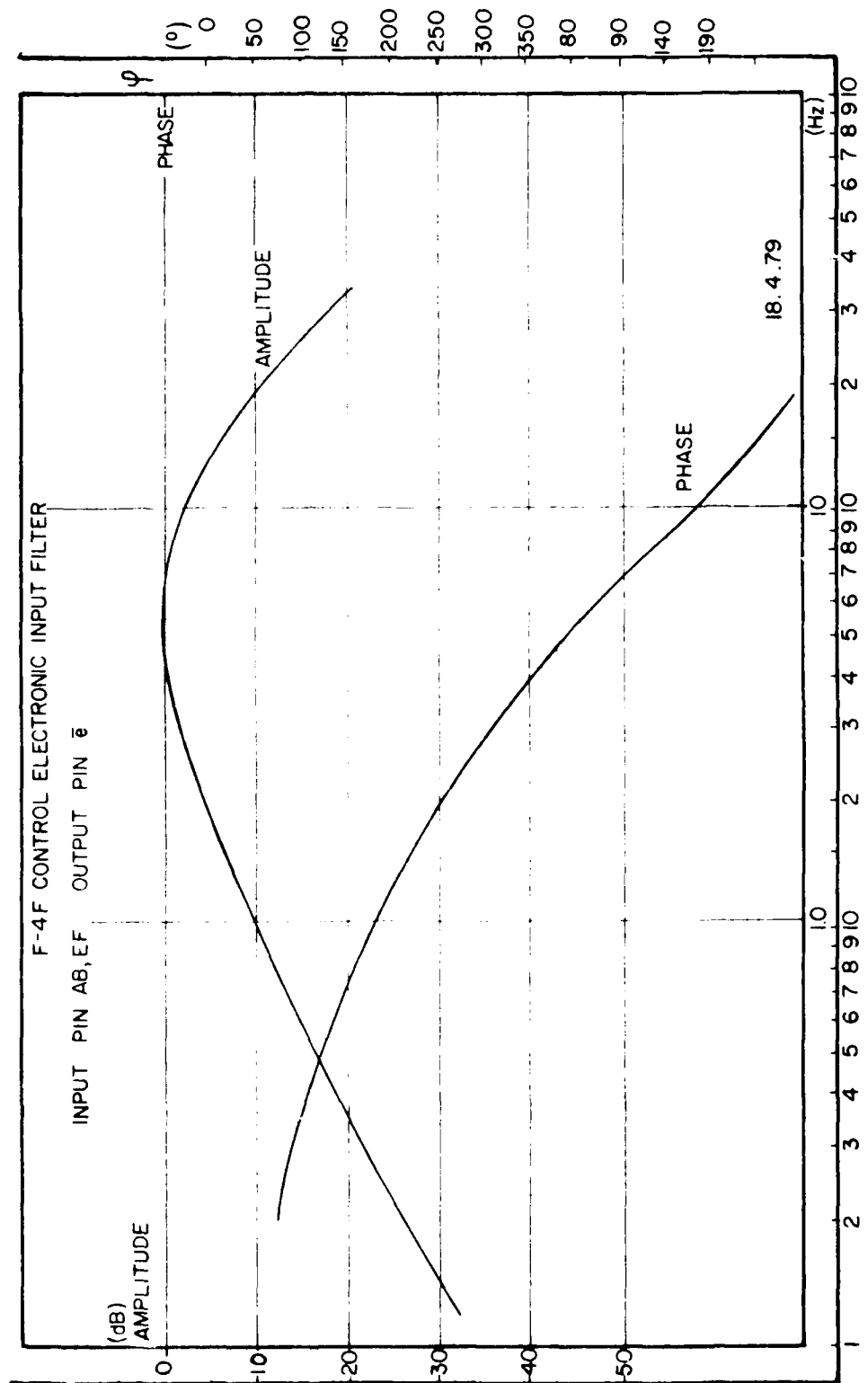
Figure 41. Transfer Function of the Control Electronics

Figure 4. Nomographic Diagram, Structural Mode Coupling Test, Store Pitch
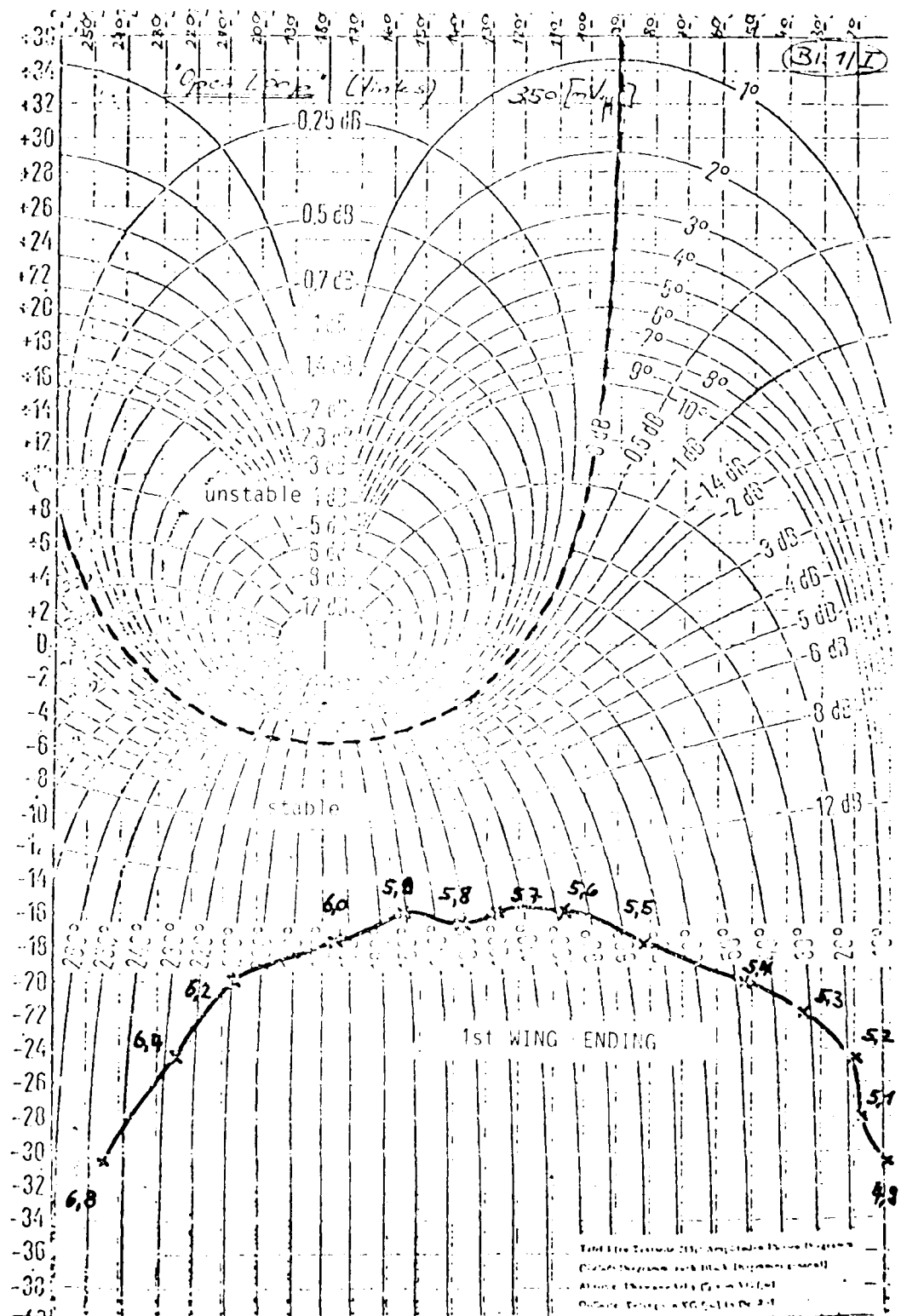
Figure 43. Nichols Diagram, Structural Coupling Test, First Wing
Bending
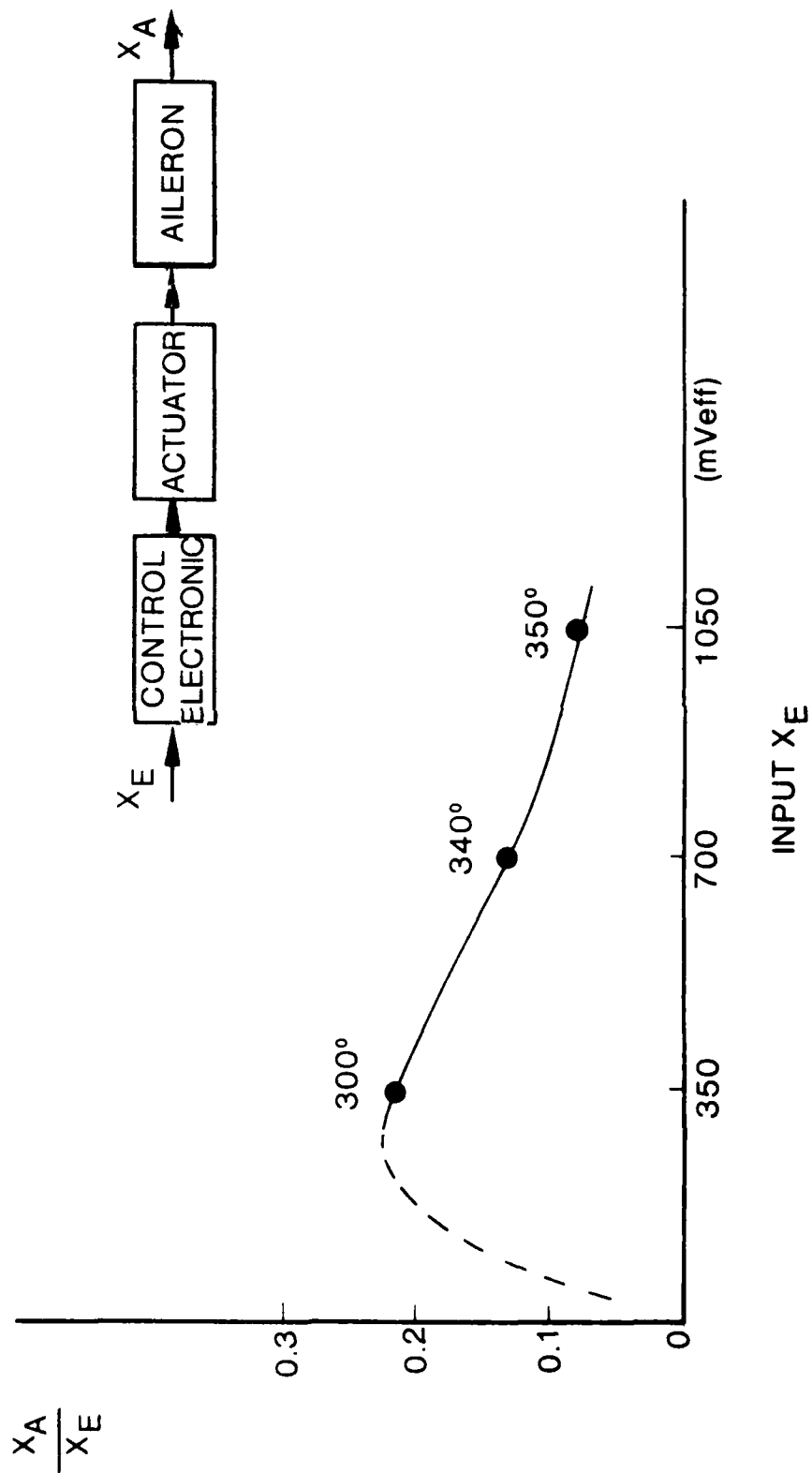
Figure 44. Effect of Non-Linearities in the Aileron Actuating System

STORE MASS 1500 kg

ρ=1.28 m

7.28 Hz
PYLON PITCH
RIGID

6.52 Hz
PYLON PITCH
1.8

6.6 Hz GVT

6.29 Hz
PYLON PITCH
1.4

5.97 Hz
PYLON PITCH
1.0
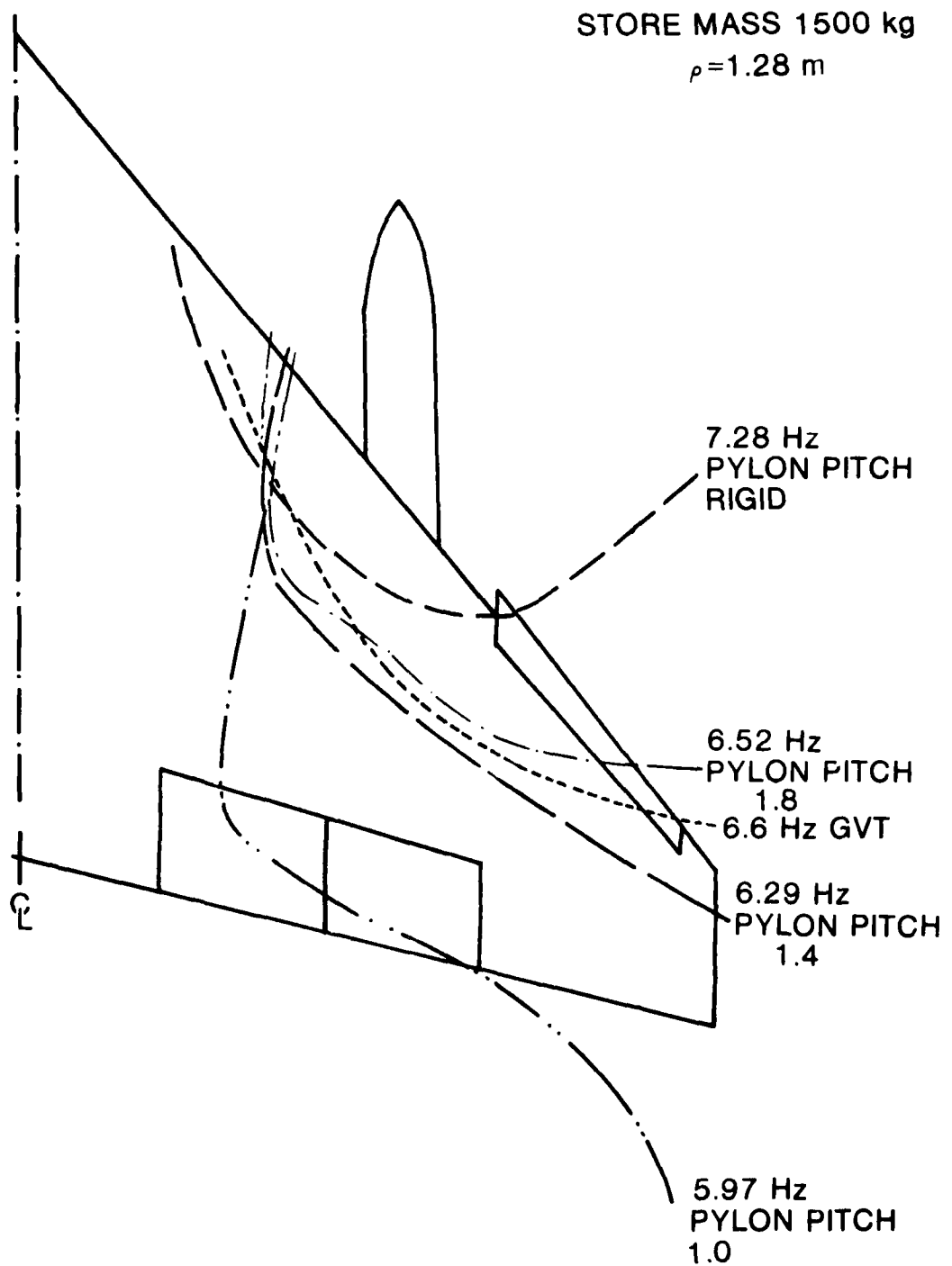
Figure 45. Shift of the Node Line for the Store Pitch Mode Due to
Variations of the Pylon Pitch Stiffness

CONFIGURATION 1

y

F4F PITCH / 1.8 : LBFK 15 $\rho = 1.28$ m

1. SYM FREQ.: 5.46 Hz

MODIFIED CALCULATION
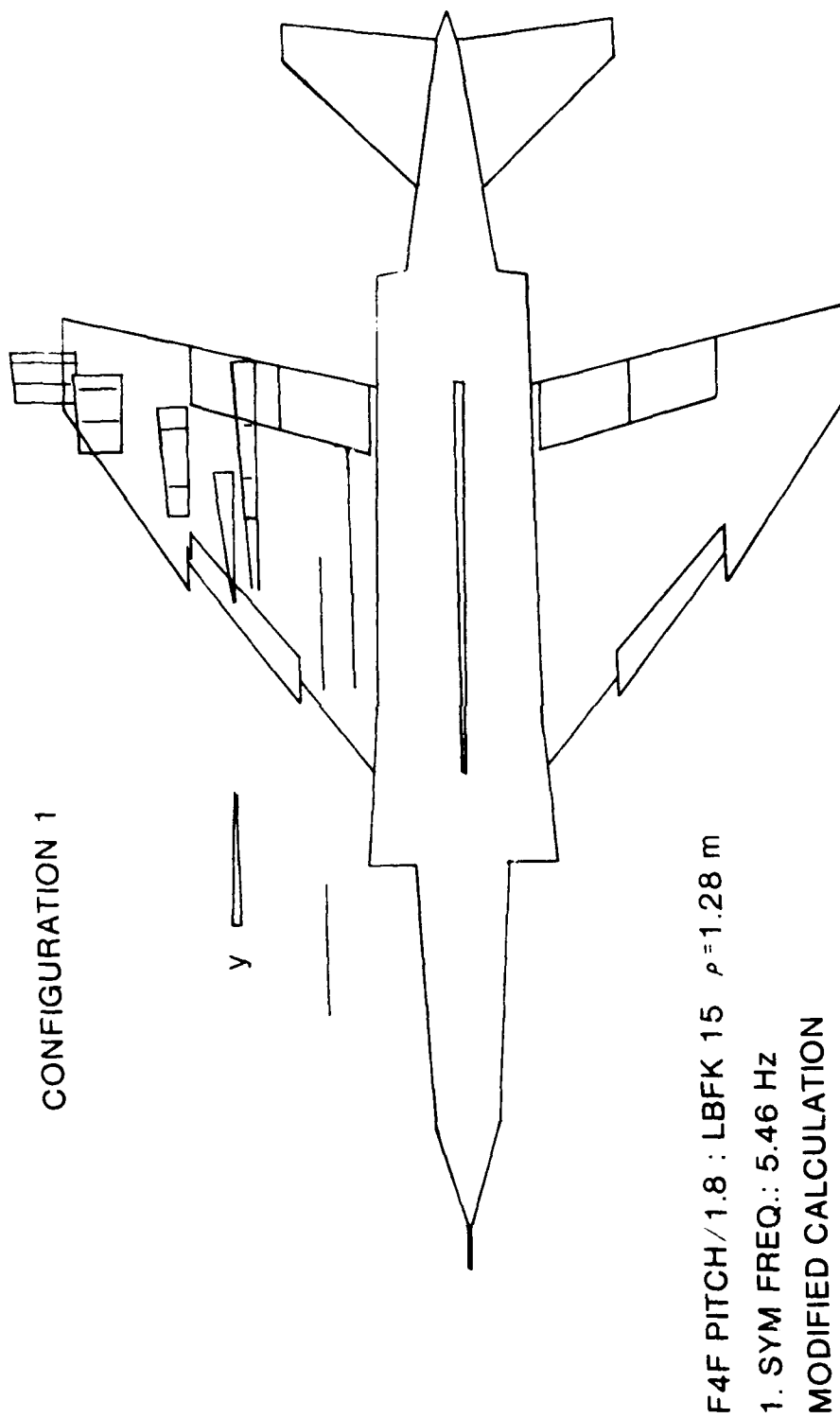
Figure 46.   Calculated 1st Wing Bending with Adjusted Pylon Pitch
Stiffness

CONFIGURATION 1

y
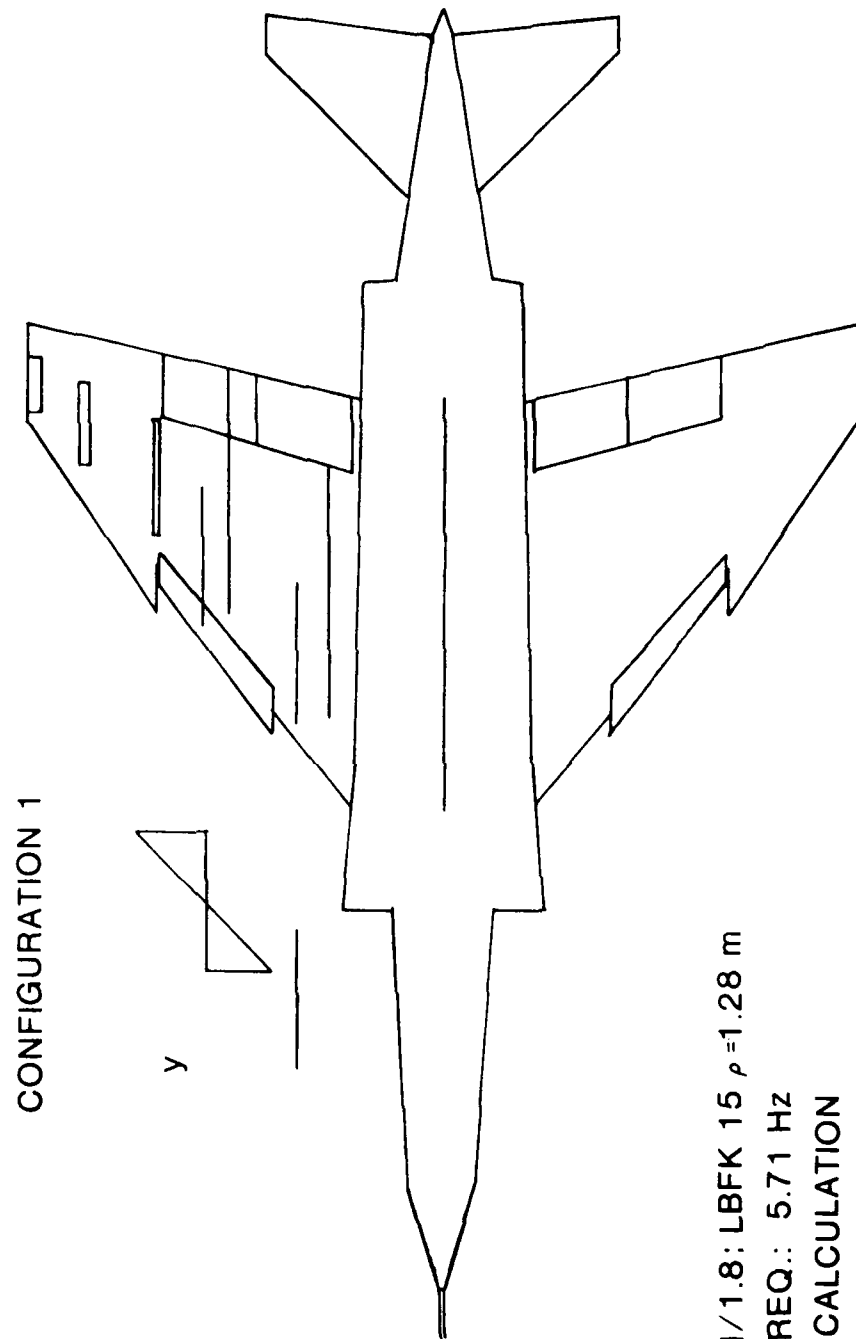
F4F PITCH/1.8: LBFK 15 ρ =1.28 m

2. SYM. FREQ.: 5.71 Hz

MODIFIED CALCULATION

Figure 47. Calculated Store Yaw Mode with Adjusted Pylon Pitch Stiffness

81

CONFIGURATION 1

y
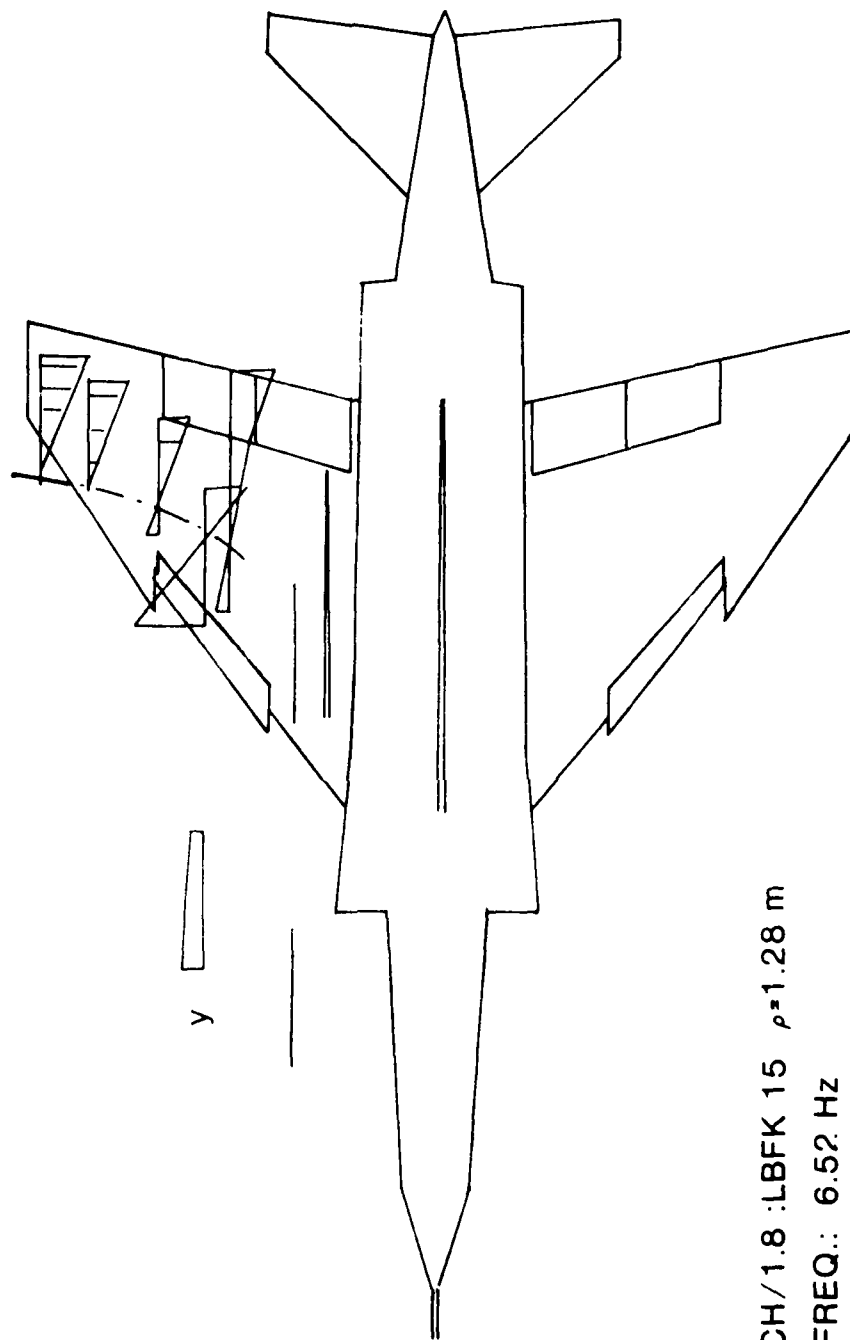
F4F PITCH/1.8 :LBFK 15 ρ=1.28 m

3.SYM FREQ.: 6.52 Hz

MODIFIED CALCULATION

Figure 48. Calculated Store Pitch Mode with Adjusted Pylon Pitch
Stiffness

CONFIGURATION 1

y

F4F PITCH/ 1.8 : LBFK 15 ρ=1.28 m

4.SYM FREQ .: 8.47 Hz

MODIFIED CALCULATION
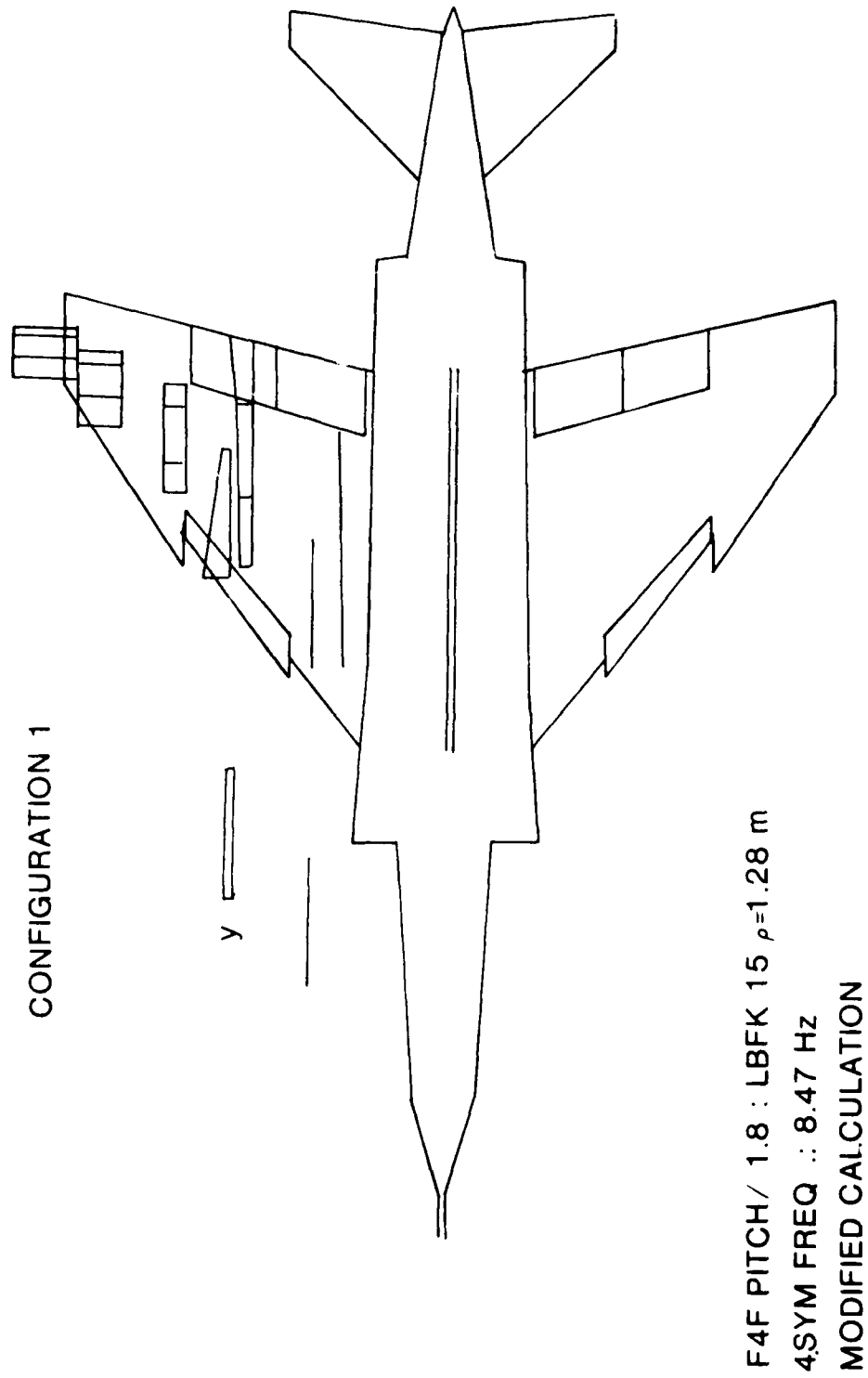
Figure 49. Calculated Store Roll Mode with Adjusted Pylon Pitch Stiffness

83

END

DATE
FILMED

DTIC

MICROCOPY RESOLUTION TEST CHART

NATIONAL BUREAU OF STANDARDS-1963-A

CONFIGURATION 2

F4F PITCH/1.8 : LBFK 18 / ρ≈1.34 m

1 SYM. FREQ.: 5.41 Hz

MODIFIED CALCULATION
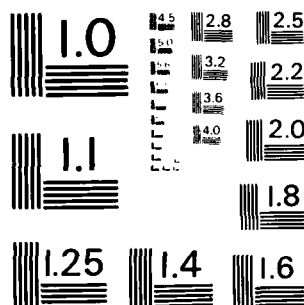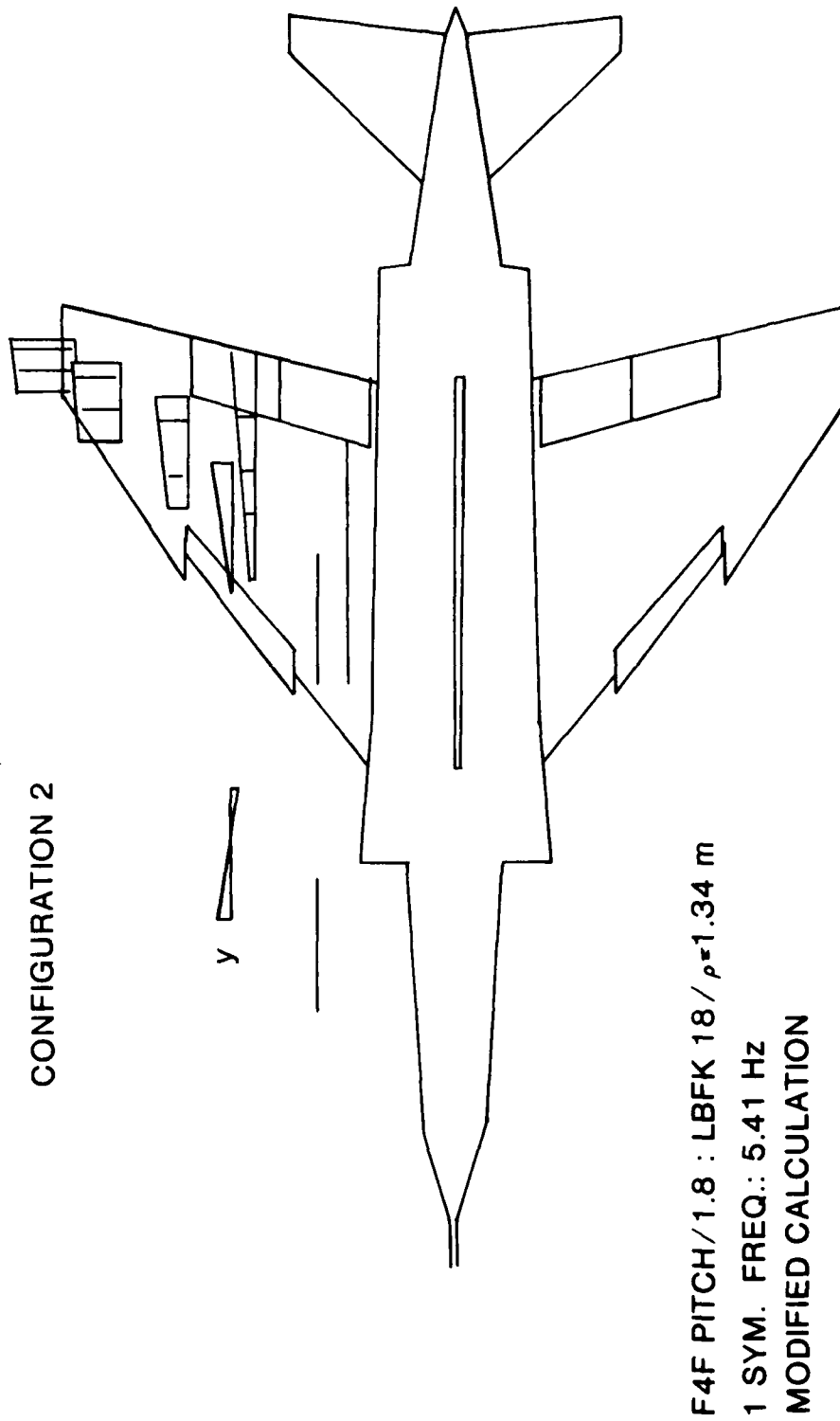
Figure 50.   Calculated 1st Wing Bending with Adjusted Pylon Pitch
Stiffness

CONFIGURATION 2

F4F PITCH/1.8 LBFK 18/ ρ=1.34 m
2 SYM FREQ.: 5.47 Hz
MODIFIED CALCULATION
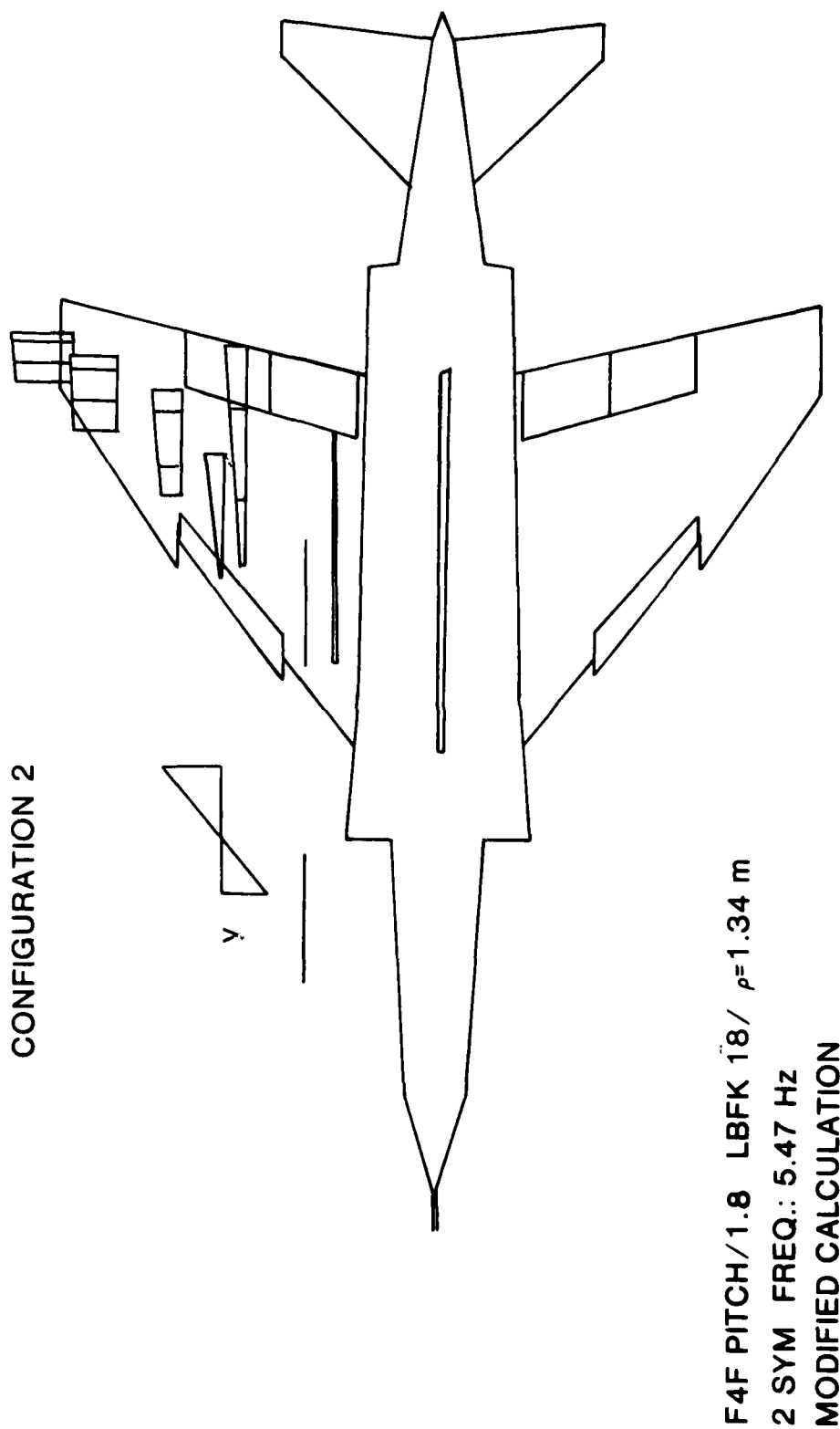
Figure 51. Calculated Store Yaw Mode with Adjusted Pylon Pitch
Stiffness

85

CONFIGURATION 2

y
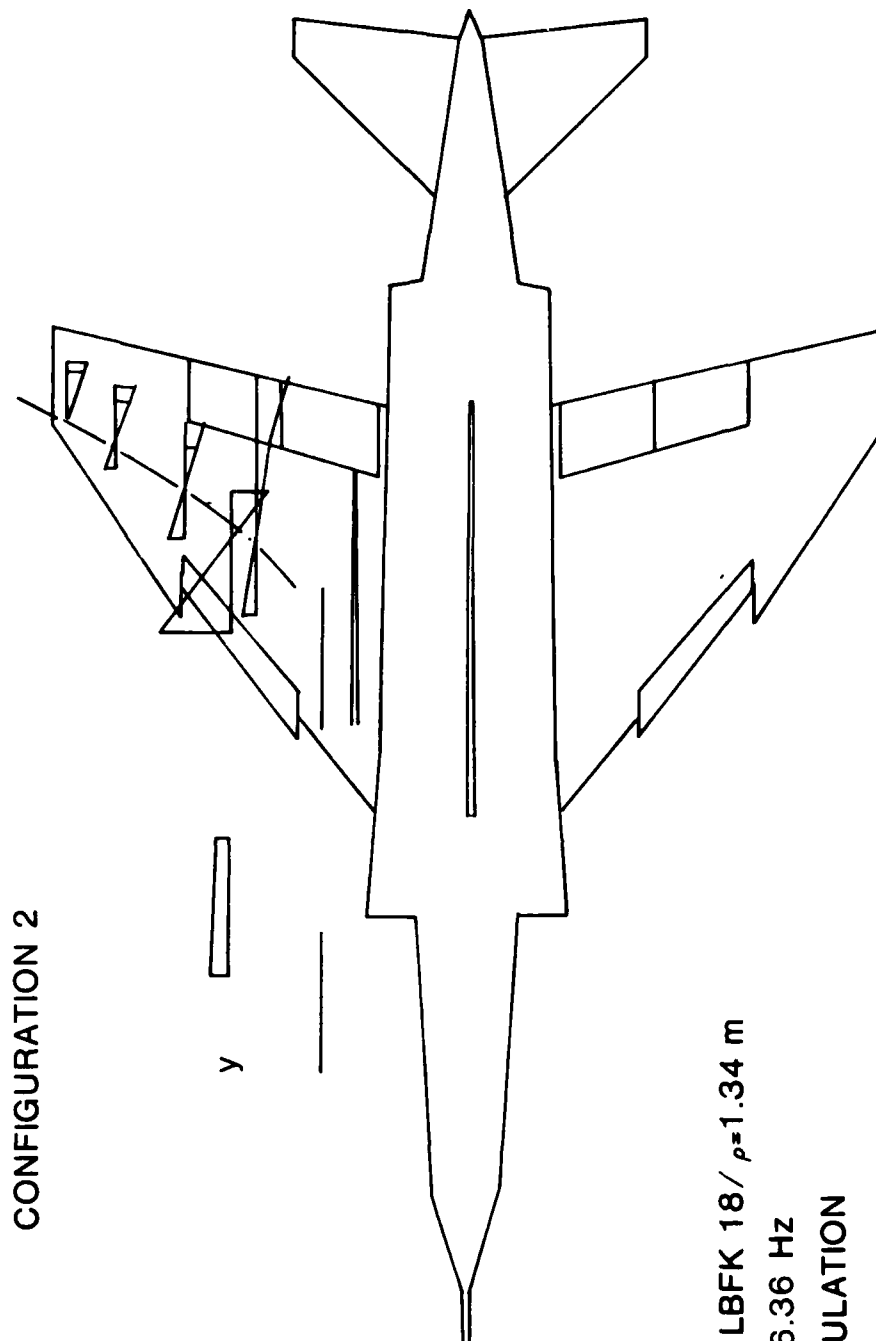
F4F PITCH/1.8 LBFK 18/ ρ=1.34 m

3. SYM FREQ.: 6.36 Hz

MODIFIED CALCULATION

Figure 52.   Calculated Store Pitch Mode with Adjusted Pylon Pitch Stiffness

CONFIGURATION 2

y

F 4 F PITCH/1.8 : LBFK 18 ρ=1.34m
4.SYM. FREQ.: 8.45 Hz
MODIFIED CALCULATION
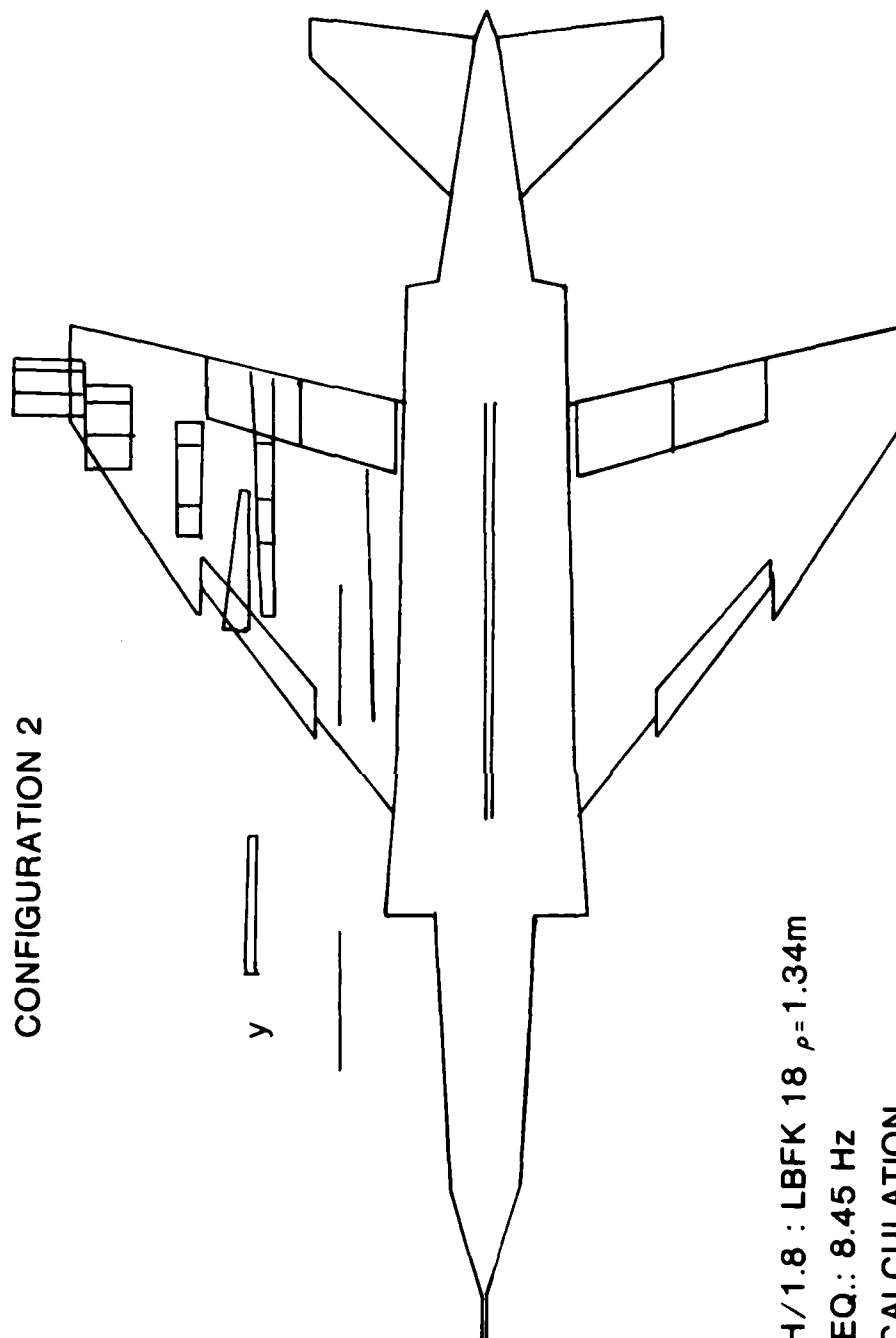
Figure 53. Calculated Store Roll Mode with Adjusted Pylon Pitch
Stiffness

CONFIGURATION 1M
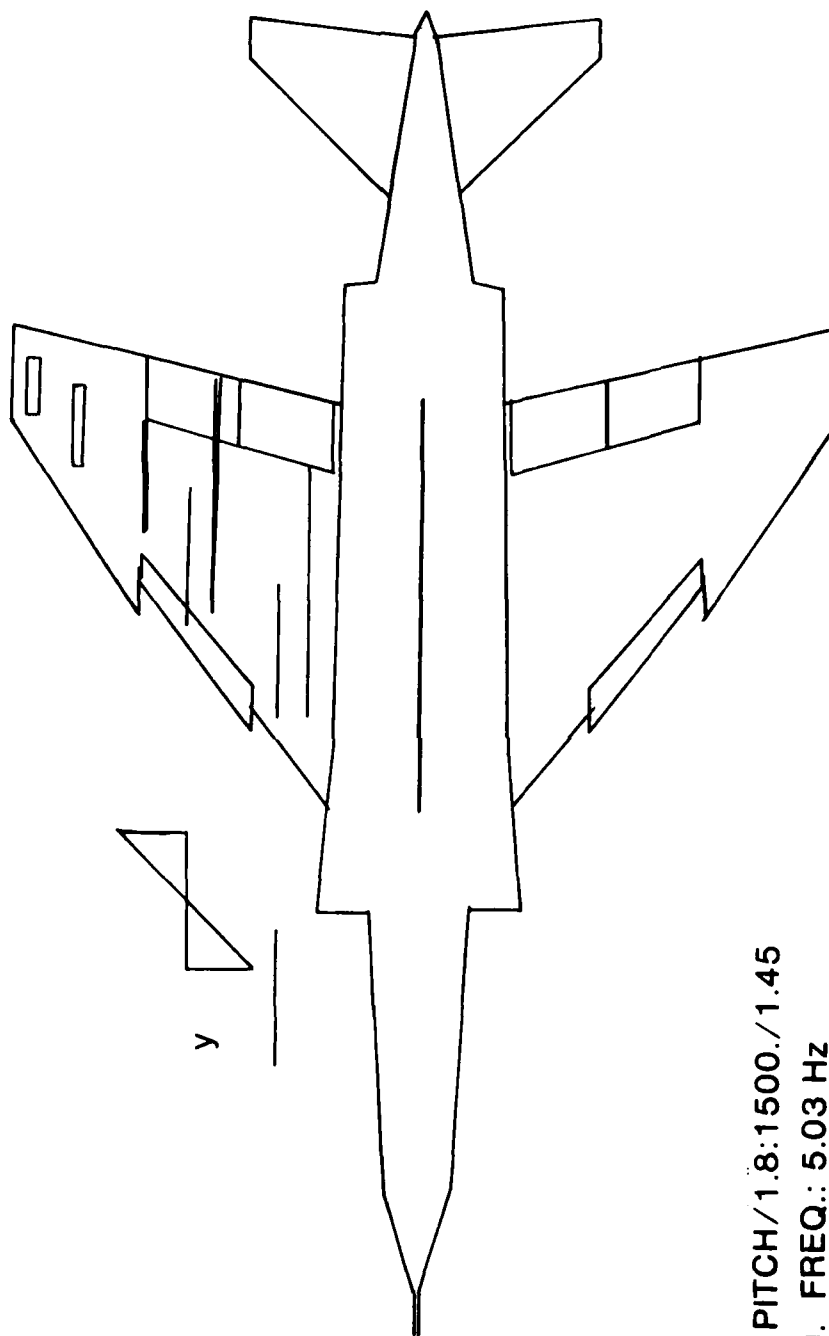
F-4 F PITCH/1.8:1500./1.45
1.SYM. FREQ.: 5.03 Hz

Figure 54. Calculated Store Yaw Mode with Modified Store Radius of Gyration and Adjusted Pylon Pitch Stiffness

CONFIGURATION 1 M

y

F-4 F PITCH/1.8:1500./1.45
2.SYM. FREQ.: 5.31 Hz
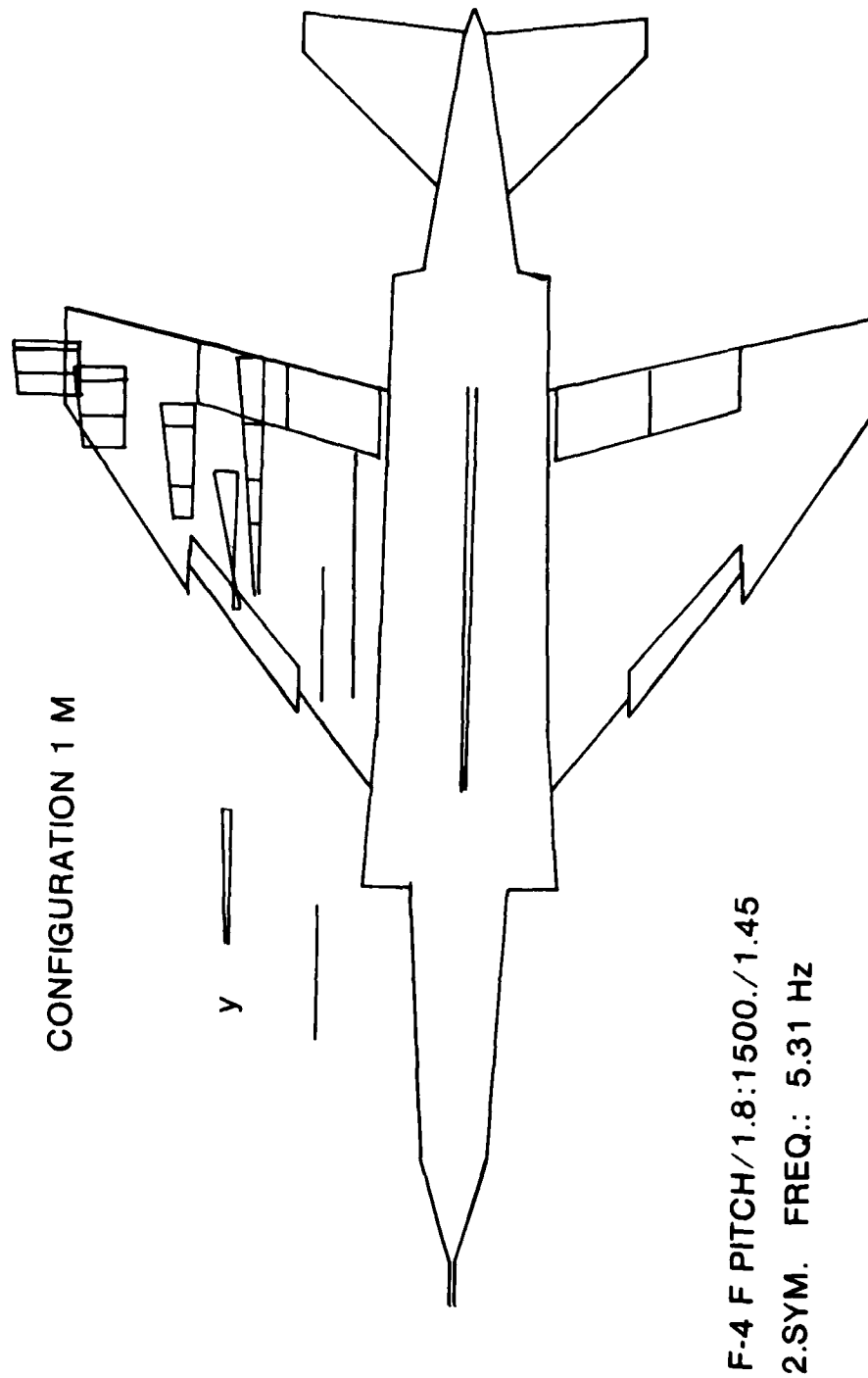
Figure 55. Calculated 1st Wing Bending Mode with Modified Store Radius of Gyration and Adjusted Pylon Pitch Stiffness

CONFIGURATION 1 M

F-4 F PITCH/1.8:1500./1.45
3.SYM. FREQ.: 6.10 HZ

y
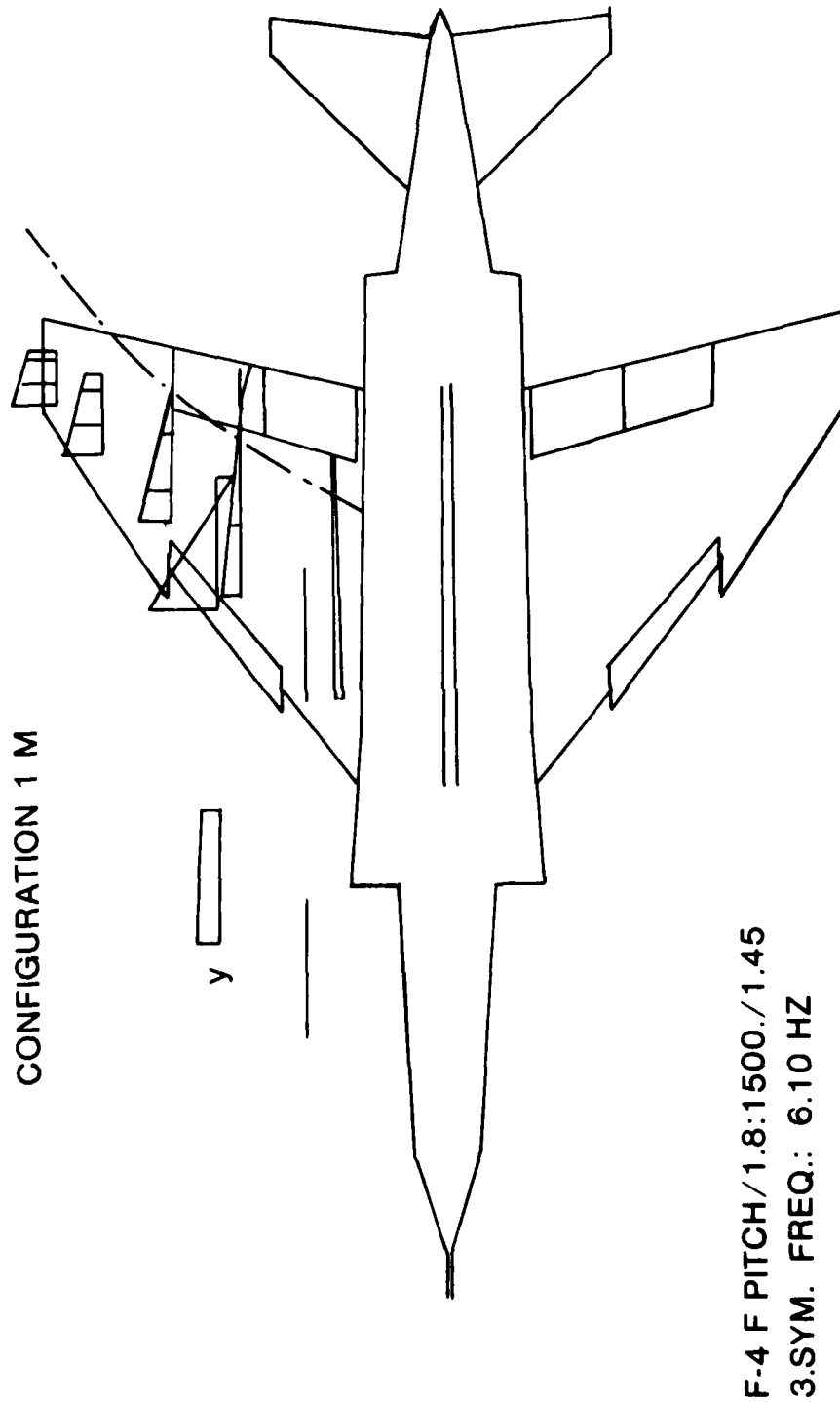
Figure 56. Calculated Store Pitch Mode with Modified Store Radius of
Gyration and Adjusted Pylon Pitch Stiffness

CONFIGURATION 1 M

F-4 F PITCH/1.8:1500./1.45

4.SYM. FREQ.: 8.41 Hz
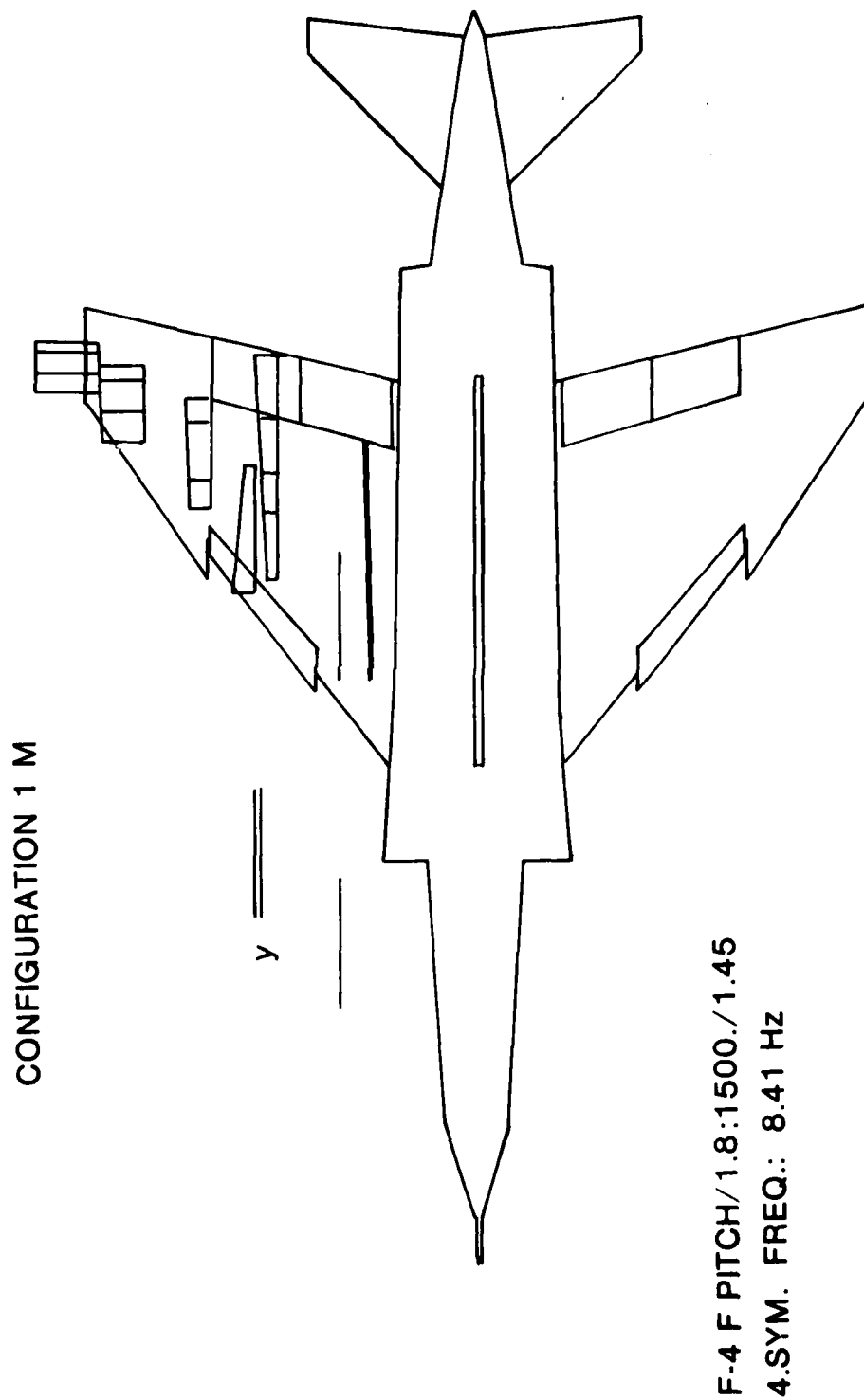
Figure 57. Calculated Store Roll Mode with Modified Store Radius of
Gyration and Adjusted Pylon Pitch Stiffness
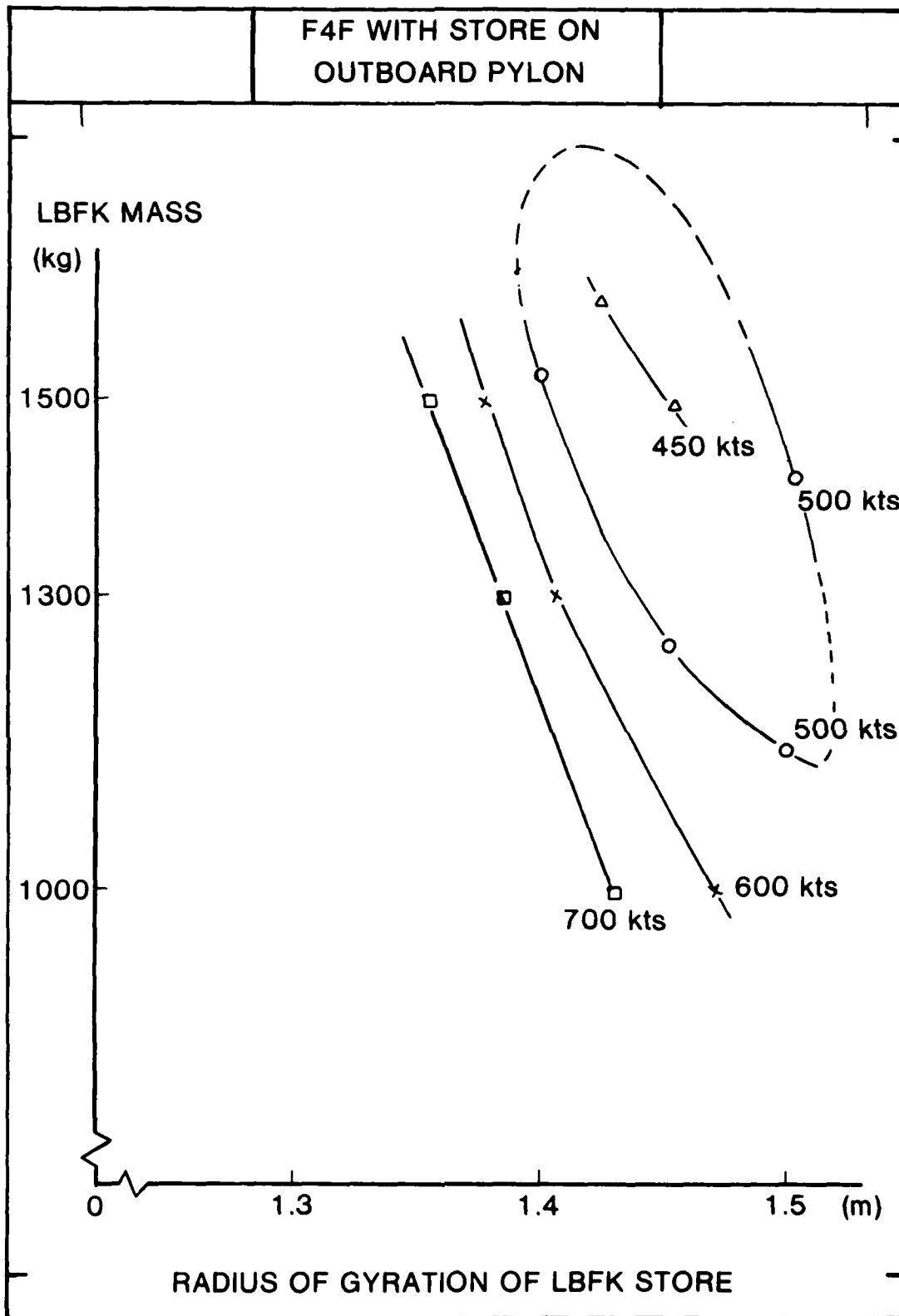
Figure 58.   Flutter Speed vs Mass and Radius of Gyration of the
LBFK-Store
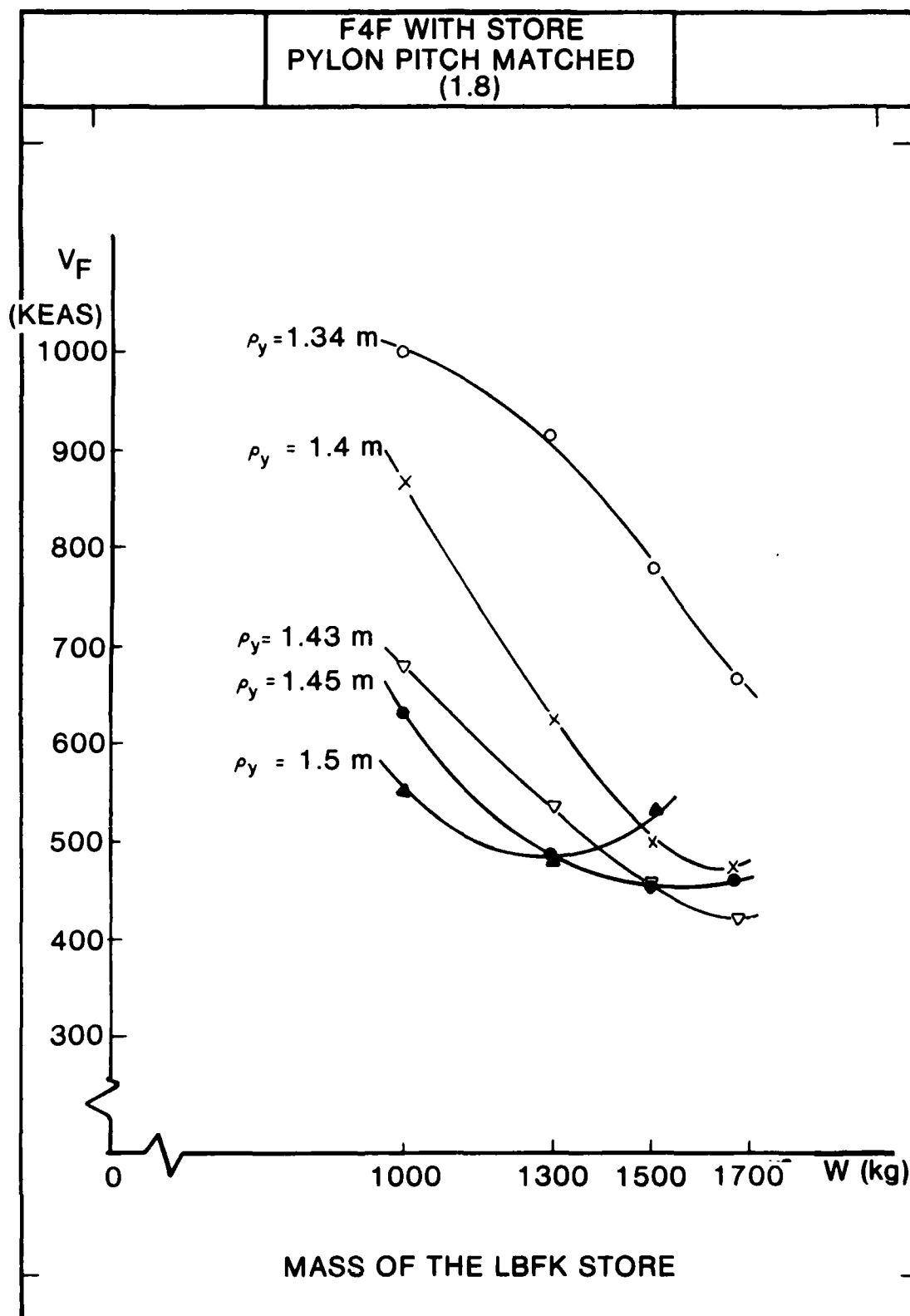
Figu⋯⋯. ⌐⌐⌐ter Speed vs Mass and Radius of Gyration of the LbFK-Store
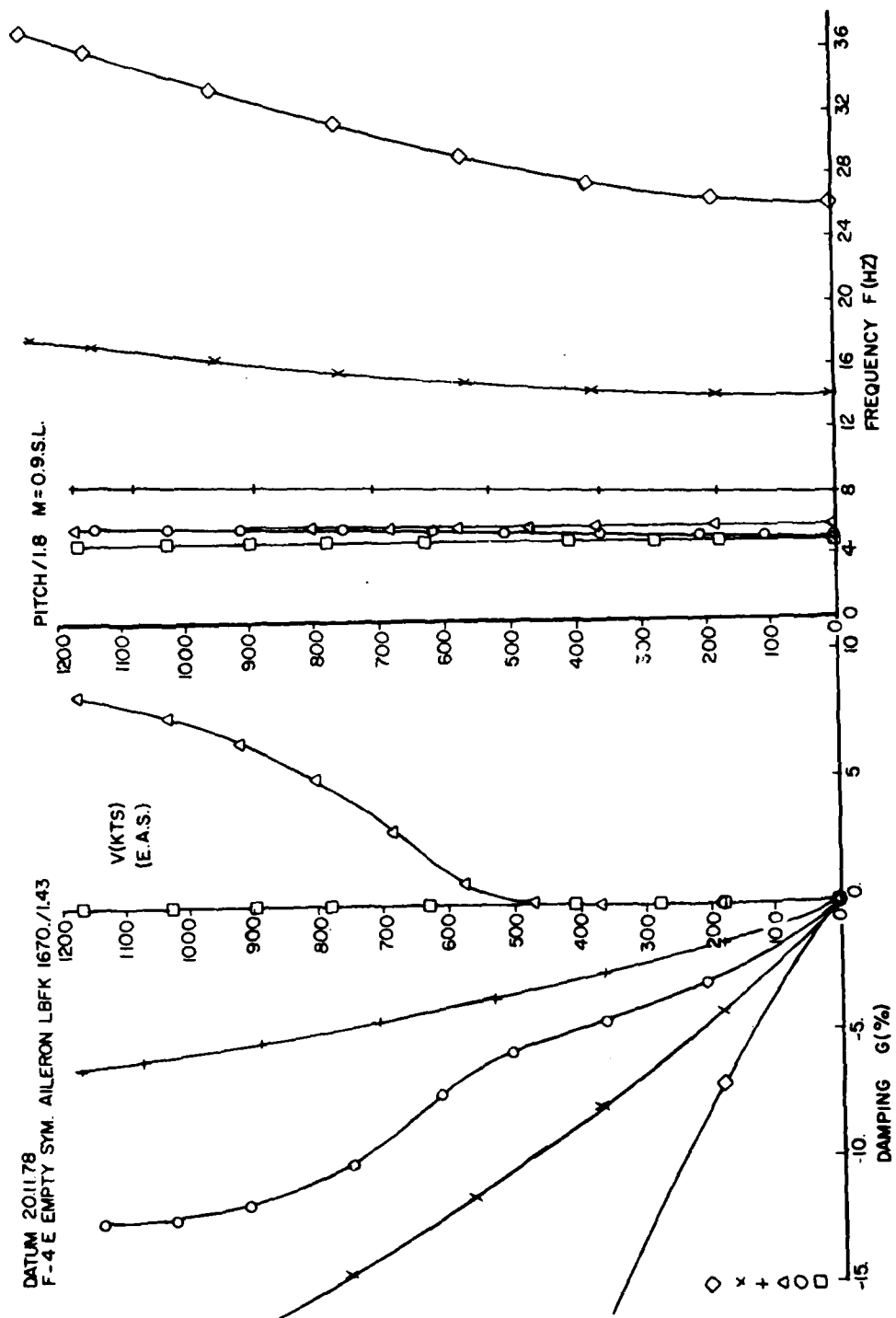
Figure 60. V-g Plot for ρ = 1.43 m
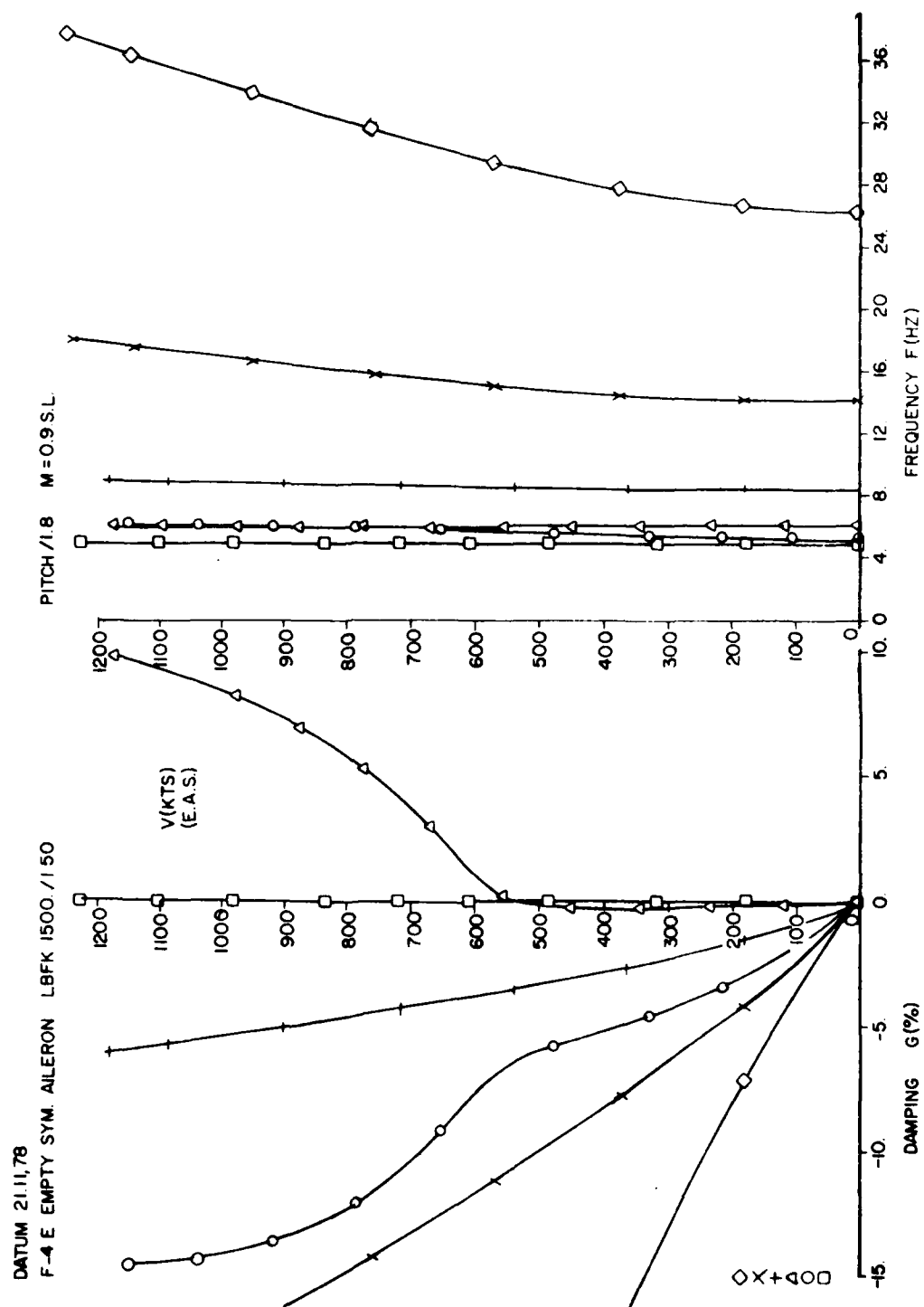
Figure 61. V-g Plot for ρ = 1.50 m
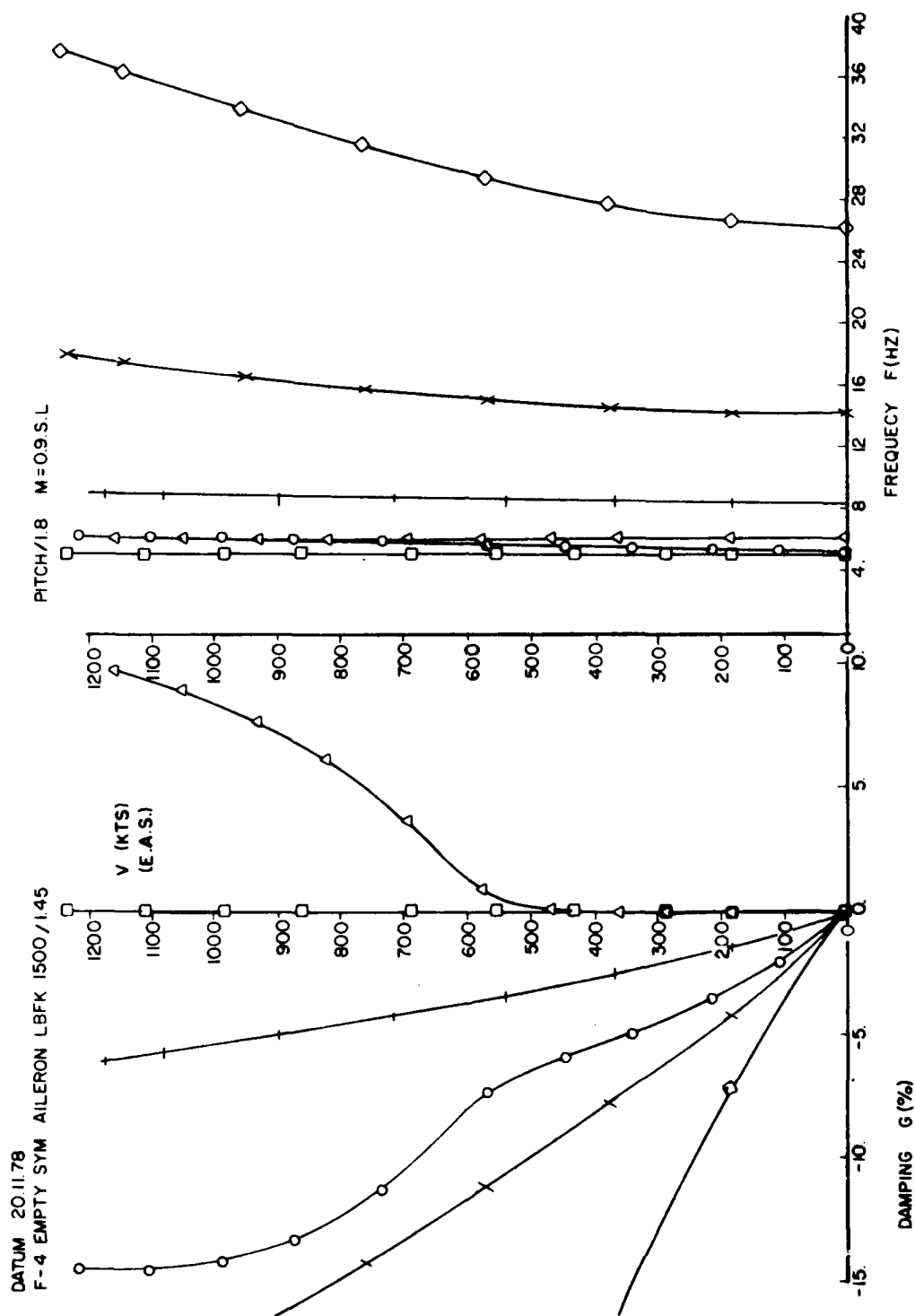
Figure 62. V-g Plot for ν = 1.45 m
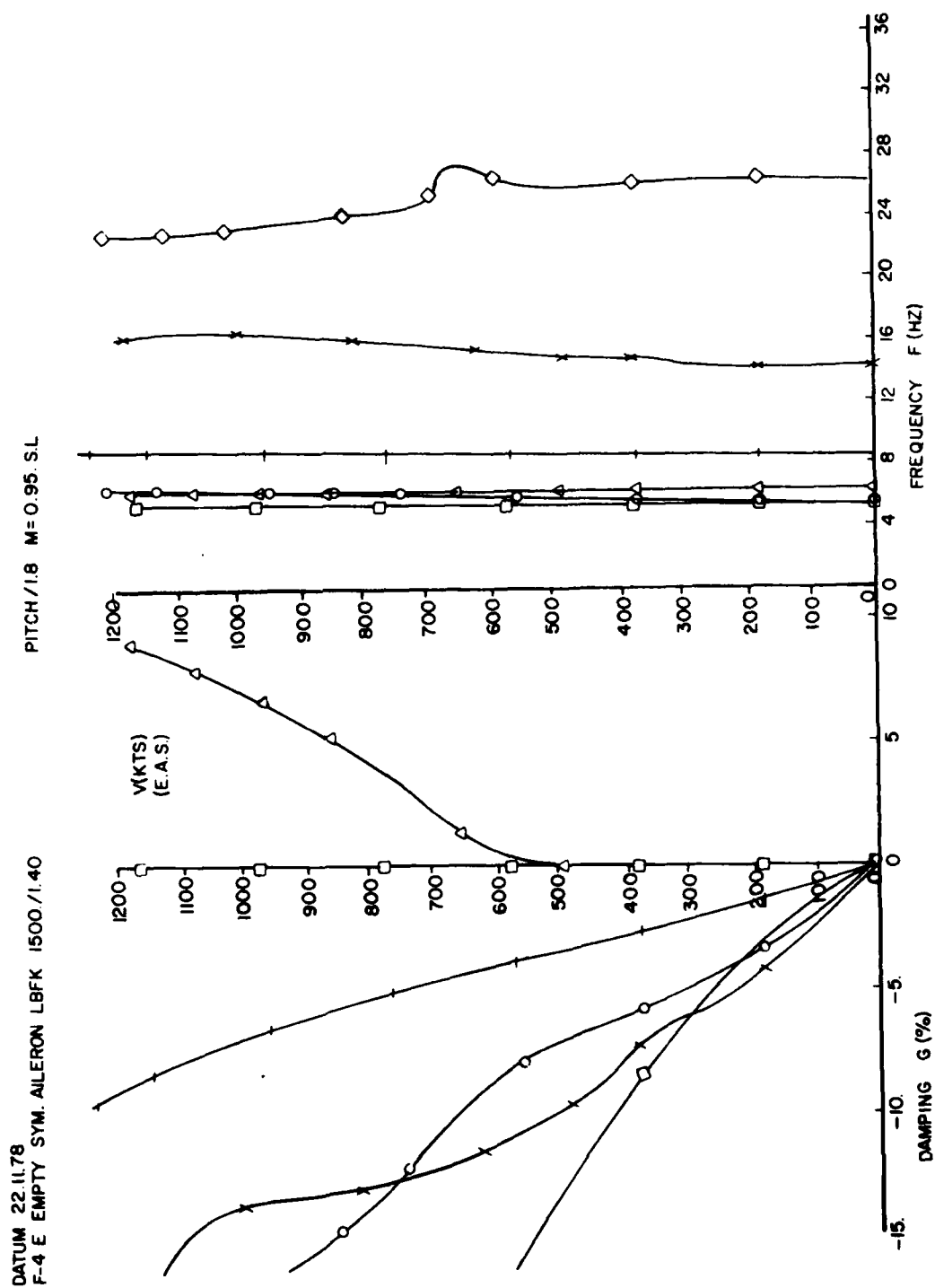
Figure 63. V-g Plot for $\rho = 1.40$ m

97
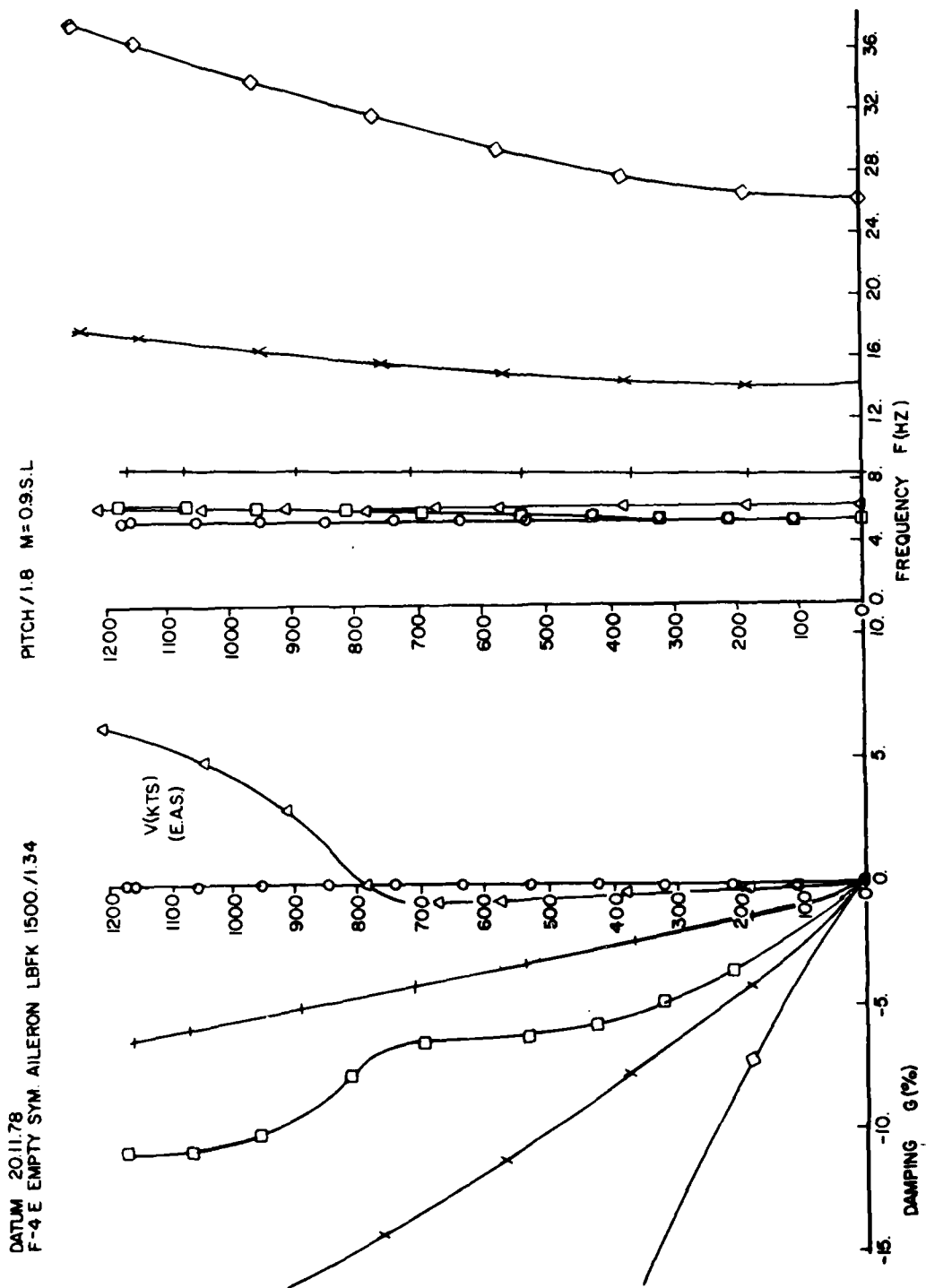
Figure 64. V-g Plot for $\dot{c}$ = 1.34 m
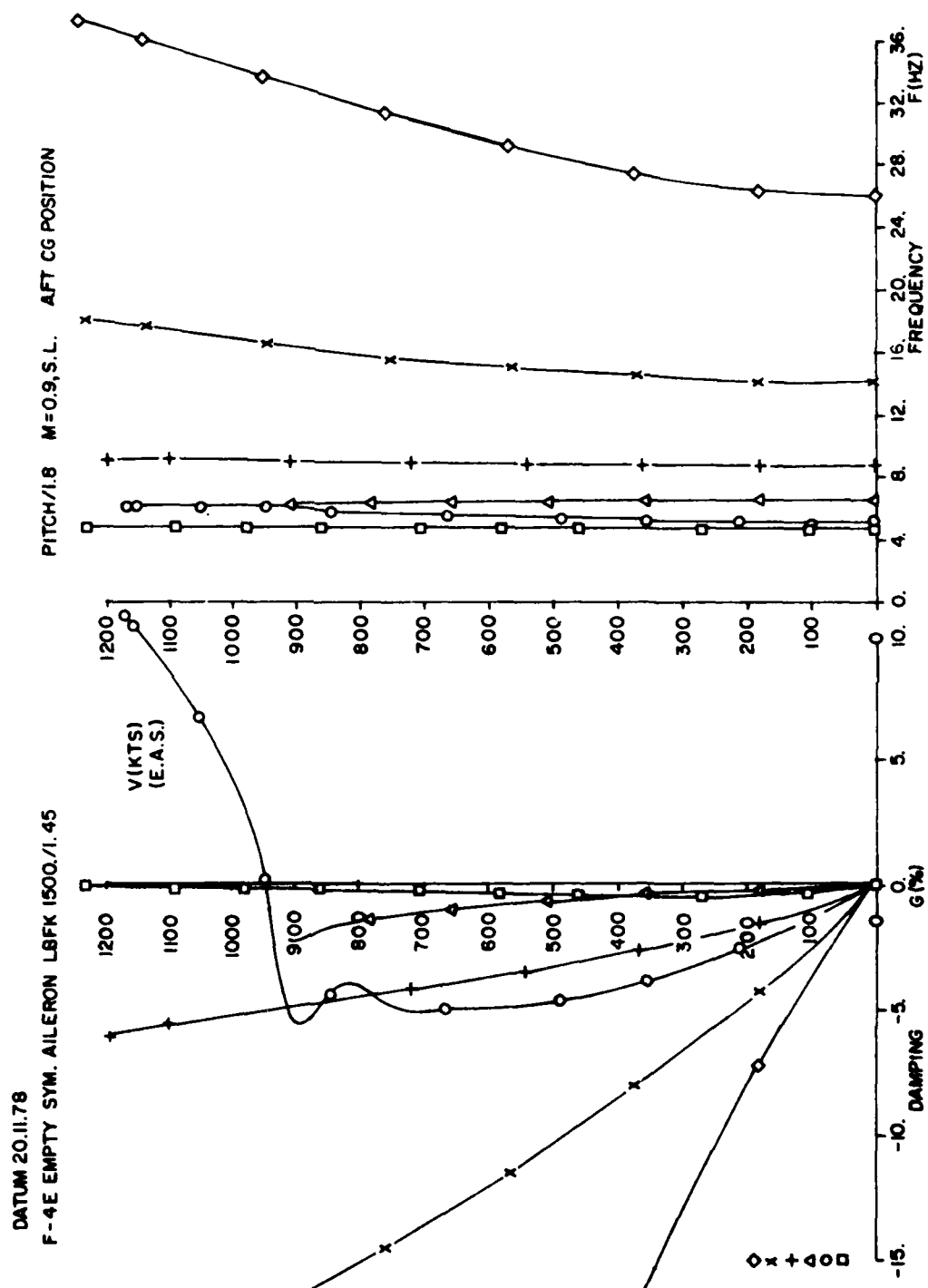
Figure 65. V-g Plot for c.g. in Aft Position
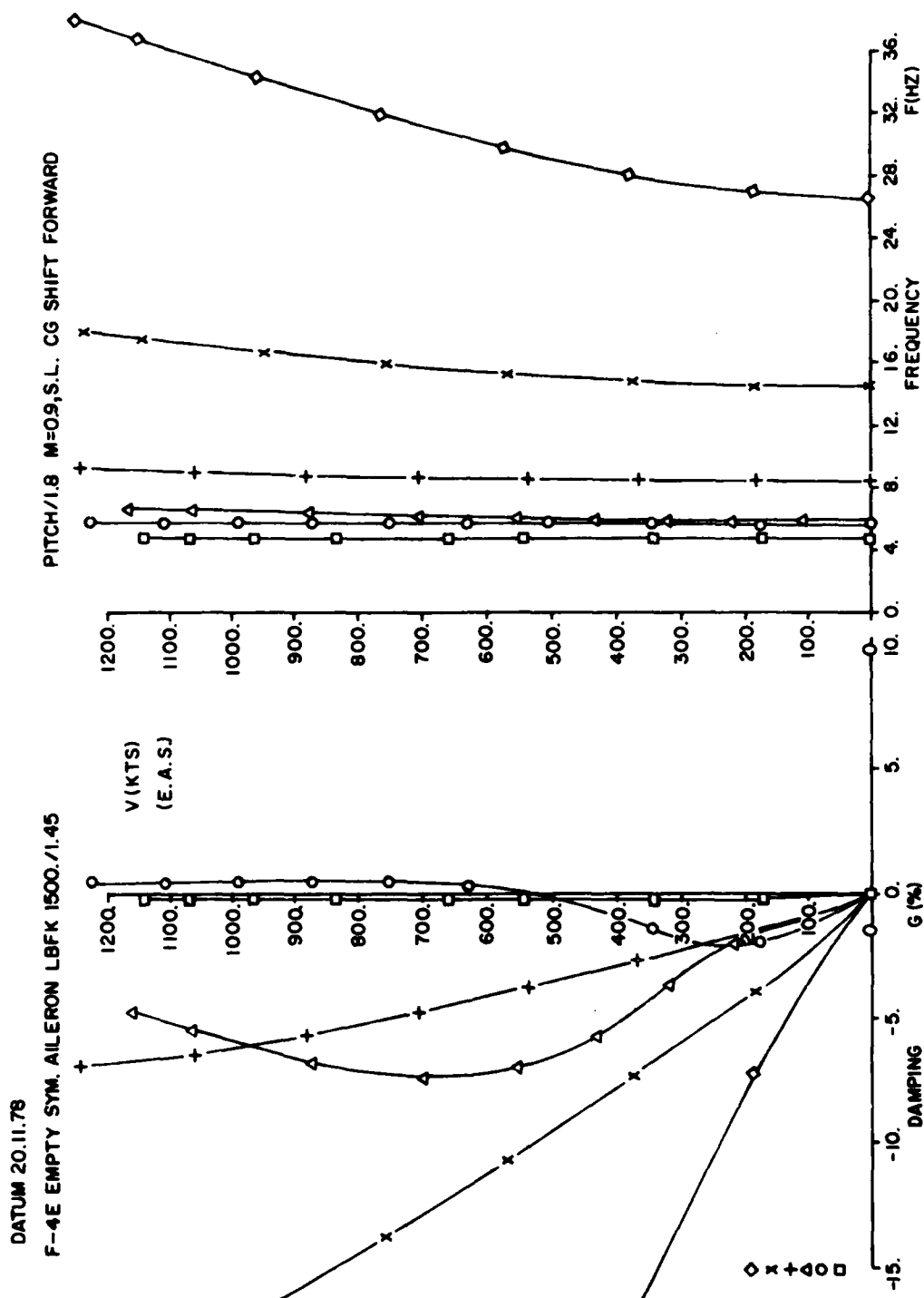
Figure 66. V-g Plot for c.g. in Forward Position
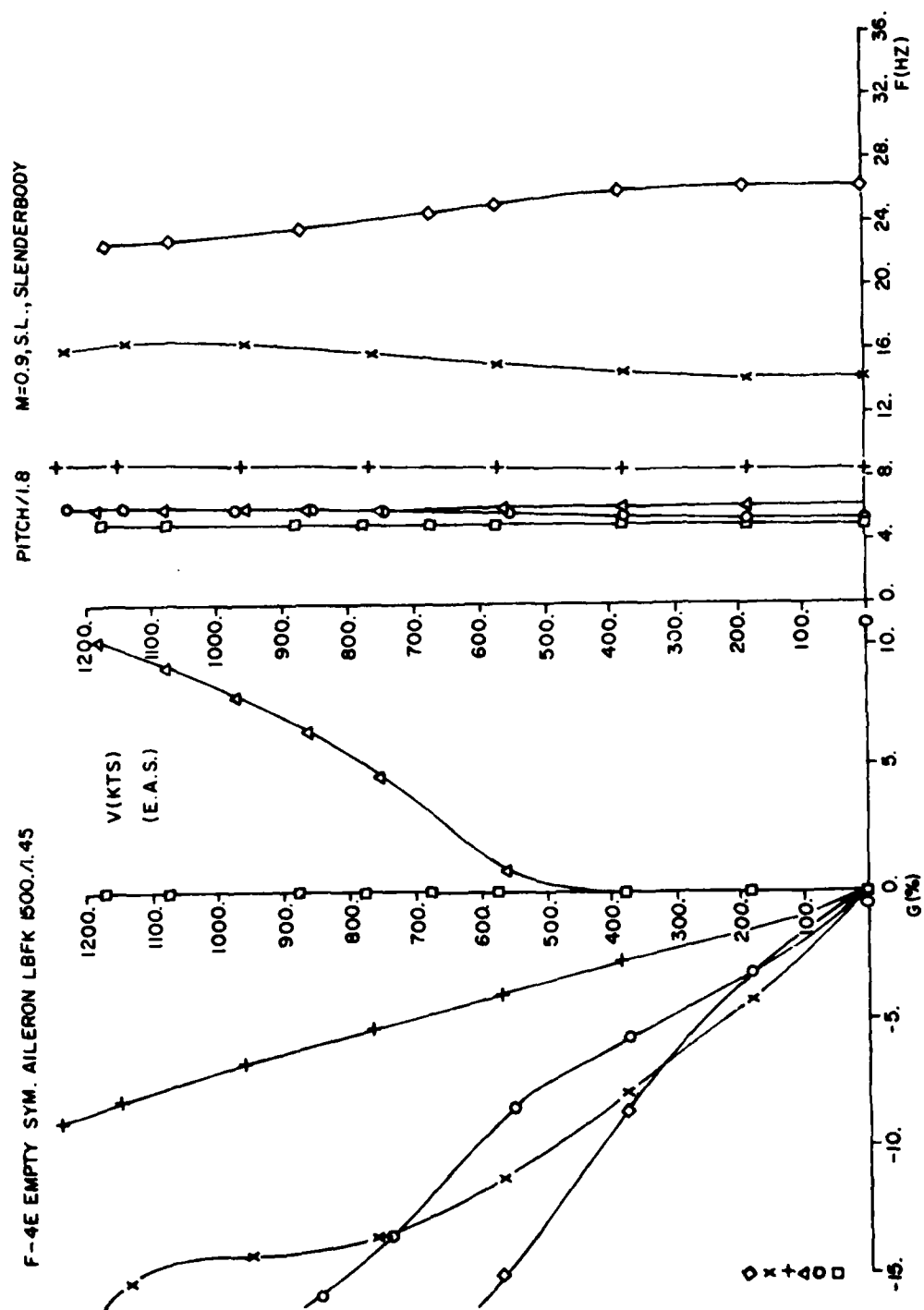
Figure 67. V-g Plot with Store Aerodynamics
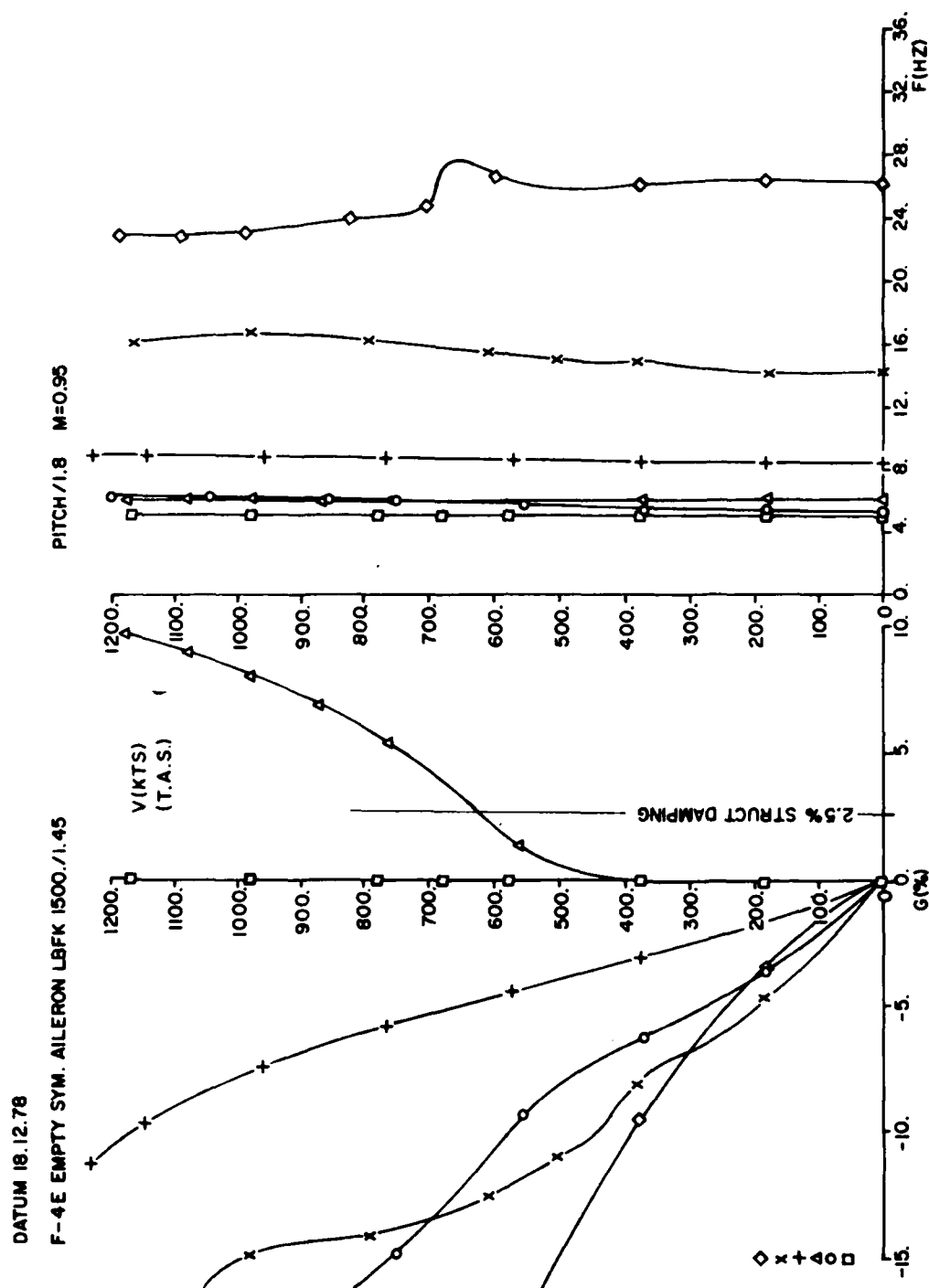
Figure 68. V-g Plot with Mach Number = 0.95
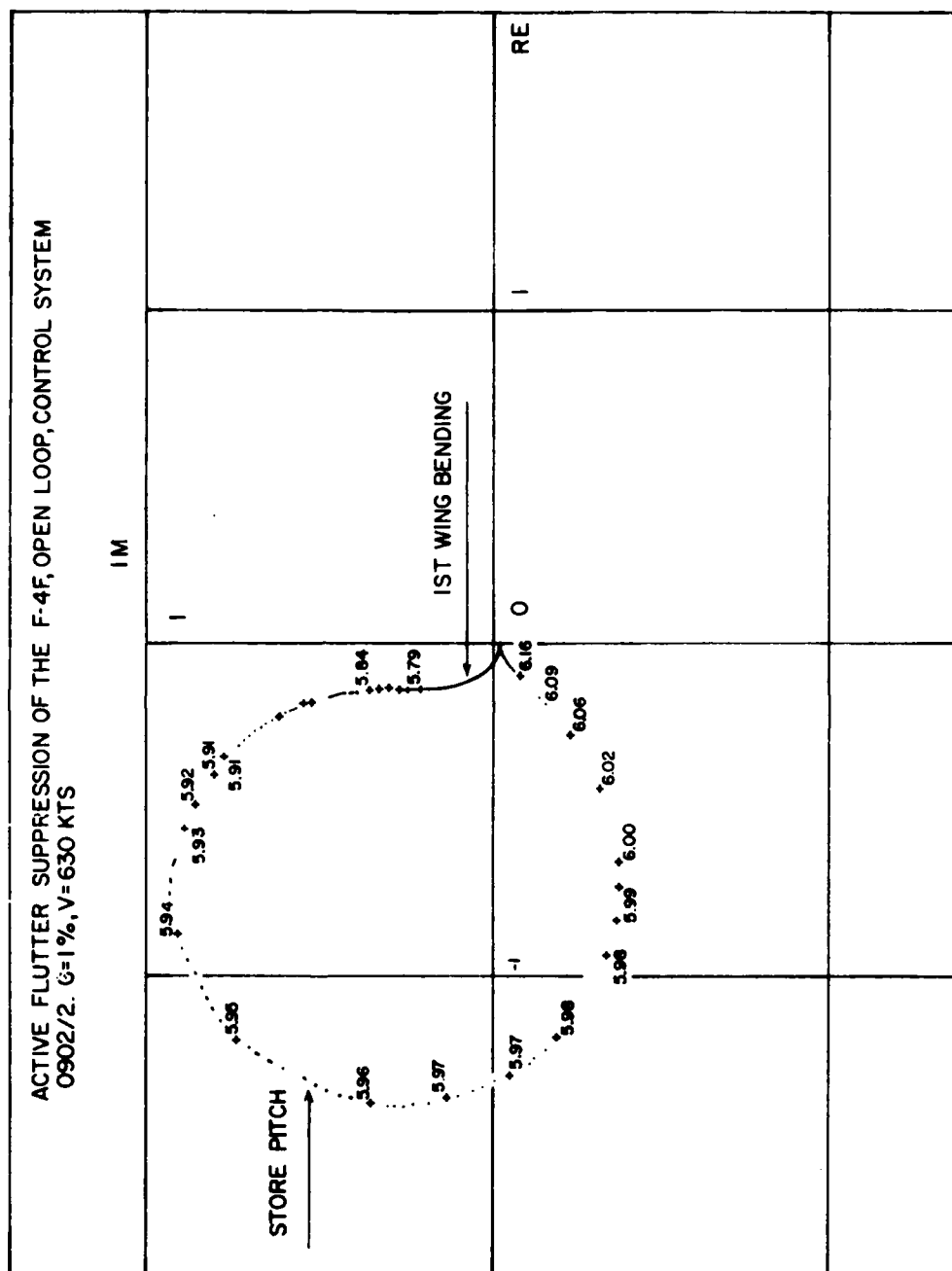
Figure 69. Nyquist Diagram for V = 630 kts
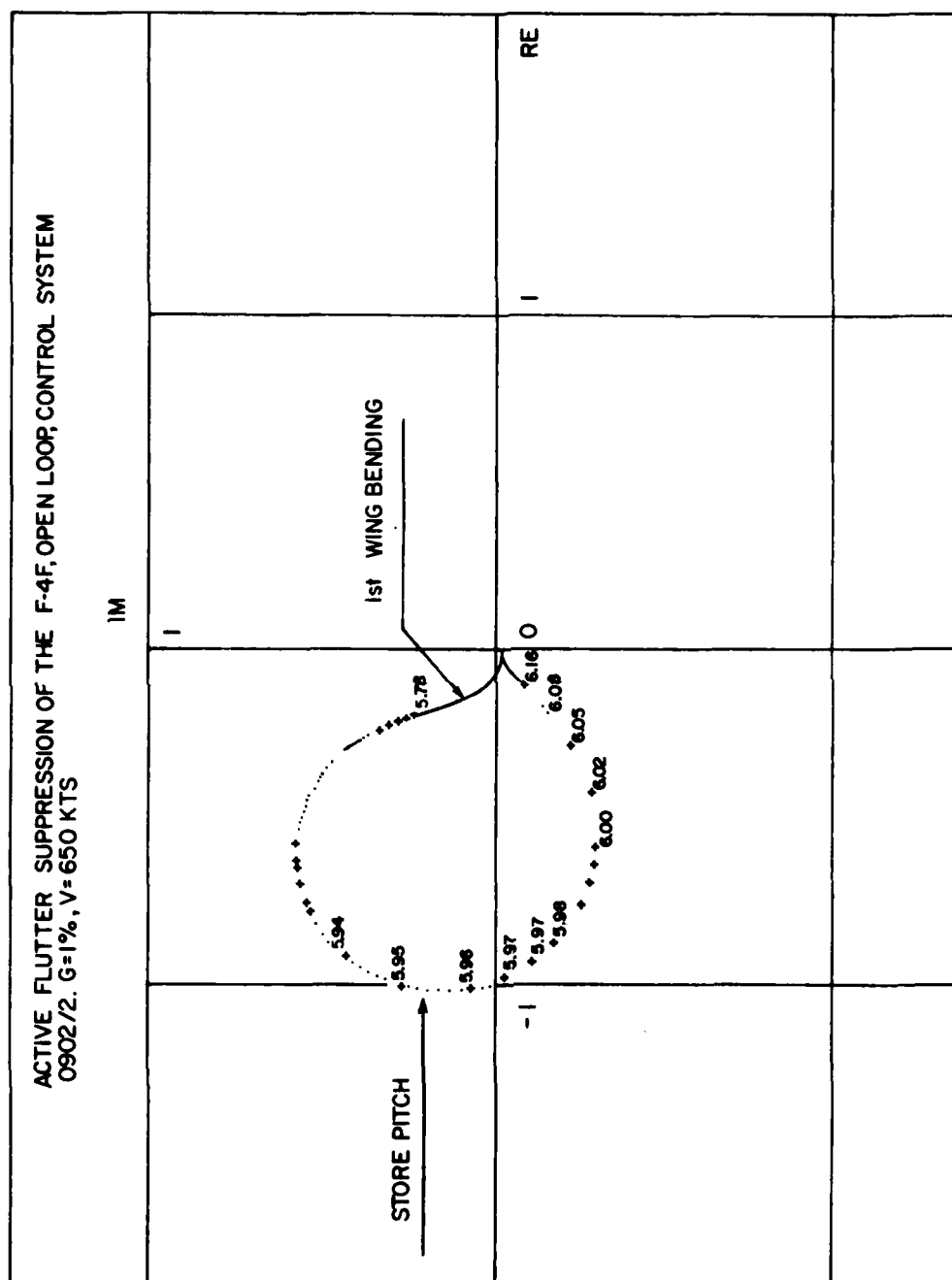
Figure 70. Nyquist Diagram for V = 650 kts
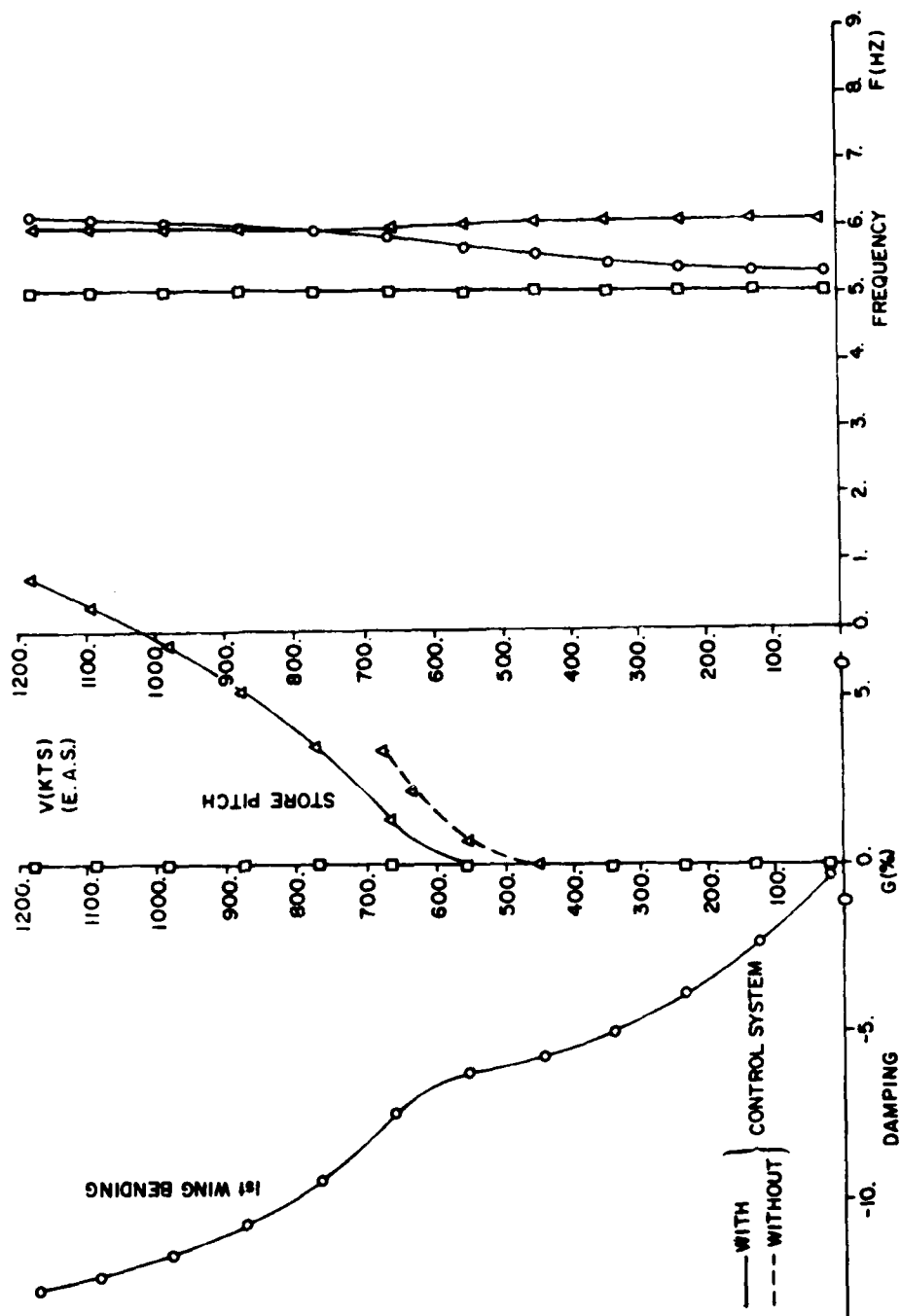
Figure 71. Flutter Calculation with Flutter Suppression System
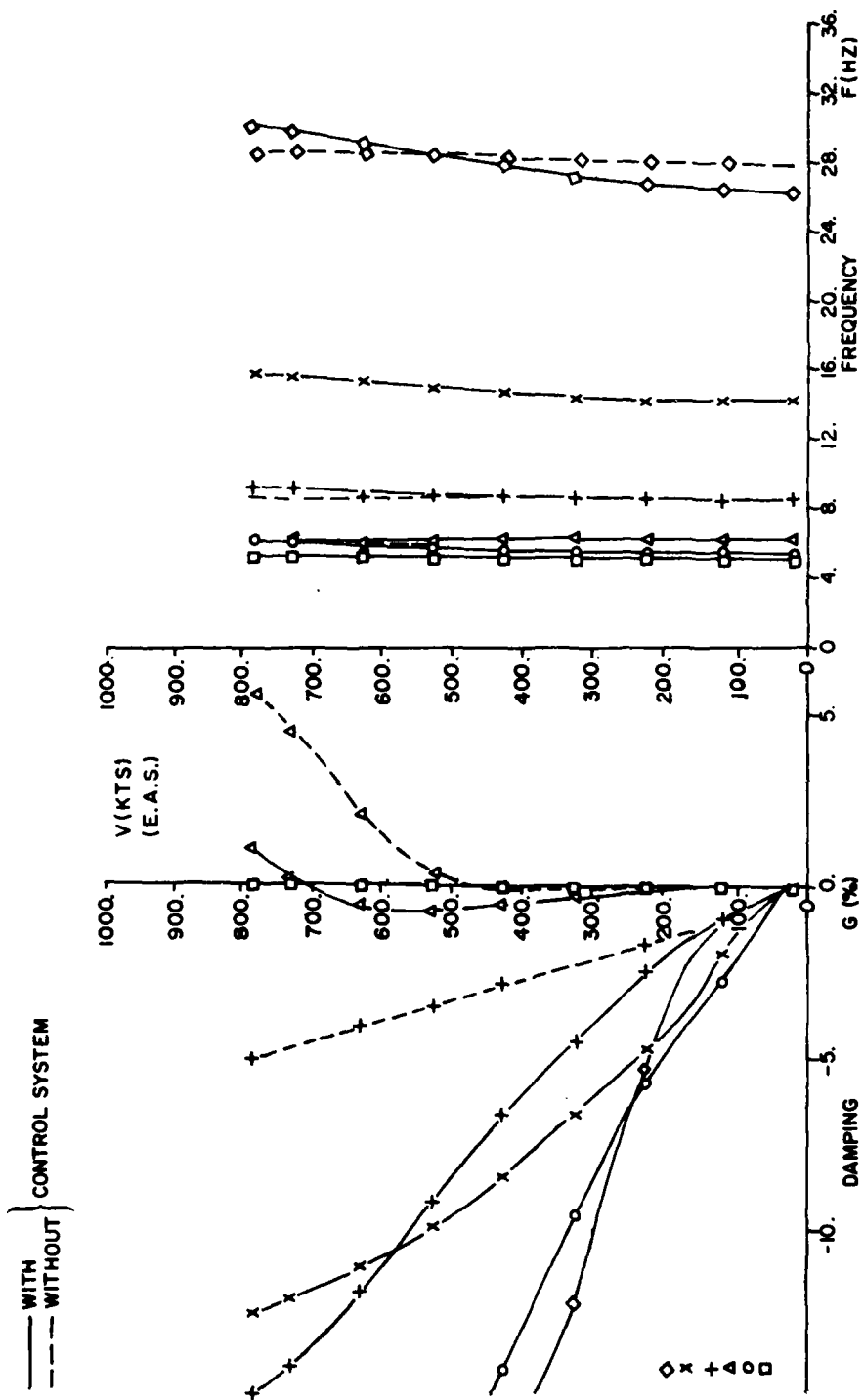
Figure 72. Flutter Calculation with Flutter Suppression System
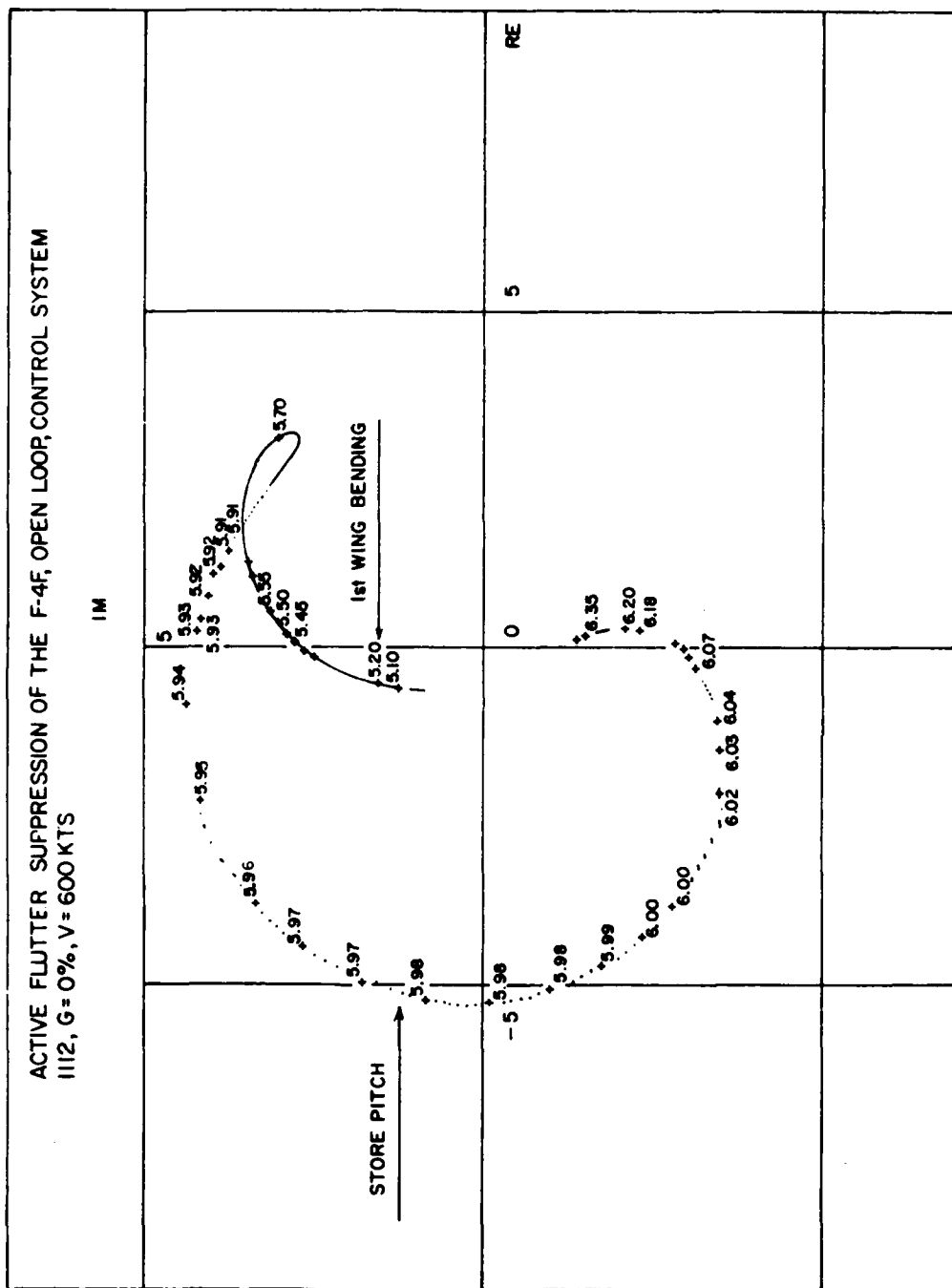
Figure 73. Nyquist Diagram for V = 600 kts

107
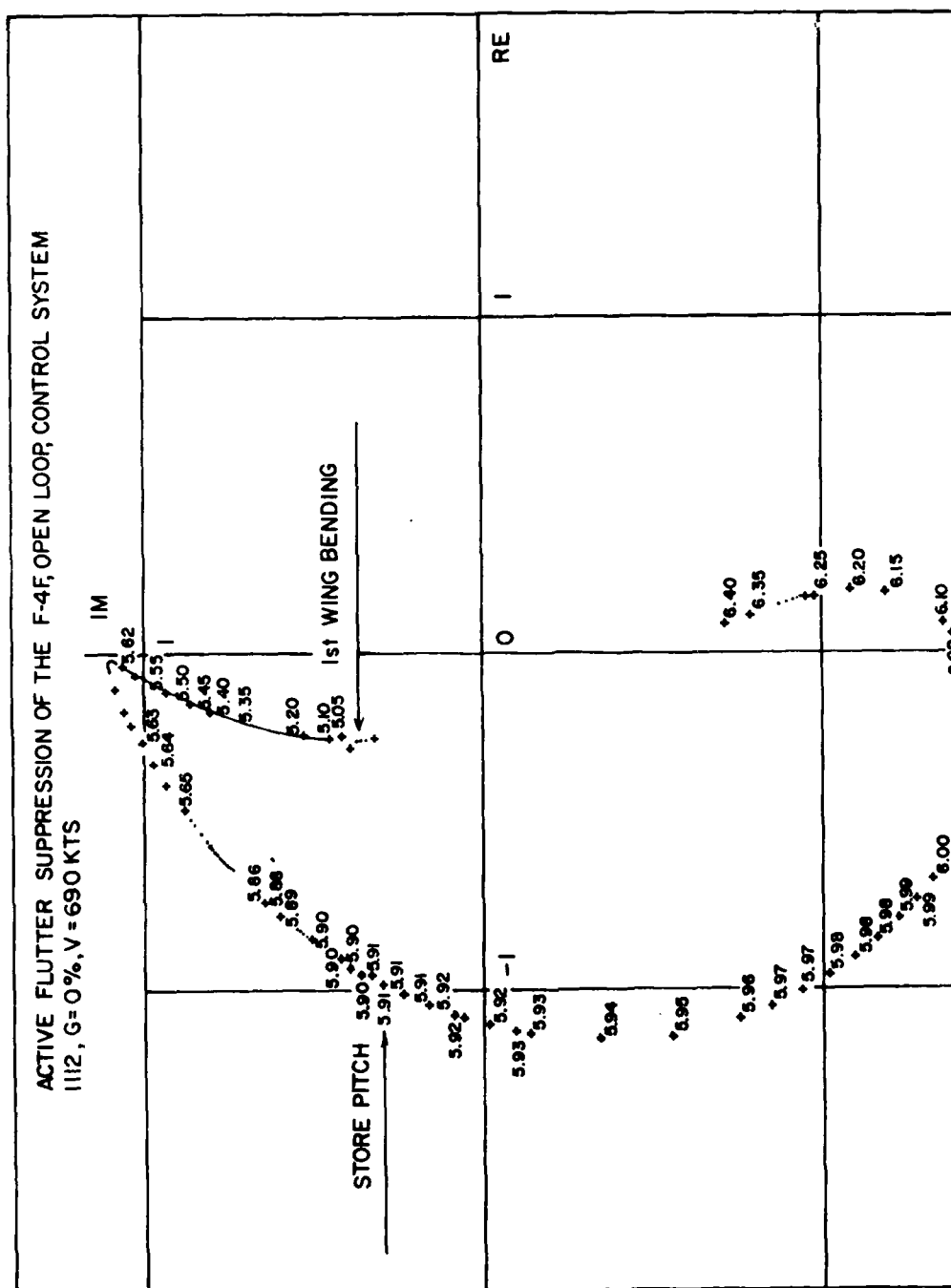
Figure 74. Nyquist Diagram for V = 690 kts
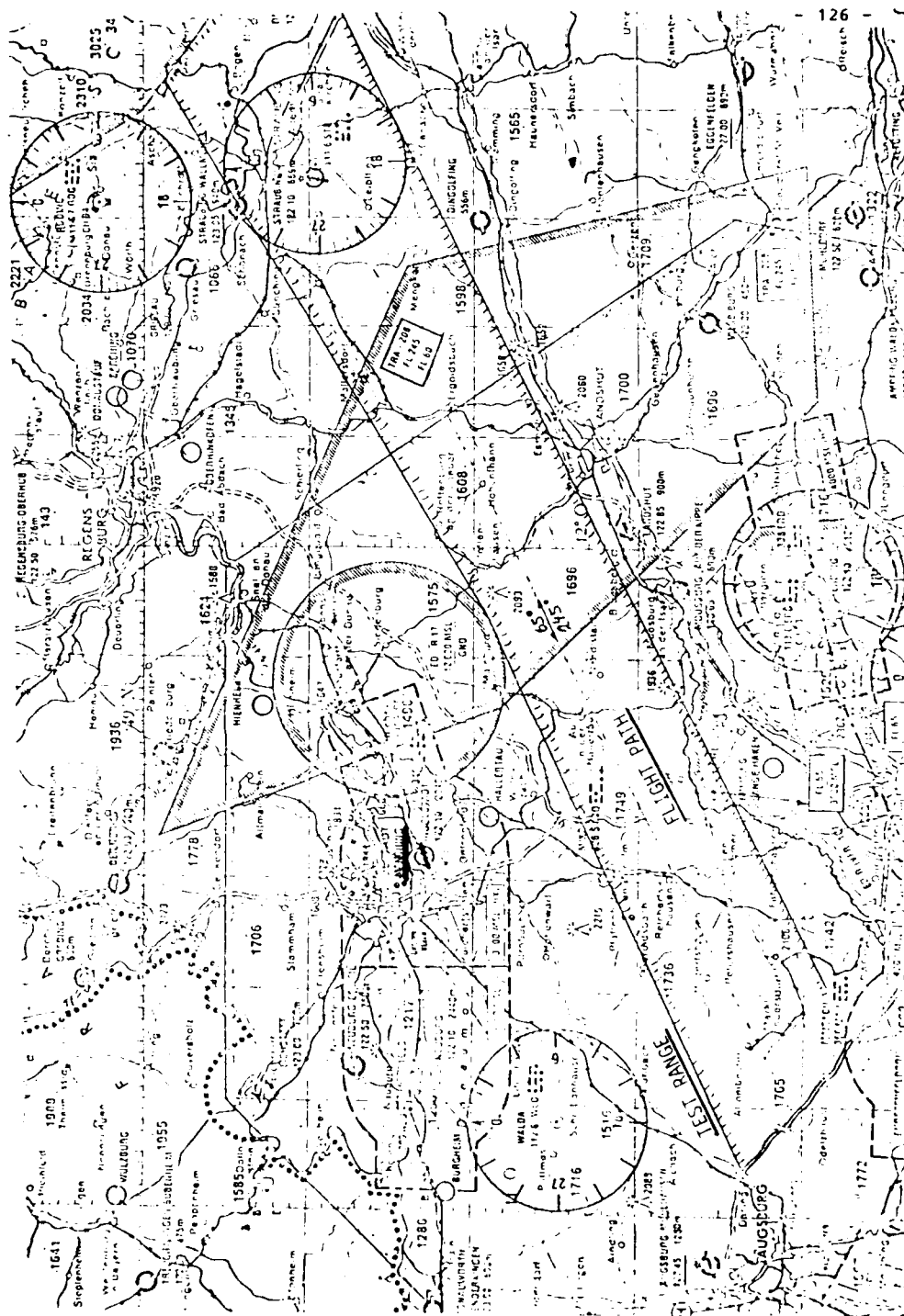
Figure 75. Test Range and Flight Path for the Flight Test at Manching
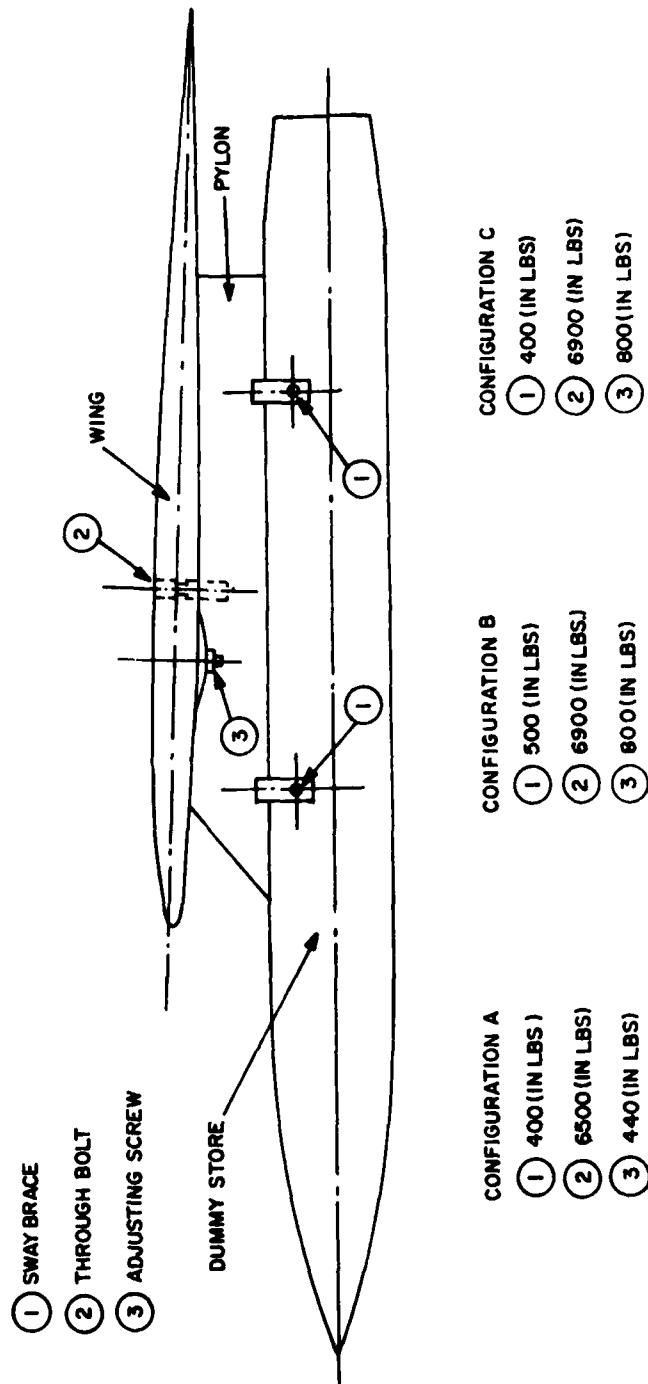
Figure 76. Torque Moments of Pylon and Store Attachment
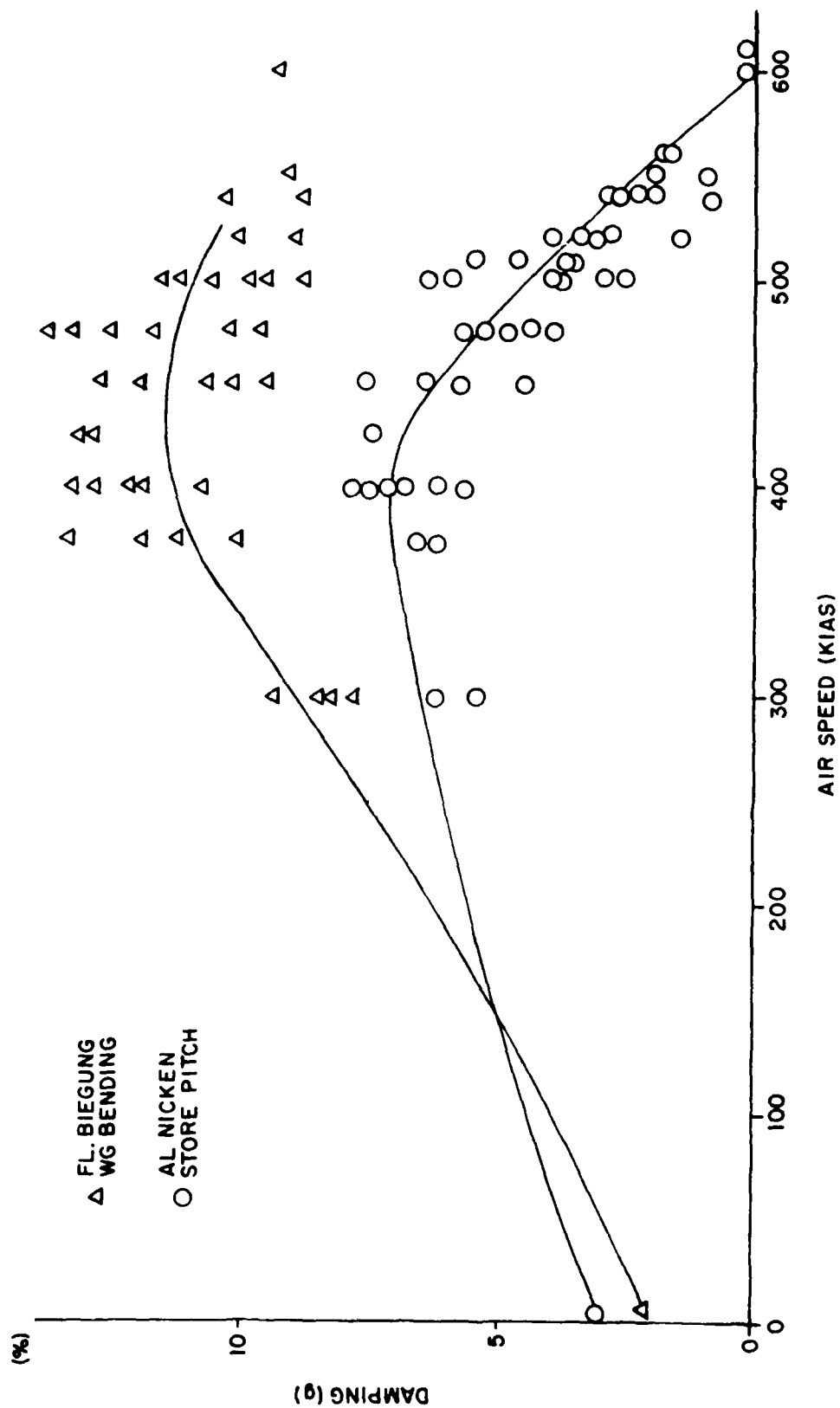
Figure 77. Damping Versus Airspeed of the Critical Store Configuration
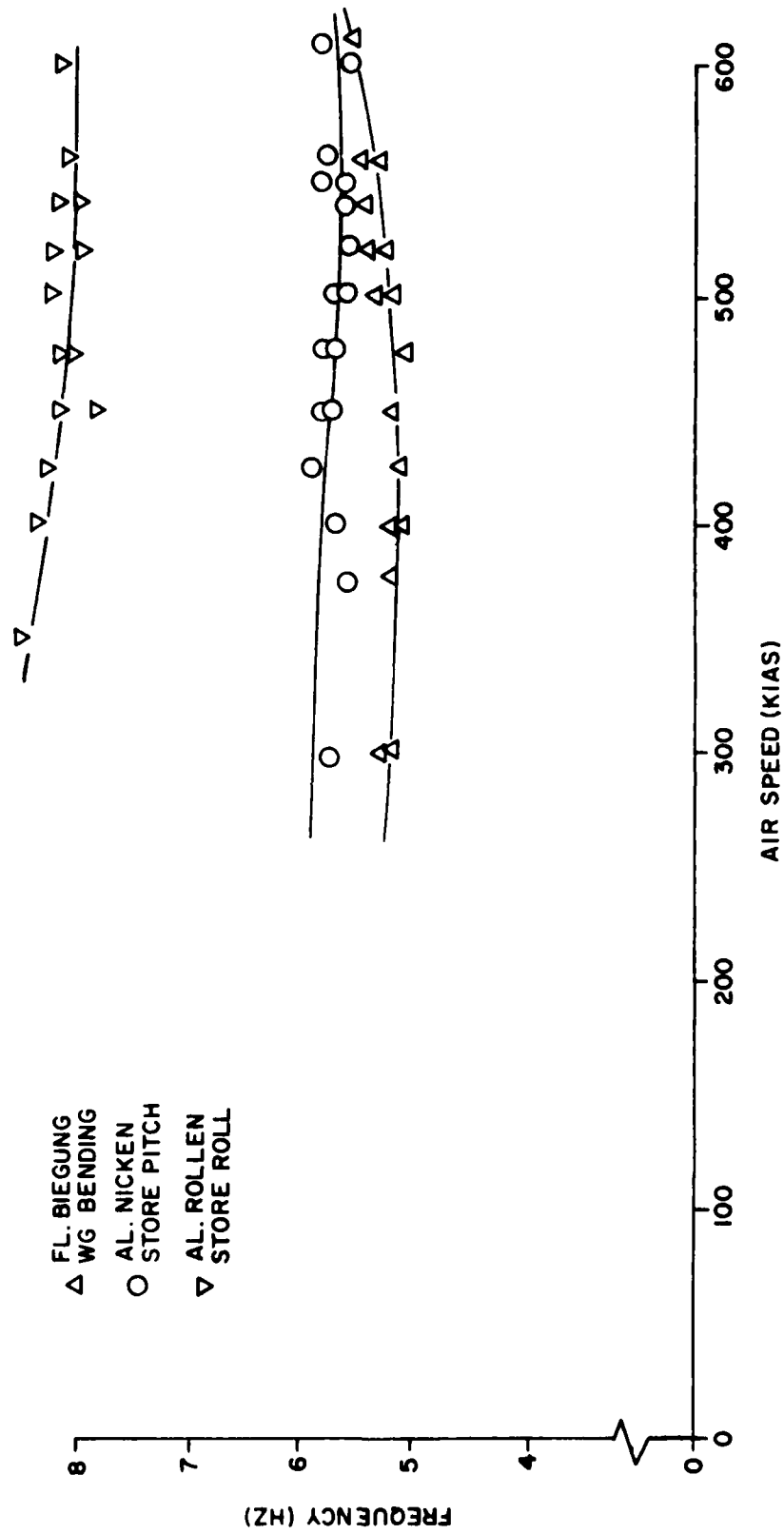
Figure 78. Frequency Versus Airspeed of the Critical Store
Configuration
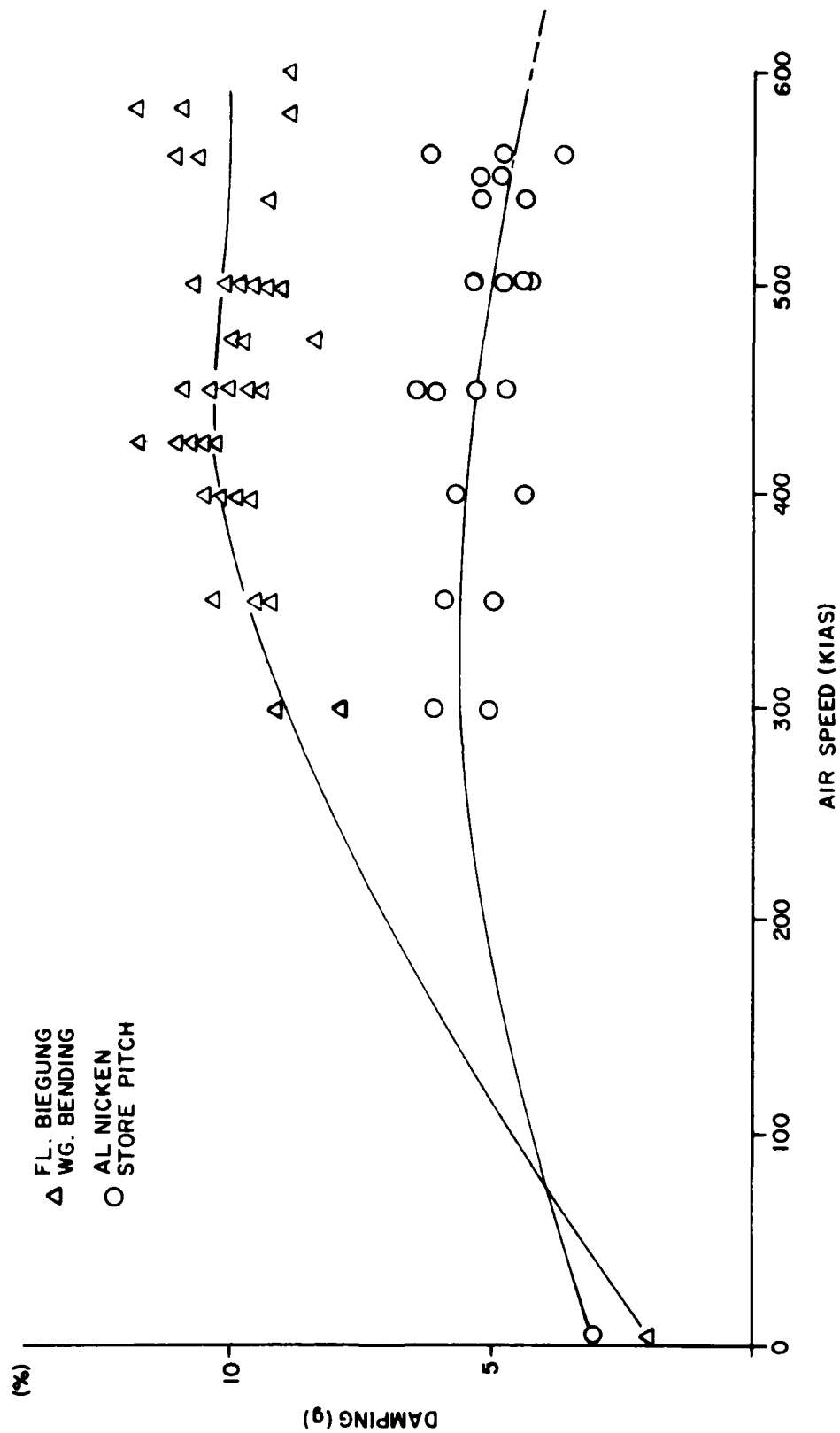
Figure 79. Damping Versus Airspeed of the Flutter Stopper
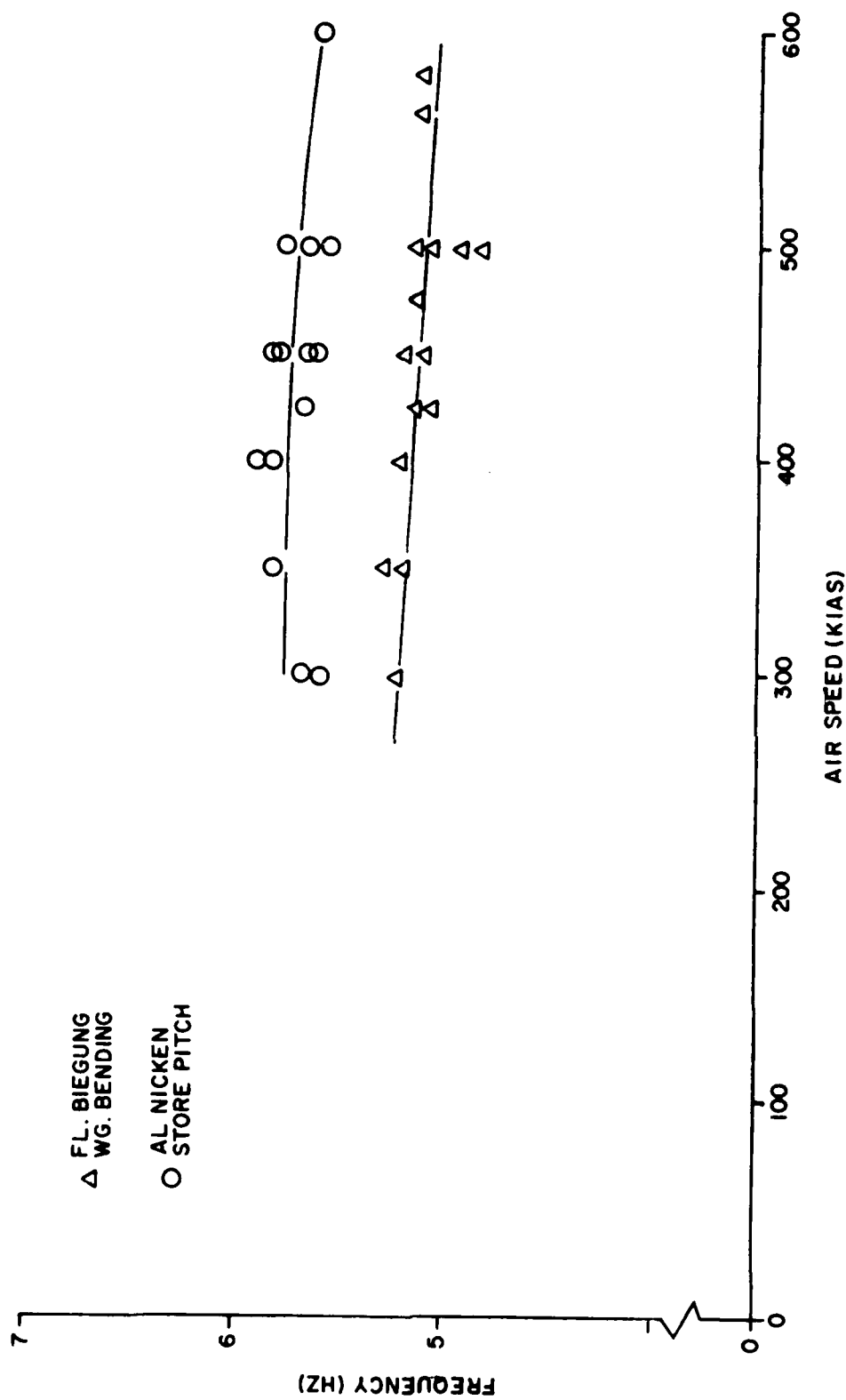
Figure 80. Frequency Versus Airspeed of the Flutter Stopper
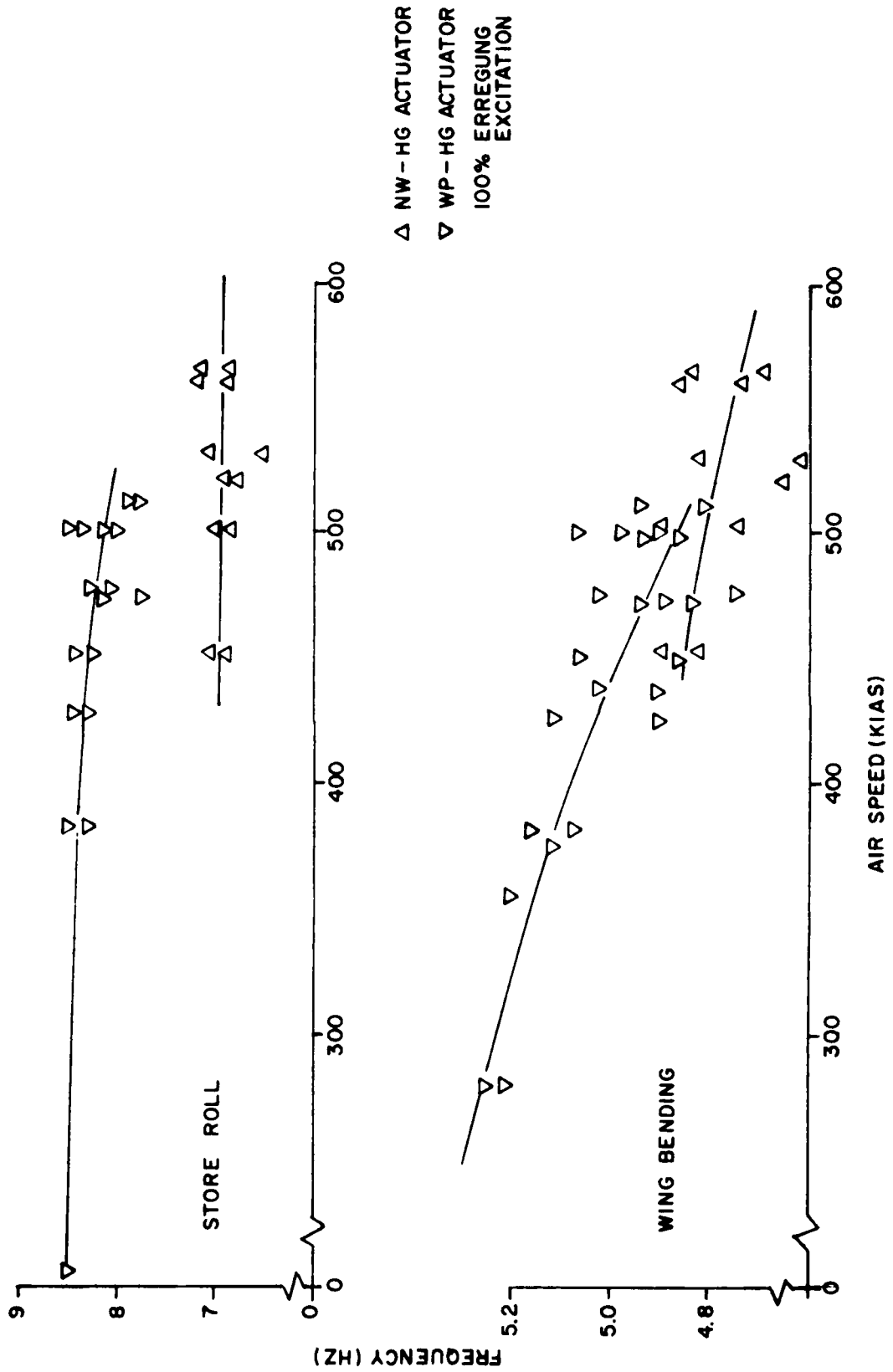
Figure 81. Frequency Shifts Due to Nonlinearities
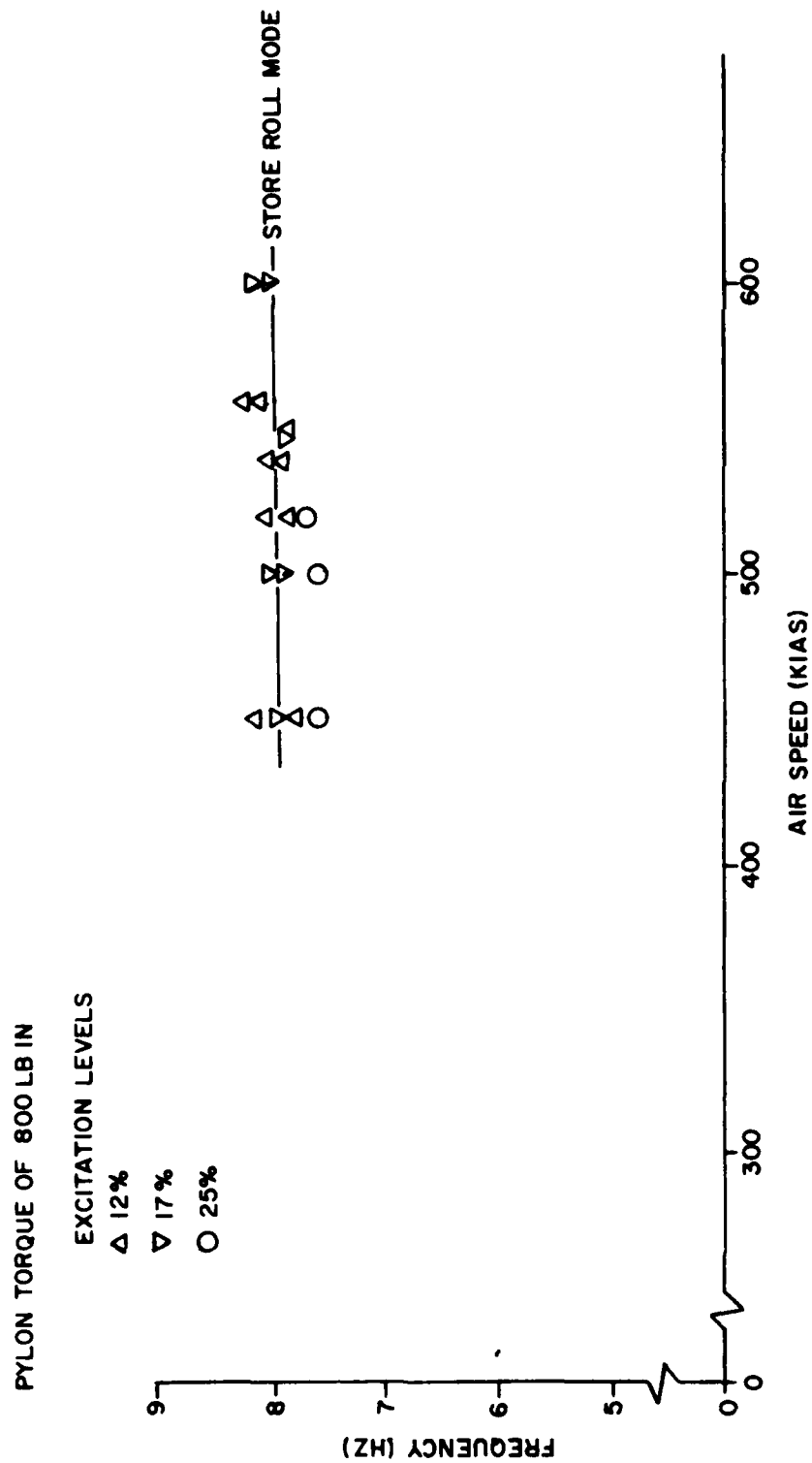
Figure 82.   Frequency Shift of the Store Roll Mode Due to Various
Excitation Levels

F-4F WITH LBFK FLUTTER STORE

$\triangledown$ V = 520 KIAS $\triangle$ V = 450 KIAS

$\triangle$ V = 540 KIAS $\triangledown$ V = 520 KIAS
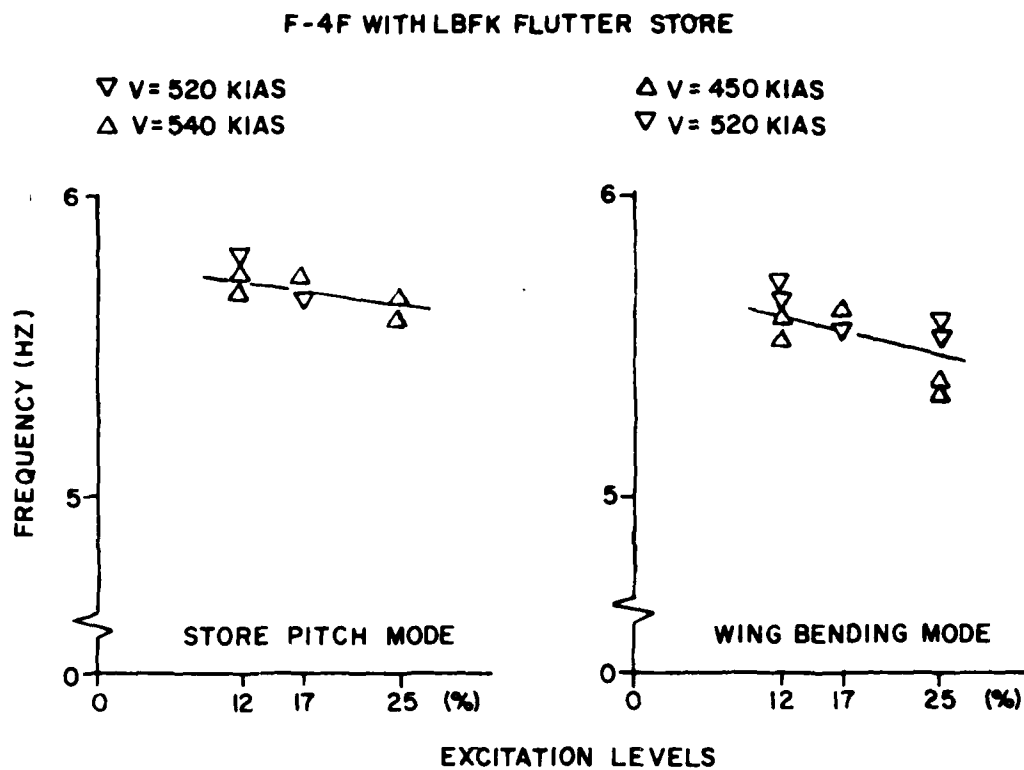
Figure 83. Frequency Shift Due to Nonlinear Effects Versus Excitation Levels
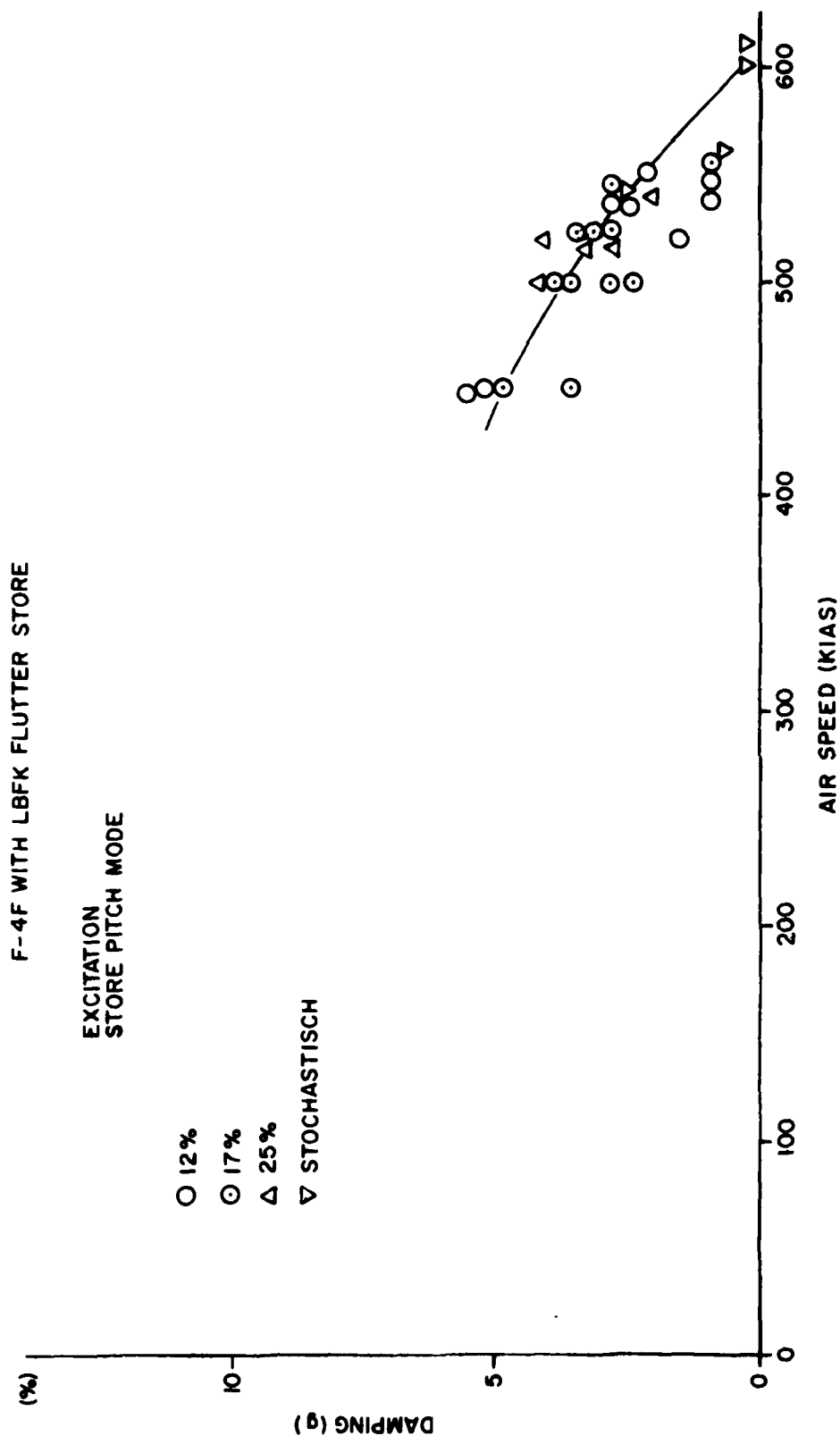
Figure 84. Damping Versus Airspeed for the Linear System
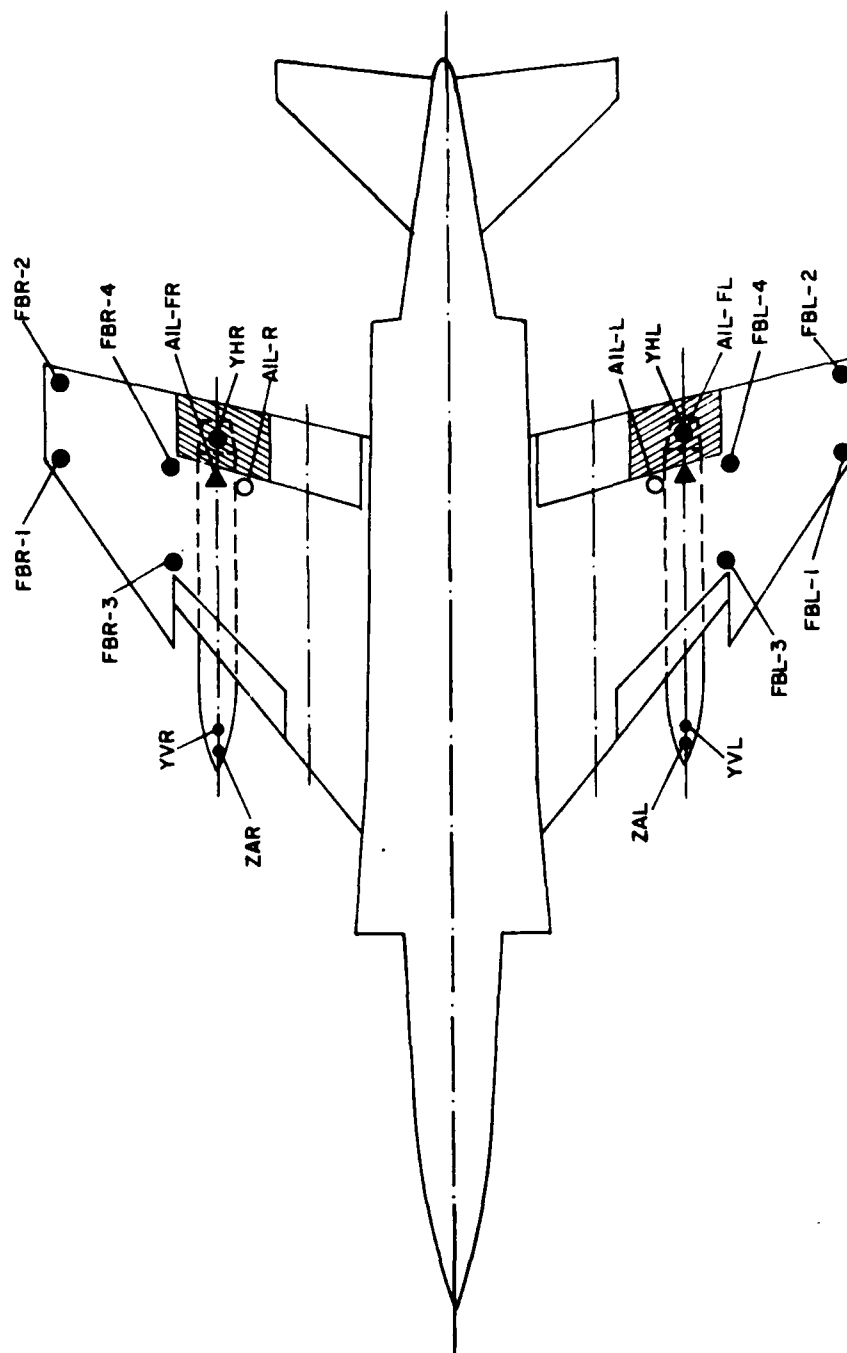
Figure 85. Locations of Sensors and Pick-ups
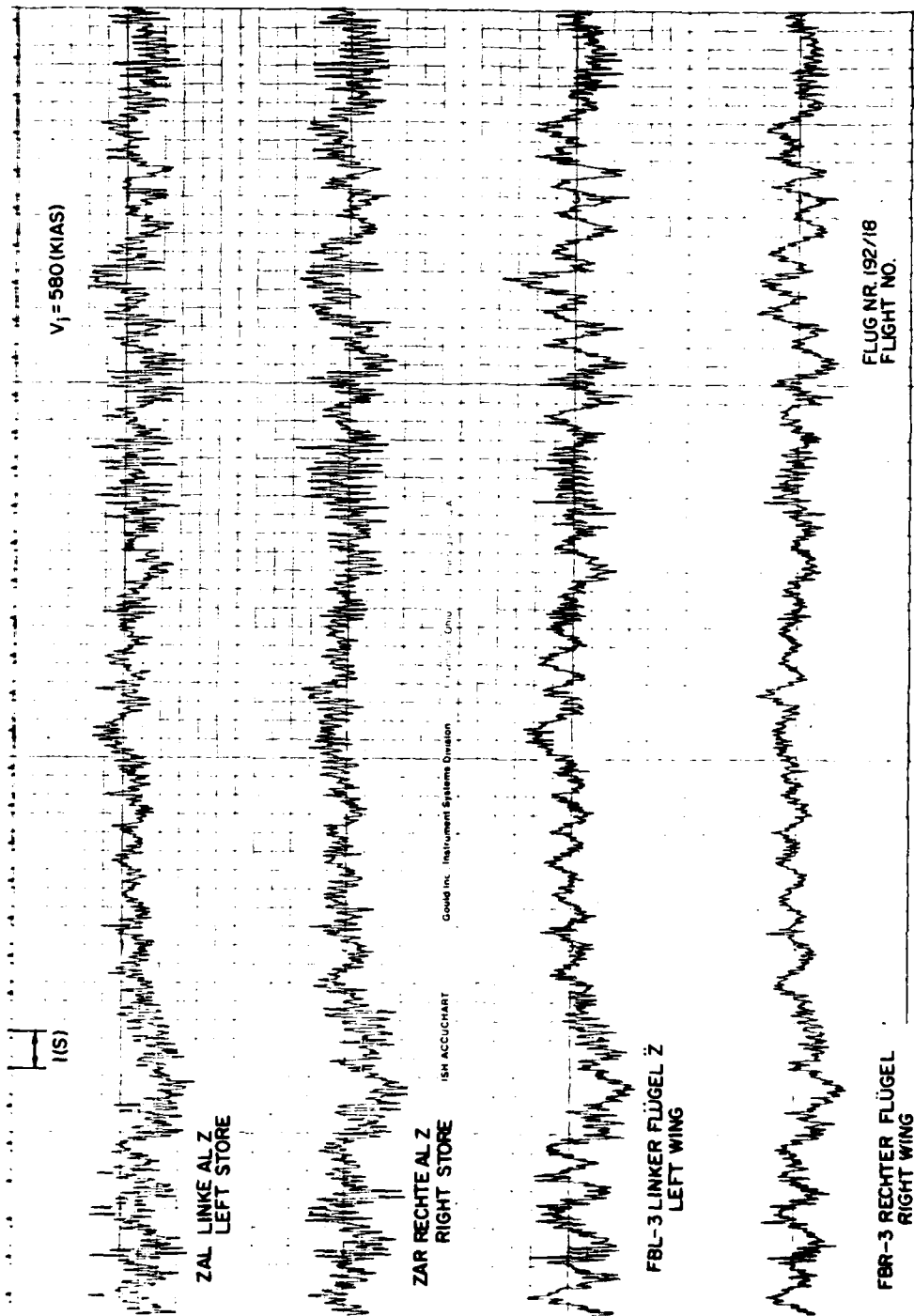
Figure 86.   Time Histories of the Critical Store Configuration at
580 KIAS
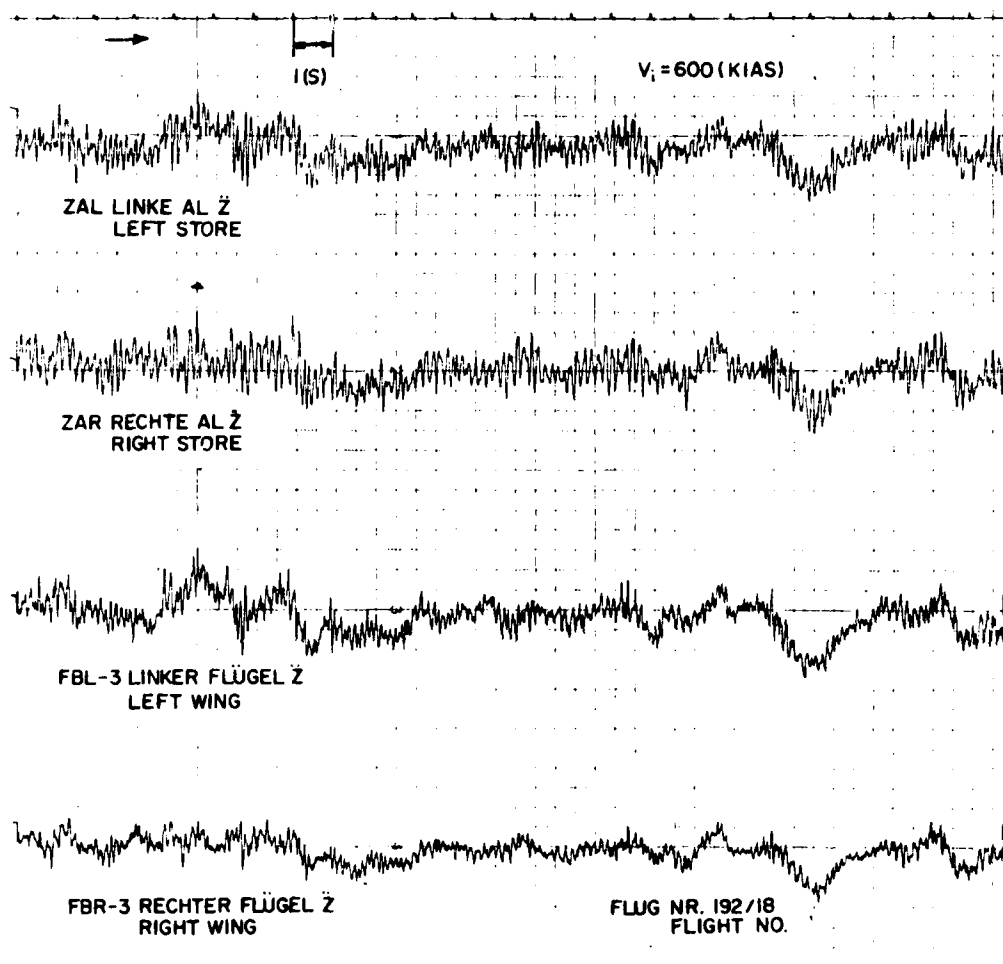
Figure 87.   Time Histories of the Critical Store Configuration at
600 KIAS

$V_i = 610 (KIAS)$

TIME ⟶ 1 SEC

ZAL LINKE AL Z
LEFT STORE

ZAR RECHTE AL Z
RIGHT STORE

FBL-3 LINKER FLÜGEL Z
LEFT WING

FBR-3 RECHTER FLÜGEL Z
RIGHT WING

FLUG NR. 192/18
FLIGHT NO.
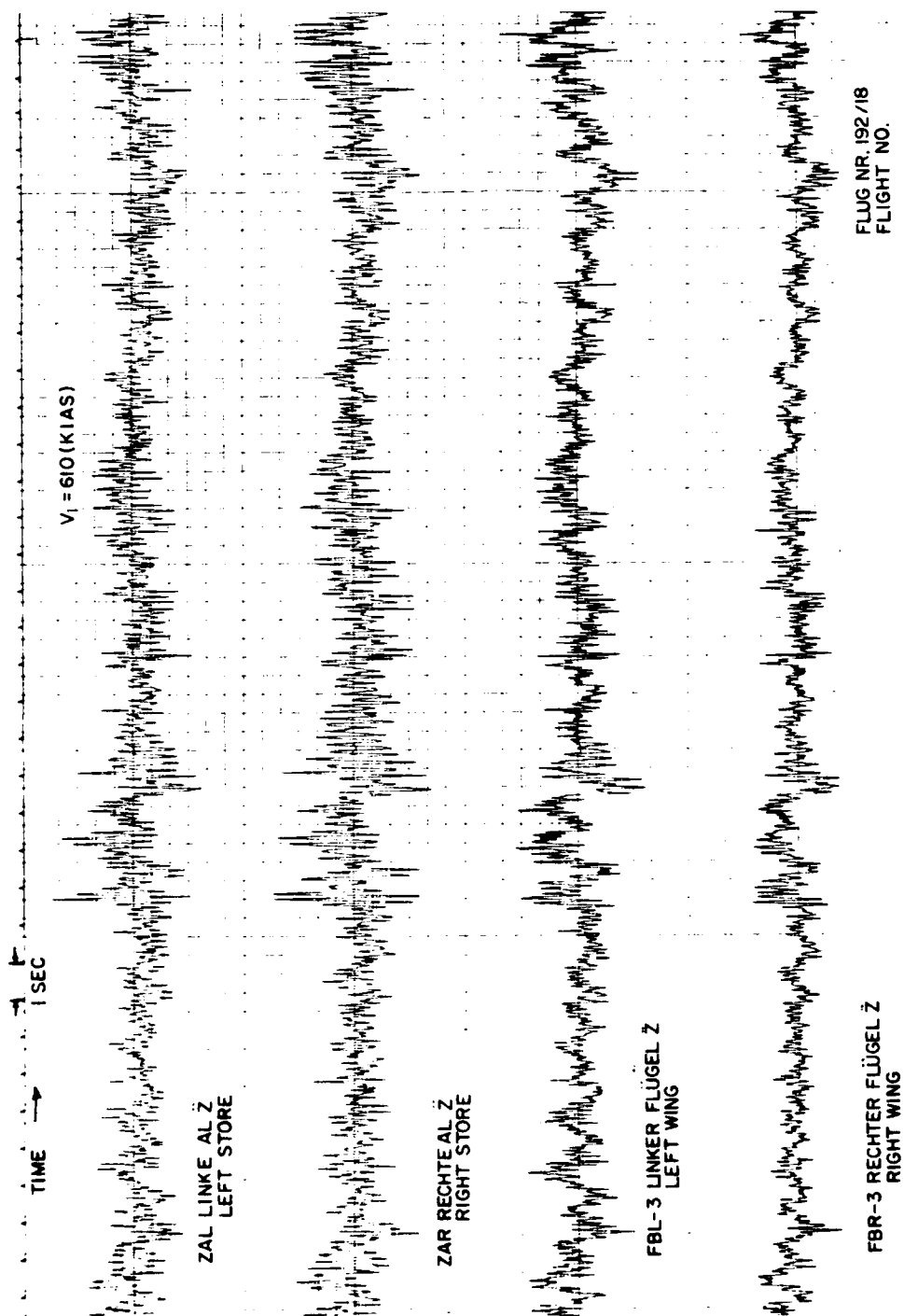
Figure 88. Time Histories of the Critical Store Configuration at
610 KIAS
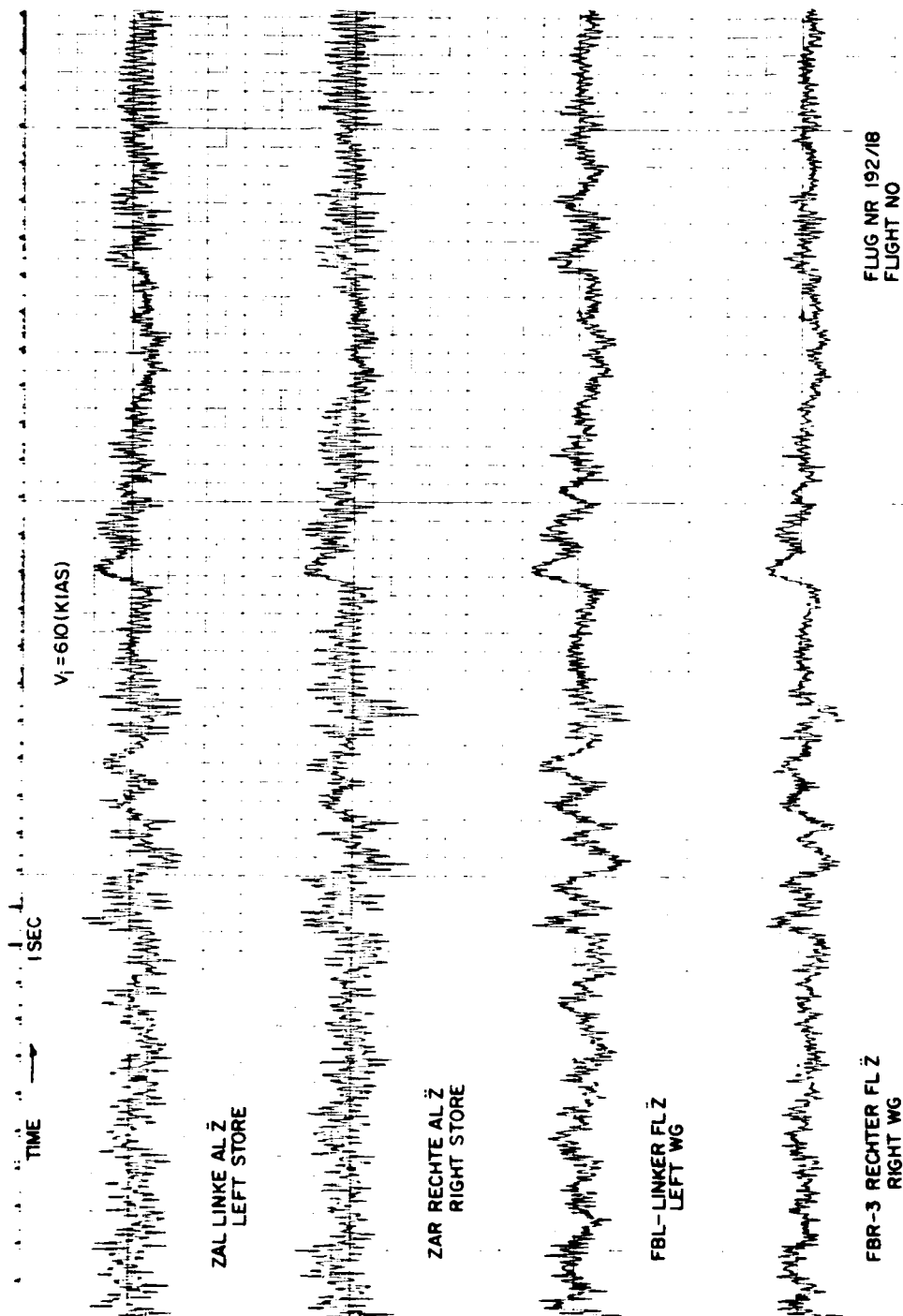
Figure 89. Time Histories of the Critical Store Configuration at
610 KIAS
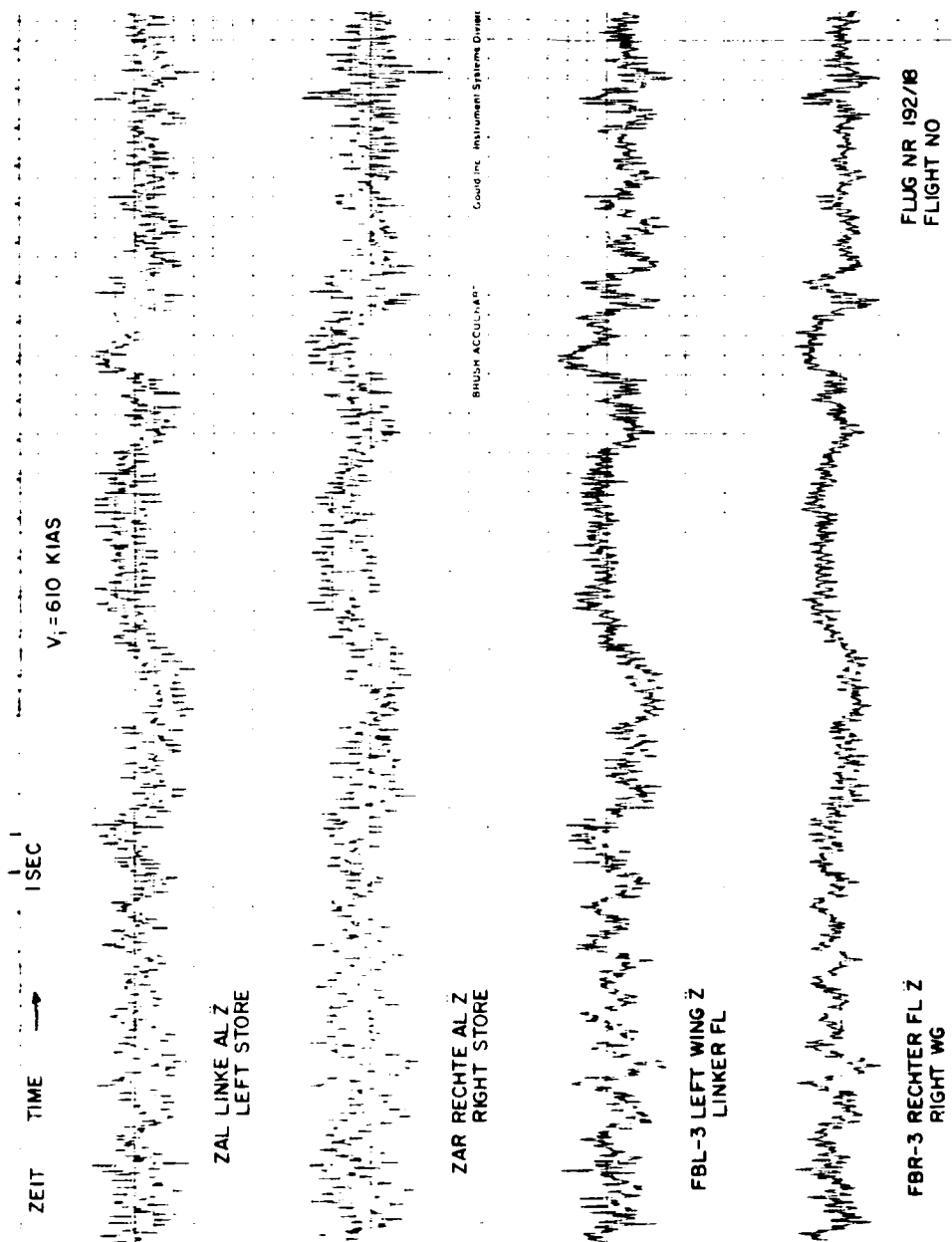
Figure 90.   Time Histories of the Critical Store Configuration at
610 KIAS
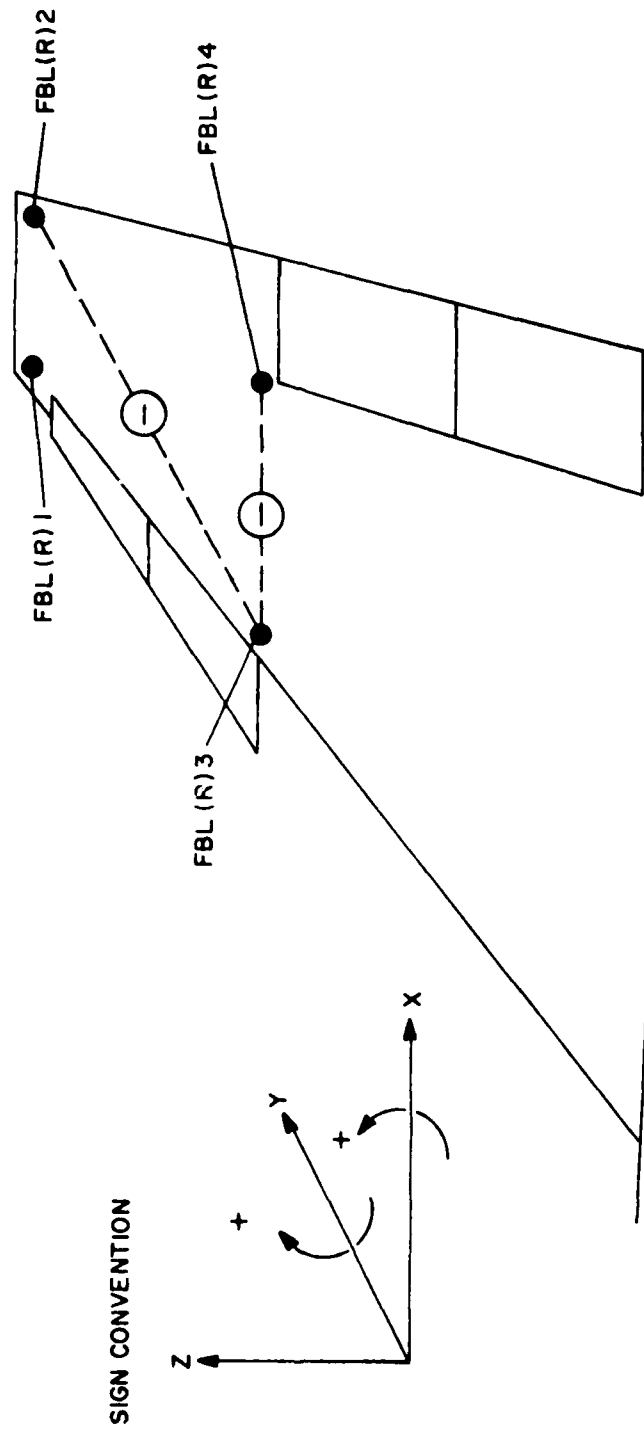
WING BENDING	φ	FBL(R)2 — FBL(R)3
STORE PITCH	θ	FBL(R)3 — FBL(R)4
VALID FOR FLIGHT 175/I - 185/II		

SIGN CONVENTION

Figure 91. Sensor Combination I

Figure 92. Sensor Combination II
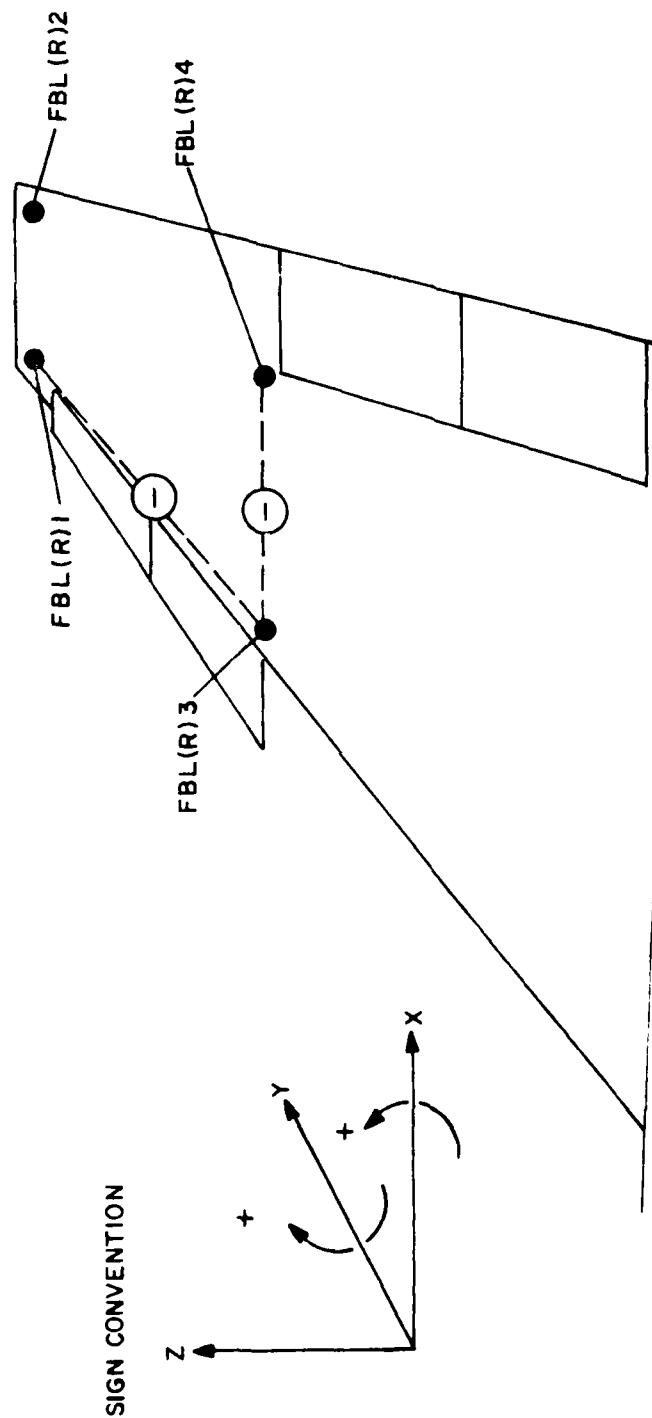
WING BENDING	φ	FBL(R)1 — FBL(R)3
STORE PITCH	θ	FBL(R)3 — FBL(R)4
VALID FOR FLIGHT 187/13—192/18		

SIGN CONVENTION
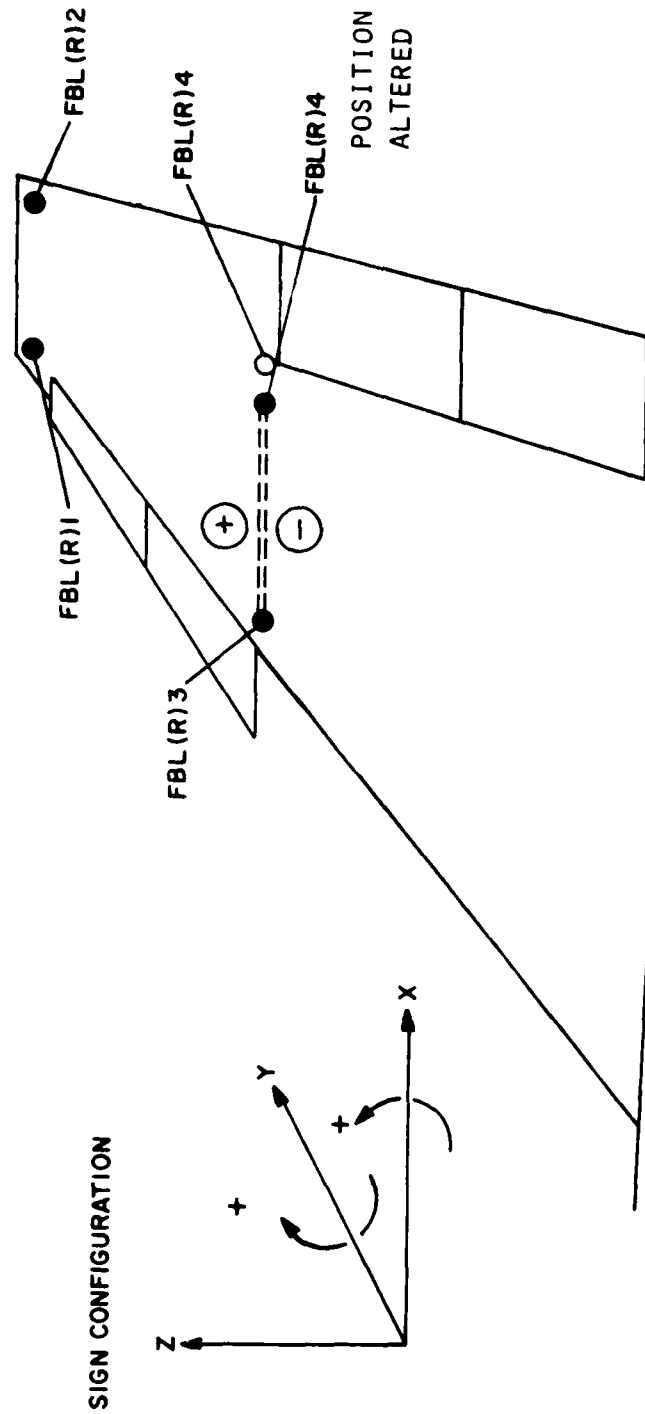
Figure 93. Sensor Combination III
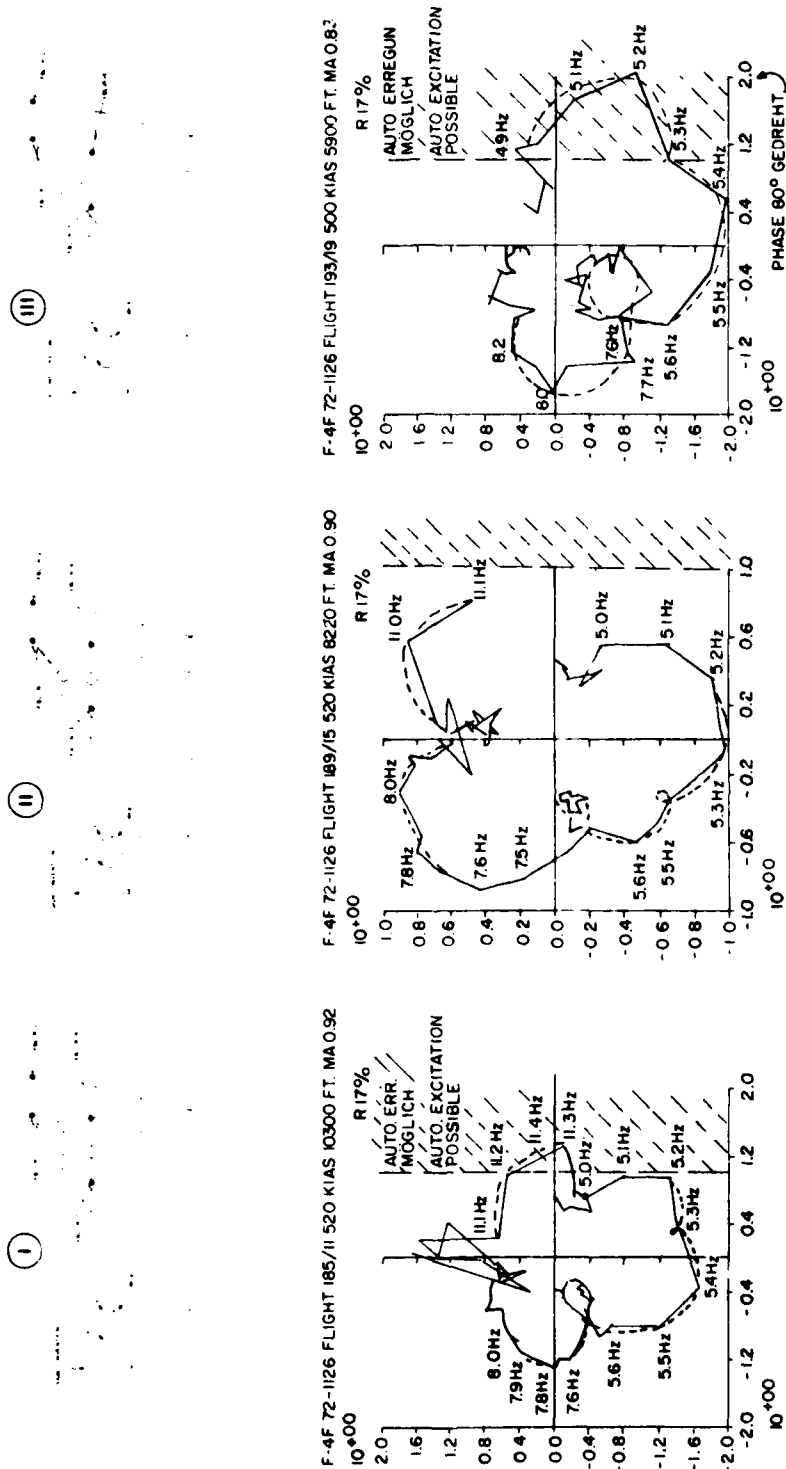
Figure 94. Nyquist Diagram for Various Sensor Combinations

F-4F 72-1126 FLIGHT 185/11 450 KIAS 10000 FT MA 0.84
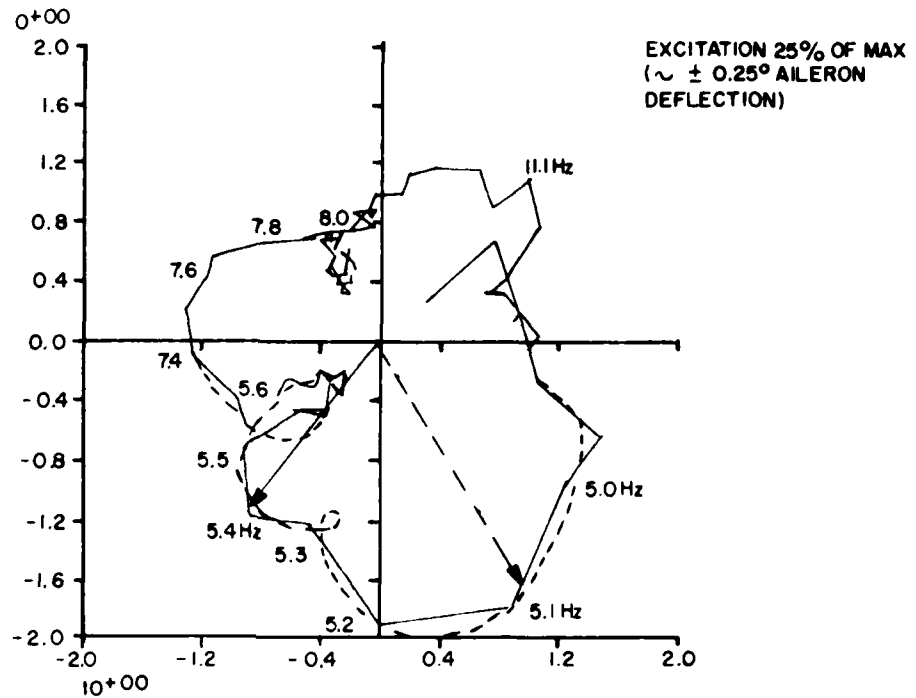
F-4F 72-1126 FLIGHT 185/11 520 KIAS 10300 FT MA 0.92
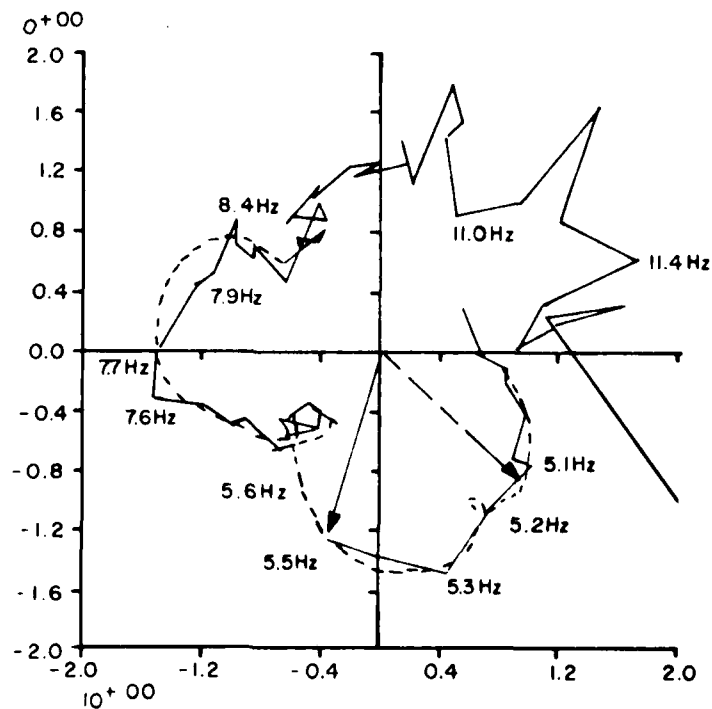
Figure 95. Nyquist Diagrams at Various Airspeeds

129
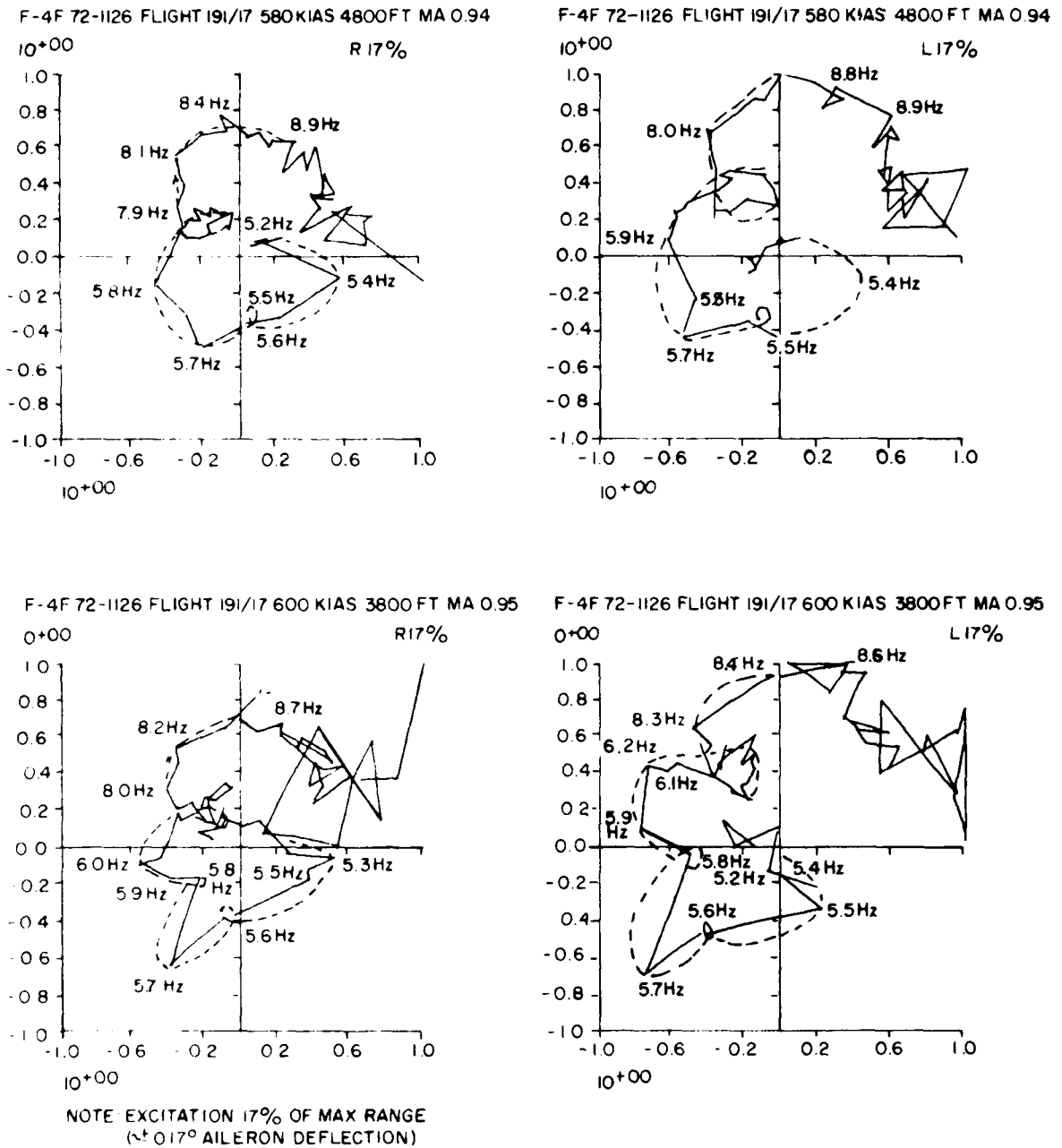
Figure 96.   Nyquist Diagrams for High Stagnation Pressures
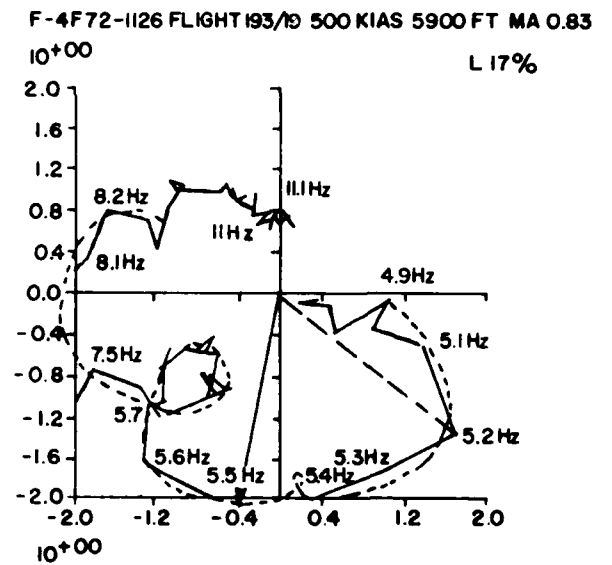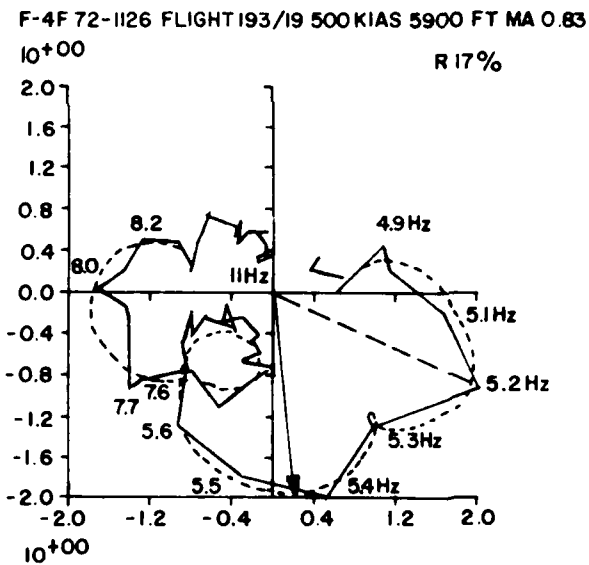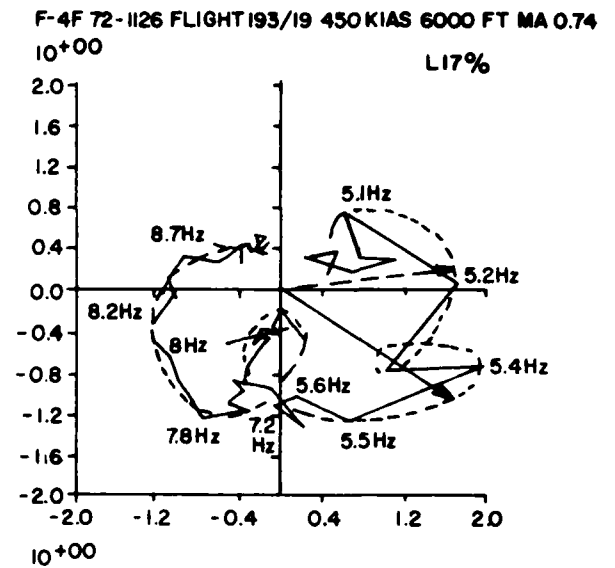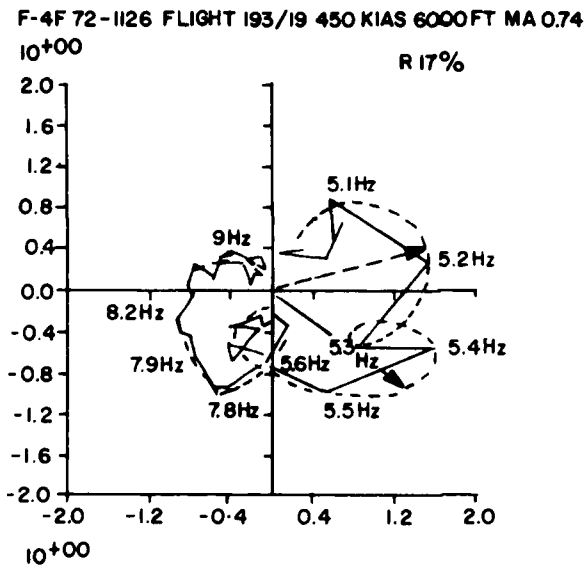
Figure 97. Nyquist Diagram of the Flutter Suppression System with
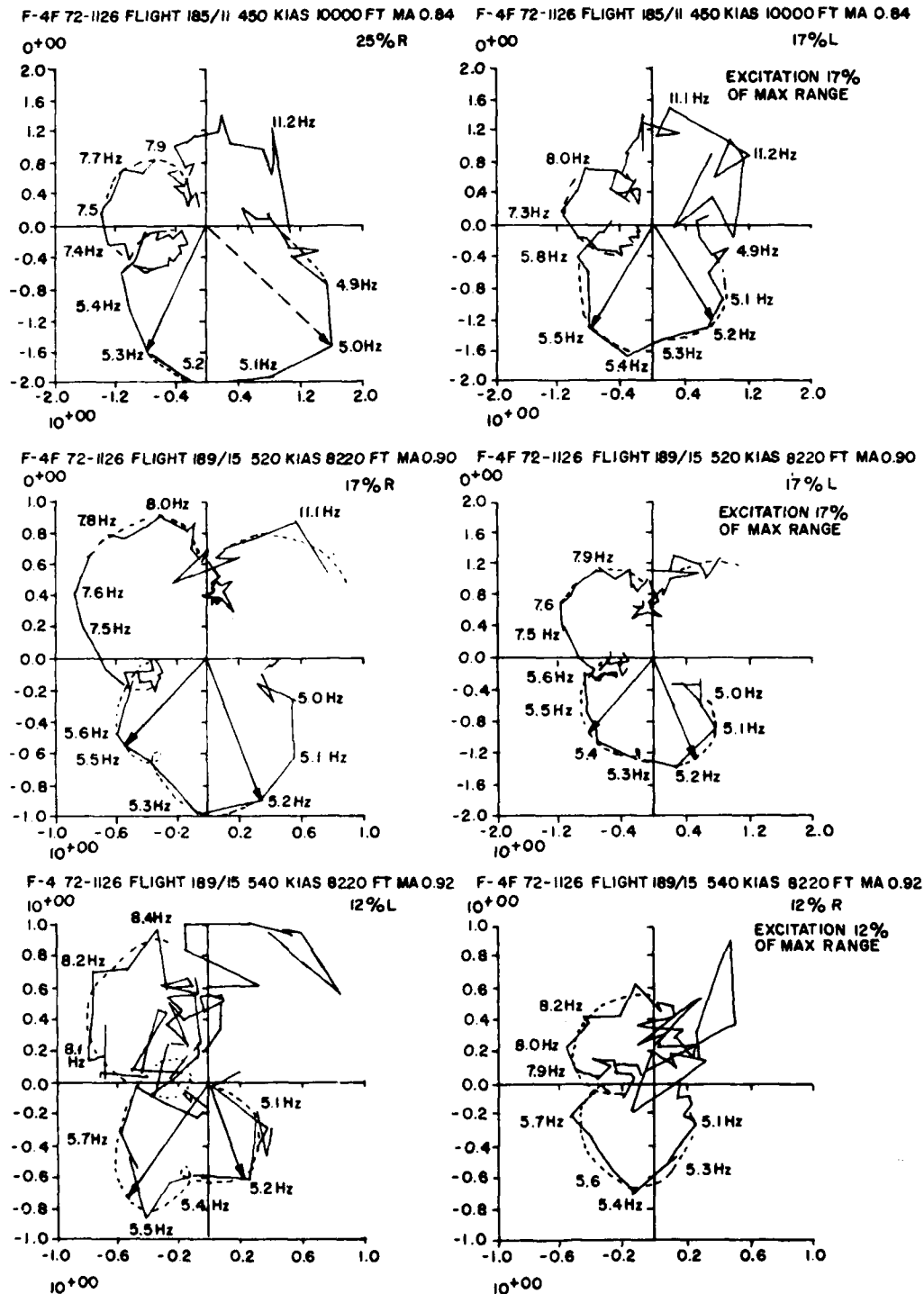Sensor Combination III, Mach Number of 0.74 and 0.83

F-4F 72-1126 FLIGHT 185/11 450 KIAS 10000 FT MA 0.84   F-4F 72-1126 FLIGHT 185/11 450 KIAS 10000 FT MA 0.84
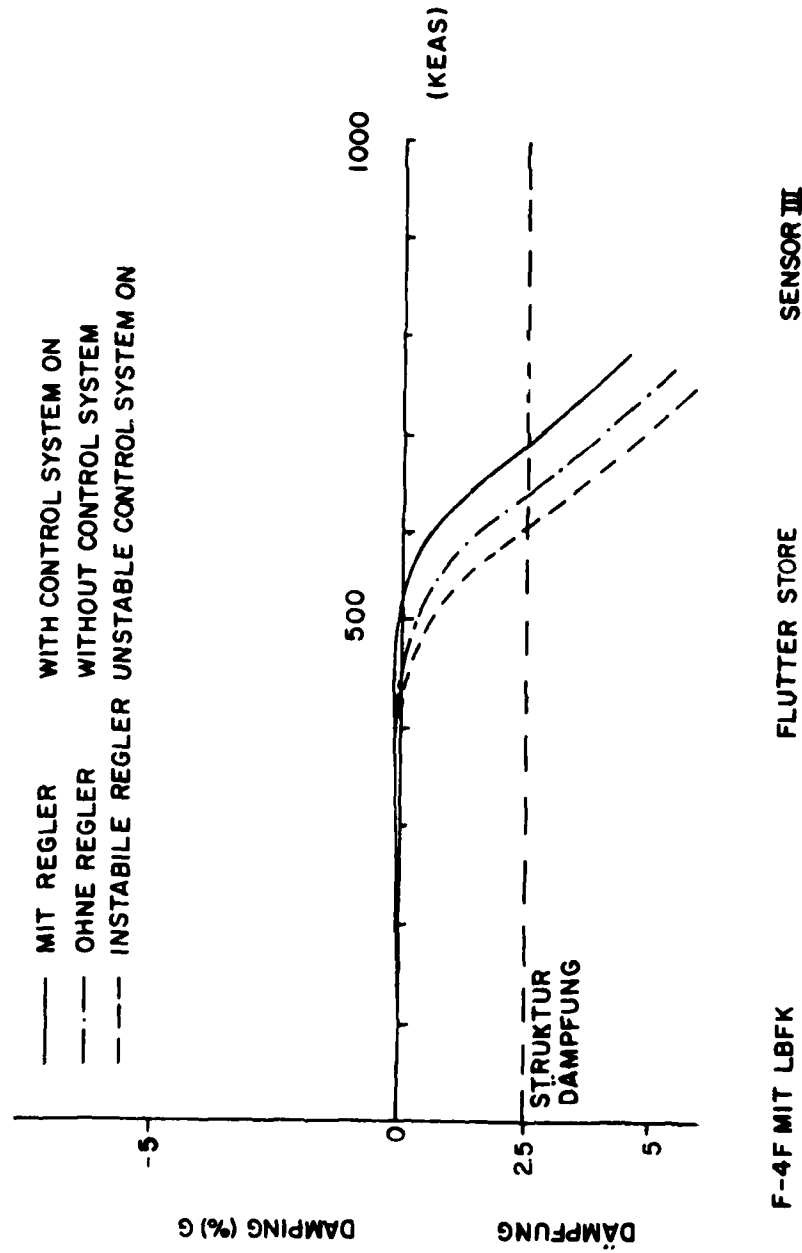
Figure 98. Nyquist Diagrams of Various Input Levels

Figure 99.   Comparison of the Calculated Damping of the Stable and
Unstable Flutter Suppression System
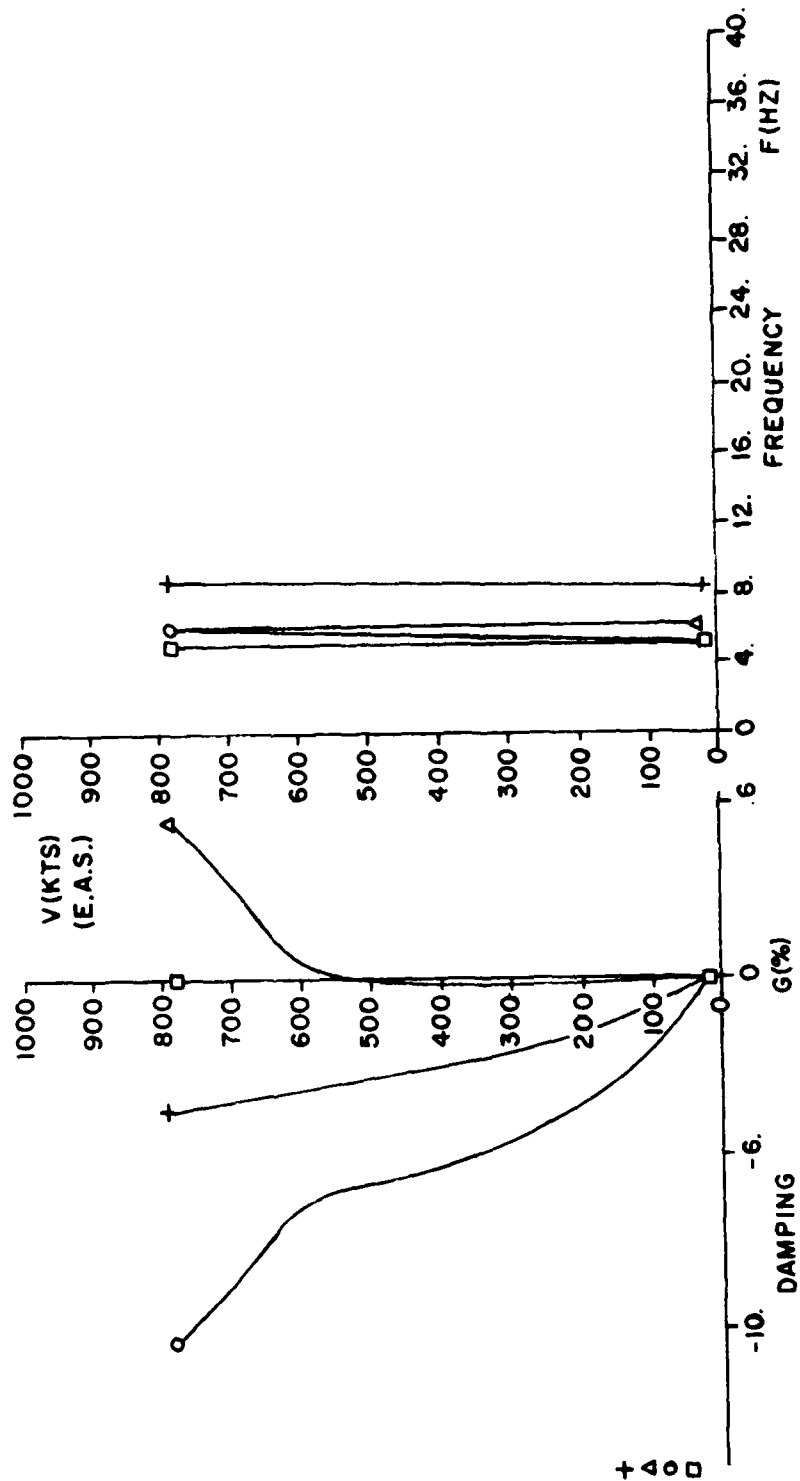
Figure 100. Flutter Calculation with FSS

Figure 101. Flutter Calculation without FSS
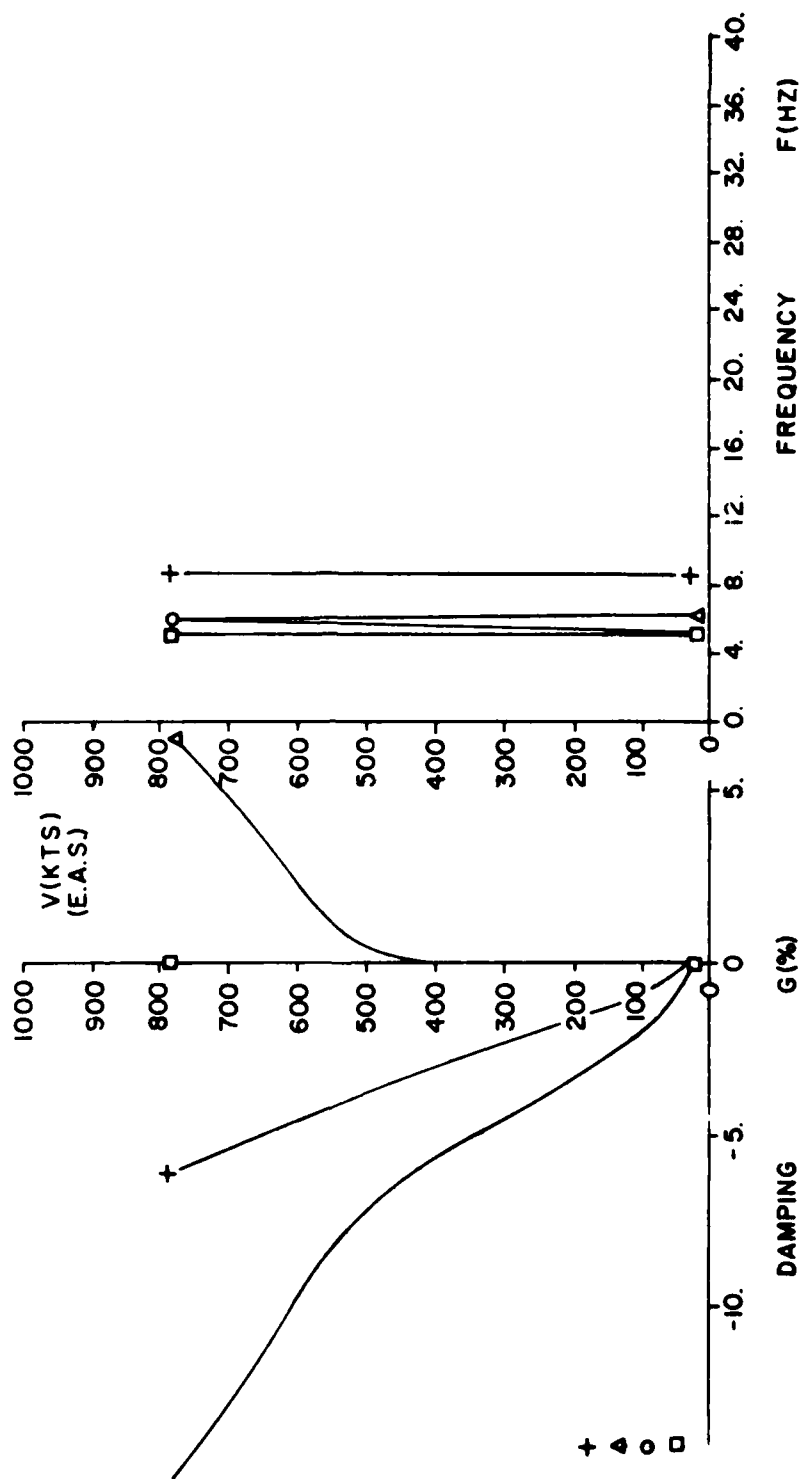
Figure 102. Flutter Calculation with Unstable FSS
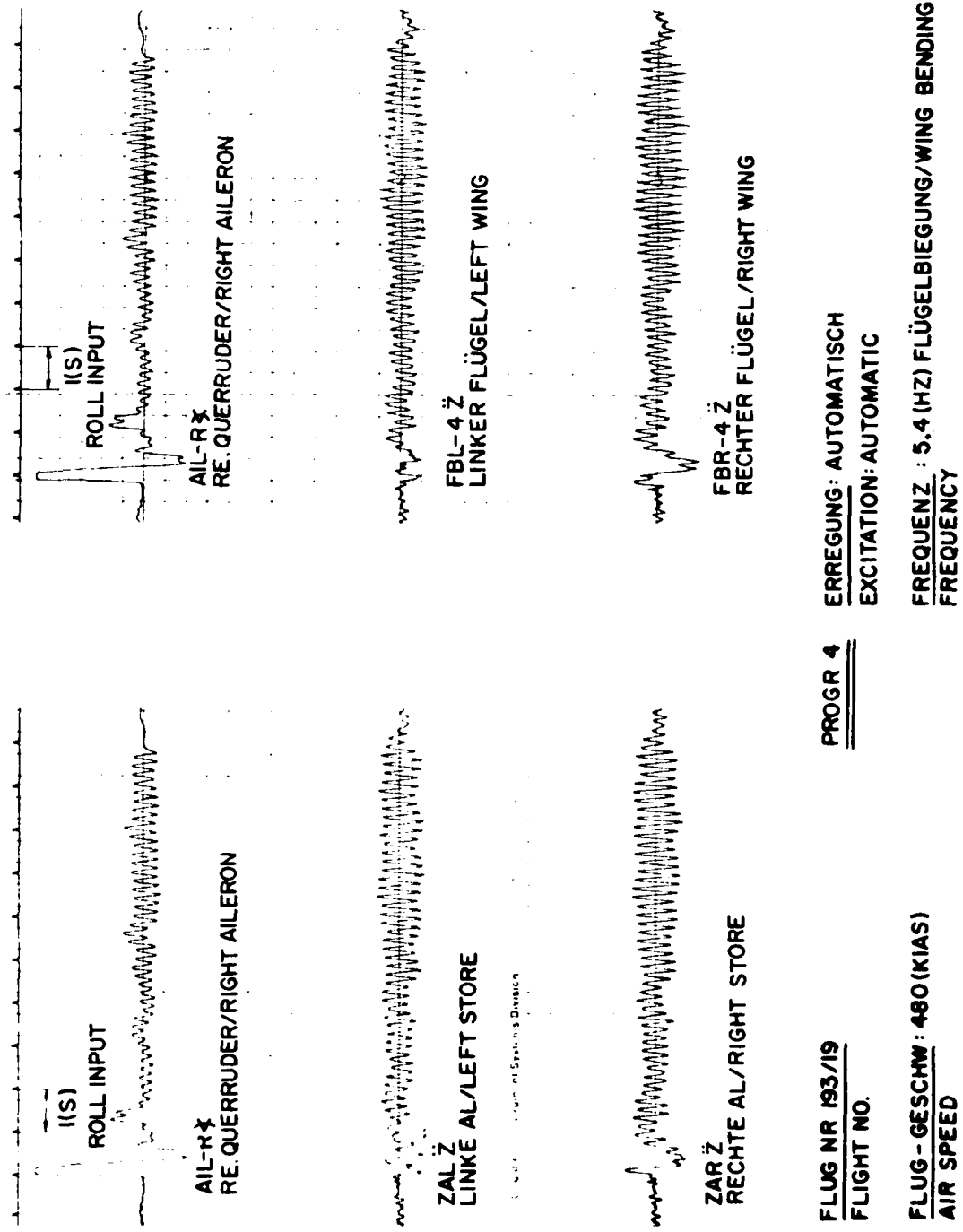
Figure 103. Time Histories with Automatic Excitation

TIME $\longrightarrow$ 1 SEC

QUERRUDER
RECHTERS FL
AIL-R
AILERON &
RIGHT WING

GEDÄMPFT
DAMPED

LINKE
ZAL LEFT STORE Ż

ERREGT
EXCITED

RECHTE AL
ZAR RIGHT STORE Ż

| FLUG NR 184/10 | PROGR. 2 | ERREGUNG | 100% | RECHTER FL | DÄMPFUNG | LINKER FL |
| FLIGHT NO | | EXCITATION | | RIGHT WING | DAMPER | LEFT WG |
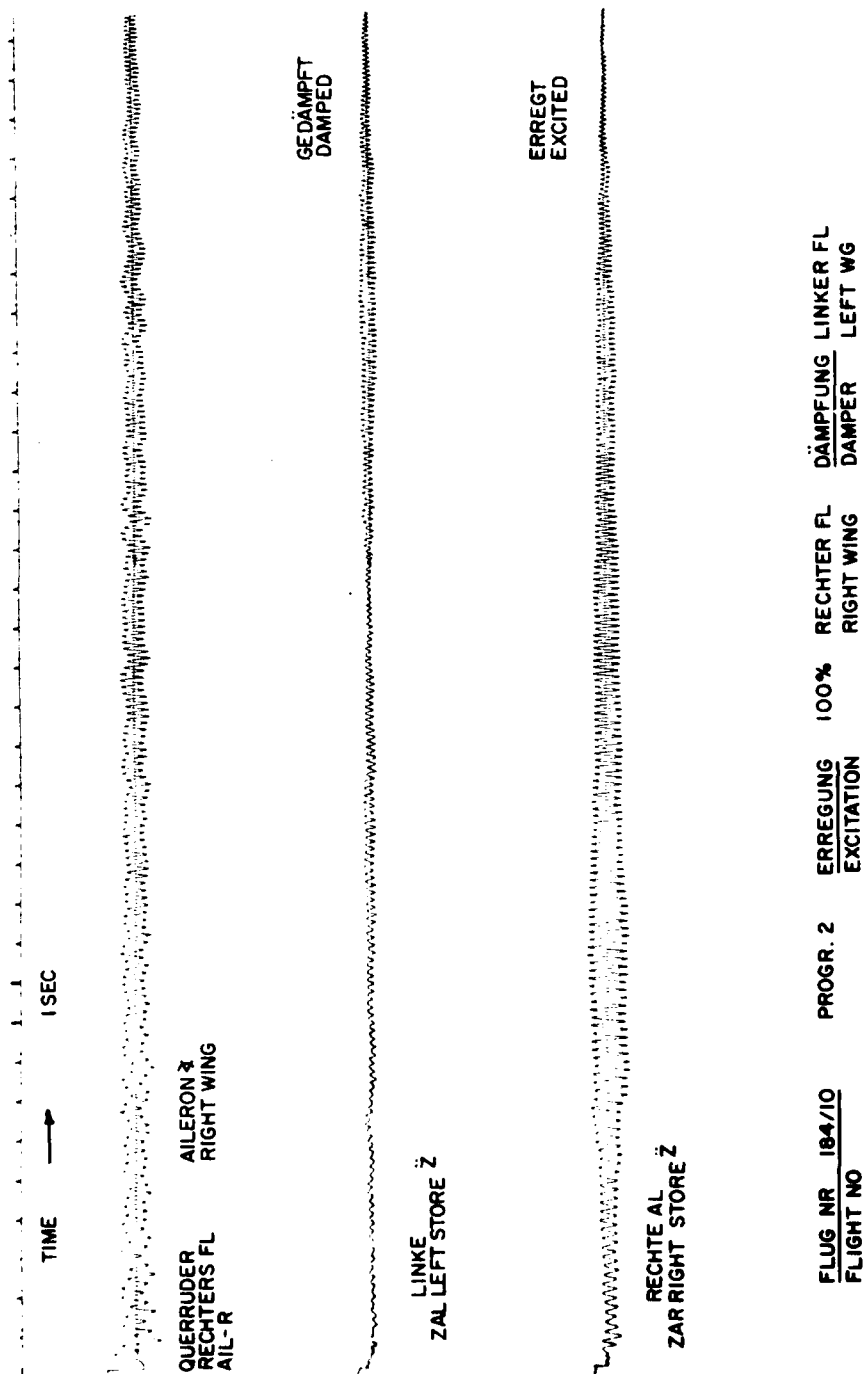
Figure 104. Tests of Vibration Suppression, 500 KIAS

TIME ⟶ I SEC

AIL-R
R.QUERRUDER R. AILERON ẍ

ZAL LINKE
LEFT STORE Z̈

ZAR RECHTE AL
RIGHT STORE Z̈

| FLUG NR 193/19 | PROGR. 2 | ERREGUNG | 100% | RECHTER FL | DÄMPFUNG | LINKER FL |
| FLIGHT NO | | EXCITATION | | RIGHT WG | DAMPER | LEFT WG |
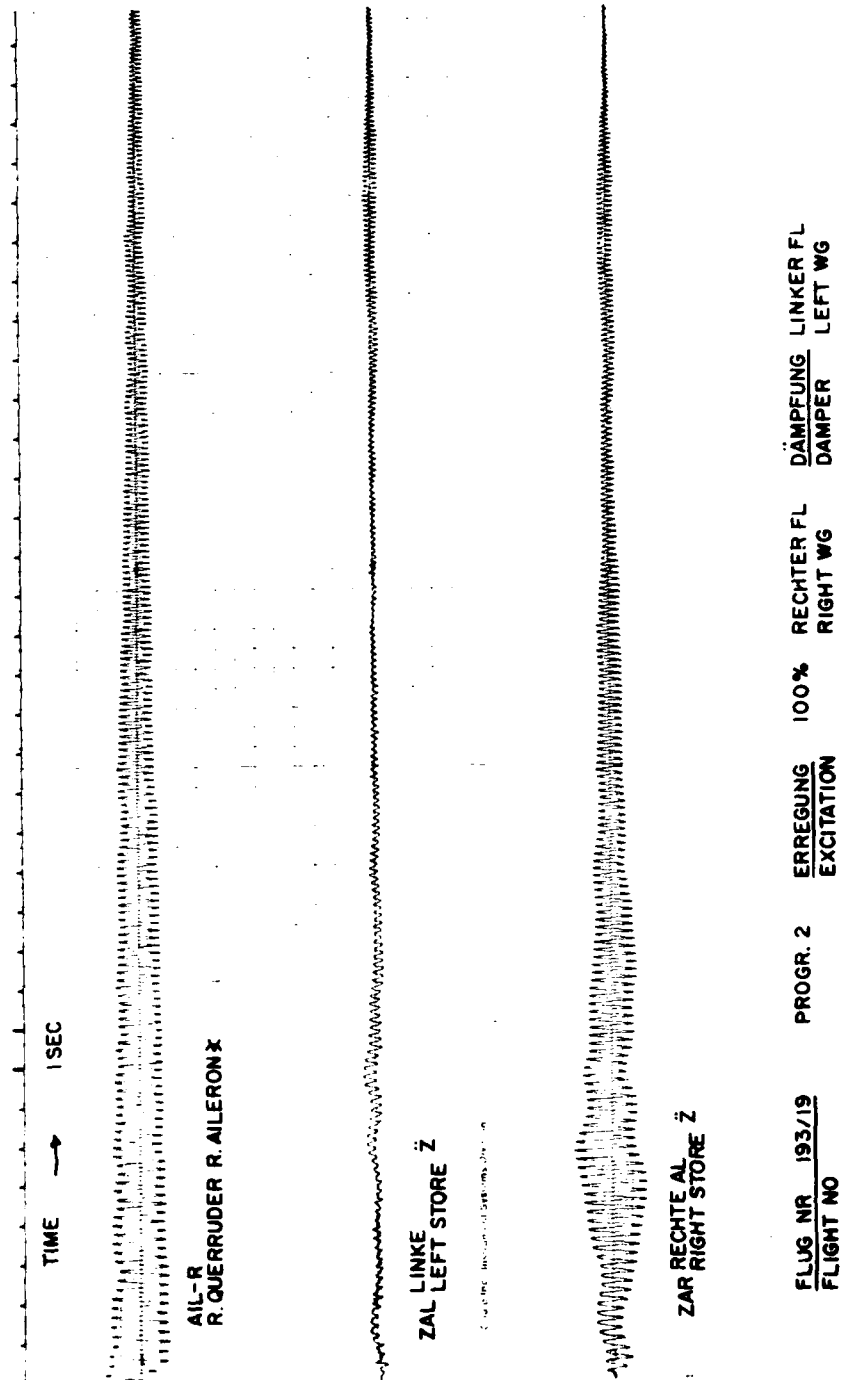
Figure 105. Tests of Vibration Suppression, 450 KIAS

139

TIME ⟶ I SEC

AIL-R R.QUERRUDER ✕
RIGHT AILERON

FBL-4 LINKER FLÜGEL Ż
RIGHT WING

BRUSH ACCUCHART   Gould Inc. Instrument Systems Division

FBR-4 RECHTER FLÜGEL Ż
RIGHT WING

| FLUG NR   193/19 | PROGR. 2 | ERREGUNG | 100% | RECHTER FLÜGEL |
| FLIGHT NO | | EXCITATION | | RIGHT WING |
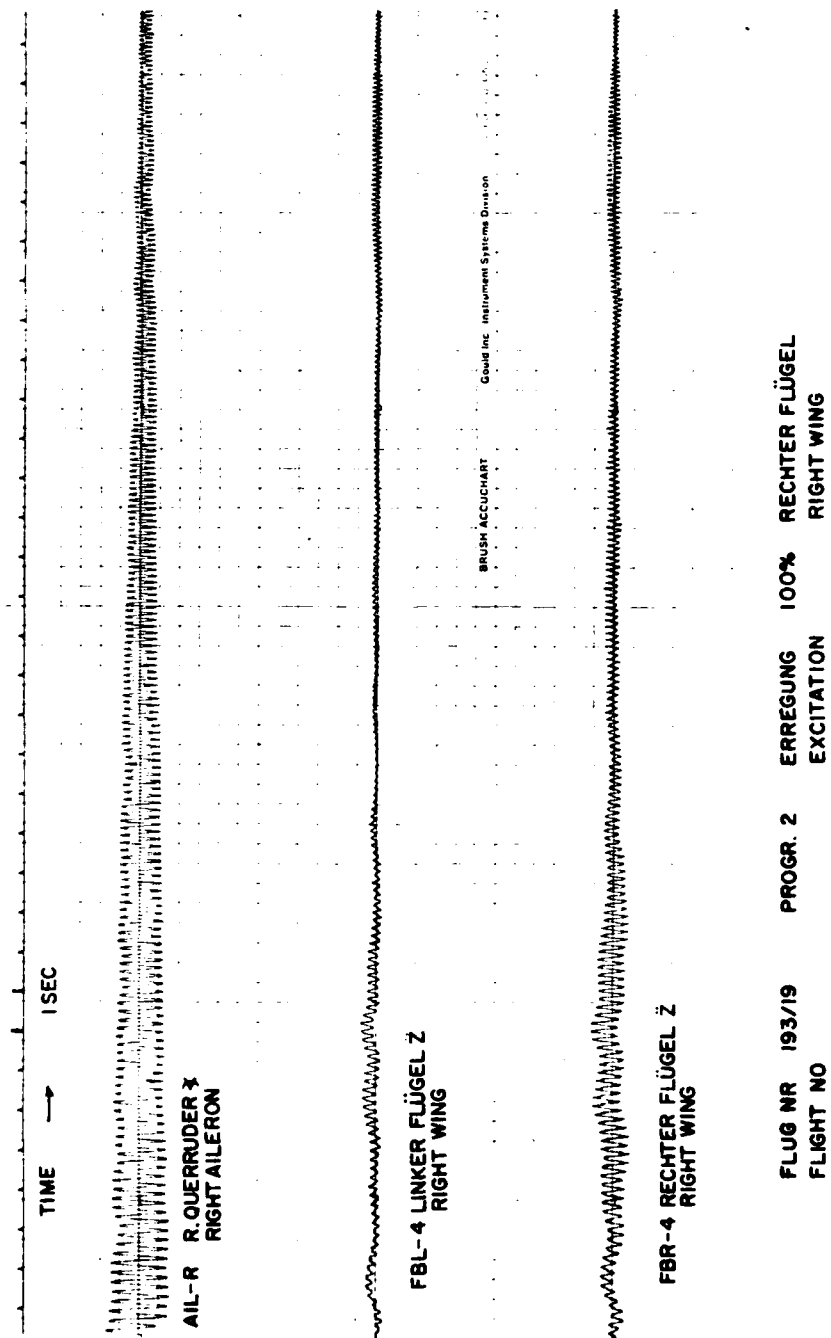
Figure 106. Tests of Vibration Suppression, 450 KIAS

140

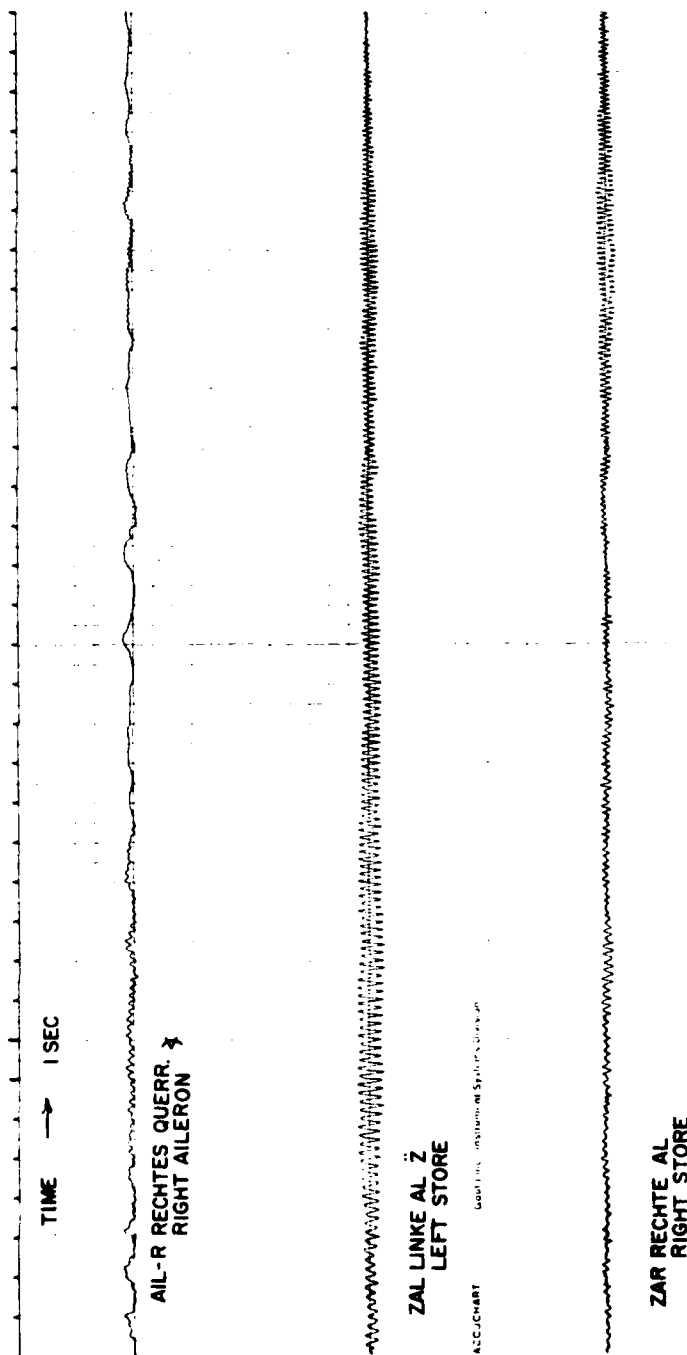Figure 107. Tests of Vibration Suppression 450 KIAS

TIME → I SEC

AIL-R
R.QUERRUDER, R.AILERON ↯

ZAL LINKE AL
LEFT STORE $\ddot{Z}$

ZAR RECHTE AL
RIGHT STORE $\ddot{Z}$

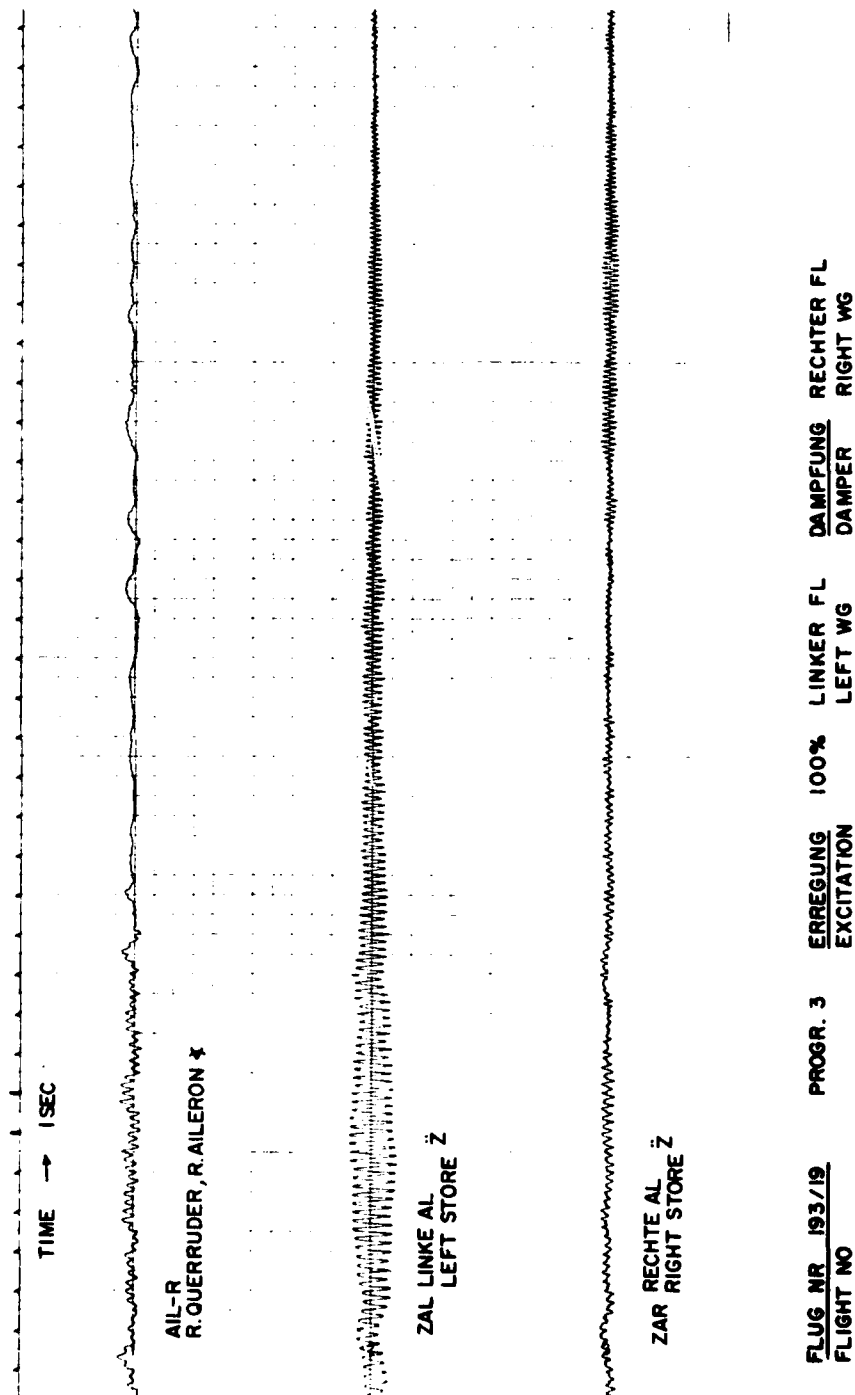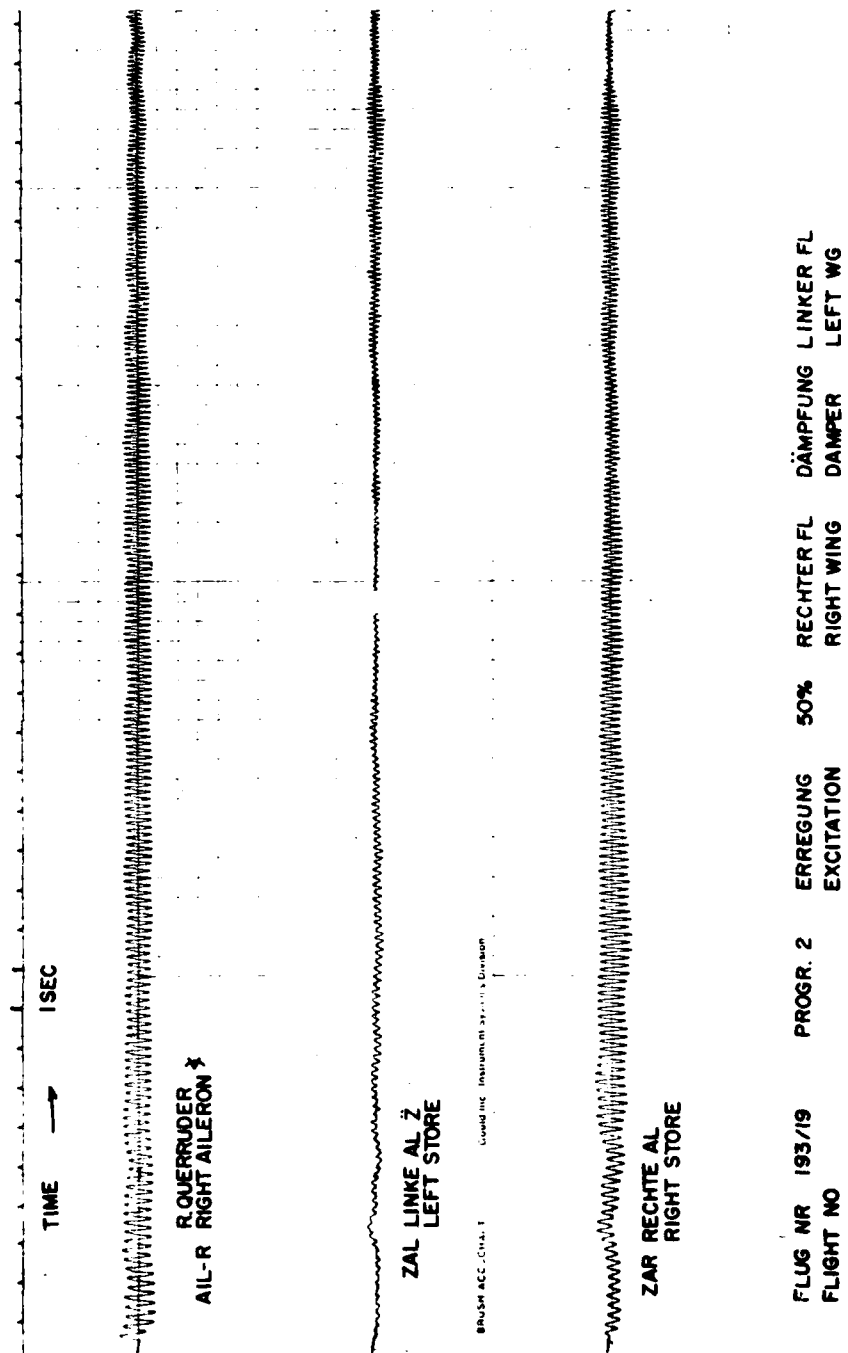| FLUG NR 193/19 | PROGR. 3 | ERREGUNG | 100% | LINKER FL | DAMPFUNG | RECHTER FL |
| FLIGHT NO | | EXCITATION | | LEFT WG | DAMPER | RIGHT WG |

Figure 108. Tests of Vibration Suppression

Figure 109. Tests of Vibration Suppresssion

END

DATE
FILMED

9 — 83

DTIC